

Utah State University

DigitalCommons@USU

All Graduate Theses and Dissertations

Graduate Studies

8-2023

Consumption of a Western Diet Enhanced Colitis-Associated Colorectal Cancer and Dysbiosis of the Fecal Microbiome in Mice Notwithstanding Dietary Intervention or Fecal Microbiome Transfer

Daphne Michelle Rodriguez Jimenez
Utah State University

Follow this and additional works at: <https://digitalcommons.usu.edu/etd>



Part of the [Animal Sciences Commons](#)

Recommended Citation

Rodriguez Jimenez, Daphne Michelle, "Consumption of a Western Diet Enhanced Colitis-Associated Colorectal Cancer and Dysbiosis of the Fecal Microbiome in Mice Notwithstanding Dietary Intervention or Fecal Microbiome Transfer" (2023). *All Graduate Theses and Dissertations*. 8802.
<https://digitalcommons.usu.edu/etd/8802>

This Dissertation is brought to you for free and open access by the Graduate Studies at DigitalCommons@USU. It has been accepted for inclusion in All Graduate Theses and Dissertations by an authorized administrator of DigitalCommons@USU. For more information, please contact digitalcommons@usu.edu.



CONSUMPTION OF A WESTERN DIET ENHANCED COLITIS-ASSOCIATED
COLORECTAL CANCER AND DYSBIOSIS OF THE FECAL MICROBIOME
IN MICE NOTWITHSTANDING DIETARY INTERVENTION OR
FECAL MICROBIOME TRANSFER

by

Daphne Michelle Rodriguez Jimenez

A dissertation submitted in partial fulfillment
of the requirements for the degree

of

DOCTOR OF PHILOSOPHY

in

Animal, Dairy and Veterinary Sciences

Approved:

Abby D. Benninghoff, Ph.D.
Major Professor

Korry J. Hintze, Ph.D.
Committee Member

Aaron Olsen, Ph.D., D.V.M
Committee Member

Kerry Rood, M.S., M.P.H., D.V.M
Committee Member

Heloisa Rutigliano, Ph.D., D.V.M.
Committee Member

D. Richard Cutler, Ph.D.
Vice Provost for Graduate Studies

UTAH STATE UNIVERSITY
Logan, Utah

2023

Copyright © Daphne Rodriguez 2023

All Rights Reserved

ABSTRACT

Consumption of a Western Diet Enhanced Colitis-Associated Colorectal Cancer and
Dysbiosis of the Fecal Microbiome in Mice Notwithstanding Dietary Intervention
or Fecal Microbiome Transfer

by

Daphne M. Rodriguez, Doctor of Philosophy

Utah State University, 2023

Major Professor: Dr. Abby D. Benninghoff
Department: Animal, Dairy, and Veterinary Sciences

Consumption of the total Western diet (TWD) in mice has been shown to increase gut inflammation, promote colon tumorigenesis and alter the fecal microbiome composition compared to mice fed a healthy diet, AIN93G (AIN). However, it is unclear whether the gut microbiome contributes directly to colitis-associated colorectal cancer (CAC) in this model. The overarching goal of this dissertation was to better understand the influence of gut microbiome on CAC development by modulating the microbiome via dietary intervention or fecal microbiota transfer (FMT). In the first project, the objective was to study if dietary supplementation with black raspberries, rich in anti-inflammatory anthocyanins, would ameliorate Western-diet enhanced gut inflammation and colon tumorigenesis. In a pilot study and follow-up experiment, we employed a mouse model of CAC to determine the effects of dietary supplementation with whole, freeze-dried black raspberry (BRB) powder in male C57BL/6J mice fed either the standard AIN diet or the TWD. Supplementation with BRB reduced tumor multiplicity and increased colon length, irrespective of the basal diet; however, BRB consumption did not significantly affect colitis symptoms or reduce colon inflammation or mucosal injury based on histopathological findings. Alternatively, BRB intake increased alpha diversity, altered beta

diversity and changed the relative abundance of various bacteria families, including some taxa with purported health benefits. The objective of the second study was to determine whether dynamic FMT from host mice fed either AIN or TWD basal diets would alter colitis symptoms or colitis-associated CRC in recipient mice, which were fed either AIN or TWD directly using a 2×2 factorial experiment design. Briefly, FMT from mice fed either basal diet with differing colitis or tumor outcomes did not shift colitis symptoms or colon tumorigenesis in recipient mice, regardless of the basal diet they consumed. These observations suggest that the gut microbiome may not contribute directly to the development of disease in this animal model. Overall, results from these two experiments using different intervention approaches to shift the gut microbiome suggest that the basal diet is the primary driving factor of gut inflammation and promotion of tumorigenesis in this mouse model of CAC.

(237 pages)

PUBLIC ABSTRACT

Consumption of a Western Diet Enhanced Colitis-Associated Colorectal Cancer and
Dysbiosis of the Fecal Microbiome in Mice Notwithstanding Dietary Intervention
or Fecal Microbiome Transfer

Daphne M. Rodriguez

Major Professor: Dr. Abby D. Benninghoff
Department: Animal, Dairy, and Veterinary Sciences

In a rodent model of inflammation-associated colorectal cancer, consumption of a Western-style diet increases gut inflammation and enhances risk of developing colon tumors. The goal of this dissertation was to understand the contribution of bacteria within the large intestine on colon inflammation and colon tumorigenesis. Two pre-clinical animal studies were performed using two different intervention strategies to shift the microbiome, and potentially gut inflammation and tumor development: 1) an experiment using dietary supplementation with black raspberries, a functional food enriched in bioactive anthocyanins with purported anti-inflammatory activity, and 2) an experiment using fecal microbiota transfer from mice fed a healthy diet with low symptoms of colitis or mice fed a Western diet with severe symptoms of colitis to recipient mice fed either the healthy or Western diet directly. Dietary supplementation with black raspberries did reduce colon tumor number, irrespective of the basal diet, and caused significant shifts in the composition of the gut microbiome. Fecal microbiota transfer from mice with severe colitis did not exacerbate colitis in recipient mice fed a healthy diet, nor did transfer from mice with low symptoms protect mice fed a Western diet. However, for both experiments, we determined that the basal diet fed to the recipient mice was the driving factor affecting the gut inflammation and colon tumorigenesis.

DEDICATION

As a graduate student, I have had many personal and professional challenges to overcome. As usual my beloved family has been in the center of my success. I would like to dedicate this dissertation to my mom Evelin Jimenez, my dad Virgilio Rodriguez, and my brother Cristian Rodriguez. They are the reason I try to achieve the most seemingly impossible tasks. I continue to be successful in my career and as a person due to their constant encouragement and unwavering support. I feel so honored to come from such an inclusive and loyal family. They have supported me through the thick and thin, respecting all the decisions I have made and encouraging me to be the best human I can be. Although, we do not live on the same continent, they are the reason I can take on the world. In our family, if one of us succeeds, we all succeed. I wouldn't have succeeded in this endeavor without them, and I will continue to succeed because of them.

ACKNOWLEDGMENTS

First and foremost, I would like to thank my mentor Dr. Abby Benninghoff, for not only supporting and guiding me through these projects and academically during my degree completion, but also being a close friend when needed. Dr. Benninghoff has been patient and understanding through the many years I have worked for her, allowing me to not only learn but also encouraged me to live my life. Working and being mentored by Dr. Benninghoff, I have accomplished and overcome many professional and personal hardships, and she always trusted me to achieve to the greatest of my potential while giving me the space to figure it out on my own. I am deeply grateful for her time spent helping me achieve my goals, but also just to be human. I am so honored I had the opportunity to work under such a dedicated, hard-working, supportive, understanding and overall inspirational person for so many years. Dr. Benninghoff is someone I aspire to be one day and even though I am moving on to other job opportunities, I will forever cherish the memories, wisdom, and guidance she provided me.

Next, I would like to thank Dr. Korry Hintze, for always lending a helping hand. Dr. Hintze mentored me very closely through my Master's and PhD degrees. Dr. Hintze's calm and encouraging words helped me not only professionally, but also in other aspects of my life. He would always be willing to help with development of protocols, guide me through various laboratory techniques and motivate me to dig deeper intellectually. Next, I want to thank my committee members Dr. Kerry Rood, Dr. Heloisa Rutigliano and Dr. Aaron Olsen. Dr. Rood for maintaining a light and uplifting spirit, reminding me to always look at the bigger picture. Dr. Rutigliano, for taking the time to conversate with me and for encouraging me to not only do better but to do it while taking time for myself. Finally, Dr. Olsen for suggesting to look past the obvious and always willing to accommodate our technical requests. I can honestly say that I had the most helpful, approachable and respectful committee members on my side.

I want to also thank all the laboratory members that made this work possible, Eliza Stewart for being my right-hand person. Abby Barton, Emily Mortensen-Curtis, Porter Green, Sam Vassar, Mohammed Alamanti, Canyon Neal, Jocelyn Cuthbert, Michaela Brubaker, Kimberly Campbell, Elizabeth Park, Tess Armbrust, Kevin Contreras, Ashli Hunter and Sumira Phatak. None of these projects would have been possible with their commitment and dedication.

Next, a special thanks to our lab manger Giovanni Rompato, for all the technical help through these projects and for providing a cheerful environment to work in. Dr. Aaron Thomas for all the guidance through the microbial sequences and a friendly face in the workspace. Lisa Desoi for always finding accommodations for our mouse projects and maintaining a warm atmosphere in the animal building.

As for personal acknowledgements, I want to send a special thanks to Dr. Tom Baldwin, Dr. Gordon Hullinger and Dr. Arnaud Van Wettere, and everyone else in the laboratory for being such a supportive and down-to-earth group during my time at the Veterinary Diagnostic Laboratory. Thank you for spending the time to teach me various techniques and providing a safe space for me during the process of this dissertation.

Finally, I want to thank Jose Bernal, for accompanying me during my time as a doctoral student. The Bernal family, Sergio, Marina, Gabriel, and Gabriela, for providing a welcoming space and making important days special, I am very grateful.

I also gratefully acknowledge financial support from the U.S. Department of Agriculture, National Institute of Food and Agriculture, grant number USDA-2018-67017-27516, and the Utah Agricultural Experiment Station, project numbers UTA-01178 and UTA-01456.

Daphne M. Rodriguez

CONTENTS

	Page
ABSTRACT	iii
PUBLIC ABSTRACT	v
DEDICATION.....	vi
ACKNOWLEDGMENTS	vii
LIST OF TABLES	xi
LIST OF FIGURES	xii
ABBREVIATIONS AND SYMBOLS	xv
CHAPTER	
1. REVIEW OF THE LITERATURE	1
1.1. Colorectal Cancer Statistics and Major Risk Factors	1
1.2. Molecular Aspects of Colorectal Cancer	3
1.3. The Immune System, Inflammation and Cancer	8
1.4. The Gut Microbiome	14
1.5. Animal Models for Gut Inflammation, Cancer, and the Microbiome	21
1.6. The Western Diet and Risk of Colitis-Associated Colorectal Cancer	25
1.7. Dietary Polyphenols and Anthocyanins	29
1.8. Project Objectives and Hypotheses	33
References	34
2. DIETARY SUPPLEMENTATION WITH BLACK RASPBERRIES ALTERED THE GUT MICROBIOME COMPOSITION IN A MOUSE MODEL OF COLITIS-ASSOCIATED COLORECTAL CANCER, ALTHOUGH WITH DIFFERING EFFECTS FOR A HEALTHY VERSUS A WESTERN BASAL DIET.....	55
Abstract	55
2.1. Introduction	56
2.2. Materials and Methods	60
2.3. Results	69
2.4. Discussion	83
2.5. Conclusions	92
References	93

3. BASAL DIET FED TO RECIPIENT MICE WAS THE DRIVING FACTOR FOR COLITIS AND COLON TUMORIGENESIS, DESPITE FECAL MICROBIOTA TRANSFER FROM MICE WITH SEVERE OR MILD DISEASE	119
Abstract	119
3.1. Introduction	120
3.2. Materials and Methods	124
3.3. Results	129
3.4. Discussion	137
3.5. Conclusions	146
References	147
4. CONCLUSIONS	168
References	175
APPENDICES	178
A. Publication Licensing Information	179
<i>Nutrients</i> Licensing Policy	179
Creative Commons CC BY License	180
B. Supplementary Material Associated with Chapter 2	187
Supplementary Figures	187
Supplementary Tables	202
Supplementary Files and Supporting Data	210
C. Supplementary Material Associated with Chapter 3	211
Supplementary Figures	211
Supplementary Tables	216
Supplementary Files and Supporting Data	220
VITA	221

LIST OF TABLES

Table		Page
2.S1.	Experimental diet formulations	202
2.S2.	Alpha diversity pairwise comparisons for effects of time point only, irrespective of basal diet or BRB supplement (experiment B)	204
2.S3.	Alpha diversity pairwise comparisons by experimental group within time points (experiment B)	205
2.S4.	Alpha diversity pairwise comparisons by time point within experimental group (experiment B)	206
2.S5.	Short-chain fatty acids pairwise comparisons for effects of time point only, irrespective of basal diet or BRB supplement (experiment B)	207
2.S6.	Short chain fatty acids pairwise comparisons by experimental group within time points (experiment B)	208
2.S7.	Short-chain fatty acids pairwise comparisons by time point within experimental group (experiment B)	209
3.S1.	Experimental diet formulations	216
3.S2.	Alpha diversity pairwise comparisons for effects of time point only, irrespective of basal diet or FMT source	217
3.S3.	Alpha diversity pairwise comparisons by experimental group within time points	218
3.S4.	Alpha diversity pairwise comparisons by time point within experimental group	219

LIST OF FIGURES

Figure	Page
2.1. Dietary supplementation with 5 to 10% BRB suppressed symptoms of colitis and colon tumorigenesis in mice fed TWD (experiment A)	102
2.2. Beta diversity of mouse microbiomes at each experimental time point (experiment A)	103
2.3. Food and energy intakes, body weight and body composition (experiment B)	104
2.4. Disease activity index and colon histopathology (experiment B)	105
2.5. Effect of BRB supplementation on colon length and colon tumorigenesis in mice fed AIN or TWD basal diets (experiment B)	106
2.6. Taxonomic classification of mouse fecal bacteria (experiment B)	107
2.7. Relative abundance of fecal microbiome at the family taxonomic level with summary of results of metagenomeSeq statistical analyses (experiment B)	108
2.8. Fecal microbiome community structures depicted as heat trees showing the relative abundance ratios for selected comparisons of basal diet and BRB supplement at each experimental time point (experiment B)	109
2.9. Relative abundance of select bacteria families of interest for each experimental time point (experiment B)	111
2.10. Ratio of Firmicutes to Bacteroidetes for each experimental time point (experiment B)	113
2.11. Alpha diversity of mouse fecal microbiomes for each experimental time point (experiment B)	114
2.12. Beta diversity of mouse fecal microbiomes for each experimental time point (experiment B)	115
2.13. Metagenome predicted functions classified using KEGG metabolism orthology with tax4fun (experiment B)	116
2.14. Longitudinal analysis of fecal microbiome taxonomy and functional capacity (experiment B)	117
2.15. Short-chain fatty acid concentrations in fecal samples from mice fed CON or BRB-supplemented diets at each experimental time point (experiment B)	118

3.1.	Food and energy intakes, body weight and body composition	155
3.2.	Disease activity index and colon histopathology	156
3.3.	Effect of recipient basal diet and FMT source on colon length and colon tumorigenesis	157
3.4.	Taxonomic classification of mouse fecal bacteria	158
3.5.	Relative abundance of fecal microbiome at the family taxonomic level with summary of results of metagenomeSeq statistical analyses	159
3.6.	Fecal microbiome community structures depicted as heat trees showing the relative abundance ratios for selected comparisons of recipient basal diet and FMT source at each experimental time point	161
3.7.	Relative abundance for select bacteria families of interest for each experimental time point	163
3.8.	Relative abundance for additional bacteria families of interest for each experimental time point	164
3.9.	Ratio of Firmicutes to Bacteroidetes for each experimental time point	165
3.10.	Alpha diversity of mouse fecal microbiomes for each experimental time point	166
3.11.	Beta diversity of mouse fecal microbiomes for each experimental time point	167

Figure in Appendices

2.S1.	Diagram depicting design of the pilot study (experiment A) and the black raspberry supplementation with standard and Western basal diets study (experiment B)	187
2.S2.	Food and energy intake, final body weight, final lean and fat mass, and glucose tolerance (experiment A)	188
2.S3.	Rarefaction curve analysis by experimental group and time point (experiment A)	189
2.S4.	Taxonomic classification of mouse fecal bacteria (experiment A)	190
2.S5.	Relative abundance of fecal microbiome at the family taxonomic level (experiment A)	191
2.S6.	Alpha diversity of mouse fecal microbiomes for each experimental time point (experiment A)	193

2.S7.	Food and energy intake over the study period (experiment B)	194
2.S8.	Relative liver, kidney, spleen, and cecum content weights (experiment B)	195
2.S9.	Rarefaction curve analysis by experimental group and time point (experiment B)	196
2.S10.	Relative abundance of selected bacteria families of interest and the ratio of Firmicutes-to-Bacteroidetes over the study time points (experiment B)	197
2.S11.	Fecal microbiome community structures depicted as heat trees showing the relative abundance ratios for comparisons across study time points within each experimental diet group (experiment B)	198
2.S12.	Beta diversity of mouse fecal microbiomes over each time point within each experimental diet group (experiment B)	199
2.S13.	Metagenome predicted functions classified using KEGG metabolism orthology with tax4fun (experiment B)	200
2.S14.	Longitudinal analysis of fecal microbiome taxonomy and functional capacity (experiment B) for AIN and TWD basal diets without BRB supplementation (AIN/CON and BRB/CON groups)	201
3.S1.	Experimental design	211
3.S2.	Relative liver, kidney, spleen, and cecum content weights	212
3.S3.	Rarefaction curve analysis by experimental group and time point	213
3.S4.	Taxonomic classification of mouse fecal bacteria at the phylum level	214
3.S5.	Relative abundance of selected bacteria families of interest over the study time points	215

LIST OF ABBREVIATIONS AND SYMBOLS

Abbreviations

AAALAC	Association for Assessment and Accreditation of Laboratory Animal Care
ACN	Anthocyanin
AIN	American Institute of Nutrition 93G diet
AOM	Azoxymethane
<i>APC</i>	Adenomatous polyposis coli gene
APCs	antigen-presenting cells
ASV	Amplicon sequence variant
BRB	Black raspberry
CAC	Colitis-associated colorectal cancer
CIN	Chromosome instability
CMS	Consensus molecular subtype
CON	Control
COX2	Cyclooxygenase-2
CRC	Colorectal cancer
CRP	C-reactive protein
DAI	Disease activity index
DAMP	Damage-associated molecular pattern
DC	Dendritic cell
DC	Dendritic cells
DMAB	3,2-dimethyl-4-aminobiphenyl
DMH	1,2-dimethylhydrazine
DNMT	DNA methyltransferase
DSS	Dextran sodium sulfate
F:B	Firmicutes-to-Bacteroidetes ratio
FAP	Familial adenomatous polyposis
FDR	False discovery rate
FMT	Fecal microbiota transfer
GB	Gnotobiotic
GIT	Gastrointestinal tract
HP	Histopathology
IBD	Inflammatory bowel disease
IgA	Immunoglobulin A
IL	Interleukin
INF- β	Interferon beta
INF- γ	Interferon gamma
LARC	Laboratory Animal Resource Center
LF/PP	Low-fat, plant polysaccharide
LPS	Lipopolysaccharide
MALT	mucosal-associated lymphoid tissue
MAM	Methylazoxymethanol
MAP	MYH-associated polyposis
MMP	Matrix metalloproteinase
MMR	Mismatch repair
MNNG	N-methyl-N-nitrosoguanidine
MNU	N-methyl-N-nitrosourea
MSI	Microsatellite instability

NK cells	Natural killer cells
NLR	NOD-like receptor
NMDS	Non-metric multidimensional scaling
OTU	Operational taxonomic unit
PAMP	Pathogen-associated molecular pattern
PBS	Phosphate buffered saline
PCA	Protocatechuic acid
PCoA	principal coordinate analysis
PGE ₂	Prostaglandin E2
PhIP	2-amino-1-methyl-6-phenylimidazo-4,5-b-pyridine
PPR	Pattern recognition receptor
RLR	Retinoic acid-inducible gene-like receptor
RNS	Reactive nitrogen species
ROS	Reactive oxygen species
ROUT	Robust outlier test
SCFA	Short-chain fatty acid
SE	Standard error
TAM	Tumor associated macrophage
TGFβ	Tumor growth factor-beta
TIR	Toll/IL-1 receptor
TLR	Toll-like receptor
TWD	Total Western diet
UC	Ulcerative colitis
VEGF	Vascular endothelial growth factors

Symbols

C	Celsius
g	Grams
h	Hour
mg	Milligram
min	Minute
ml	Milliliter
μg	Microgram
μl	Microliter
ng	Nanogram

CHAPTER 1

REVIEW OF THE LITERATURE

1.1 Colorectal Cancer Statistics and Major Risk Factors

After lung cancer and either prostate or breast cancers, colorectal cancer (CRC) is the third leading cause of cancer-related death in the United States [1], with an estimated 52,580 deaths and 106,180 new cases in 2022 [2]. Recently, the National Cancer Institute reported an increase in CRC in young adults 20 to 39 years of age [3]; this increase coincided with a decline in incidence among older age groups, thus lowering the median age of CRC diagnosis to 66 years [4]. CRC disproportionately affects men worldwide, as men are diagnosed with CRC at a rate 44% higher than women, and the mortality rate is 25% higher in men compared to women [5].

Approximately 30% of CRC patients report having a family history of the disease or colon adenomatous polyps in one or more first-degree relatives, resulting in future generations experiencing a 4- to 6-fold higher risk of developing the disease [6]. The presence of other chronic diseases doubles the risk of developing CRC [7], such as obesity, characterized by individuals being excessively overweight, or ulcerative colitis (UC), a type of inflammatory bowel disease (IBD) restricted to the colon mucosa [8]. Various lifestyle factors also increase CRC risk, including lack of exercise, tobacco use, excessive alcohol consumption and poor diet [9]. A meta-analysis reviewed 116 articles and determined a positive correlation between developing colorectal cancer and excess alcohol consumption, family history of colon polyps, presence of inflammatory bowel disease or obesity, smoking and consumption of red meat [10].

A combination of these factors can further increase CRC risk as a global epidemiological review reported up to 50% higher CRC risk when an individual combines a sedentary routine with a high body mass index (BMI) [11]. Additionally, patients diagnosed with IBD have a 2.93-fold greater risk of developing CRC compared to healthy controls, suggesting the importance of gut

inflammation in the etiology of CRC [10]. Several factors were correlated with a decrease in CRC risk including whole food consumption, physical activity and aspirin use.

The 5-year survival rate for CRC patients is 90%, contingent on early detection of disease and mass localization. As the disease advances, the probability of survival decreases to 70%, depending on the regionality of the mass; survival rates fall to 15% for patients with metastatic disease [12]. Furthermore, CRC survival rates are disproportionately lower in individuals from low socioeconomic and poorly educated communities [9]. Patients with CRC normally require surgery and chemotherapy as treatment for all stages of the disease and endure the second-highest expenditure in clinical oncology [13]. In addition, cancer survivors lose an average of \$1,000 annually due to reduced work productivity originating from an increase in disease-related sick days and employment disabilities [14]. Detection of CRC in younger age groups, poor survival rates for those diagnosed with advanced disease, the high financial burden and a variety of modifiable behaviors support research efforts focused on developing preventative strategies to combat colorectal cancer.

Colorectal cancer occurs in the large intestine with approximately 60% developing in the colon and 38% in the rectum [15]. As the largest section of the intestine, the colon tissues facilitate water and electrolyte absorption and the secretion of mucus to maintain the protective mucus layer. Microorganisms, especially bacteria, inhabit this mucus layer and are essential for the degradation of undigested dietary material. The colon intestinal wall is composed of four layers including the serosa, muscularis, submucosa and mucosa; the mucosa is in direct contact with the colon lumen and its components [16]. The mucosa layer is divided into inner and outer layers. The outer mucosal layer creates an environment ideal for microorganism attachment and survival which in turn provides generous amounts of vitamins and other micronutrients, regularly absorbed by the host. On the other hand, the inner layer is highly dense and provides a protective barrier between host cells and foreign microorganisms [17]. Disruption of the colonic

microenvironment can trigger a low-grade inflammatory response similar to the chronic low-grade inflammation described in other tissues of patients with other non-communicable diseases including type 2 diabetes, cardiovascular disease, depression, autoimmune diseases, neurodegenerative disease, osteoporosis, immunosenescence and cancer [18].

CRC takes years to progress due to all the oncogenic modifications the colonocytes must sustain to reach a balance with the microenvironment necessary for survival, giving rise to various windows of opportunity to develop preventative therapeutics [19]. Preventative therapies for CRC may target carcinogenesis at different stages of the cell cycle to prevent the initiation of cell proliferation and block the progression of cell growth or before the development of metastasis. A general example is the consumption of non-steroidal anti-inflammatory drugs (NSAIDs) to reduce inflammation in the colon of humans and animal models [20].

The risk of developing CRC during a lifetime in the general population is as low as 5%; however, up to 30% of all CRC patients have a family history of polyps or cancer [21]. Furthermore, only about 5 to 10% of colorectal cancer burden is inherited in an autosomal dominant nature [22]. Subtypes of heritable CRC include familial adenomatous polyposis (FAP) and MYH-associated polyposis (MAP) characterized in 1% of CRC patients and lynch syndrome characterized in 3% of CRC patients [23]. Approximately 88-94% of CRC develops spontaneously via chromosome instability (CIN), which affects 65% of CRC cases, or microsatellite instability (MSI) pathways, affecting 15% of CRC cases and described in patients with Lynch syndrome [24].

1.2 Molecular Aspects of Colorectal Cancer

1.2.1 Cancer-Critical Gene Pathways

In 1990, Fearon and Vogelstein [25] proposed the multi-hit model of carcinogenesis, which requires multiple mutations for the disease to progress from an initial mutating event to the development of neoplasia and ultimately cancer. The multi-hit model describes how new

mutations (“hits”) can confer new capabilities on the neoplastic cells. Tumor development requires that neoplastic cells acquire the capacity for prolonged survival, evasion of growth suppressors and immune responses, constant proliferation, induction of angiogenesis and replicative immortality. Ultimately, as the disease progresses, neoplastic cells become cancerous and acquire the ability to invade surrounding tissues, ultimately establishing metastases at distant locations within the body [26]. Cancerous cells have the ability to constantly multiply by producing growth factor ligands that stimulate cell proliferation via autocrine or paracrine signaling [27]. Tumor cells have a higher expression of growth factor protein receptors, which also stimulates sustained cell proliferation [28]. Mutations in genes responsible for activating the negative feedback loop, such as the Ras GTPase, which regulates active Ras signaling, lead to uncontrolled cell proliferation [26]. Another cancer-critical pathway involves *PTEN*, which functions as a tumor suppressor gene by controlling PI3K signaling pathways; loss-of-function mutations in *PTEN* can lead to inappropriate activation of PI3K signaling and aberrant cell growth and survival [26]. Transcription factor protein p53, considered the guardian of the genome, regulates cell proliferation by activating senescence, arresting cell growth or initiating apoptosis through intrinsic (mitochondrial pathway) or extrinsic mechanisms (death receptor-induced apoptotic pathways) [29]. In CRC, *TP53* is mutated in 43% of tumors, normally observed as missense mutations, resulting in loss-of-function of p53 which promotes cancer cell proliferation [30]. DNA damage, growth factors, hypoxia, oncogene activation, nutrient deprivation and oxidative stress are some of the stress signals that normally stimulate cell cycle arrest by activating the apoptotic functions of p53 [31].

Neoplastic cells must send molecular signals that avoid apoptosis (*e.g.*, P53) or that promote cell proliferation (*e.g.*, TGF β) [26]. Tumor cells avoid apoptosis through various pathways including loss-of-function mutations in proteins, such as P53, or an increase in the expression of antiapoptotic proteins, such as BCL-2 and BCL-X_L. Additionally, reduced

expression of proapoptotic proteins including BAX, CIMA and PUMA, enhances the secretion of survival proteins such as IGF1/2 [26]. Likewise, tumor cells must escape replicative senescence by the preservation of telomeres, known as regions of repetitive nucleotide sequences that normally protect chromosome ends. In a healthy cell, telomeres shorten with every cell replication until their complete loss signals for cessation of cell divisions. Cancer cell survival often requires upregulation of telomerase activity, which elongates short telomeres and permits constant cell growth [32]. Finally, as tumor cells grow and multiply, cells require higher quantities of available nutrients and oxygen which triggers the formation of new blood vessels. Activation of matrix metalloproteinase genes involved in the inflammatory response and remodeling of the extracellular matrix (*e.g.*, *MMP9*) are implicated in angiogenesis regulation including vasculogenesis and lymphangiogenesis. *MMP9* activation promotes endothelial cell migration and can be induced by angiogenic factors such as vascular endothelial growth factors (VEGF), also releasing VEGF during carcinogenesis [33,34]. As the tumor microenvironment stabilizes for cell replication and invasion, the tumor cells must also evade identification by the immune system. Furthermore, the interaction between tumor-promoting cells and the immune system can be influenced by the gut microbiome population, as discussed below.

1.2.2 *Wnt/β-Catenin Pathway*

In 2012, a comprehensive characterization of CRC found that up to 80% of tumor tissues expressed mutations in the adenomatous polyposis coli (*APC*) gene, while 93% had altered Wnt signaling pathways [35]. Mutations in the *APC* gene are responsible for the FAP phenotype and maintain an essential role in sporadic cancer development in connection to the Wnt pathway. While APC proteins participate in various cellular functions including cell adhesion and migration, signal transduction, assembly of the mitotic spindle and chromosome segregation, the main cancerogenic role seems to come from its capacity to regulate β-catenin levels [36]. Wnt signals normally regulate the activation of genes critical for cell proliferation and cell cycle, such

as *MYC* and *CCND1* [37]. Two Wnt pathways exist, the β -catenin independent non-canonical pathway responsible for cell movement during morphogenesis [38] and the canonical β -catenin dependent pathway, notably studied for its complexity. β -catenin is regularly destroyed by a protein complex via phosphorylation and ubiquitination resulting in proteasome degradation [39]. Activation of the Wnt signaling pathway prevents the complex from forming, which grants β -catenin access to translocate to the nucleus, further activating and silencing target genes [39].

1.2.3 Chromosome Instability Pathway

The majority of CRC cases are characterized by chromosomal instability (CIN), a type of genome instability in which whole chromosomes or portions of chromosomes are either lost or duplicated. Colon tumors that initiate via the CIN pathway are regularly characterized by base deletions or insertion or the loss of chromosomal heterozygosity [40]. Karyotypic irregularities coupled with mutations initiate tumorigenesis by activating oncogenes (i.e., *KRAS* and *BRAF*), and silencing tumor suppressor genes (i.e., *APC* and *TP53*) [41]. As CRC advances, mutational inactivation of the *APC* gene is generally followed by an accumulation of mutated genes including *KRAS*, *PI3K*, *SMAD2*, *SMAD4*, and *TP53* [42]. CIN tumors develop in this stepwise manner, as the cell takes multiple hits [41]. A tumor that develops through the CIN pathway typically acquires mutations in the *APC* gene early on in disease development [41]. The *APC* gene is responsible for regulating cell growth [36]. Next, mutations in the oncogene *KRAS* lead to aberrant cell proliferation [41]. Finally, the inactivation of the tumor suppressor gene *TP53* is observed in the advanced stages of CIN tumors [41]. Moreover, the *TP53* gene is commonly mutated in various cancer types and has been correlated with early-onset CRC [43]. The loss of function of tumor suppressor genes requires a bi-allelic loss. Common genes normally mutated in spontaneous cancer include *TP53*, *APC*, and *DCC/SMAD* [44]. Various molecular mechanisms controlling mutation, activation or deactivation of critical pathways involved in cancer

development are being studied giving way to therapeutic opportunities for preventing CRC initiation.

1.2.4 Microsatellite Instability

Microsatellites are short, repetitive segments of DNA scattered through non-coding regions of the genome. Microsatellite instability is caused by mutations in DNA mismatch repair (MMR) genes, such as *MLH1*, *MSH2*, *MSH6*, and *PMS2* [45]. Normally, MMR proteins function to repair errors that occur during normal DNA replication. However, mutations in the MMR pathways can lead to the replication of improperly matched DNA and the accumulation of sequence errors that result in further genetic irregularities [46]. Tumors that develop via the MSI pathway express higher mutations in the *BRAF* gene and fewer abnormalities in *APC* and *TP53* genes, which are typically mutated in tumors arising from chromosome instability pathways [47]. Most MSI tumors have mutations in the *TGFBR2* gene that cause structural changes in the receptor, thus preventing the binding of its ligand [48]. Appropriate binding of TGF β to its receptor induces cell death by apoptosis; however, the mutation-induced aberrant structure of this receptor can lead to upregulation of cell proliferation [49]. Tumors originating via MSI are reported in relatively fewer patients, although these tumors develop more rapidly than the alternative CIN pathway. Excess MSI in colon tumors is associated with a hypermutable environment and shorter progression time, with the disease developing in a few years as compared to a few decades in patients without MSI [24]. Cases of CRC characterized by MSI typically have a favorable prognosis due to highly successful immune checkpoint co-inhibitory drugs targeting the programmed cell-death receptor 1. These drugs outcompete the natural tumor ligand that suppresses T-cell activity leading to reactivation of T-cell effects promoting antitumor immune response [19].

1.2.5 CpG Island Methylator Phenotype

Another distant molecular subtype of CRC is the CpG island methylator phenotype (CIMP). CpG islands are clusters of cytosine and guanine linked by a phosphate located in promoter regions of genes. Hypermethylation by DNA methyltransferase (DNMT) causes epigenetic silencing of these CpG-rich regions [50]. Hypermethylation of CpG islands inactivates tumor suppressor genes, such as *MLH1*, leading to CRC development. Silencing of CpG island in combination with mutations of oncogenes *BRAF* and *KRAS* results in abnormal mass formation [47].

1.2.6 Molecular Subtypes of Colorectal Cancer

In 2015, the College of American Pathologists declared four consensus molecular subtypes (CMS) of CRC with differing features, as follows: 1) CMS1 present in 14% of all cancer described as MSI immune pathway, demonstrates hypermutation, deficient MMR, microsatellite instability and strong immune activation; 2) CMS2, present in 37% of cancers, is characterized as the canonical pathway revealing high chromosomal instability, and WNT and MY signaling activation; 3) CMS3, present in 13% of cancer, is considered the metabolic pathway that exhibits KRAS mutations and metabolic dysregulation; and 4) CMS4, present in 23% of cases, known as the mesenchymal pathway, presents with CpG hypermethylation, TGF β activation, angiogenesis and stromal invasion [44].

1.3 Immune System, Inflammation and Cancer

1.3.1 Colitis-Associated Colorectal Cancer

Approximately 20% of all cancers can be linked to pre-cancerous inflammation [51], and CRC is no exception as chronic inflammation of the colon is a major contributing factor to the development of this disease. An estimated 3 million people suffer from IBD in the U.S., including patients diagnosed with UC and Crohn's disease, resulting in an overall healthcare cost of more

than \$1.7 billion [52]. IBD patients with prolonged colitis, pan-colitis or severe intestinal inflammation are at high risk for developing CRC [53,54].

The progression of both spontaneous CRC and colitis-associated CRC (CAC) occurs in a dysplasia-adenoma-carcinoma sequence [55] requiring multiple (epi)mutations and chromosomal instability as outlined above. However, in colitis-associated disease, these mutations generally occur at a faster pace, more frequently and in an apparently different sequence with respect to spontaneous CRC. Importantly, inflamed colon mucosa tissues exhibit abnormalities in cancer-critical pathways before these tissues show signs of dysplasia or cancer, with elevated oxidative stress a likely major contributing factor. For example, reactive oxygen (ROS) and nitrogen species (RNS) can lead to aberrant signaling of P53, DNA mismatch repair proteins, and methylation pathways [56]. Importantly, in CAC, mutations to *TP53* often precede the loss of APC function, which normally occurs later in the progression of the disease [53].

Proinflammatory pathways involved in the pathogenesis of colitis-associated tumor initiation include COX2/PGE2, NF κ B, IL6/STAT3, and IL23/Th17 signaling pathways providing inflammatory mediation and influence over the tumor microenvironment [57]. The tumor microenvironment is composed of tumor stem cells, extracellular matrix, fibroblasts, lymphocytes, tumor-infiltrating macrophages, and local microbiota which maintain constant communication with each other [58]. The diverse cells within this microenvironment communicate through an autocrine or paracrine manner via chemokine and cytokine production providing structure and control of tumor growth [51]. Thus, the acceleration of cancer progression in colitis-associated cancer is likely a consequence of high levels of inflammation and the consequent increase in cell proliferation rate that is pervasive in the colon mucosa.

Endogenous ROS, a subset of free radicals, are primarily produced from the mitochondrial respiratory chain and organelles, such as the endoplasmic reticulum, peroxisomes, and the nucleus, via electron leakage for biological defense against pathogenic agents [59].

Reactive oxygen species, including superoxide (O_2^-), hydroxyl radical (OH^\bullet), peroxy (ROO^\bullet), alkoxy (RO^\bullet), and hydroperoxy (HOO^\bullet), potentially damage protein structures, lipids, and DNA through oxidative reactions [60]. Oxidative stress, or overproduction of reactive species, contributes to the development of IBD and subsequent tumor formation via damage to the mucosal layer of the colon increasing membrane permeability, granting pathogenic and opportunistic bacteria access to epithelial cells, and enhancing immune response [61,62].

1.3.2 Immune Signaling Pathways and Cancer

The immune system of mammals consists of a network of cells responsible for the prevention, elimination and removal of pathogenic bacteria, toxins, viruses and damaged tissue, among others. The immune system can be divided into two components: 1) innate immunity, a defense mechanism consisting of physical barriers and non-specific front-line immune cells and other molecules that attack invaders within hours, and 2) adaptive immunity, a specific and long-term recognition defense mechanism [63]. Various front-line immune cells reside throughout the body including neutrophils, basophils, eosinophils, natural killer cells (NKs), mast cells and sentinel cells. Sentinel cells, such as monocytes, macrophages and dendritic cells (DCs), function to recognize pathogens and damage tissue initiating an immune response. Sentinel cells can be found in various tissues mainly in places of high infection risk, such as the mucosa of the lungs and gut. Macrophages, dendritic cells and mast cells express pattern recognition receptors (PRRs). Four subtypes of PRRs have been identified including membrane-bound toll-like receptors (TLRs), C-type lectin receptors, cytosolic NOD-like receptors (NLRs) and retinoic acid-inducible gene-like receptors (RLRs) [64]. These receptors recognize molecular patterns such as bacterial antigens known as pathogen-associated molecular patterns (PAMPs) and endogenous danger signals molecules released by host cells recognized as damage-associated molecular patterns (DAMPs) [65].

Of particular interest, TLRs are expressed in innate immune cells, including DCs and macrophages. TLRs are transmembrane receptors localized on the cell surface that recognize bacteria-derived lipopolysaccharides (LPS), as in the case of TLR4. Most toll-like receptors share the same immunological pathway which activates transcription factors such as NF κ B, AP1 and interferon beta (IFN β) [66]. Activation of TLR2, TLR4 or TLR6 leads to recruitment of the toll/IL-1 receptor (TIR) domain-containing adaptor protein MyD88 to the intracellular domain of the receptor, triggering an intracellular signaling pathway which leads to NF κ B activation and induction of gene expression for a variety of inflammatory cytokines [67]. Activation of the NF κ B signaling pathway first requires inactivation and degradation of its inhibitor I κ B kinase (IKK), which then allows for translocation of active NF κ B to the nucleus where this transcription factor induces transcription of *TNF*, *IL6* and *IL1*, among others [68]. TNF α binds to the TNF receptor and induces the production of free radicals and proangiogenic chemokines [69,70]. NF κ B activated IL6 recruits and phosphorylates Jak2 which mediates STAT3 and then proceeds to enhance apoptotic expression of BCL2 and BCLX_L, which stimulate cell survival and proliferation [71]. IL6 also activates RAS/ERK and PI3K/AKT pathways leading to increased cell proliferation and survival [71]. Moreover, TGF β signals reduce IL6 secretion and inhibit tumor development. Contrarily, the suppression of TGF β signals promotes IL6 secretion which activates STAT3 encouraging tumor growth [72]. CRC patients have high levels of serum IL6 [73] and express mutations in TGF β receptor II (TGF β 2) [74]. Normally, the activation of TGF β 2 receptors promotes the phosphorylation of SMAD2/3 which then binds with cytosolic SMAD4. The SMAD complex then translocates to the nucleus and is involved in cell growth regulation and development [75]. Furthermore, IL6 activates peroxisome proliferator-activated receptor gamma (PPAR δ) through the PI3K/Akt signaling pathway, which is a downstream target of the COX2/ PGE₂ pathway that contributes to inflammation via a self-amplifying loop [57]. High levels of IL6 expression in macrophages, DCs and T-cells are observed in the murine model of

CAC during tumor formation [76]. Furthermore, interleukin 1 (IL1) family cytokines bind to IL1 receptors, which also harbor TIR intracellular domains and similarly activate the MyD88/IRAK/NF κ B pathway leading to cell survival and proliferation [77,78].

The immune system responds to cancer cells similar to viral infections. Three ways the immune system interacts with tumor cells include: 1) elimination of the tumor cells; 2) greater elimination of highly immunogenic tumor cells while low immunogenic tumor cells survive; or 3) tumor cells are completely unaffected by the immune system [79]. The immune response depends on whether the tumor antigens are recognized as self or non-self peptides. Sentinel cells recognize tumor antigens either through a foreign, mutated peptide, reactivation of embryonic cells which are not normally expressed in adult cells or overexpression of a self-peptide. Examples of this include the overexpression of large transmembrane mucin glycoprotein 1 (MUC1) in adenocarcinomas compared to healthy tissue [80]; or through neoantigens that originate from mutations in regulatory oncogenes and tumor suppressor genes (*KRAS*, *BRAF*, *TP53*, *PIK3CA*) [81]. Otherwise, cells can express MICA/B proteins which function as stress ligands for NKs and gamma-delta T cells ($\gamma\delta$ -T cells) [82]. During immunosurveillance, neoantigens and DAMPs amplify the innate immune response, recruiting effector cells via cytokine secretion, including IL1 and TNF α [83]. Macrophages and DCs engulf tumor cells through phagocytosis. While NKs secrete interferon-gamma (IFN γ), a pluripotent antitumor cytokine [84], which creates a positive feedback loop that recruits more NKs and activates macrophages. Macrophages can be activated into two functional states. M1 macrophages are classically activated macrophages by IFN γ and TNF α , which produce proinflammatory and immunostimulatory cytokines such as IL12 and IL23. M1 macrophages find and destroy phagocytosed tumor cells and stimulate T-cell type 1 response. Contrarily, M2 macrophages are activated by cytokines IL4 and IL10 and are considered tumor-associated macrophages (TAMs) [85]. After macrophages and DCs phagocytize tumor cells and process tumor antigens, they activate T and B lymphocytes by presenting these antigens via major

histocompatibility complex I or II (MHC-I/II). These antigen-presenting cells (APCs), which are mainly DCs that contain higher quantities of MHC-peptide complex and costimulatory compounds, travel to secondary lymphoid organs such as the lymph nodes, spleen and mucosal-associated lymphoid tissue (MALT). In lymphoid organs, naïve T-cells are activated into effector cells. CD4 T-cells are activated by exogenous antigen presentation via MHC-II and function as helper T-cells that recognize pathogens and trigger cytokine production. Whereas, endogenous antigens are presented to naïve CD8 T-cells via MHC-I, which differentiates into cytotoxic T-cells that can directly kill infected cells [86]. Additionally, when B cells encounter antigens, they can differentiate into memory cells or plasma cells that secrete immunoglobulin A in the colon mucosa [87].

Tumor cells need to not only evade immunosurveillance but also undergo immunoediting for prolonged survival [88]. Immunoediting is characterized as tumor cells maintaining low immunogenicity in the tumor microenvironment. Further, cells that survive this equilibrium phase evolve to the escape phase in which tumor cells can proliferate without immune recognition [89]. Tumor-infiltrating macrophages can reprogram the tumor microenvironment into an immunosuppressive state promoting cell proliferation, invasion and metastasis. In addition, colon infiltration of TAMs activates the expression of cyclooxygenase-2 (COX-2), which in turn generates prostaglandins (mostly prostaglandin E2) from arachidonic acid [90]. Prostaglandins modulate several different cell signaling pathways via activation of specific membrane-bound G-protein coupled receptors (EP1, EP2, EP3 or EP4), ultimately leading to modulation of multiple cancer critical pathways (e.g., mitogen-activated protein kinase pathways, β -catenin signaling, AKT pathways, etc.) [91-94]. For example, prostaglandin E2 (PGE₂) mediates COX2 in the development of IBD and CRC by acting through cell surface receptors, primarily EP1 and EP3 [95]. Then PGE2 induces expression of CXC motif ligand 1 (CXCL1), a proangiogenic chemokine that promotes microvascular tube formation and tumor growth [96]. COX2

contributes to cell survival by inducing antiapoptotic protein production such as BCL2 and elevated levels of MMPs, which increases malignant cell migration [97]. The high proliferative state of cancer cells requires high nutrient intake, which deprives nearby healthy cells of access to these essential components to support their own metabolism and growth, allowing tumor cells to outcompete. In addition, cancer cells accumulate a high waste load and decrease locally available oxygen. Locally high hypoxia lowers acidity, which forces infiltrating immune cells to endure metabolic changes and promote tolerant phenotypes [98].

Although in most cases the specific cause of colitis is unknown, viral, parasitic and bacterial infections can influence colitis symptoms. Rutter, et al. [99] made the critical observation that recovery from colitis in IBD patients restored their CRC risk level to that of the general population. Thus, intervention strategies to reduce colonic inflammation could markedly reduce the risk of progression to CRC. Due to the enhanced inflammatory response associated with IBD and CRC, anti-inflammatory therapeutics provided insight into possible prevention strategies against these non-communicable diseases. Examples of nonsteroidal anti-inflammatory drugs used as therapeutics for IBD and CRC, inhibit COX2. Upregulation of COX2 enhances growth factors and secretion of proinflammatory cytokines [100]. In IBD patients, COX2 overexpression is observed during active inflammation and inflammatory-associated dysplasia in the colon [101]. Additionally, the expression of COX2 was elevated in up to 85% of CRC patients [97]. Finally, as reviewed by Gupta and Dubois, there is substantial evidence from murine models of intestinal neoplasia that use of a COX2-selective inhibitor or deletion of the COX2 gene suppresses colorectal cancer cell growth [97].

1.4 The Gut Microbiome

1.4.1 The Gut Microbiome and Gut Homeostasis

The intestinal tract is unique in that its structure consists largely of a continuous tube within the body that encounters the external environment, thus making these tissues vulnerable to

pathogens and toxins. The intestinal barrier system consists of several components, including a physical barrier (mucosal layer) that harbors protective proteins, such as antibacterial peptides and immunoglobulin A (IgA). Further, intercellular tight junctions regulate the absorption of dietary components via intra- and extracellular signals [102]. Particles can cross the epithelium via passive permeability, transcellular transport, or extracellular transport through tight junction regions between epithelial cells [103]. Tight junctions consist of transmembrane proteins including claudin, occludin, tricellulin and junctional adhesion molecule-A [103]. Goblet cells in the epithelial layer secrete mucus to form a thick protective layer known as the mucus layer. This mucus layer provides a surface for immunoglobins and peptides to attach, which functions to prevent bacterial contact and cellular translocation. In a healthy patient, maintaining a strong epithelial barrier is essential to maintain gut homeostasis and protect from pathobionts in the gut lumen. Impairment of the intestinal barrier can result in leaked toxins and microbial fermentation byproducts from the colon lumen into the body. Weakening of the intestinal barrier leads to irregular barrier function, intestinal inflammation and high gut permeability. Chronic gut leakiness is linked to gut inflammatory diseases [104].

The microbiome is a vast collection of microorganisms that live in association with the human body, including bacteria, viruses, fungi and protists that reside on various surfaces, such as the skin, mouth, nose, lung, gastrointestinal tract and genital tract [105]. The microbiome of the gastrointestinal tract is the most populated and diverse microbial niche associated with the human body. The gut microbiome includes more than a trillion microorganisms with over three million accumulated genes among them, 150-fold more than the human genome [106]. The human gut microbiome is composed of more than 50 phyla with Firmicutes, Bacteroidetes, Actinobacteria and Proteobacteria as the most dominant, composing 90% of the total microbial population [107]. The National Center for Biotechnology Information recently renamed these phyla as Bacillota,

Bacteroidota, Actinomycetota and Pseudomonadota, respectively, to improve systemic taxonomic nomenclature [108].

Gut microorganisms maintain communication with the host via bacteria-derived metabolites or through immunologic and endocrine signals. In a state of homeostasis, the microbiome-host relationship is mutually beneficial, as microorganisms are provided with undigested nutrients and the host is provided with fiber derived-short chain fatty acids (SCFAs), anti-inflammatory lipids and microbially derived vitamins, such as K and B [109,110]. SCFAs influence numerous cellular processes, such as histone acetylation, histone acetyltransferase, epigenetic mechanisms and hormone release, while also providing energy for colonocytes [111,112]. Moreover, the gut microbiome maintains bidirectional communication with the host through the vagus nerve, called the brain-gut axis, which influences the host's mood and other nervous system disorders [113]. The continuous interaction between the gut microbiome and host epithelial cells is tightly regulated by a combination of secreted antimicrobial peptides such as regenerating family member 3 gamma (Reg3 γ), and mucosal IgA harbored in the inner mucosa layer [114]. The goblet cells in colon epithelial secrete MUC2 which creates a protective inner barrier impenetrable to bacteria [115]. The presence of microbes is necessary for the mucus layer to achieve mature structure and function. The mucosa layer is essential in host-microbiota interaction and the host's innate immune system [115].

Mammals have minimal to no interaction with microorganisms before birth. In utero, the fetus is isolated within the mother's womb from most environmental microbes and will experience its first major exposure at birth. This exposure helps to kickstart the newborn's immune, metabolic, hormonal and nervous systems [116,117]. Newborns birthed through the vaginal canal harbor large numbers of *Lactobacillus spp.* and *Bifidobacterium spp.*, both considered to be probiotics, which are bacteria that promote health and gut homeostasis [118]. Conversely, neonates born through cesarean section are first colonized with microbial populations

predominated by species belonging to the *Staphylococcus* genus, a skin-related microbial family. Cesarean births are associated with a higher risk of immune-related disorders later in life [119]. A newborn's microbiome fluctuates during the first three years of life, ultimately reaching an equilibrium that remains relatively constant unless affected by external factors [120]. During the first months of life, breast milk positively influences infant development and health. Breast milk is composed of an ideal balance of immunoglobins, hormones and oligosaccharides [121]. Human milk oligosaccharides modulate the immune system due to anti-adhesive properties and influence the gut flora by stimulating levels of *Bifidobacterium* species, known to promote a healthy gut microbiome [121]. The diversity of the colon microbiome can be influenced by other external factors as the infant develops, such as living in rural versus urban settings, the presence of disease, the use of antibiotics and the child's diet [118].

1.4.2 Dysbiosis of the Gut Microbiome

Patients suffering from diseases characterized by chronic inflammation, such as obesity, metabolic syndrome, CRC or IBD, present with a less diverse microbiome compared to healthy individuals [122]. A disruption to healthy microbial communities leads to dysbiosis, an imbalance in microbial populations that is associated with persistent inflammation, pathobiont invasion and systemic disease [123,124]. Cross-sectional studies found that obese individuals had a higher Firmicute-to-Bacteroidetes ratio compared to lean individuals [125]. However, a meta-analysis found that studies correlating obesity with microbial communities had weak associations due to confounding factors such as sample size and interpersonal variations [126]. Individuals with type 1 diabetes have a high abundance of Bacteroidetes, whereas type 2 diabetics have more Proteobacteria and Firmicutes resulting in high quantities of SCFA production and increased energy harvest [107]. The intestinal microbiome of patients with IBD or CRC differs from healthy individuals in a variety of ways, including reduced gut microbial load, decreased diversity, increased pro-inflammatory taxa, and alterations in the relative abundance of certain

taxa [127-129]. A decrease in general microbial diversity and an increase in abundance of specific taxa such as Enterobacteriaceae, Bacilli, Erysipelotrichaceae and Streptococcaceae, all belonging to the Firmicutes phylum, is reported in the gut microbiome of IBD and CRC patients [130]. Aside from general microbial profile shifts, overpopulation or depletion of certain taxa has also been closely associated with non-communicable diseases [122]. Furthermore, the microbiome of healthy tissues is different than tumor tissue at different developmental stages of CRC giving light to the interaction between the gut microbiome and disease progression [131].

Repeated insult, whether by consumption of a nutritionally deficient diet or long-term antibiotic exposure, can degrade the mucosal layer by decreasing MUC2 production, secretion and viscosity creating an unfavorable environment for existing taxa [132]. The reduction of beneficial bacteria species grants pathogenic and opportunistic bacteria a chance to overpopulate. Overpopulation of proinflammatory bacteria enhances the inflammatory response which causes further loss of epithelial function and consequent high cell turnover [124]. In the colon, gut microbiome composition directly influences the activation of certain transcription factors that promote uncontrolled cell proliferation, facilitate evasion of apoptosis and induce inflammatory cell infiltration. Jointly these factors promote a chronic inflammatory microenvironment that is ideal for tumor development [133]. An association was found among host cells, host immune system and gut microbiome (and metabolites), all of which have a dynamic role in tumor microenvironment modulation [58].

Bacteria species drive colitis and other hallmarks of cancer by activating various pro-inflammatory cytokine production and metabolic pathways. Secretion of pro-inflammatory cytokines IL6, IL17 and IL22 are involved in the activation of NF κ B and STAT3 which increases cell proliferation, and anti-apoptosis proteins BCL2 and BCLX_L, essential for cell survival [134]. Ablation of bacteria-sensing TLR 2, 4, and 9 and their signaling adaptor MyD88 reduced inflammatory cytokine production; this finding supports the hypothesis that bacteria are drivers of

tumor-promoting inflammation when the bacterial surface barrier is compromised [135]. In addition, changes in the environment increase the abundance of some bacteria that overproduce genotoxins (e.g., colibactin from *Escherichia Coli*) or detrimental metabolites (i.e., secondary bile acids or hydrogen sulfides broken down from diet) that lead to DNA damage in epithelial cells and activation of Wnt/ β -catenin oncogenic signals [136].

Due to the high connection between CAC and IBD, it has been argued that pro-inflammatory bacteria may be linked to colon tumorigenesis [137]. Martin et al. observed high proportions of Proteobacteria and a low abundance of Bacteroidetes, coupled with increased Enterobacteriaceae abundance in IBD and CRC patients compared to healthy individuals [138]. Furthermore, mucosa-associated adhesive-invasive *E. Coli* strains can invade the mucosa and create cancer-driving ROS [139]. Additionally, *Enterococcus faecalis*, part of the Firmicutes phylum observed in high levels in CRC patients, promotes colon inflammation via expression of TGF β in intestinal epithelial cells leading to activation of SMAD signaling pathways [140,141]. In vitro, *E. faecalis* has been observed to generate extracellular superoxide and hydrogen peroxide. ROS species induce DNA damage and increase mutations rate by upregulation of COX2 [142]. In a cross-sectional study that characterized bacteria adherent to adenomas compared to healthy tissue, researchers found a greater abundance of *Dorea spp.* and *Faecalibacterium spp.* species and decreased *Bacteroides spp.* and *Coproccoccus spp.* abundance which increased the firmicute to Bacteroidetes ratio [143]. Associated with later stages of CRC, enterotoxigenic *Bacteroides fragilis* (ETBF) produces toxins that cleave to E-cadherin proteins and induce IL17 production [144,145]. Finally, *Fusobacterium* seems to be a key factor in the colon tumor microenvironment as various strains are associated with primary tumors and metastasis of colorectal cancer [146]. A 10-15% increase in *Fusobacterium nucleatum* has been observed in various stages of colorectal cancer development [147]. High quantities of this taxa are associated with high recurrence risk and decreased survival rates [147]. A connection between

F. nucleatum and abnormal molecular features, including mutation in the *BRAF* gene and other key mutations suggests that this taxon contributes to CRC development [148]. *F. nucleatum* selectively binds to E-cadherin and then activates β -catenin signals within the colonic epithelium which upregulate the expression of oncogenic and pro-inflammatory genes in mice and humans [149]. *F. nucleatum* is associated with IL17A and TNF α production, both of which have proinflammatory properties [150].

The knowledge gap lies in whether microbial shifts are a cause or consequence of inflammatory disease development. In other words, is the tumor microenvironment providing a hospitable environment for certain bacteria to colonize and thrive or is gut dysbiosis promoting inflammation and early neoplasia? A variety of therapeutic strategies have been studied to alter the composition and, hence, the function of the gut microbiome. These strategies include prebiotics (substances that promote the growth of certain bacteria), probiotics (bacteria that support gut health), postbiotics (nutrients and antimicrobial peptides that slow the growth of harmful bacteria), antibiotics (drugs that kill certain bacteria) and fecal microbiota transfer. Interventions with *Lactobacillus* and *Bifidobacterium* species have been shown to reduce levels of pro-inflammatory cytokines, increase bacterial diversity and reduce CRC-associated taxa [151,152]. Additionally, alterations of the gut microbiome happen concurrently with inflammation onset revealing a great capacity for the gut to recover homeostasis in a longitudinal IBD mice model [153]. Sharpton et al., observed similar significant changes in the taxonomical and functional structure of the gut microbiome during IBD development in an established mouse model correlating with immune activation [154]. These studies, as well as numerous others, suggest that strategies to manipulate the gut microbiome may lead to favorable outcomes, however, further evaluation of potential risks is needed.

1.5 Animal Models for Gut Inflammation, Cancer, and the Microbiome

1.5.1 Models of Gut Inflammation

Laboratory rodents are the most common animal models for experimental research due to physiological and genetic similarities to humans, accessibility and minimal husbandry requirements. Different models are developed to mimic disease progression. IBD rodent model types include chemical induction, cell transfer, spontaneous, congenital and genetically engineered models. Genetically engineered mice can overexpress or lack certain genes critical in inflammatory signaling; for example, *IL10*^{-/-} mice and *STAT3*^{-/-} are knock-out models used to study IBD susceptibility genes [155]. IL10 is a regulatory cytokine that, when knocked out, mice spontaneously develop colitis at three months of age. Nucleotide-binding oligomerization domain containing 2 (NOD2) was the first susceptibility gene for Crohn's disease discovered in 2001. Mice deficient in NOD2 receptors were found to be in gut dysbiosis and experienced severe colitis [156]. More recently, a large-scale genetic study employed data from 75,000 individuals with onset IBD and identified 163 loci susceptible to IBD, of which 23 were unique to UC [157]. In addition to knockout models, chemical models are common in IBD research, such as the administration of dextran sodium sulfate (DSS). DSS is a polymer of sulfated polysaccharides that induces acute intestinal injury characterized by shortening of colon length, inflammation, tissue loss, ulcerations and bloody stool. Administration of DSS in drinking water is documented at various concentrations, from 1% to 5% (v/v), with varying time intervals of administration [158]. C3H/HeJ mice have previously been observed to be more susceptible to DSS treatment compared to other strains, such as the C57BL/6, while males tend to be more vulnerable compared to females [155,159]. In contrast to most of the IBD models, chemically induced models allow for an opportunity to follow the recovery process, including regulatory immune cell development necessary for healing. While this chemical model of colitis is convenient and

recapitulates many features of ulcerative colitis in humans, the variable protocols employed in pre-clinical experiments in rodents may complicate comparisons across studies.

1.5.2 Models of Colorectal Cancer

Rodent models for CRC include spontaneous, chemically induced, syngeneic and xenograft models (reviewed in [160]). The use of a chemically induced model of intestinal cancer in rodents was first reported by Lorenz and Stewart in 1940 [161]; in this work, researchers used chemical carcinogens dibenzanthracene or methylcholanthrene resulting in the development of adenocarcinomas in the small intestine. Various chemical models of CRC have been developed since, including use of 3,2-dimethyl-4-aminobiphenyl (DMAB); alkylnitrosamines such as N-methyl-N-nitrosourea (MNU) and N-methyl-N-nitrosoguanidine (MNNG); 1,2-dimethylhydrazine (DMH), azoxymethane (AOM), and 2-amino-1-methyl-6-phenylimidazo-4,5-b-pyridine (PhIP), all of which must be metabolized to their respective bioactive forms [162]. AOM is a potent inducer of carcinomas in the large intestine of various strains of rats, such as the F344 strain, and mice, such as the C57BL/6 and SWR/J strains [163,164]. Although DMH has been frequently used in the past, its bioactive metabolite AOM has better chemical stability and is highly effective at inducing colon carcinogenesis [165]. AOM is an indirect carcinogenic compound that requires bioactivation by cytochrome P450 2E1 in the liver via *N*-oxidation, which generates the mutagenic form, methylazoxymethanol (MAM) [166]. Of note, the response of mice to AOM-induced CRC emulates the development of non-familial CRC in humans, including the molecular pathogenesis [167] and the preponderance of polyps that form in the distal colon, similar to tumors that form on the descending human colon [168]. In 2003, Tanaka et al. described a new model of inflammation-associated CRC, in which male Crj: CD-1 mice were injected intraperitoneally with AOM (10 mg/kg of body weight) and received 2% (w/v) DSS in their water for seven days; these mice developed colonic dysplasia that progressed to the development of colon adenocarcinomas at an incidence rate of 100% [169]. AOM is generally

used coupled with DSS to represent the long-standing inflammation that is associated with the increase of colorectal cancer development [162]. Chronic mucosal inflammation results in genetic mutations, an increase in cell proliferation, a change in crypt cell metabolism, and alterations in the bacterial flora [169]. One noted limitation of the AOM/DSS CAC model is the limited ability to study disease metastasis, as colon tumors become so large that bowel obstructions requiring humane euthanasia before advanced disease can develop are common.

1.5.3 Models to Explore the Gut Microbiome

Researchers have developed multiple pre-clinical murine models in which the composition of the gut microbiome is manipulated to determine subsequent effects on gut health parameters. First among these is the gnotobiotic (GB) mouse model, for which the composition of the microbiome is known. Generally, GB mice are developed from a germ-free animal, either conceived via *in vitro* fertilization of a germ-free dam or birthed via a cesarian section and then maintained in a pathogen-free environment. Then, the desired microbe(s) can be introduced to colonize the germ-free mouse and establish a gnotobiotic model [170]. However, the absence of microbiota has been associated with aberrant immune system development [171]. Turnbaugh et al., colonized germ-free mice with microbiota obtained from obese or lean human donors; the microbiome of recipient mice had a higher Firmicutes-to-Bacteroidetes ratio, increased capacity for harvesting energy, and higher total body fat compared to their counterparts that received microbiota from lean donors. However, it should be noted that the authors followed their recipients for only two weeks after inoculation, and it is not known whether these effects were transient or long-term [172]. Previously, we reported that inoculation of antibiotic-treated mice with fecal microbiota from lean or obese human donors did not drive long-term phenotype or microbiome profiles of recipient mice [173]; rather, this study determined that the basal diet provided to the recipients – either a standard AIN93G diet, the total Western diet, or a 60% fat diet – was the driving factor affecting body weight gain, body composition, and fecal microbiome

profiles. Lastly, colonization of germ-free mice using fecal microbiota from mice with CAC significantly increased colon tumorigenesis compared to mice colonized with conventional healthy bacteria; furthermore, a reduction in tumors was observed when these mice were administered antibiotics [137].

A possible therapeutic approach for colitis and associated colorectal cancer involves the exchange of fecal material from a healthy individual to individuals with gut dysbiosis, termed fecal microbiota transfer (FMT). Experimentally, the FMT method can be applied to determine whether the host traits (*e.g.*, inflammation, cancer development, dysbiosis, etc.) can be conferred to the recipient. In other words, one can attempt to determine whether the microbiota are a cause of disease or a consequence or symptom of disease. The use of FMT dates back to the fourth century in China, at which time a so-called “yellow soup” prepared with human fecal material was used in patients with poisoning or severe diarrhea [174]. Borody et al. described the first successful application of FMT in 1989, in which FMT was performed on a male with unmanageable ulcerative colitis; the patient experienced full and lasting beneficial effects of the donor’s healthy microbiome [175]. FMT has emerged as one of the only successful therapies for *Clostridium difficile* infections and has been recently studied to be used as IBD and CRC therapeutics [176,177]. Although FMT has been widely studied in preclinical settings, clinical trials are necessary for the accurate interpretation of results [178]. A few clinical trials are currently active to understand the effect of FMT in combination with chemotherapy against various cancers including metastatic colorectal cancer. In addition, other clinical trials have focused on FMT as a treatment for UC.

The use of germ-free mice for FMT has been known to be the most reliable method as this model lacks any resident microbe competition for gut colonization; however, they are expensive and difficult to maintain, resulting in alternative methods developed to investigate the effect of the microbiome in mouse disease models. Thus, researchers have employed some

alternate methods to deplete, at least partially, the resident gut microbiome of rodents. Wrzosek et al. determined that cleansing the gut with polyethylene glycol four times reduces the bacterial population by 90% in C57BL/6J mice [179]; after this treatment, they determined that weekly FMT was necessary to achieve a stable microbiota community. In addition to bowel cleansings and the use of germ-free mice, the use of antibiotics has been shown to be efficient in preparing the gut for FMT [180]. Hintze et al. depleted the microbiome of C57BL/6J mice using a broad-scope cocktail of antibiotics followed by administration of FMT with material obtained from either obese or lean human donors to recipient mice, which acquired about 68 to 75% of the human microbiome [181]. The success rate for establishing the donor microbiome in a recipient via FMT is higher if the microbial load of the recipient is low [182]. The most common method of administering FMT in the murine model includes oral gastric gavage. However, stress-induced death and accidental injuries to the trachea, esophagus and stomach can occur [173,183,184]. Other methods include co-housing mice to facilitate the acquisition of gut microbes via coprophagy and mice that are colonized via vertical transmission [170].

Limitations to consider for rodent pre-clinical studies investigating the role of the gut microbiome in health and disease include obvious anatomical and physiologic differences that influence the gut environment, and thus the array of microbes that can inhabit the mouse gut as compared to humans [173]. A universal protocol for FMT has not yet been established, although various methods have been explored with germ-free mice being the most reliable and FMT protocols incorporating an antibiotic regimen as the most common method for microbial manipulation [185].

1.6 Consumption of a Western Diet and Risk of Colitis-Associated Colorectal Cancer

The link between diet and inflammatory disease was initially observed in epidemiological studies. Accounting for various environmental and lifestyle factors, dietary pattern was connected to a high incidence of inflammatory disease in Westernized countries compared to developing

countries [186]. Malnutrition is reported in various immunodeficiency and inflammatory diseases and is prevalent in developed countries, where individuals commonly consume meals characterized as calorie-dense, high palatability and low nutritional profiles [187]. Children who consumed a greater intake of processed foods high in refined sugar, dietary fats and animal protein had elevated prevalence of IBD [188]. Furthermore, low dietary quality scores were associated with high levels of pro-inflammatory proteins such as IL6, which suggests a poor diet promotes subclinical chronic inflammation [189,190]. High consumption of red meat, sugars and fried food is typical in a Western diet which promotes pro-inflammatory reactions [187,191]. In a cross-sectional study, researchers found a positive correlation between the consumption of a Western dietary pattern and high levels of pro-inflammatory proteins C-reactive protein (CRP) and IL6 in the blood [192]. High consumption of n-6 poly-unsaturated fatty acids (PUFA) obtained from oils and meat-based products promote cytokine production and elevated inflammatory response [193]. Vitamin deficiencies are commonly found in IBD patients, whether by consequence or as a risk factor of the disease is yet to be determined [194]. Due to the lack of vegetables and fruits intake and high ultra-processed food consumption in the Western-style diet, essential vitamins and minerals are deficient which can adversely affect the regulation of the inflammation response [195]. Finally, a Western diet contains high amounts of processed and pre-packaged foods which are associated with a high risk of cardiovascular disease and colorectal cancer development [196-198].

The differences between dietary patterns can be observed when comparing CRC between countries. CRC development is higher in African American than native Americans due to mucosal proliferation rates caused by higher consumption of animal products [199]. Western dietary patterns are associated with an increased risk of developing CRC or colon adenomas [200-202] and is inversely associated with quality of life [203,204]. In a meta-analysis of 40 studies, researchers observed an increased risk of CRC when coupled with a Western-style diet [205].

Furthermore, a Western diet pattern led to tumor development in the distal colon and had a strong association with KRAS and BRAF wildtype but with little to no CIMP or microsatellite instability phenotypes [206].

Additionally, high consumption of sugars, animal protein, trans and saturated fats are associated with shifts in the gut microbiome towards compositions dominated by *Bacteroides* [207]. Dietary elements, such as sweeteners, highly consumed in Western diets modulate the microbiome by decreasing *Bifidobacterium spp.* and *Lactobacillus* levels [208]. However, high dietary fiber intake, particularly from fruit and vegetables reduced IBD risk [209,210]. The Mediterranean, indigenous African, traditional East-Asian and plant-based diets have reduced immune parameters including IL6 and CRP levels [211]. A prudent diet such as the Mediterranean diet is characterized by intakes of plant-based foods, legumes, whole grains, vegetables, fruit, nuts and fish [212]. Rural populations characterized by low industrialization environments consume diets high in fiber which results in a microbiome dominated by the *Prevotella* genus, also observed in a vegetarian diet [207]. Age and sex-matched fresh fecal samples of African natives had a *Prevotella*-dominated gut microbiome while African Americans had a gut microbiome dominated by *Bacteroides*. Additionally, fecal samples of native Africans had significantly higher total bacteria and major butyrate-producing taxa which result in higher quantities of SCFAs in feces [213]. Oppositely, African Americans harbor a microbiome that favors secondary bile production [199].

We see similar a phenomenon in animal models. A high fat/high sugar Western-style diet impairs the epithelial barrier and enhances inflammatory response in mice colitis models [214,215]. In addition, diets enriched in simple sugars aggravated colitis and reduce mucosa thickness in rodent models [216-218]. Aside from the high components of simple sugars in the Western diet, these sugary foods also contain high levels of colorants, emulsifiers and additives which drive colitis levels in mouse models [219-221]. Interestingly, in an IBD rodent model, a

high-fat/high sucrose diet-induced colitis and gut dysbiosis in healthy mice. However, these microbiome and inflammatory alterations were improved when mice were given normal chow [215]. After a day of shifting from a low-fat, plant polysaccharide diet to a high fat/ high sucrose diet, changes were detected in the microbiota profile, metabolic pathways and microbial gene expression of germ-free mice transplanted with fresh adult fecal microbial communities [222]. However, initial microbial communities shifts were rapidly changed when the diet was altered [222]. In 2009, mice colonized with microbiota from one healthy adult were fed either a high-fat, high-sugar western-style diet or a low-fat, plant polysaccharide (LF/PP) rich diet, after 12 weeks cecal microbiota was collected for further FMT to the second generation of mice also fed the western or LF/PP diet. The microbiota of mice fed the LF/PP diet had subtle distinctions between fecal sample storage methods and source of FMT with clear distinctions of microbial communities due to the basal diet given to recipient mice [222]. A distinct microbiome and different Bacteroidetes to Firmicute ratio were observed in mice fed a low-fat purified diet compared to a low-fat chow diet [223]. In a FMT study done by our group using fecal material from lean or obese human donors, we found a higher influence of diet on gut microbiome profiles compared to the FMT source [173].

Research on the impact of different dietary patterns on disease has been of interest for years, however, the focus has been on manipulation of macronutrients in the diet, such as carbohydrate and fat components. However, a critical overlook of micronutrient presence in a diet results in incomplete findings on how diet affects health. Newark et al. explored this knowledge gap by creating a 'stress diet' from AIN76G that was depleted in some micronutrients, such as methyl donors, vitamin D and calcium; consumption of this stress diet enhanced tumor formation in mice [224]. Previous diets used to represent the Western-dietary pattern typically alter only the macronutrients, such as fat or carbohydrate content; use of these model diets has led to limited information on the interaction of gut epithelium and other important dietary factors, including

micronutrients and other dietary bioactives. With that limitation in mind, Hintze and colleagues formulated the total Western diet (TWD) for rodents which emulates a typical American dietary pattern using an energy density approach to determine the macro-and-micronutrient on a per-calorie basis, based on the 50th percentile of the NHANES survey [225]. In repeated studies, mice develop enhanced colitis symptoms and colon tumorigenesis when fed a TWD compared to the AIN93G diet in a colitis-associated colorectal cancer model using either C57BL/6J mice or the *APC^{min/+}* mice [226]. Consumption of the Western nutrient profile activates pro-inflammatory and aberrant immune response pathways in mice colon mucosa [226], without triggering systemic inflammation response characteristic of metabolic phenotypes [227]. Prior work in our laboratory used a mouse model of diet-induced obesity with FMT from either lean or obese human donors to recipient C57BL/6J male mice fed a standard optimum diet for rodents, a high-fat diet, or the TWD; we found that the basal diet fed to the recipient mice was the driving factor for the phenotype of those recipient mice and the composition of the gut microbiome as opposed to the phenotype of the human FMT donor [173].

Limitations of many preclinical studies lie in the limited selection of ingredients found in purified mouse diets. These purified diets lack the complex bioactive and diverse fiber sources present in whole foods humans regularly eat. To address this limitation, studies should employ a diet that emulates the complex food matrix and dietary fiber profile of human diets.

1.7 Dietary Polyphenols and Anthocyanins

Polyphenols are plant-derived compounds composed of at least one aromatic ring and one or more hydroxyl groups [228]. Dietary polyphenols can be subdivided into five subclasses based on their structure: flavonoids, phenolic acids, lignans, stilbenes and others [229]. The most common two are flavonoids and phenolic acids, composed of 60% and 30% of all-natural polyphenols, respectively. Flavonoids can be subdivided into six further subgroups including flavanols, flavanones, flavones, isoflavones, flavonols and anthocyanins [230]. Anthocyanins are

naturally occurring in the outer layer of flowers, fruits and vegetables that have red, blue, purple, and black coloring, and have structures composed of two aromatic rings connected by a pyran ring [231]. Factors that influence the color of the anthocyanins include acidity, light intensity and temperature of the environment; for example, anthocyanins appear redder in color in acidic conditions, whereas in basic conditions these compounds appear purple-blue [232]. Examples of vegetables, fruits and flowers with high levels of naturally occurring anthocyanins include berries, purple corn, eggplant, and lavender, among others [233]. Anthocyanins can be identified as anthocyanin glycoside compounds or their sugar-free anthocyanidin aglycone structures. Anthocyanidin aglycones include 3-hydroxyanthocyanidins, 3-deoxyanthocyanidins, and *O*-methylated anthocyanidins with the most common types being pelargonidin, cyanidin, delphinidin, peonidin, petunidin and malvidin [232]. Delphinidin and cyanidin proved to be cytotoxic toward tumor cells in the Caco-2 and metastatic LoVo and LoVo/ADR cell lines, via cellular accumulation of ROS [234]. Cyanidin and delphinidin both thrive in acid conditions and are highly water soluble [231]. Cyanidin, delphinidin and pelargonidin are the most common anthocyanidins found in plants distributed at 50%, 12% and 12%, respectively in various fruits and vegetables [232]. However, anthocyanidins are unstable and rarely found in nature due to the presence of flavylum ions [235]. Anthocyanins are modifiable via hydroxylation, methylation, acylation and glycosylation, chemical modifications that also contribute to the color and stability of the compound [236]. Anthocyanins refer to the glycosylated form of anthocyanidins, normally facilitated by glycosyl transferase in the cytoplasm which binds a common sugar such as glucose or rutin to anthocyanidins [231]. The antioxidant properties of anthocyanins are attributed to their chemical structures, as the hydroxyl motifs are capable of scavenging free radicals. Conversely, the substitution of those hydroxyl groups in the B-ring reduces their antioxidant capacity [231]. Anthocyanins are usually unstable in gastric acid which results in only 1% of anthocyanins reaching the colon for further bacterial digestion. Most polyphenols that reach the colon are

further metabolized by local microbiota into smaller, more bioavailable compounds. For example, cyanidin-3-O-glucoside is primarily metabolized into protocatechuic acid (PCA), a metabolite reported to have antioxidant, antidiabetic, anti-proliferative and pro-apoptotic capabilities [237]. Berries contain the greatest quantity of anthocyanins, more specifically dark-colored berries like chokeberries, elderberries, and black raspberries. These three berries contain the highest amount of total anthocyanin per serving [238].

Black raspberry (*Rubus occidentalis*) contains high quantities of anthocyanins and other important micronutrients (vitamins A, E and C, calcium and folic acid), dietary fibers and phytochemicals (ellagic acid, ferulic acid, ellagitannins and other flavonoids) [238].

Anthocyanins are the most abundant polyphenol in black raspberries (BRB), which have an average total anthocyanin weight of 845 mg per serving, dominated by cyanidin-3-O-glucoside and cyanidin-3-O-rutinoside [232]. The average American consumes approximately 12.5 mg a day of anthocyanins per day [238]. Research in anthocyanins has revealed anti-inflammatory and anti-cancer properties in animal models. In a murine model of UC, mice were provided 5 or 10% (w/v) BRB-supplemented AIN76 basal diets as colitis was induced by administering 3% DSS via drinking water [239]. BRB exposure modulated inflammatory pathways which result in a dampened inflammatory state by suppression of TNF α and IL-1 β expression in the colon. Additionally, the downregulation of I κ B α further inhibits NF κ B activity and decreases COX2 action [239]. In an AOM-induced aberrant crypt foci model using Fisher 344 rats, researchers observed reduced colon tumor multiplicity and burden in mice that consumed a diet supplemented with BRB ranging from 2.5 – 10% (w/w) [240]. In an esophageal cancer model, F344 rats administered N-nitroso methylbenzylamine and fed an AIN76G diet supplemented with 5% whole freeze-dried black raspberries, reported evidence of cell proliferation inhibition, decrease in an inflammatory response, reduced angiogenesis and apoptosis induction [241]. In models of colitis, *APC1838*^{+/-} and *Muc2*^{-/-} mice fed a western-style diet supplemented by 10%

(w/w) BRB for 12 weeks had suppressed colon tumorigenesis [242]. Feeding black raspberries to *APC^{min/+}* mice suppressed colon tumor formation by hypomethylating regions involved in immune regulation, inflammation response and ROS production [243]. Furthermore, BRB supplemented in an AIN76 diet, fed to *APC^{min/+}* mice, suppressed colonic adenoma development and changed mucosa, liver and fecal metabolites production [244]. However, the question remains if BRB supplements reduce inflammation and tumorigenesis in mice consuming a TWD. Moreover, past studies do not account for the longitudinal effects of BRB supplementation on colitis, tumor progression and microbiome composition.

Black raspberry-supplemented diets used in murine models of inflammatory disease and colorectal cancer are reported to decrease adenomas and polyp growth, reduce ulcerations in colon mucosa and regulate cytokine expression including IL6 and IL10 [239,244-247]. Indeed, black raspberries are rich in anthocyanins but also contain a high abundance of other bioactive such as ellagic acid known to have anti-inflammatory and anticancer properties. Ellagic acid supplementation to a normal rodent diet suppresses acute and chronic colitis by regulating IL6, TNF α and IFN γ and other stress modulators such as COX2 and iNOS [248]. Anthocyanins and other bioactive compounds found in whole foods have the potential to modulate inflammation response and modify the gut microbiome.

Diets supplemented with BRB shift microbiome profiles by promotion of *Akkermansia muciniphila*, *Bifidobacterium spp.*, and *Lactobacillus spp.* abundance while inhibiting pathogenic strains like *Helicobacter pylori* [249,250]. BRB consumption results in Firmicute and Bacteroidetes ratio and abundance alterations. Additionally, SCFAs found in berries are not digested in the small intestine and reach the colon where local microbiota ferments complex compounds into SCFAs, mainly butyrate, acetate and propionate [251]. Anthocyanin-rich berries increased short-chain fatty acids production, namely butyric acid, in the colon and serum of rats and cyanidin-3-glucoside in their urine [252]. In vitro, butyrate arrested new cell growth and

hyperproliferation in colon cells, displaying anticancer properties [253]. Additionally, PCA exerts chemoprotective effects towards colorectal cancer by modulating inflammatory and metabolic pathways in the APC^{min/+} mouse model administered AIN76A diet supplemented with 5% BRB or 500 ppm of PCA [254]. High quantities of phenolic acid, specifically PCA, were detected in the GI tract of pigs following the consumption of freeze-dried BRB powder [255].

1.8. Project Objectives and Hypotheses

Although there is evidence pointing to the health benefits of BRB consumption for suppression of colitis and colon tumor development, it is not known whether BRB intake in the context of a Western diet would affect gut inflammation and CAC or whether BRB would alter the composition of the microbiome. Furthermore, multiple studies have pointed to gut dysbiosis as a common feature of colitis and/or colon tumorigenesis in humans and animal models, although it is not clear whether changes in the gut microbiome population associated with different nutritional patterns are drivers of this disease process. The overarching goal of studies reported here is to better understand how the gut microbiome contributes to CRC. In order to study this relationship, these two different approaches were taken one leveraging diet intervention and the other leveraging FMT modulation, in mice models of CAC fed a Western-style diet.

Thus, the objectives of the projects were first to determine the effects of dietary intervention with whole freeze-dried BRB on the dynamic composition of the gut microbiome, inflammation status and colon tumorigenesis in mice fed a Western diet. Based on prior evidence for the protective effects of BRB reported in the literature, we hypothesized a dietary supplementation with BRB would improve recovery from colon injury and prevent progression to CAC, and this effect would be more pronounced in mice consuming a Western diet. We also hypothesized that consumption of BRB would result in changes to the gut microbiota composition, shifting the population in favor of commensal species that promote gut homeostasis. Secondly, to better understand the involvement of the microbiome in the development and/or

exacerbation of colitis and colon tumorigenesis, we designed an FMT experiment using fecal material collected from the first study in which donor mice fed either AIN93G or TWD and subjected to our standard protocol for mouse CAC [256]. This experiment design incorporated the standard AIN93G or the total Western diet for the donor animals as well as for the recipient mice. We hypothesized that FMT from donor mice fed TWD that experienced severe colitis and high tumor burden would exacerbate symptoms of colitis and increase tumorigenesis in recipient mice fed AIN93G. Conversely, we hypothesized that FMT from donor mice fed AIN93G with mild colitis and low tumor burden would alleviate colitis symptoms and reduce tumorigenesis in recipient mice fed TWD.

References

1. U.S. Cancer Statistics Working Group. U.S. Cancer Statistics Data Visualizations Tool, based on 2021 submission data (1999-2019): U.S. Department of Health and Human Services, Centers for Disease Control and Prevention and National Cancer Institute. Available online: www.cdc.gov/cancer/dataviz (accessed on November 2022).
2. American Society of Cancer. Cancer Statistic Center, 2022. Available online: <http://cancerstatisticscenter.cancer.org> (accessed on November 14, 2022).
3. Wong, M.C.S.; Huang, J.; Lok, V.; Wang, J.; Fung, F.; Ding, H.; Zheng, Z.J. Differences in incidence and mortality trends of colorectal cancer worldwide based on sex, age, and anatomic location. *Clin Gastroenterol Hepatol* **2021**, *19*, 955-966 e961, doi:10.1016/j.cgh.2020.02.026.
4. Siegel, R.L.; Miller, K.D.; Goding Sauer, A.; Fedewa, S.A.; Butterly, L.F.; Anderson, J.C.; Cercek, A.; Smith, R.A.; Jemal, A. Colorectal cancer statistics, 2020. *CA Cancer J Clin* **2020**, *70*, 145-164, doi:10.3322/caac.21601.
5. Bray, F.; Ferlay, J.; Soerjomataram, I.; Siegel, R.L.; Torre, L.A.; Jemal, A. Global cancer statistics 2018: GLOBOCAN estimates of incidence and mortality worldwide for 36 cancers in 185 countries. *CA Cancer J Clin* **2018**, *68*, 394-424, doi:10.3322/caac.21492.
6. Amersi, F.; Agustin, M.; Ko, C.Y. Colorectal cancer: epidemiology, risk factors, and health services. *Clin Colon Rectal Surg* **2005**, *18*, 133-140, doi:10.1055/s-2005-916274.
7. Bucagu, M.; Bizimana Jde, D.; Muganda, J.; Humblet, C.P. Socio-economic, clinical and biological risk factors for mother - to - child transmission of HIV-1 in Muhima health centre (Rwanda): a prospective cohort study. *Arch Public Health* **2013**, *71*, 4, doi:10.1186/0778-7367-71-4.

8. Seyedian, S.S.; Nokhostin, F.; Malamir, M.D. A review of the diagnosis, prevention, and treatment methods of inflammatory bowel disease. *J Med Life* **2019**, *12*, 113-122, doi:10.25122/jml-2018-0075.
9. Doubeni, C.A.; Laiyemo, A.O.; Major, J.M.; Schootman, M.; Lian, M.; Park, Y.; Graubard, B.I.; Hollenbeck, A.R.; Sinha, R. Socioeconomic status and the risk of colorectal cancer: an analysis of more than a half million adults in the National Institutes of Health-AARP Diet and Health Study. *Cancer* **2012**, *118*, 3636-3644, doi:10.1002/cncr.26677.
10. Johnson, C.M.; Wei, C.; Ensor, J.E.; Smolenski, D.J.; Amos, C.I.; Levin, B.; Berry, D.A. Meta-analyses of colorectal cancer risk factors. *Cancer Causes Control* **2013**, *24*, 1207-1222, doi:10.1007/s10552-013-0201-5.
11. Rawla, P.; Sunkara, T.; Barsouk, A. Epidemiology of colorectal cancer: incidence, mortality, survival, and risk factors. *Prz Gastroenterol* **2019**, *14*, 89-103, doi:10.5114/pg.2018.81072.
12. American Cancer Society. *Cancer Facts & Figures 2022*; Atlanta, 2022.
13. Park, J.; Look, K.A. Health care expenditure burden of cancer care in the united states. *Inquiry* **2019**, *56*, 46958019880696, doi:10.1177/0046958019880696.
14. Ekwueme, D.U.; Yabroff, K.R.; Guy, G.P., Jr.; Banegas, M.P.; de Moor, J.S.; Li, C.; Han, X.; Zheng, Z.; Soni, A.; Davidoff, A., et al. Medical costs and productivity losses of cancer survivors--United States, 2008-2011. *MMWR Morb Mortal Wkly Rep* **2014**, *63*, 505-510.
15. Xi, Y.; Xu, P. Global colorectal cancer burden in 2020 and projections to 2040. *Transl Oncol* **2021**, *14*, 101174, doi:10.1016/j.tranon.2021.101174.
16. Azzouz, L.L.; Sharma, S. Physiology, Large Intestine. In *StatPearls*, Treasure Island (FL), 2022.
17. Johansson, M.E.; Larsson, J.M.; Hansson, G.C. The two mucus layers of colon are organized by the MUC2 mucin, whereas the outer layer is a legislator of host-microbial interactions. *Proc Natl Acad Sci U S A* **2011**, *108 Suppl 1*, 4659-4665, doi:10.1073/pnas.1006451107.
18. Furman, D.; Campisi, J.; Verdin, E.; Carrera-Bastos, P.; Targ, S.; Franceschi, C.; Ferrucci, L.; Gilroy, D.W.; Fasano, A.; Miller, G.W., et al. Chronic inflammation in the etiology of disease across the life span. *Nat Med* **2019**, *25*, 1822-1832, doi:10.1038/s41591-019-0675-0.
19. Yaghoubi, N.; Soltani, A.; Ghazvini, K.; Hassanian, S.M.; Hashemy, S.I. PD-1/ PD-L1 blockade as a novel treatment for colorectal cancer. *Biomed Pharmacother* **2019**, *110*, 312-318, doi:10.1016/j.biopha.2018.11.105.
20. Drew, D.A.; Cao, Y.; Chan, A.T. Aspirin and colorectal cancer: the promise of precision chemoprevention. *Nat Rev Cancer* **2016**, *16*, 173-186, doi:10.1038/nrc.2016.4.

21. Lewandowska, A.; Rudzki, G.; Lewandowski, T.; Strykowska-Gora, A.; Rudzki, S. Risk factors for the diagnosis of colorectal cancer. *Cancer Control* **2022**, *29*, 10732748211056692, doi:10.1177/10732748211056692.
22. Lynch, H.T.; de la Chapelle, A. Hereditary colorectal cancer. *N Engl J Med* **2003**, *348*, 919-932, doi:10.1056/NEJMra012242.
23. Weitz, J.; Koch, M.; Debus, J.; Hohler, T.; Galle, P.R.; Buchler, M.W. Colorectal cancer. *Lancet* **2005**, *365*, 153-165, doi:10.1016/S0140-6736(05)17706-X.
24. Nguyen, L.H.; Goel, A.; Chung, D.C. Pathways of Colorectal Carcinogenesis. *Gastroenterology* **2020**, *158*, 291-302, doi:10.1053/j.gastro.2019.08.059.
25. Fearon, E.R.; Vogelstein, B. A genetic model for colorectal tumorigenesis. *Cell* **1990**, *61*, 759-767, doi:10.1016/0092-8674(90)90186-i.
26. Hanahan, D.; Weinberg, R.A. Hallmarks of cancer: the next generation. *Cell* **2011**, *144*, 646-674, doi:10.1016/j.cell.2011.02.013.
27. Witsch, E.; Sela, M.; Yarden, Y. Roles for growth factors in cancer progression. *Physiology (Bethesda)* **2010**, *25*, 85-101, doi:10.1152/physiol.00045.2009.
28. Lemmon, M.A.; Schlessinger, J. Cell signaling by receptor tyrosine kinases. *Cell* **2010**, *141*, 1117-1134, doi:10.1016/j.cell.2010.06.011.
29. Aubrey, B.J.; Strasser, A.; Kelly, G.L. Tumor-suppressor functions of the TP53 pathway. *Cold Spring Harb Perspect Med* **2016**, *6*, doi:10.1101/cshperspect.a026062.
30. Liebl, M.C.; Hofmann, T.G. The role of p53 signaling in colorectal cancer. *Cancers (Basel)* **2021**, *13*, doi:10.3390/cancers13092125.
31. Strzyz, P. Cell signalling: Signalling to cell cycle arrest. *Nat Rev Mol Cell Biol* **2016**, *17*, 536, doi:10.1038/nrm.2016.108.
32. Blasco, M.A. Telomeres and human disease: ageing, cancer and beyond. *Nat Rev Genet* **2005**, *6*, 611-622, doi:10.1038/nrg1656.
33. Carmeliet, P. VEGF as a key mediator of angiogenesis in cancer. *Oncology* **2005**, *69* Suppl 3, 4-10, doi:10.1159/000088478.
34. Bergers, G.; Brekken, R.; McMahon, G.; Vu, T.H.; Itoh, T.; Tamaki, K.; Tanzawa, K.; Thorpe, P.; Itohara, S.; Werb, Z., et al. Matrix metalloproteinase-9 triggers the angiogenic switch during carcinogenesis. *Nat Cell Biol* **2000**, *2*, 737-744, doi:10.1038/35036374.
35. Cancer Genome Atlas, N. Comprehensive molecular characterization of human colon and rectal cancer. *Nature* **2012**, *487*, 330-337, doi:10.1038/nature11252.
36. Fodde, R. The APC gene in colorectal cancer. *Eur J Cancer* **2002**, *38*, 867-871, doi:10.1016/s0959-8049(02)00040-0.

37. Schatoff, E.M.; Leach, B.I.; Dow, L.E. Wnt Signaling and Colorectal Cancer. *Curr Colorectal Cancer Rep* **2017**, *13*, 101-110, doi:10.1007/s11888-017-0354-9.
38. Veeman, M.T.; Axelrod, J.D.; Moon, R.T. A second canon. Functions and mechanisms of beta-catenin-independent Wnt signaling. *Dev Cell* **2003**, *5*, 367-377, doi:10.1016/s1534-5807(03)00266-1.
39. Cheng, X.; Xu, X.; Chen, D.; Zhao, F.; Wang, W. Therapeutic potential of targeting the Wnt/beta-catenin signaling pathway in colorectal cancer. *Biomed Pharmacother* **2019**, *110*, 473-481, doi:10.1016/j.biopha.2018.11.082.
40. Pino, M.S.; Chung, D.C. The chromosomal instability pathway in colon cancer. *Gastroenterology* **2010**, *138*, 2059-2072, doi:10.1053/j.gastro.2009.12.065.
41. Malki, A.; ElRuz, R.A.; Gupta, I.; Allouch, A.; Vranic, S.; Al Moustafa, A.E. Molecular Mechanisms of Colon Cancer Progression and Metastasis: Recent Insights and Advancements. *Int J Mol Sci* **2020**, *22*, doi:10.3390/ijms22010130.
42. Raskov, H.; Pommergaard, H.C.; Burcharth, J.; Rosenberg, J. Colorectal carcinogenesis--update and perspectives. *World J Gastroenterol* **2014**, *20*, 18151-18164, doi:10.3748/wjg.v20.i48.18151.
43. Yurgelun, M.B.; Masciari, S.; Joshi, V.A.; Mercado, R.C.; Lindor, N.M.; Gallinger, S.; Hopper, J.L.; Jenkins, M.A.; Buchanan, D.D.; Newcomb, P.A., et al. Germline TP53 Mutations in Patients With Early-Onset Colorectal Cancer in the Colon Cancer Family Registry. *JAMA Oncol* **2015**, *1*, 214-221, doi:10.1001/jamaoncol.2015.0197.
44. Lotfollahzadeh, S.; Recio-Boiles, A.; Cagir, B. Colon Cancer. In *StatPearls*, Treasure Island (FL), 2022.
45. De' Angelis, G.L.; Bottarelli, L.; Azzoni, C.; De' Angelis, N.; Leandro, G.; Di Mario, F.; Gaiani, F.; Negri, F. Microsatellite instability in colorectal cancer. *Acta Biomed* **2018**, *89*, 97-101, doi:10.23750/abm.v89i9-S.7960.
46. Boland, C.R.; Thibodeau, S.N.; Hamilton, S.R.; Sidransky, D.; Eshleman, J.R.; Burt, R.W.; Meltzer, S.J.; Rodriguez-Bigas, M.A.; Fodde, R.; Ranzani, G.N., et al. A National Cancer Institute Workshop on Microsatellite Instability for cancer detection and familial predisposition: development of international criteria for the determination of microsatellite instability in colorectal cancer. *Cancer Res* **1998**, *58*, 5248-5257.
47. Bessa, X.; Balleste, B.; Andreu, M.; Castells, A.; Bellosillo, B.; Balaguer, F.; Castellvi-Bel, S.; Paya, A.; Jover, R.; Alenda, C., et al. A prospective, multicenter, population-based study of BRAF mutational analysis for Lynch syndrome screening. *Clin Gastroenterol Hepatol* **2008**, *6*, 206-214, doi:10.1016/j.cgh.2007.10.011.
48. Parsons, R.; Myeroff, L.L.; Liu, B.; Willson, J.K.; Markowitz, S.D.; Kinzler, K.W.; Vogelstein, B. Microsatellite instability and mutations of the transforming growth factor beta type II receptor gene in colorectal cancer. *Cancer Res* **1995**, *55*, 5548-5550.
49. Biswas, S.; Trobridge, P.; Romero-Gallo, J.; Billheimer, D.; Myeroff, L.L.; Willson, J.K.; Markowitz, S.D.; Grady, W.M. Mutational inactivation of TGFBR2 in microsatellite

- unstable colon cancer arises from the cooperation of genomic instability and the clonal outgrowth of transforming growth factor beta resistant cells. *Genes Chromosomes Cancer* **2008**, *47*, 95-106, doi:10.1002/gcc.20511.
50. Greenberg, M.V.C.; Bourc'his, D. The diverse roles of DNA methylation in mammalian development and disease. *Nat Rev Mol Cell Biol* **2019**, *20*, 590-607, doi:10.1038/s41580-019-0159-6.
 51. Grivennikov, S.I.; Greten, F.R.; Karin, M. Immunity, inflammation, and cancer. *Cell* **2010**, *140*, 883-899, doi:10.1016/j.cell.2010.01.025.
 52. Centers for Disease Control and Prevention. Irritable Bowel Syndrome. Available online: <http://www.cdc.gov/ibd/> (accessed on May 29, 2014).
 53. Dyson, J.K.; Rutter, M.D. Colorectal cancer in inflammatory bowel disease: what is the real magnitude of the risk? *World journal of gastroenterology : WJG* **2012**, *18*, 3839-3848, doi:10.3748/wjg.v18.i29.3839.
 54. Grivennikov, S.I. Inflammation and colorectal cancer: colitis-associated neoplasia. *Sem. Immunopath.* **2013**, *35*, 229-244, doi:10.1007/s00281-012-0352-6.
 55. Rhodes, J.M.; Campbell, B.J. Inflammation and colorectal cancer: IBD-associated and sporadic cancer compared. *Trends. Mol. Med.* **2002**, *8*, 10-16.
 56. Itzkowitz, S.H.; Yio, X. Inflammation and cancer IV. Colorectal cancer in inflammatory bowel disease: the role of inflammation. *Am J Physiol Gastrointest Liver Physiol* **2004**, *287*, G7-17, doi:10.1152/ajpgi.00079.2004.
 57. Luo, C.; Zhang, H. The role of proinflammatory pathways in the pathogenesis of colitis-associated colorectal cancer. *Mediators Inflamm* **2017**, *2017*, 5126048, doi:10.1155/2017/5126048.
 58. Hanus, M.; Parada-Venegas, D.; Landskron, G.; Wielandt, A.M.; Hurtado, C.; Alvarez, K.; Hermoso, M.A.; Lopez-Kostner, F.; De la Fuente, M. Immune System, Microbiota, and Microbial Metabolites: The Unresolved Triad in Colorectal Cancer Microenvironment. *Front Immunol* **2021**, *12*, 612826, doi:10.3389/fimmu.2021.612826.
 59. Valko, M.; Leibfritz, D.; Moncol, J.; Cronin, M.T.; Mazur, M.; Telser, J. Free radicals and antioxidants in normal physiological functions and human disease. *Int J Biochem Cell Biol* **2007**, *39*, 44-84, doi:10.1016/j.biocel.2006.07.001.
 60. Pizzino, G.; Irrera, N.; Cucinotta, M.; Pallio, G.; Mannino, F.; Arcoraci, V.; Squadrito, F.; Altavilla, D.; Bitto, A. Oxidative Stress: Harms and Benefits for Human Health. *Oxid Med Cell Longev* **2017**, *2017*, 8416763, doi:10.1155/2017/8416763.
 61. Liou, G.Y.; Storz, P. Reactive oxygen species in cancer. *Free Radic Res* **2010**, *44*, 479-496, doi:10.3109/10715761003667554.
 62. Tian, T.; Wang, Z.; Zhang, J. Pathomechanisms of Oxidative Stress in Inflammatory Bowel Disease and Potential Antioxidant Therapies. *Oxid Med Cell Longev* **2017**, *2017*, 4535194, doi:10.1155/2017/4535194.

63. Arneth, B. Trained innate immunity. *Immunol Res* **2021**, *69*, 1-7, doi:10.1007/s12026-021-09170-y.
64. Takeuchi, O.; Akira, S. Pattern recognition receptors and inflammation. *Cell* **2010**, *140*, 805-820, doi:10.1016/j.cell.2010.01.022.
65. Netea, M.G.; Schlitzer, A.; Placek, K.; Joosten, L.A.B.; Schultze, J.L. Innate and Adaptive Immune Memory: an Evolutionary Continuum in the Host's Response to Pathogens. *Cell Host Microbe* **2019**, *25*, 13-26, doi:10.1016/j.chom.2018.12.006.
66. Sameer, A.S.; Nissar, S. Toll-like receptors (TLRs): structure, functions, signaling, and role of their polymorphisms in colorectal cancer susceptibility. *Biomed Res Int* **2021**, *2021*, 1157023, doi:10.1155/2021/1157023.
67. Kawasaki, T.; Kawai, T. Toll-like receptor signaling pathways. *Front Immunol* **2014**, *5*, 461, doi:10.3389/fimmu.2014.00461.
68. Atreya, I.; Atreya, R.; Neurath, M.F. NF-kappaB in inflammatory bowel disease. *J Intern Med* **2008**, *263*, 591-596, doi:10.1111/j.1365-2796.2008.01953.x.
69. Mehrad, B.; Keane, M.P.; Strieter, R.M. Chemokines as mediators of angiogenesis. *Thromb Haemost* **2007**, *97*, 755-762.
70. Popivanova, B.K.; Kitamura, K.; Wu, Y.; Kondo, T.; Kagaya, T.; Kaneko, S.; Oshima, M.; Fujii, C.; Mukaida, N. Blocking TNF-alpha in mice reduces colorectal carcinogenesis associated with chronic colitis. *J Clin Invest* **2008**, *118*, 560-570, doi:10.1172/JCI32453.
71. Atreya, R.; Neurath, M.F. Involvement of IL-6 in the pathogenesis of inflammatory bowel disease and colon cancer. *Clin Rev Allergy Immunol* **2005**, *28*, 187-196, doi:10.1385/CRIAI:28:3:187.
72. Becker, C.; Fantini, M.C.; Schramm, C.; Lehr, H.A.; Wirtz, S.; Nikolaev, A.; Burg, J.; Strand, S.; Kiesslich, R.; Huber, S., et al. TGF-beta suppresses tumor progression in colon cancer by inhibition of IL-6 trans-signaling. *Immunity* **2004**, *21*, 491-501, doi:10.1016/j.immuni.2004.07.020.
73. Chung, Y.C.; Chang, Y.F. Serum interleukin-6 levels reflect the disease status of colorectal cancer. *J Surg Oncol* **2003**, *83*, 222-226, doi:10.1002/jso.10269.
74. Souza, R.F.; Lei, J.; Yin, J.; Appel, R.; Zou, T.T.; Zhou, X.; Wang, S.; Rhyu, M.G.; Cymes, K.; Chan, O., et al. A transforming growth factor beta 1 receptor type II mutation in ulcerative colitis-associated neoplasms. *Gastroenterology* **1997**, *112*, 40-45, doi:10.1016/s0016-5085(97)70217-8.
75. Fleming, N.I.; Jorissen, R.N.; Mouradov, D.; Christie, M.; Sakthianandeswaren, A.; Palmieri, M.; Day, F.; Li, S.; Tsui, C.; Lipton, L., et al. SMAD2, SMAD3 and SMAD4 mutations in colorectal cancer. *Cancer Res* **2013**, *73*, 725-735, doi:10.1158/0008-5472.CAN-12-2706.
76. Grivennikov, S.; Karin, E.; Terzic, J.; Mucida, D.; Yu, G.Y.; Vallabhapurapu, S.; Scheller, J.; Rose-John, S.; Cheroutre, H.; Eckmann, L., et al. IL-6 and Stat3 are required

- for survival of intestinal epithelial cells and development of colitis-associated cancer. *Cancer Cell* **2009**, *15*, 103-113, doi:10.1016/j.ccr.2009.01.001.
77. Mantovani, A.; Barajon, I.; Garlanda, C. IL-1 and IL-1 regulatory pathways in cancer progression and therapy. *Immunol Rev* **2018**, *281*, 57-61, doi:10.1111/imr.12614.
 78. Dinarello, C.A. Overview of the IL-1 family in innate inflammation and acquired immunity. *Immunol Rev* **2018**, *281*, 8-27, doi:10.1111/imr.12621.
 79. Schumacher, T.N.; Schreiber, R.D. Neoantigens in cancer immunotherapy. *Science* **2015**, *348*, 69-74, doi:10.1126/science.aaa4971.
 80. Maleki, F.; Rezaadeh, F.; Varmira, K. MUC1-targeted radiopharmaceuticals in cancer imaging and therapy. *Mol Pharm* **2021**, *18*, 1842-1861, doi:10.1021/acs.molpharmaceut.0c01249.
 81. Finn, O.J. Cancer immunology. *N Engl J Med* **2008**, *358*, 2704-2715, doi:10.1056/NEJMra072739.
 82. McGilvray, R.W.; Eagle, R.A.; Watson, N.F.; Al-Attar, A.; Ball, G.; Jafferji, I.; Trowsdale, J.; Durrant, L.G. NKG2D ligand expression in human colorectal cancer reveals associations with prognosis and evidence for immunoediting. *Clin Cancer Res* **2009**, *15*, 6993-7002, doi:10.1158/1078-0432.CCR-09-0991.
 83. Alberts B, J.A., Lewis J, et al. *Molecular Biology of the Cell*, 4th edition ed.; New York: Garland Science: 2002; Vol. Innate Immunity.
 84. Mojic, M.; Takeda, K.; Hayakawa, Y. The dark side of IFN-gamma: its role in promoting cancer immunoevasion. *Int J Mol Sci* **2017**, *19*, doi:10.3390/ijms19010089.
 85. Liu, J.; Geng, X.; Hou, J.; Wu, G. New insights into M1/M2 macrophages: key modulators in cancer progression. *Cancer Cell Int* **2021**, *21*, 389, doi:10.1186/s12935-021-02089-2.
 86. Smith-Garvin, J.E.; Koretzky, G.A.; Jordan, M.S. T cell activation. *Annu Rev Immunol* **2009**, *27*, 591-619, doi:10.1146/annurev.immunol.021908.132706.
 87. Spencer, J.; Sollid, L.M. The human intestinal B-cell response. *Mucosal Immunol* **2016**, *9*, 1113-1124, doi:10.1038/mi.2016.59.
 88. Gajewski, T.F.; Schreiber, H.; Fu, Y.X. Innate and adaptive immune cells in the tumor microenvironment. *Nat Immunol* **2013**, *14*, 1014-1022, doi:10.1038/ni.2703.
 89. Dunn, G.P.; Old, L.J.; Schreiber, R.D. The immunobiology of cancer immunosurveillance and immunoediting. *Immunity* **2004**, *21*, 137-148, doi:10.1016/j.immuni.2004.07.017.
 90. Mizuno, R.; Kawada, K.; Sakai, Y. Prostaglandin E2/EP signaling in the tumor microenvironment of colorectal cancer. *Int J Mol Sci* **2019**, *20*, doi:10.3390/ijms20246254.

91. Greenhough, A.; Smartt, H.J.; Moore, A.E.; Roberts, H.R.; Williams, A.C.; Paraskeva, C.; Kaidi, A. The COX-2/PGE2 pathway: key roles in the hallmarks of cancer and adaptation to the tumour microenvironment. *Carcinogenesis* **2009**, *30*, 377-386, doi:10.1093/carcin/bgp014.
92. Kalinski, P. Regulation of immune responses by prostaglandin E2. *J Immunol* **2012**, *188*, 21-28, doi:10.4049/jimmunol.1101029.
93. Sheng, J.; Sun, H.; Yu, F.B.; Li, B.; Zhang, Y.; Zhu, Y.T. The role of cyclooxygenase-2 in colorectal cancer. *Int J Med Sci* **2020**, *17*, 1095-1101, doi:10.7150/ijms.44439.
94. Liu, Y.; Sun, H.; Hu, M.; Zhang, Y.; Chen, S.; Tighe, S.; Zhu, Y. The role of cyclooxygenase-2 in colorectal carcinogenesis. *Clin Colorectal Cancer* **2017**, *16*, 165-172, doi:10.1016/j.clcc.2016.09.012.
95. Wang, D.; Dubois, R.N. The role of COX-2 in intestinal inflammation and colorectal cancer. *Oncogene* **2010**, *29*, 781-788, doi:10.1038/onc.2009.421.
96. Wang, D.; Wang, H.; Brown, J.; Daikoku, T.; Ning, W.; Shi, Q.; Richmond, A.; Strieter, R.; Dey, S.K.; DuBois, R.N. CXCL1 induced by prostaglandin E2 promotes angiogenesis in colorectal cancer. *J Exp Med* **2006**, *203*, 941-951, doi:10.1084/jem.20052124.
97. Gupta, R.A.; Dubois, R.N. Colorectal cancer prevention and treatment by inhibition of cyclooxygenase-2. *Nat Rev Cancer* **2001**, *1*, 11-21, doi:10.1038/35094017.
98. Bader, J.E.; Voss, K.; Rathmell, J.C. Targeting metabolism to improve the tumor microenvironment for cancer immunotherapy. *Mol Cell* **2020**, *78*, 1019-1033, doi:10.1016/j.molcel.2020.05.034.
99. Rutter, M.D.; Saunders, B.P.; Wilkinson, K.H.; Rumbles, S.; Schofield, G.; Kamm, M.A.; Williams, C.B.; Price, A.B.; Talbot, I.C.; Forbes, A. Thirty-year analysis of a colonoscopic surveillance program for neoplasia in ulcerative colitis. *Gastroenterology* **2006**, *130*, 1030-1038, doi:10.1053/j.gastro.2005.12.035.
100. Simon, L.S. Role and regulation of cyclooxygenase-2 during inflammation. *Am J Med* **1999**, *106*, 37S-42S, doi:10.1016/s0002-9343(99)00115-1.
101. Agoff, S.N.; Brentnall, T.A.; Crispin, D.A.; Taylor, S.L.; Raaka, S.; Haggitt, R.C.; Reed, M.W.; Afonina, I.A.; Rabinovitch, P.S.; Stevens, A.C., et al. The role of cyclooxygenase 2 in ulcerative colitis-associated neoplasia. *Am J Pathol* **2000**, *157*, 737-745, doi:10.1016/S0002-9440(10)64587-7.
102. Greenwood-Van Meerveld, B.; Johnson, A.C.; Grundy, D. Gastrointestinal physiology and function. *Handb Exp Pharmacol* **2017**, *239*, 1-16, doi:10.1007/164_2016_118.
103. Suzuki, T. Regulation of the intestinal barrier by nutrients: The role of tight junctions. *Anim Sci J* **2020**, *91*, e13357, doi:10.1111/asj.13357.
104. Camilleri, M.; Madsen, K.; Spiller, R.; Greenwood-Van Meerveld, B.; Verne, G.N. Intestinal barrier function in health and gastrointestinal disease. *Neurogastroenterol Motil* **2012**, *24*, 503-512, doi:10.1111/j.1365-2982.2012.01921.x.

105. Sekirov, I.; Russell, S.L.; Antunes, L.C.; Finlay, B.B. Gut microbiota in health and disease. *Physiol Rev* **2010**, *90*, 859-904, doi:10.1152/physrev.00045.2009.
106. Holmes, E.; Li, J.V.; Marchesi, J.R.; Nicholson, J.K. Gut microbiota composition and activity in relation to host metabolic phenotype and disease risk. *Cell Metab* **2012**, *16*, 559-564, doi:10.1016/j.cmet.2012.10.007.
107. Gomaa, E.Z. Human gut microbiota/microbiome in health and diseases: a review. *Antonie Van Leeuwenhoek* **2020**, *113*, 2019-2040, doi:10.1007/s10482-020-01474-7.
108. Oren, A.; Garrity, G.M. Valid publication of the names of forty-two phyla of prokaryotes. *Int J Syst Evol Microbiol* **2021**, *71*, doi:10.1099/ijsem.0.005056.
109. Martin, A.M.; Sun, E.W.; Rogers, G.B.; Keating, D.J. The Influence of the Gut Microbiome on Host Metabolism Through the Regulation of Gut Hormone Release. *Front Physiol* **2019**, *10*, 428, doi:10.3389/fphys.2019.00428.
110. Durack, J.; Lynch, S.V. The gut microbiome: relationships with disease and opportunities for therapy. *J Exp Med* **2019**, *216*, 20-40, doi:10.1084/jem.20180448.
111. Stilling, R.M.; Dinan, T.G.; Cryan, J.F. Microbial genes, brain & behaviour - epigenetic regulation of the gut-brain axis. *Genes Brain Behav* **2014**, *13*, 69-86, doi:10.1111/gbb.12109.
112. Frost, G.; Sleeth, M.L.; Sahuri-Arisoylu, M.; Lizarbe, B.; Cerdan, S.; Brody, L.; Anastasovska, J.; Ghourab, S.; Hankir, M.; Zhang, S., et al. The short-chain fatty acid acetate reduces appetite via a central homeostatic mechanism. *Nat Commun* **2014**, *5*, 3611, doi:10.1038/ncomms4611.
113. Margolis, K.G.; Cryan, J.F.; Mayer, E.A. The microbiota-gut-brain axis: from motility to mood. *Gastroenterology* **2021**, *160*, 1486-1501, doi:10.1053/j.gastro.2020.10.066.
114. Allaire, J.M.; Crowley, S.M.; Law, H.T.; Chang, S.Y.; Ko, H.J.; Vallance, B.A. The Intestinal Epithelium: Central Coordinator of Mucosal Immunity. *Trends Immunol* **2018**, *39*, 677-696, doi:10.1016/j.it.2018.04.002.
115. Paone, P.; Cani, P.D. Mucus barrier, mucins and gut microbiota: the expected slimy partners? *Gut* **2020**, *69*, 2232-2243, doi:10.1136/gutjnl-2020-322260.
116. Palmer, C.; Bik, E.M.; DiGiulio, D.B.; Relman, D.A.; Brown, P.O. Development of the human infant intestinal microbiota. *PLoS Biol* **2007**, *5*, e177, doi:10.1371/journal.pbio.0050177.
117. Yao, Y.; Cai, X.; Ye, Y.; Wang, F.; Chen, F.; Zheng, C. The Role of Microbiota in Infant Health: From Early Life to Adulthood. *Front Immunol* **2021**, *12*, 708472, doi:10.3389/fimmu.2021.708472.
118. Barko, P.C.; McMichael, M.A.; Swanson, K.S.; Williams, D.A. The gastrointestinal microbiome: a review. *J Vet Intern Med* **2018**, *32*, 9-25, doi:10.1111/jvim.14875.

119. Dominguez-Bello, M.G.; Costello, E.K.; Contreras, M.; Magris, M.; Hidalgo, G.; Fierer, N.; Knight, R. Delivery mode shapes the acquisition and structure of the initial microbiota across multiple body habitats in newborns. *Proc Natl Acad Sci U S A* **2010**, *107*, 11971-11975, doi:10.1073/pnas.1002601107.
120. Dunn, A.B.; Jordan, S.; Baker, B.J.; Carlson, N.S. The Maternal Infant Microbiome: Considerations for Labor and Birth. *MCN Am J Matern Child Nurs* **2017**, *42*, 318-325, doi:10.1097/NMC.0000000000000373.
121. Wicinski, M.; Sawicka, E.; Gebalski, J.; Kubiak, K.; Malinowski, B. Human milk oligosaccharides: health benefits, potential applications in infant formulas, and pharmacology. *Nutrients* **2020**, *12*, doi:10.3390/nu12010266.
122. Ahn, J.; Sinha, R.; Pei, Z.; Dominianni, C.; Wu, J.; Shi, J.; Goedert, J.J.; Hayes, R.B.; Yang, L. Human gut microbiome and risk for colorectal cancer. *J. Natl. Cancer Inst.* **2013**, *105*, 1907-1911, doi:10.1093/jnci/djt300.
123. Bernstein, C.N.; Forbes, J.D. Gut Microbiome in Inflammatory Bowel Disease and Other Chronic Immune-Mediated Inflammatory Diseases. *Inflamm Intest Dis* **2017**, *2*, 116-123, doi:10.1159/000481401.
124. DeGruttola, A.K.; Low, D.; Mizoguchi, A.; Mizoguchi, E. Current Understanding of Dysbiosis in Disease in Human and Animal Models. *Inflamm Bowel Dis* **2016**, *22*, 1137-1150, doi:10.1097/MIB.0000000000000750.
125. Ley, R.E.; Turnbaugh, P.J.; Klein, S.; Gordon, J.I. Microbial ecology: human gut microbes associated with obesity. *Nature* **2006**, *444*, 1022-1023, doi:10.1038/4441022a.
126. Sze, M.A.; Schloss, P.D. Looking for a signal in the noise: revisiting obesity and the microbiome. *mBio* **2016**, *7*, doi:10.1128/mBio.01018-16.
127. Manichanh, C.; Rigottier-Gois, L.; Bonnaud, E.; Gloux, K.; Pelletier, E.; Frangeul, L.; Nalin, R.; Jarrin, C.; Chardon, P.; Marteau, P., et al. Reduced diversity of faecal microbiota in Crohn's disease revealed by a metagenomic approach. *Gut* **2006**, *55*, 205-211, doi:10.1136/gut.2005.073817.
128. Nishida, A.; Inoue, R.; Inatomi, O.; Bamba, S.; Naito, Y.; Andoh, A. Gut microbiota in the pathogenesis of inflammatory bowel disease. *Clin J Gastroenterol* **2018**, *11*, 1-10, doi:10.1007/s12328-017-0813-5.
129. Frank, D.N.; St Amand, A.L.; Feldman, R.A.; Boedeker, E.C.; Harpaz, N.; Pace, N.R. Molecular-phylogenetic characterization of microbial community imbalances in human inflammatory bowel diseases. *Proc Natl Acad Sci U S A* **2007**, *104*, 13780-13785, doi:10.1073/pnas.0706625104.
130. Hansen, J.J. Immune responses to intestinal microbes in inflammatory bowel diseases. *Curr Allergy Asthma Rep* **2015**, *15*, 61, doi:10.1007/s11882-015-0562-9.
131. Nakatsu, G.; Li, X.; Zhou, H.; Sheng, J.; Wong, S.H.; Wu, W.K.; Ng, S.C.; Tsoi, H.; Dong, Y.; Zhang, N., et al. Gut mucosal microbiome across stages of colorectal carcinogenesis. *Nat Commun* **2015**, *6*, 8727, doi:10.1038/ncomms9727.

132. Velcich, A.; Yang, W.; Heyer, J.; Fragale, A.; Nicholas, C.; Viani, S.; Kucherlapati, R.; Lipkin, M.; Yang, K.; Augenlicht, L. Colorectal cancer in mice genetically deficient in the mucin Muc2. *Science* **2002**, *295*, 1726-1729, doi:10.1126/science.1069094.
133. Song, M.; Chan, A.T.; Sun, J. Influence of the gut microbiome, diet, and environment on risk of colorectal cancer. *Gastroenterology* **2020**, *158*, 322-340, doi:10.1053/j.gastro.2019.06.048.
134. Schmitt, M.; Greten, F.R. The inflammatory pathogenesis of colorectal cancer. *Nat Rev Immunol* **2021**, *21*, 653-667, doi:10.1038/s41577-021-00534-x.
135. Grivennikov, S.I.; Wang, K.; Mucida, D.; Stewart, C.A.; Schnabl, B.; Jauch, D.; Taniguchi, K.; Yu, G.Y.; Osterreicher, C.H.; Hung, K.E., et al. Adenoma-linked barrier defects and microbial products drive IL-23/IL-17-mediated tumour growth. *Nature* **2012**, *491*, 254-258, doi:10.1038/nature11465.
136. Sinha, S.R.; Haileselassie, Y.; Nguyen, L.P.; Tropini, C.; Wang, M.; Becker, L.S.; Sim, D.; Jarr, K.; Spear, E.T.; Singh, G., et al. Dysbiosis-induced secondary bile acid deficiency promotes intestinal inflammation. *Cell Host Microbe* **2020**, *27*, 659-670 e655, doi:10.1016/j.chom.2020.01.021.
137. Zackular, J.P.; Baxter, N.T.; Iverson, K.D.; Sadler, W.D.; Petrosino, J.F.; Chen, G.Y.; Schloss, P.D. The gut microbiome modulates colon tumorigenesis. *mBio* **2013**, *4*, e00692-00613, doi:10.1128/mBio.00692-13.
138. Martin, H.M.; Campbell, B.J.; Hart, C.A.; Mpofo, C.; Nayar, M.; Singh, R.; Englyst, H.; Williams, H.F.; Rhodes, J.M. Enhanced *Escherichia coli* adherence and invasion in Crohn's disease and colon cancer. *Gastroenterology* **2004**, *127*, 80-93, doi:10.1053/j.gastro.2004.03.054.
139. Bonnet, M.; Buc, E.; Sauvanet, P.; Darcha, C.; Dubois, D.; Pereira, B.; Dechelotte, P.; Bonnet, R.; Pezet, D.; Darfeuille-Michaud, A. Colonization of the human gut by *E. coli* and colorectal cancer risk. *Clin Cancer Res* **2014**, *20*, 859-867, doi:10.1158/1078-0432.CCR-13-1343.
140. Steck, N.; Hoffmann, M.; Sava, I.G.; Kim, S.C.; Hahne, H.; Tonkonogy, S.L.; Mair, K.; Krueger, D.; Pruteanu, M.; Shanahan, F., et al. *Enterococcus faecalis* metalloprotease compromises epithelial barrier and contributes to intestinal inflammation. *Gastroenterology* **2011**, *141*, 959-971, doi:10.1053/j.gastro.2011.05.035.
141. Ruiz, P.A.; Shkoda, A.; Kim, S.C.; Sartor, R.B.; Haller, D. IL-10 gene-deficient mice lack TGF-beta/Smad-mediated TLR2 degradation and fail to inhibit proinflammatory gene expression in intestinal epithelial cells under conditions of chronic inflammation. *Ann N Y Acad Sci* **2006**, *1072*, 389-394, doi:10.1196/annals.1326.023.
142. Huycke, M.M.; Abrams, V.; Moore, D.R. *Enterococcus faecalis* produces extracellular superoxide and hydrogen peroxide that damages colonic epithelial cell DNA. *Carcinogenesis* **2002**, *23*, 529-536, doi:10.1093/carcin/23.3.529.
143. Shen, X.J.; Rawls, J.F.; Randall, T.; Burcal, L.; Mpande, C.N.; Jenkins, N.; Jovov, B.; Abdo, Z.; Sandler, R.S.; Keku, T.O. Molecular characterization of mucosal adherent

- bacteria and associations with colorectal adenomas. *Gut Microbes* **2010**, *1*, 138-147, doi:10.4161/gmic.1.3.12360.
144. Dejea, C.M.; Fathi, P.; Craig, J.M.; Boleij, A.; Taddese, R.; Geis, A.L.; Wu, X.; DeStefano Shields, C.E.; Hechenbleikner, E.M.; Huso, D.L., et al. Patients with familial adenomatous polyposis harbor colonic biofilms containing tumorigenic bacteria. *Science* **2018**, *359*, 592-597, doi:10.1126/science.aah3648.
 145. Purcell, R.V.; Pearson, J.; Aitchison, A.; Dixon, L.; Frizelle, F.A.; Keenan, J.I. Colonization with enterotoxigenic *Bacteroides fragilis* is associated with early-stage colorectal neoplasia. *PLoS One* **2017**, *12*, e0171602, doi:10.1371/journal.pone.0171602.
 146. Bullman, S.; Peadarallu, C.S.; Sicinska, E.; Clancy, T.E.; Zhang, X.; Cai, D.; Neuberg, D.; Huang, K.; Guevara, F.; Nelson, T., et al. Analysis of *Fusobacterium* persistence and antibiotic response in colorectal cancer. *Science* **2017**, *358*, 1443-1448, doi:10.1126/science.aal5240.
 147. Yu, T.; Guo, F.; Yu, Y.; Sun, T.; Ma, D.; Han, J.; Qian, Y.; Kryczek, I.; Sun, D.; Nagarsheth, N., et al. *Fusobacterium nucleatum* promotes chemoresistance to colorectal cancer by modulating autophagy. *Cell* **2017**, *170*, 548-563 e516, doi:10.1016/j.cell.2017.07.008.
 148. Ito, M.; Kanno, S.; Noshō, K.; Sukawa, Y.; Mitsuhashi, K.; Kurihara, H.; Igarashi, H.; Takahashi, T.; Tachibana, M.; Takahashi, H., et al. Association of *Fusobacterium nucleatum* with clinical and molecular features in colorectal serrated pathway. *Int J Cancer* **2015**, *137*, 1258-1268, doi:10.1002/ijc.29488.
 149. Rubinstein, M.R.; Wang, X.; Liu, W.; Hao, Y.; Cai, G.; Han, Y.W. *Fusobacterium nucleatum* promotes colorectal carcinogenesis by modulating E-cadherin/beta-catenin signaling via its FadA adhesin. *Cell Host Microbe* **2013**, *14*, 195-206, doi:10.1016/j.chom.2013.07.012.
 150. Ye, X.; Wang, R.; Bhattacharya, R.; Boulbes, D.R.; Fan, F.; Xia, L.; Adoni, H.; Ajami, N.J.; Wong, M.C.; Smith, D.P., et al. *Fusobacterium nucleatum* subspecies *animalis* influences proinflammatory cytokine expression and monocyte activation in human colorectal tumors. *Cancer Prev Res (Phila)* **2017**, *10*, 398-409, doi:10.1158/1940-6207.CAPR-16-0178.
 151. Hibberd, A.A.; Lyra, A.; Ouwehand, A.C.; Rolny, P.; Lindegren, H.; Cedgard, L.; Wettergren, Y. Intestinal microbiota is altered in patients with colon cancer and modified by probiotic intervention. *BMJ Open Gastroenterol* **2017**, *4*, e000145, doi:10.1136/bmjgast-2017-000145.
 152. Zaharuddin, L.; Mokhtar, N.M.; Muhammad Nawawi, K.N.; Raja Ali, R.A. A randomized double-blind placebo-controlled trial of probiotics in post-surgical colorectal cancer. *BMC Gastroenterol* **2019**, *19*, 131, doi:10.1186/s12876-019-1047-4.
 153. Schwab, C.; Berry, D.; Rauch, I.; Rennisch, I.; Ramesmayer, J.; Hainzl, E.; Heider, S.; Decker, T.; Kenner, L.; Muller, M., et al. Longitudinal study of murine microbiota activity and interactions with the host during acute inflammation and recovery. *ISME J* **2014**, *8*, 1101-1114, doi:10.1038/ismej.2013.223.

154. Sharpton, T.; Lyalina, S.; Luong, J.; Pham, J.; Deal, E.M.; Armour, C.; Gaulke, C.; Sanjabi, S.; Pollard, K.S. Development of inflammatory bowel disease is linked to a longitudinal restructuring of the gut metagenome in mice. *mSystems* **2017**, *2*, doi:10.1128/mSystems.00036-17.
155. Mizoguchi, A. Animal models of inflammatory bowel disease. *Prog Mol Biol Transl Sci* **2012**, *105*, 263-320, doi:10.1016/B978-0-12-394596-9.00009-3.
156. Couturier-Maillard, A.; Secher, T.; Rehman, A.; Normand, S.; De Arcangelis, A.; Haesler, R.; Huot, L.; Grandjean, T.; Bressenot, A.; Delanoye-Crespin, A., et al. NOD2-mediated dysbiosis predisposes mice to transmissible colitis and colorectal cancer. *J Clin Invest* **2013**, *123*, 700-711, doi:10.1172/JCI62236.
157. McGovern, D.P.; Kugathasan, S.; Cho, J.H. Genetics of Inflammatory Bowel Diseases. *Gastroenterology* **2015**, *149*, 1163-1176 e1162, doi:10.1053/j.gastro.2015.08.001.
158. Das, S.; Batra, S.K.; Rachagani, S. Mouse model of dextran sodium sulfate (DSS)-induced colitis. *Bio Protoc* **2017**, *7*, e2515, doi:10.21769/BioProtoc.2515.
159. Dieleman, L.A.; Ridwan, B.U.; Tennyson, G.S.; Beagley, K.W.; Bucy, R.P.; Elson, C.O. Dextran sulfate sodium-induced colitis occurs in severe combined immunodeficient mice. *Gastroenterology* **1994**, *107*, 1643-1652, doi:10.1016/0016-5085(94)90803-6.
160. Nascimento-Goncalves, E.; Mendes, B.A.L.; Silva-Reis, R.; Faustino-Rocha, A.I.; Gama, A.; Oliveira, P.A. Animal Models of Colorectal Cancer: From Spontaneous to Genetically Engineered Models and Their Applications. *Vet Sci* **2021**, *8*, doi:10.3390/vetsci8040059.
161. Lorenz, E.; Stewart, H.L. Intestinal carcinoma and other lesions in mice following oral administration of 1,2,5,6-dibenzanthracene and 20-methylcholanthrene. *J Nat Cancer Inst* **1940**, *1*, 17-40, doi:10.1093/jnci/1.1.17.
162. Tanaka, T. Colorectal carcinogenesis: Review of human and experimental animal studies. *J Carcinog* **2009**, *8*, 5, doi:10.4103/1477-3163.49014.
163. Bissahoyo, A.; Pearsall, R.S.; Hanlon, K.; Amann, V.; Hicks, D.; Godfrey, V.L.; Threadgill, D.W. Azoxymethane is a genetic background-dependent colorectal tumor initiator and promoter in mice: effects of dose, route, and diet. *Toxicol Sci* **2005**, *88*, 340-345, doi:10.1093/toxsci/kfi313.
164. Reddy, B.S. Studies with the azoxymethane-rat preclinical model for assessing colon tumor development and chemoprevention. *Environ Mol Mutagen* **2004**, *44*, 26-35, doi:10.1002/em.20026.
165. Papanikolaou, A.; Wang, Q.S.; Delker, D.A.; Rosenberg, D.W. Azoxymethane-induced colon tumors and aberrant crypt foci in mice of different genetic susceptibility. *Cancer Lett* **1998**, *130*, 29-34, doi:10.1016/s0304-3835(98)00101-3.
166. Sohn, O.S.; Fiala, E.S.; Puz, C.; Hamilton, S.R.; Williams, G.M. Enhancement of rat liver microsomal metabolism of azoxymethane to methylazoxymethanol by chronic ethanol

- administration: similarity to the microsomal metabolism of N-nitrosodimethylamine. *Cancer Res* **1987**, *47*, 3123-3129.
167. Chen, J.; Huang, X.-F. The signal pathways in azoxymethane-induced colon cancer and preventive implications. *Cancer Biol Ther* **2009**, *8*, 1313-1317.
168. Chang, W.W. Histogenesis of symmetrical 1,2-dimethylhydrazine-induced neoplasms of the colon in the mouse. *J Natl Cancer Inst* **1978**, *60*, 1405-1418, doi:10.1093/jnci/60.6.1405.
169. Tanaka, T.; Kohno, H.; Suzuki, R.; Yamada, Y.; Sugie, S.; Mori, H. A novel inflammation-related mouse colon carcinogenesis model induced by azoxymethane and dextran sodium sulfate. *Cancer Sci* **2003**, *94*, 965-973, doi:10.1111/j.1349-7006.2003.tb01386.x.
170. Gheorghe, C.E.; Ritz, N.L.; Martin, J.A.; Wardill, H.R.; Cryan, J.F.; Clarke, G. Investigating causality with fecal microbiota transplantation in rodents: applications, recommendations and pitfalls. *Gut Microbes* **2021**, *13*, 1941711, doi:10.1080/19490976.2021.1941711.
171. Fiebigler, U.; Bereswill, S.; Heimesaat, M.M. Dissecting the interplay between intestinal microbiota and host immunity in health and disease: lessons learned from germfree and gnotobiotic animal models. *Eur J Microbiol Immunol (Bp)* **2016**, *6*, 253-271, doi:10.1556/1886.2016.00036.
172. Turnbaugh, P.J.; Ley, R.E.; Mahowald, M.A.; Magrini, V.; Mardis, E.R.; Gordon, J.I. An obesity-associated gut microbiome with increased capacity for energy harvest. *Nature* **2006**, *444*, 1027-1031, doi:10.1038/nature05414.
173. Rodriguez, D.M.; Benninghoff, A.D.; Aardema, N.D.J.; Phatak, S.; Hintze, K.J. Basal diet determined long-term composition of the gut microbiome and mouse phenotype to a greater extent than fecal microbiome transfer from lean or obese human donors. *Nutrients* **2019**, *11*, doi:10.3390/nu11071630.
174. Zhang, F.; Luo, W.; Shi, Y.; Fan, Z.; Ji, G. Should we standardize the 1,700-year-old fecal microbiota transplantation? *Am J Gastroenterol* **2012**, *107*, 1755; author reply p 1755-1756, doi:10.1038/ajg.2012.251.
175. Borody, T.J.; George, L.; Andrews, P.; Brandl, S.; Noonan, S.; Cole, P.; Hyland, L.; Morgan, A.; Maysey, J.; Moore-Jones, D. Bowel-flora alteration: a potential cure for inflammatory bowel disease and irritable bowel syndrome? *Med J Aust* **1989**, *150*, 604, doi:10.5694/j.1326-5377.1989.tb136704.x.
176. Weingarden, A.R.; Vaughn, B.P. Intestinal microbiota, fecal microbiota transplantation, and inflammatory bowel disease. *Gut Microbes* **2017**, *8*, 238-252, doi:10.1080/19490976.2017.1290757.
177. Fong, W.; Li, Q.; Yu, J. Gut microbiota modulation: a novel strategy for prevention and treatment of colorectal cancer. *Oncogene* **2020**, *39*, 4925-4943, doi:10.1038/s41388-020-1341-1.

178. Ortigao, R.; Pimentel-Nunes, P.; Dinis-Ribeiro, M.; Libanio, D. Gastrointestinal microbiome - what we need to know in clinical practice. *GE Port J Gastroenterol* **2020**, *27*, 336-351, doi:10.1159/000505036.
179. Wrzosek, L.; Ciocan, D.; Borentain, P.; Spatz, M.; Puchois, V.; Hugot, C.; Ferrere, G.; Mayeur, C.; Perlemuter, G.; Cassard, A.M. Transplantation of human microbiota into conventional mice durably reshapes the gut microbiota. *Sci Rep* **2018**, *8*, 6854, doi:10.1038/s41598-018-25300-3.
180. Ji, S.K.; Yan, H.; Jiang, T.; Guo, C.Y.; Liu, J.J.; Dong, S.Z.; Yang, K.L.; Wang, Y.J.; Cao, Z.J.; Li, S.L. Preparing the Gut with Antibiotics Enhances Gut Microbiota Reprogramming Efficiency by Promoting Xenomicrobiota Colonization. *Front Microbiol* **2017**, *8*, 1208, doi:10.3389/fmicb.2017.01208.
181. Hintze, K.J.; Cox, J.E.; Rompato, G.; Benninghoff, A.D.; Ward, R.E.; Broadbent, J.; Lefevre, M. Broad scope method for creating humanized animal models for animal health and disease research through antibiotic treatment and human fecal transfer. *Gut Microbes* **2014**, *5*, 183-191, doi:10.4161/gmic.28403.
182. Sarrabayrouse, G.; Landolfi, S.; Pozuelo, M.; Willamil, J.; Varela, E.; Clark, A.; Campos, D.; Herrera, C.; Santiago, A.; Machiels, K., et al. Mucosal microbial load in Crohn's disease: A potential predictor of response to faecal microbiota transplantation. *EBioMedicine* **2020**, *51*, 102611, doi:10.1016/j.ebiom.2019.102611.
183. de Meijer, V.E.; Le, H.D.; Meisel, J.A.; Puder, M. Repetitive orogastric gavage affects the phenotype of diet-induced obese mice. *Physiol Behav* **2010**, *100*, 387-393, doi:10.1016/j.physbeh.2010.04.001.
184. Kinder, J.M.; Then, J.E.; Hansel, P.M.; Molinero, L.L.; Bruns, H.A. Long-term repeated daily use of intragastric gavage hinders induction of oral tolerance to ovalbumin in mice. *Comp Med* **2014**, *64*, 369-376.
185. Bokoliya, S.C.; Dorsett, Y.; Panier, H.; Zhou, Y. Procedures for fecal microbiota transplantation in murine microbiome studies. *Front Cell Infect Microbiol* **2021**, *11*, 711055, doi:10.3389/fcimb.2021.711055.
186. Kaplan, G.G.; Ng, S.C. Understanding and preventing the global increase of inflammatory bowel disease. *Gastroenterology* **2017**, *152*, 313-321 e312, doi:10.1053/j.gastro.2016.10.020.
187. Garcia-Montero, C.; Fraile-Martinez, O.; Gomez-Lahoz, A.M.; Pekarek, L.; Castellanos, A.J.; Nogueras-Fraguas, F.; Coca, S.; Guijarro, L.G.; Garcia-Honduvilla, N.; Asunsolo, A., et al. Nutritional components in Western diet versus Mediterranean diet at the gut microbiota-immune system interplay. implications for health and disease. *Nutrients* **2021**, *13*, doi:10.3390/nu13020699.
188. D'Souza, S.; Levy, E.; Mack, D.; Israel, D.; Lambrette, P.; Ghadirian, P.; Deslandres, C.; Morgan, K.; Seidman, E.G.; Amre, D.K. Dietary patterns and risk for Crohn's disease in children. *Inflamm Bowel Dis* **2008**, *14*, 367-373, doi:10.1002/ibd.20333.

189. Tabung, F.K.; Smith-Warner, S.A.; Chavarro, J.E.; Wu, K.; Fuchs, C.S.; Hu, F.B.; Chan, A.T.; Willett, W.C.; Giovannucci, E.L. Development and validation of an empirical dietary inflammatory index. *J Nutr* **2016**, *146*, 1560-1570, doi:10.3945/jn.115.228718.
190. Fung, T.T.; McCullough, M.L.; Newby, P.K.; Manson, J.E.; Meigs, J.B.; Rifai, N.; Willett, W.C.; Hu, F.B. Diet-quality scores and plasma concentrations of markers of inflammation and endothelial dysfunction. *Am J Clin Nutr* **2005**, *82*, 163-173, doi:10.1093/ajcn.82.1.163.
191. Christ, A.; Lauterbach, M.; Latz, E. Western diet and the immune system: an inflammatory connection. *Immunity* **2019**, *51*, 794-811, doi:10.1016/j.immuni.2019.09.020.
192. Lopez-Garcia, E.; Schulze, M.B.; Fung, T.T.; Meigs, J.B.; Rifai, N.; Manson, J.E.; Hu, F.B. Major dietary patterns are related to plasma concentrations of markers of inflammation and endothelial dysfunction. *Am J Clin Nutr* **2004**, *80*, 1029-1035, doi:10.1093/ajcn/80.4.1029.
193. D'Angelo, S.; Motti, M.L.; Meccariello, R. Omega-3 and omega-6 polyunsaturated fatty Acids, obesity and cancer. *Nutrients* **2020**, *12*, doi:10.3390/nu12092751.
194. Weisshof, R.; Chermesh, I. Micronutrient deficiencies in inflammatory bowel disease. *Curr Opin Clin Nutr Metab Care* **2015**, *18*, 576-581, doi:10.1097/MCO.0000000000000226.
195. Martinez Steele, E.; Popkin, B.M.; Swinburn, B.; Monteiro, C.A. The share of ultra-processed foods and the overall nutritional quality of diets in the US: evidence from a nationally representative cross-sectional study. *Popul Health Metr* **2017**, *15*, 6, doi:10.1186/s12963-017-0119-3.
196. Srour, B.; Fezeu, L.K.; Kesse-Guyot, E.; Alles, B.; Mejean, C.; Andrianasolo, R.M.; Chazelas, E.; Deschasaux, M.; Herberg, S.; Galan, P., et al. Ultra-processed food intake and risk of cardiovascular disease: prospective cohort study (NutriNet-Sante). *BMJ* **2019**, *365*, 11451, doi:10.1136/bmj.11451.
197. Jafari, F.; Yarmand, S.; Nouri, M.; Nejad, E.T.; Ramezani, A.; Sohrabi, Z.; Rashidkhani, B. Ultra-processed food intake and risk of colorectal cancer: a matched case-control study. *Nutr Cancer* **2022**, 10.1080/01635581.2022.2125990, 1-10, doi:10.1080/01635581.2022.2125990.
198. Blanco-Rojo, R.; Sandoval-Insausti, H.; Lopez-Garcia, E.; Graciani, A.; Ordovas, J.M.; Banegas, J.R.; Rodriguez-Artalejo, F.; Guallar-Castillon, P. Consumption of ultra-processed foods and mortality: a national prospective cohort in Spain. *Mayo Clin Proc* **2019**, *94*, 2178-2188, doi:10.1016/j.mayocp.2019.03.035.
199. O'Keefe, S.J.; Chung, D.; Mahmoud, N.; Sepulveda, A.R.; Manafe, M.; Arch, J.; Adada, H.; van der Merwe, T. Why do African Americans get more colon cancer than Native Africans? *J Nutr* **2007**, *137*, 175S-182S, doi:10.1093/jn/137.1.175S.

200. Magalhaes, B.; Bastos, J.; Lunet, N. Dietary patterns and colorectal cancer: a case-control study from Portugal. *Eur J Cancer Prev* **2011**, *20*, 389-395, doi:10.1097/CEJ.0b013e328347220a.
201. Yusof, A.S.; Isa, Z.M.; Shah, S.A. Dietary patterns and risk of colorectal cancer: a systematic review of cohort studies (2000-2011). *Asian Pac J Cancer Prev* **2012**, *13*, 4713-4717, doi:10.7314/apjcp.2012.13.9.4713.
202. Bahrami, A.; Houshyari, M.; Jafari, S.; Rafiei, P.; Mazandarani, M.; Hekmatdoost, A.; Sadeghi, A.; Hejazi, E. Dietary patterns and the risk of colorectal cancer and adenoma: a case control study in Iran. *Gastroenterol Hepatol Bed Bench* **2019**, *12*, 217-225.
203. Gigic, B.; Boeing, H.; Toth, R.; Bohm, J.; Habermann, N.; Scherer, D.; Schrotz-King, P.; Abbenhardt-Martin, C.; Skender, S.; Brenner, H., et al. Associations between dietary patterns and longitudinal quality of life changes in colorectal cancer patients: the ColoCare study. *Nutr Cancer* **2018**, *70*, 51-60, doi:10.1080/01635581.2018.1397707.
204. Gupta, D.; Lis, C.G.; Granick, J.; Grutsch, J.F.; Vashi, P.G.; Lammersfeld, C.A. Malnutrition was associated with poor quality of life in colorectal cancer: a retrospective analysis. *J Clin Epidemiol* **2006**, *59*, 704-709, doi:10.1016/j.jclinepi.2005.08.020.
205. Feng, Y.L.; Shu, L.; Zheng, P.F.; Zhang, X.Y.; Si, C.J.; Yu, X.L.; Gao, W.; Zhang, L. Dietary patterns and colorectal cancer risk: a meta-analysis. *Eur J Cancer Prev* **2017**, *26*, 201-211, doi:10.1097/CEJ.0000000000000245.
206. Mehta, R.S.; Song, M.; Nishihara, R.; Drew, D.A.; Wu, K.; Qian, Z.R.; Fung, T.T.; Hamada, T.; Masugi, Y.; da Silva, A., et al. Dietary patterns and risk of colorectal cancer: analysis by tumor location and molecular subtypes. *Gastroenterology* **2017**, *152*, 1944-1953 e1941, doi:10.1053/j.gastro.2017.02.015.
207. Bresser, L.R.F.; de Goffau, M.C.; Levin, E.; Nieuwdorp, M. Gut microbiota in nutrition and health with a special focus on specific bacterial clusters. *Cells* **2022**, *11*, doi:10.3390/cells11193091.
208. Ceballos, D.; Hernandez-Camba, A.; Ramos, L. Diet and microbiome in the beginning of the sequence of gut inflammation. *World J Clin Cases* **2021**, *9*, 11122-11147, doi:10.12998/wjcc.v9.i36.11122.
209. Ananthakrishnan, A.N.; Khalili, H.; Konijeti, G.G.; Higuchi, L.M.; de Silva, P.; Korzenik, J.R.; Fuchs, C.S.; Willett, W.C.; Richter, J.M.; Chan, A.T. A prospective study of long-term intake of dietary fiber and risk of Crohn's disease and ulcerative colitis. *Gastroenterology* **2013**, *145*, 970-977, doi:10.1053/j.gastro.2013.07.050.
210. Hou, J.K.; Abraham, B.; El-Serag, H. Dietary intake and risk of developing inflammatory bowel disease: a systematic review of the literature. *Am J Gastroenterol* **2011**, *106*, 563-573, doi:10.1038/ajg.2011.44.
211. Gill, P.A.; Inniss, S.; Kumagai, T.; Rahman, F.Z.; Smith, A.M. The role of diet and gut microbiota in regulating gastrointestinal and inflammatory disease. *Front Immunol* **2022**, *13*, 866059, doi:10.3389/fimmu.2022.866059.

212. Davis, C.; Bryan, J.; Hodgson, J.; Murphy, K. Definition of the Mediterranean diet; a literature review. *Nutrients* **2015**, *7*, 9139-9153, doi:10.3390/nu7115459.
213. Ou, J.; Carbonero, F.; Zoetendal, E.G.; DeLany, J.P.; Wang, M.; Newton, K.; Gaskins, H.R.; O'Keefe, S.J. Diet, microbiota, and microbial metabolites in colon cancer risk in rural Africans and African Americans. *Am J Clin Nutr* **2013**, *98*, 111-120, doi:10.3945/ajcn.112.056689.
214. Agus, A.; Denizot, J.; Thevenot, J.; Martinez-Medina, M.; Massier, S.; Sauvanet, P.; Bernalier-Donadille, A.; Denis, S.; Hofman, P.; Bonnet, R., et al. Western diet induces a shift in microbiota composition enhancing susceptibility to adherent-invasive *E. coli* infection and intestinal inflammation. *Sci Rep* **2016**, *6*, 19032, doi:10.1038/srep19032.
215. Arnone, D.; Vallier, M.; Hergalant, S.; Chabot, C.; Ndiaye, N.C.; Moulin, D.; Aignatoaei, A.M.; Alberto, J.M.; Louis, H.; Boulard, O., et al. Long-term overconsumption of fat and sugar causes a partially reversible Pre-inflammatory bowel disease state. *Front Nutr* **2021**, *8*, 758518, doi:10.3389/fnut.2021.758518.
216. Khan, S.; Waliullah, S.; Godfrey, V.; Khan, M.A.W.; Ramachandran, R.A.; Cantarel, B.L.; Behrendt, C.; Peng, L.; Hooper, L.V.; Zaki, H. Dietary simple sugars alter microbial ecology in the gut and promote colitis in mice. *Sci Transl Med* **2020**, *12*, doi:10.1126/scitranslmed.aay6218.
217. Montrose, D.C.; Nishiguchi, R.; Basu, S.; Staab, H.A.; Zhou, X.K.; Wang, H.; Meng, L.; Johncilla, M.; Cubillos-Ruiz, J.R.; Morales, D.K., et al. Dietary fructose alters the composition, localization, and metabolism of gut microbiota in association with worsening colitis. *Cell Mol Gastroenterol Hepatol* **2021**, *11*, 525-550, doi:10.1016/j.jcmgh.2020.09.008.
218. Kawabata, K.; Kanmura, S.; Morinaga, Y.; Tanaka, A.; Makino, T.; Fujita, T.; Arima, S.; Sasaki, F.; Nasu, Y.; Tanoue, S., et al. A high-fructose diet induces epithelial barrier dysfunction and exacerbates the severity of dextran sulfate sodium-induced colitis. *Int J Mol Med* **2019**, *43*, 1487-1496, doi:10.3892/ijmm.2018.4040.
219. He, Z.; Chen, L.; Catalan-Dibene, J.; Bongers, G.; Faith, J.J.; Suebsuwong, C.; DeVita, R.J.; Shen, Z.; Fox, J.G.; Lafaille, J.J., et al. Food colorants metabolized by commensal bacteria promote colitis in mice with dysregulated expression of interleukin-23. *Cell Metab* **2021**, *33*, 1358-1371 e1355, doi:10.1016/j.cmet.2021.04.015.
220. Laudisi, F.; Di Fusco, D.; Dinallo, V.; Stolfi, C.; Di Grazia, A.; Marafini, I.; Colantoni, A.; Ortenzi, A.; Alteri, C.; Guerrieri, F., et al. The food additive maltodextrin promotes endoplasmic reticulum stress-driven mucus depletion and exacerbates intestinal inflammation. *Cell Mol Gastroenterol Hepatol* **2019**, *7*, 457-473, doi:10.1016/j.jcmgh.2018.09.002.
221. Chassaing, B.; Koren, O.; Goodrich, J.K.; Poole, A.C.; Srinivasan, S.; Ley, R.E.; Gewirtz, A.T. Dietary emulsifiers impact the mouse gut microbiota promoting colitis and metabolic syndrome. *Nature* **2015**, *519*, 92-96, doi:10.1038/nature14232.

222. Turnbaugh, P.J.; Ridaura, V.K.; Faith, J.J.; Rey, F.E.; Knight, R.; Gordon, J.I. The effect of diet on the human gut microbiome: a metagenomic analysis in humanized gnotobiotic mice. *Sci Transl Med* **2009**, *1*, 6ra14, doi:10.1126/scitranslmed.3000322.
223. Dalby, M.J.; Ross, A.W.; Walker, A.W.; Morgan, P.J. Dietary uncoupling of gut microbiota and energy harvesting from obesity and glucose tolerance in mice. *Cell Rep* **2017**, *21*, 1521-1533, doi:10.1016/j.celrep.2017.10.056.
224. Newmark, H.L.; Yang, K.; Kurihara, N.; Fan, K.; Augenlicht, L.H.; Lipkin, M. Western-style diet-induced colonic tumors and their modulation by calcium and vitamin D in C57Bl/6 mice: a preclinical model for human sporadic colon cancer. *Carcinogenesis* **2009**, *30*, 88-92, doi:10.1093/carcin/bgn229.
225. Hintze, K.J.; Benninghoff, A.D.; Ward, R.E. Formulation of the total Western diet (TWD) as a basal diet for rodent cancer studies. *J Agric Food Chem* **2012**, *60*, 6736-6742, doi:10.1021/jf204509a.
226. Benninghoff, A.D.; Hintze, K.J.; Monsanto, S.P.; Rodriguez, D.M.; Hunter, A.H.; Phatak, S.; Pestka, J.J.; Wettere, A.J.V.; Ward, R.E. Consumption of the total Western diet promotes colitis and inflammation-associated colorectal cancer in mice. *Nutrients* **2020**, *12*, doi:10.3390/nu12020544.
227. Monsanto, S.P.; Hintze, K.J.; Ward, R.E.; Larson, D.P.; Lefevre, M.; Benninghoff, A.D. The new total Western diet for rodents does not induce an overweight phenotype or alter parameters of metabolic syndrome in mice. *Nutr Res* **2016**, *36*, 1031-1044, doi:10.1016/j.nutres.2016.06.002.
228. Manach, C.; Scalbert, A.; Morand, C.; Remesy, C.; Jimenez, L. Polyphenols: food sources and bioavailability. *Am J Clin Nutr* **2004**, *79*, 727-747, doi:10.1093/ajcn/79.5.727.
229. Tsao, R. Chemistry and biochemistry of dietary polyphenols. *Nutrients* **2010**, *2*, 1231-1246, doi:10.3390/nu2121231.
230. Zhou, Y.; Zheng, J.; Li, Y.; Xu, D.P.; Li, S.; Chen, Y.M.; Li, H.B. Natural polyphenols for prevention and treatment of cancer. *Nutrients* **2016**, *8*, doi:10.3390/nu8080515.
231. Alappat, B.; Alappat, J. Anthocyanin Pigments: Beyond Aesthetics. *Molecules* **2020**, *25*, doi:10.3390/molecules25235500.
232. Khoo, H.E.; Azlan, A.; Tang, S.T.; Lim, S.M. Anthocyanidins and anthocyanins: colored pigments as food, pharmaceutical ingredients, and the potential health benefits. *Food Nutr Res* **2017**, *61*, 1361779, doi:10.1080/16546628.2017.1361779.
233. Fang, J. Classification of fruits based on anthocyanin types and relevance to their health effects. *Nutrition* **2015**, *31*, 1301-1306, doi:10.1016/j.nut.2015.04.015.
234. Cvorovic, J.; Tramer, F.; Granzotto, M.; Candussio, L.; Decorti, G.; Passamonti, S. Oxidative stress-based cytotoxicity of delphinidin and cyanidin in colon cancer cells. *Arch Biochem Biophys* **2010**, *501*, 151-157, doi:10.1016/j.abb.2010.05.019.

235. Smeriglio, A.; Barreca, D.; Bellocco, E.; Trombetta, D. Chemistry, Pharmacology and Health Benefits of Anthocyanins. *Phytother Res* **2016**, *30*, 1265-1286, doi:10.1002/ptr.5642.
236. Mattioli, R.; Francioso, A.; Mosca, L.; Silva, P. Anthocyanins: A Comprehensive Review of Their Chemical Properties and Health Effects on Cardiovascular and Neurodegenerative Diseases. *Molecules* **2020**, *25*, doi:10.3390/molecules25173809.
237. Peiffer, D.S.; Zimmerman, N.P.; Wang, L.S.; Ransom, B.W.; Carmella, S.G.; Kuo, C.T.; Siddiqui, J.; Chen, J.H.; Oshima, K.; Huang, Y.W., et al. Chemoprevention of esophageal cancer with black raspberries, their component anthocyanins, and a major anthocyanin metabolite, protocatechuic acid. *Cancer Prev Res (Phila)* **2014**, *7*, 574-584, doi:10.1158/1940-6207.CAPR-14-0003.
238. Wu, X.; Beecher, G.R.; Holden, J.M.; Haytowitz, D.B.; Gebhardt, S.E.; Prior, R.L. Concentrations of anthocyanins in common foods in the United States and estimation of normal consumption. *J Agric Food Chem* **2006**, *54*, 4069-4075, doi:10.1021/jf060300l.
239. Montrose, D.C.; Horelik, N.A.; Madigan, J.P.; Stoner, G.D.; Wang, L.S.; Bruno, R.S.; Park, H.J.; Giardina, C.; Rosenberg, D.W. Anti-inflammatory effects of freeze-dried black raspberry powder in ulcerative colitis. *Carcinogenesis* **2011**, *32*, 343-350, doi:10.1093/carcin/bgq248.
240. Harris, G.K.; Gupta, A.; Nines, R.G.; Kresty, L.A.; Habib, S.G.; Frankel, W.L.; LaPerle, K.; Gallaher, D.D.; Schwartz, S.J.; Stoner, G.D. Effects of lyophilized black raspberries on azoxymethane-induced colon cancer and 8-hydroxy-2'-deoxyguanosine levels in the Fischer 344 rat. *Nutr Cancer* **2001**, *40*, 125-133, doi:10.1207/S15327914NC402_8.
241. Wang, L.S.; Hecht, S.S.; Carmella, S.G.; Yu, N.; Larue, B.; Henry, C.; McIntyre, C.; Rocha, C.; Lechner, J.F.; Stoner, G.D. Anthocyanins in black raspberries prevent esophageal tumors in rats. *Cancer Prev Res (Phila)* **2009**, *2*, 84-93, doi:10.1158/1940-6207.CAPR-08-0155.
242. Bi, X.; Fang, W.; Wang, L.S.; Stoner, G.D.; Yang, W. Black raspberries inhibit intestinal tumorigenesis in *apc1638*^{+/-} and *Muc2*^{-/-} mouse models of colorectal cancer. *Cancer Prev Res (Phila)* **2010**, *3*, 1443-1450, doi:10.1158/1940-6207.CAPR-10-0124.
243. Huang, Y.W.; Mo, Y.Y.; Echeveste, C.E.; Oshima, K.; Zhang, J.; Yearsley, M.; Lin, C.W.; Yu, J.; Liu, P.; Du, M., et al. Black raspberries attenuate colonic adenoma development in *Apc* (Min) mice: Relationship to hypomethylation of promoters and gene bodies. *Food Front* **2020**, *1*, 234-242, doi:10.1002/fft2.45.
244. Pan, P.; Skaer, C.W.; Wang, H.T.; Stirdivant, S.M.; Young, M.R.; Oshima, K.; Stoner, G.D.; Lechner, J.F.; Huang, Y.W.; Wang, L.S. Black raspberries suppress colonic adenoma development in *ApcMin*⁺ mice: relation to metabolite profiles. *Carcinogenesis* **2015**, *36*, 1245-1253, doi:10.1093/carcin/bgv117.
245. Wang, L.S.; Kuo, C.T.; Huang, T.H.; Yearsley, M.; Oshima, K.; Stoner, G.D.; Yu, J.; Lechner, J.F.; Huang, Y.W. Black raspberries protectively regulate methylation of Wnt pathway genes in precancerous colon tissue. *Cancer Prev Res (Phila)* **2013**, *6*, 1317-1327, doi:10.1158/1940-6207.CAPR-13-0077.

246. Wang, L.S.; Kuo, C.T.; Stoner, K.; Yearsley, M.; Oshima, K.; Yu, J.; Huang, T.H.; Rosenberg, D.; Peiffer, D.; Stoner, G., et al. Dietary black raspberries modulate DNA methylation in dextran sodium sulfate (DSS)-induced ulcerative colitis. *Carcinogenesis* **2013**, *34*, 2842-2850, doi:10.1093/carcin/bgt310.
247. Lu, H.; Li, J.; Zhang, D.; Stoner, G.D.; Huang, C. Molecular mechanisms involved in chemoprevention of black raspberry extracts: from transcription factors to their target genes. *Nutr Cancer* **2006**, *54*, 69-78, doi:10.1207/s15327914nc5401_8.
248. Marin, M.; Maria Giner, R.; Rios, J.L.; Recio, M.C. Intestinal anti-inflammatory activity of ellagic acid in the acute and chronic dextrane sulfate sodium models of mice colitis. *J Ethnopharmacol* **2013**, *150*, 925-934, doi:10.1016/j.jep.2013.09.030.
249. Chen, L.; Jiang, B.; Zhong, C.; Guo, J.; Zhang, L.; Mu, T.; Zhang, Q.; Bi, X. Chemoprevention of colorectal cancer by black raspberry anthocyanins involved the modulation of gut microbiota and SFRP2 demethylation. *Carcinogenesis* **2018**, *39*, 471-481, doi:10.1093/carcin/bgy009.
250. Tu, P.; Bian, X.; Chi, L.; Gao, B.; Ru, H.; Knobloch, T.J.; Weghorst, C.M.; Lu, K. Characterization of the functional changes in mouse gut microbiome associated with increased *Akkermansia muciniphila* population modulated by dietary black raspberries. *ACS Omega* **2018**, *3*, 10927-10937, doi:10.1021/acsomega.8b00064.
251. Koh, A.; De Vadder, F.; Kovatcheva-Datchary, P.; Backhed, F. From dietary fiber to host physiology: short-chain fatty acids as key bacterial metabolites. *Cell* **2016**, *165*, 1332-1345, doi:10.1016/j.cell.2016.05.041.
252. Jakobsdottir, G.; Nilsson, U.; Blanco, N.; Sterner, O.; Nyman, M. Effects of soluble and insoluble fractions from bilberries, black currants, and raspberries on short-chain fatty acid formation, anthocyanin excretion, and cholesterol in rats. *J Agric Food Chem* **2014**, *62*, 4359-4368, doi:10.1021/jf5007566.
253. Velazquez, O.C.; Lederer, H.M.; Rombeau, J.L. Butyrate and the colonocyte. Implications for neoplasia. *Dig Dis Sci* **1996**, *41*, 727-739, doi:10.1007/BF02213129.
254. Dong, A.; Lin, C.W.; Echeveste, C.E.; Huang, Y.W.; Oshima, K.; Yearsley, M.; Chen, X.; Yu, J.; Wang, L.S. Protocatechuic acid, a gut bacterial metabolite of black raspberries, inhibits adenoma development and alters gut microbiome profiles in Apc (Min/+) mice. *J Cancer Prev* **2022**, *27*, 50-57, doi:10.15430/JCP.2022.27.1.50.
255. Wu, X.; Pittman Iii, H.E.; Hager, T.; Hager, A.; Howard, L.; Prior, R.L. Phenolic acids in black raspberry and in the gastrointestinal tract of pigs following ingestion of black raspberry. *Mol Nutr Food Res* **2009**, *53 Suppl 1*, S76-84, doi:10.1002/mnfr.200800231.
256. Rodriguez, D.M.; Hintze, K.J.; Rompato, G.; Wettore, A.J.V.; Ward, R.E.; Phatak, S.; Neal, C.; Armbrust, T.; Stewart, E.C.; Thomas, A.J., et al. Dietary supplementation with black raspberries altered the gut microbiome composition in a mouse model of colitis-associated colorectal cancer, although with differing effects for a healthy versus a Western basal diet. *Nutrients* **2022**, *14*, doi:10.3390/nu14245270.

CHAPTER 2

DIETARY SUPPLEMENTATION WITH BLACK RASPBERRIES ALTERED THE GUT MICROBIOME COMPOSITION IN A MOUSE MODEL OF COLITIS-ASSOCIATED COLORECTAL CANCER, ALTHOUGH WITH DIFFERING EFFECTS FOR A HEALTHY VERSUS A WESTERN BASAL DIET¹

Abstract

Black raspberries (BRB) are rich in anthocyanins with purported anti-inflammatory properties. However, it is not known whether dietary supplementation would ameliorate Western-diet enhanced gut inflammation and colon tumorigenesis. We employed a mouse model of colitis-associated colorectal cancer (CAC) to determine the effects of dietary supplementation with 5 to 10% (*w/w*) whole, freeze-dried BRB in male C57BL/6J mice fed either a standard healthy diet (AIN93G) or the total Western diet (TWD). In a pilot study, BRB suppressed colitis and colon tumorigenesis while also shifting the composition of the fecal microbiome in favor of taxa with purported health benefits, including *Bifidobacterium pseudolongum*. In a follow-up experiment using a 2 × 2 factorial design with AIN and TWD basal diets with and without 10% (*w/w*) BRB, supplementation with BRB reduced tumor multiplicity and increased colon length, irrespective of the basal diet, but it did not apparently affect colitis symptoms, colon inflammation or mucosal injury based on histopathological findings. However, BRB intake increased alpha diversity,

¹ This chapter has been previously published in: Rodriguez, D.M.; Hintze, K.J.; Rompato, G.; Wettere, A.J.V.; Ward, R.E.; Phatak, S.; Neal, C.; Armbrust, T.; Stewart, E.C.; Thomas, A.J., Benninghoff, A.D. Dietary supplementation with black raspberries altered the gut microbiome composition in a mouse model of colitis-associated colorectal cancer, although with differing effects for a healthy versus a Western basal diet. *Nutrients* 2022, 14, doi:10.3390/nu14245270. Author Contributions: Conceptualization, D.M.R., K.J.H. and A.D.B.; methodology, D.M.R., K.J.H., G.R., R.E.W., A.J.V., A.T., S.P., C.N., T.A., and A.D.B; data curation, D.M.R., K.J.H., S.P., and A.D.B.; writing—original draft preparation, D.M.R. and A.D.B.; writing—review and editing, D.M.R., K.J.H., C.N., and A.D.B.; visualization, D.M.R. and A.D.B; project administration, A.D.B.; funding acquisition, A.D.B.

altered beta diversity and changed the relative abundance of Erysipelotrichaceae, Bifidobacteriaceae, Streptococcaceae, Rikenellaceae, Ruminococcaceae and Akkermansiaceae, among others, of the fecal microbiome. Notably, changes in microbiome profiles were inconsistent with respect to the basal diet consumed. Overall, these studies provide equivocal evidence for in vivo anti-inflammatory effects of BRB on colitis and colon tumorigenesis; yet, BRB supplementation led to dynamic changes in the fecal microbiome composition over the course of disease development.

2.1. Introduction

Inflammatory bowel disease (IBD) encompasses a group of disorders characterized by chronic intestinal inflammation, including ulcerative colitis (UC) and Crohn's disease (CD). IBD is an idiopathic disorder, with causative factors linked to heredity, genetics and environmental risk factors. While the risk factors for both conditions are similar [1,2], UC is characterized by inflammation limited to the colon, whereas CD may involve any part of the digestive tract. As of 2015, an estimated 3.1 million adults in the United States had been diagnosed with IBD, according to the Centers for Disease Control and Prevention [3], and recent reports indicate that global prevalence of IBD has increased markedly in the past thirty years [4].

Patients diagnosed with IBD have a two to six times higher risk of developing colorectal cancer (CRC) compared to healthy individuals [5], and they tend to be affected at a younger age than those who develop sporadic CRC [6]. The National Cancer Institute estimated 149,500 new cases of colorectal cancer in 2021, placing this disease as the fourth most diagnosed cancer in the United States [7]. Colorectal cancer is estimated to be the third leading cause of cancer death in the United States, with approximately 52,980 deaths reported in 2021. The risk of developing colitis-associated colorectal cancer (CAC) begins to increase eight to ten years after the onset of inflammation and increases with prolonged intestinal inflammation [6]. Other factors contributing to the risk of developing CRC include African American descent, male sex, metabolic status,

excessive consumption of red or processed meat, alcohol and/or tobacco habits and chronic inflammation associated with IBD, among others [8]. However, IBD and CRC risk can be reduced with changes in lifestyle, such as regular physical activity, consumption of a prudent diet and intake of non-steroid anti-inflammatory drugs in elderly populations [6].

Diet is a major risk factor affecting the pathogenesis of IBD and CRC. The typical American diet is energy dense and nutrient poor, characterized by high proportions of red meat, animal fat and sugar coupled with low fiber intake [9]. Chronic deficiencies of essential micronutrients typified by the Western dietary pattern can lead to chronic disease by disrupting metabolic and other biological pathways [10]. To better understand the contribution of a Western dietary pattern to the development of colon inflammation and CAC, our group previously developed a novel basal diet that emulates typical American nutrient intakes, including macro- and micronutrient profiles, on an energy-density basis for rodents [11]. In repeated studies using this total Western diet (TWD), we have shown that chronic consumption of this Western nutrition profile in mice markedly exacerbates colitis and promotes development of colorectal tumors, likely through activation of pro-inflammatory and aberrant immune response pathways in the colon mucosa [12], although without triggering systemic inflammation or metabolic syndrome [13].

Anthocyanins are water-soluble compounds that impart blue, red and purple colors to certain fruits and vegetables, such as cranberries, blueberries, blackberries, strawberries, black currant, bilberry and purple corn [14]. Anthocyanins are characterized as either the anthocyanin glycosides (e.g., cyanidin-3-glucoside) or the sugar-free anthocyanidin aglycone. Because anthocyanins are poorly absorbed in the gastrointestinal tract, a large fraction of these bioactive chemicals reach the colon and are available for microbial metabolism to generate the more bioavailable metabolite protocatechuic acid, which has reported antioxidant, anti-diabetic, anti-proliferative and pro-apoptotic capabilities [15]. Moreover, researchers have reported two

anthocyanidins, delphinidin and cyanidin, exhibiting cytotoxicity toward metastasizing colorectal cancer cells via oxidative stress [16].

The black raspberry (*Rubus occidentalis*) is a good source of vitamins A, C, E, calcium, folic acid and fiber, as well as an abundant source of bioactive phytochemicals, including anthocyanins, ellagic acid, ferulic acid, ellagitannins and other bioflavonoids [17]. Anthocyanins comprise the most abundant polyphenol class in black raspberries (BRB), with an estimated total concentration of 669 mg anthocyanin per 100 g berries [18]. The average American is estimated to consume 12.5 mg of anthocyanins a day [18]. Black raspberries (BRB) contain phytochemicals regularly metabolized by host microbes, generating secondary metabolites that exhibit antioxidant, antiproliferation and pro-apoptotic properties [19,20]. Cyanidin-3-*O*-glucoside is the most abundant anthocyanin present in fruits and veggies [21]. In one report, the consumption of a diet enriched with 5% BRB (*w/w*) resulted in reduced cell proliferation, inflammation and angiogenesis and increased apoptosis in a rat model of esophageal cancer [22]. BRB consumption has been shown to modulate inflammatory pathways in the colon by reducing expression of TNF and IL-1 β , as well as other key mediators of inflammation, such as NF κ B and COX-2 [23]. In addition, BRB promotes the production of short-chain fatty acids (SCFAs) via microbe fermentation, as seen in rats [24]. Various studies have also observed a shift in the gut microbiota composition due to BRB consumption promoting beneficial gut bacteria growth, such as *Akkermansia muciniphila*, *Bifidobacterium spp.* and *Lactobacillus spp.*, while inhibiting pathogenic strains, such as *Helicobacter pylori* [25,26].

When considering the role of diet in modulating gut inflammation and development of intestinal cancer, one cannot ignore the potential involvement of the gut microbiome, that is, the collection of thousands of diverse organisms within the intestinal tract that help maintain gut homeostasis [27]. However, dysbiosis can occur when certain taxa become aberrantly abundant, or pathogenic bacteria are present. Importantly, the gut microbiome modulates physiological

functions related to cancer development, including inflammation, cell proliferation, apoptosis and angiogenesis. In the pathogenesis of IBD, a shift in the microbiota population, triggered by a combination of genetic and environmental factors, leads to dysregulation of the immune system, disruption of the epithelial barrier, increased production of pro-inflammatory and pro-tumorigenic cytokines, metabolic activation of various mutagens, loss of protective bacteria species and accumulation of opportunistic pathobionts (reviewed in Refs [reviewed in 28,29]). The gut microbiomes of IBD patients are distinct from healthy controls, with consistent reduced gut microbial biomass, decreased diversity and richness of the microbial community and/or altered relative abundance of members of the dominant phyla, Firmicutes (synonym Bacillota) and Bacteroidetes (synonym Bacteroidota) [30-33]. In a longitudinal study assessing the structure and function of the mouse microbiome during active colitis and during a subsequent period of recovery, Schwab et al. [34] determined that changes in the microbiome caused by exposure to the colonic irritant dextran sodium sulfate (DSS) were temporary, with functional recovery of the metagenome occurring shortly after cessation of DSS exposure and the taxonomic composition returning within 25 days. These findings illustrate the remarkable ability of the gut microbiome to recover host-microbiota homeostasis after gut injury in this chemically induced animal model of UC.

Although there is evidence pointing to health benefits of BRB consumption for suppression of colitis and colon tumor development, it is not known whether BRB intake in the context of a Western diet would affect gut inflammation and CAC or whether BRB would alter the composition of the microbiome. Thus, the objective of this study was to determine the effects of dietary intervention with whole freeze-dried black raspberries on the dynamic composition of the gut microbiome, inflammation status and colon tumorigenesis in mice fed a Western diet. Based on prior evidence for protective effects of BRB reported in the literature, we hypothesized a dietary supplementation with BRB would improve recovery from colon injury and prevent

progression to CAC, and this effect would be more pronounced in mice consuming a Western diet. We also hypothesized that consumption of BRB would result in changes to the gut microbiota composition, shifting the population in favor of commensal species that promote gut homeostasis.

2.2. Materials and Methods

2.2.1. Chemicals and Reagents

Azoxymethane (AOM) was purchased from Sigma-Aldrich (St. Louis, MO, USA; CAS No. 25843-45-2). Dextran sodium sulfate (DSS; reagent grade at mol. wt. ~40 kDa) was obtained from Thermo Fisher Scientific (Waltham, MA, USA). All other chemicals were obtained from general laboratory suppliers at reagent grade. Other reagents and kits are described below.

2.2.2. Animals and Experimental Diets

The Utah State University Institutional Animal Care and use Committee approved all procedures for the handling and treatment of mice used for this study (protocol 2818). Mice were housed in a specific pathogen-free vivarium in the Laboratory Animal Research Center (LARC) at Utah State University, an AAALAC-approved facility. To be consistent with previous work on the role of the TWD in CAC [12,13,35,36], male C57BL/6J mice were obtained from Jackson Laboratories (Bar Harbor, ME) at five weeks of age. Mice were group-housed in sterile microisolator cages with Bed-o'Cobs[®] ¼ bedding (Andersons, Cincinnati, OH, USA) supplied with HEPA-filtered microisolator cages in an IVC Air Handling Solutions ventilated housing system (Tecniplast, Buguggiate, Italy). Mice were maintained in a 12:12 h dark:light cycle, with 50% humidity and in a specific pathogen-free vivarium with temperature ranging from 18 to 23 °C. Following one week of quarantine, mice were randomized and allocated to one of four experimental groups, as outlined below. Ear notching was performed to allow for repeated

individual mouse weight measurements weekly. Mice were provided with autoclaved drinking water *ad libitum* throughout the study.

Experimental diets were formulated by Envigo (Hackensack, NJ; formerly Harlan-Teklad), as outlined in Table 2.S1, obtained from the vendor as one lot and maintained at 4 °C for the duration of the study. The two basal diets included AIN93G (AIN, cat. no. TD.160421), formulated to promote rodent health with energy density of 3.8 kcal/g, or the total Western diet (TWD, cat. no. TD.160422, formulation previously published [11]) with energy density of 4.4 kcal/g, designed to emulate typical U.S. intakes of macro- and micronutrients on an energy density basis. Fresh food was provided twice a week, and food consumption was monitored at each change (including accounting for spillage into the cage).

Black raspberry (*Rubus occidentalis*, Munger variety) powder (BRB) was obtained from Berri Health (Corvallis, OR). This powder consists of 6.94% (w/w) total phenolics with 3.72% (w/w) total anthocyanins with cyanidin-3-rutinoside as the dominant form and small quantities of cyanidin-3-glucoside, cyanidin-3-xyloside and cyanidin-3-arabinoside (via Certificate of Analysis and personal communication, J. Stephen Dunfield, President, Berri Products LLC). Other phenolics and flavonoids include caffeic acid, ellagic acid and quercetin. AIN and TWD basal diets were supplemented with 5 or 10% (w/w) BRB, with adjustments made to equalize total carbohydrates with respect to the appropriate basal diet. Given an estimated daily food intake of 3.5 g per day per mouse (equating to 13.3 or 15.1 kcal/day for AIN and TWD diets, respectively), this concentration of BRB will deliver approximately 7 to 13 mg anthocyanins per mouse per day, for 5 and 10% supplementation levels, respectively. These concentrations correspond to energy densities of 489 and 978 µg/kcal for the AIN basal diet or 432 and 864 µg/kcal for the TWD basal diet for the high and low BRB concentration, respectively. The black raspberry Munger variety was estimated to provide 394 mg total anthocyanins per 100 g serving, or 190 µg/kcal for one serving per day with a total caloric intake of 2070 kcal/day (U.S. average). Thus, the 5% and

10% BRB supplementation for the mouse diets would approximate two or five servings, respectively, of whole BRB fruit per day on an energy density basis.

2.2.3. *Experiment Designs*

2.2.3.1. Pilot Study (Experiment A)

A pilot study was performed to explore the potential benefit of dietary supplementation with black raspberries in mice fed the TWD. Experimental groups included 1) AIN93G basal diet alone as negative control (AIN), 2) TWD basal diet alone as positive control for promotion of colitis and CAC (TWD), 3) TWD supplemented with 5% (*w/w*) BRB (TWD+5% BRB) and 4) TWD supplemented with 10% (*w/w*) BRB (TWD+10% BRB). At five weeks of age, mice were assigned to these diet groups using a random block design to equalize group body weight at the start of the experiment ($n = 32$ per diet group) (Figure 2.S1a). Mice were provided either the AIN diet (group 1) or the TWD diet (groups 2–4) for seven days, at which time the BRB-supplemented diets were introduced (groups 3–4). On day 21, all mice were dosed *i.p.* with 10 mg/kg AOM prepared in sterile PBS and provided 1% (*w/v*) DSS, a colonic irritant, in their drinking water for 10 days, followed by plain drinking water for the remainder of the study. On experiment days 33 and 45, mice were temporarily placed in new cages blinded to treatment, and then, the disease activity index (DAI) was determined, as previously described [12]. On day 105, body composition was determined for all mice using an MRI scan (EchoMRI-700; EchoMRI, Houston, TX, USA). On day 112, mice were euthanized by CO₂ asphyxiation and necropsied. Colons were isolated ($n = 23$ to 26 per group), flushed with PBS, cut open longitudinally and stored at 4 °C in 70% (*v/v*) ethanol until further assessment of colon tumors, as described previously [12]. A randomly selected subset of colon tissues ($n = 6$ per group) was preserved in 10% phosphate-buffered formalin for histopathological classification of cancer stage.

2.2.3.2. BRB Supplementation with Standard and Western Basal Diets (Experiment B)

To determine the effect of BRB supplementation on colitis and CAC in mice fed either a standard diet or a Western diet, a 2×2 factorial study design was used with *basal diet* and *BRB supplementation* as the two main factors with the following experimental groups: (1) AIN control (AIN/CON), (2) AIN + 10% BRB (AIN/BRB), (3) TWD control (TWD/CON) and (4) TWD+10% BRB (TWD/BRB). At five weeks of age, mice were assigned to these diet groups using a random block design to equalize group body weight at the start of the experiment ($n = 32$ per diet group) (Figure 2.S1b). Mice were provided either the AIN diet (groups 1,3) or the TWD diet (groups 2,4) for seven days, at which time BRB-supplemented diets were introduced (groups 3–4). On day 21, all mice were dosed intraperitoneally with 10 mg/kg AOM prepared in sterile PBS and provided 1% (*w/v*) DSS in their drinking water for 10 days, followed by plain drinking water for the remainder of the study. On experiment days 33 and 45, mice were temporarily placed in new cages blinded to treatment, and then, the DAI was determined, as previously described [12]. Additionally, on days 33 and 45, a randomly selected subset of mice ($n = 9$ to 12 per group) was euthanized by CO₂ asphyxiation, necropsied and their colon tissues preserved in 10% phosphate-buffered formalin for histopathological assessment of epithelial inflammation and mucosal injury by a board-certified veterinary pathologist at the Utah Veterinary Diagnostic Laboratory, as previously described [12]. On day 113, body composition was determined for all mice using an MRI scan (EchoMRI-700). On day 115, the remaining mice were euthanized by CO₂ asphyxiation and necropsied, as described above. Colons were isolated ($n = 23$ to 26 per group), flushed with PBS, cut open longitudinally and stored at 4 °C in 70% (*v/v*) ethanol until further assessment of colon tumors, as described previously [12]. A randomly selected subset of colon tissues ($n = 6$ per group) was preserved in 10% phosphate-buffered formalin for histopathological verification of cancer stage.

2.2.4. Microbiota Profiling by 16S rRNA Sequencing

2.2.4.1. Microbiome Sequencing (Experiment A)

For experiment A, fresh fecal samples were collected by cage on day 21 (pre-DSS), day 33 (colitis), day 45 (recovery) and day 112 (terminal) and stored at -80°C until analysis. Obtaining fecal samples on a per cage basis avoided the potential confounding effects of coprophagia among co-housed mice for microbiome analyses. The complete methods for sample preparation, sequencing and data processing are described by Rodriguez et al. [36]. Briefly, the QIAamp DNA Stool Mini Kit (Qiagen, Frederick, MD, USA) was used to isolate DNA from mouse fecal pellets according to the manufacturer's protocol, with the added step of mechanical disruption with zirconia/silica beads (Thermo Fisher) for 5 min. DNA concentration and sample purity were determined by UV spectrophotometry (NanoDrop 2000, Thermo Fisher). All DNA samples were then diluted to 20 ng/mL in tris-EDTA buffer (TE, pH 8.0). Fecal DNA was then amplified using the Roche High Fidelity dNTP Pack according to the manufacturer's protocol (Millipore Sigma, St. Louis, MO, USA). Samples were assigned a barcoded primer and a universal primer; the barcoded primers were directed against the V3 region of the 16s rRNA [36]. PCR amplification, product purification and product pooling prior to sequencing were performed as previously described [36]. Samples were sequenced using an Ion Personal Genome Machine (PGM) sequencer with a 318 Chip kit and an Ion PGM Hi-Q View OT2 kit for library preparation (Thermo Fisher) by the USU Center for Integrated BioSystems Genomics Core Laboratory. Sequences were processed using QIIME [37], with mapping of sequences to the GreenGenes OTU database (gg_13_8_otus), as previously described [36]. File 2.S1 provides the resulting count data at the species level.

2.2.4.2. Microbiome Sequencing (Experiment B)

For experiment B, fresh fecal samples were collected by cage on day 21 (pre-DSS), day 33 (colitis), day 45 (recovery) and day 115 (terminal) and stored at -80°C until analysis. Because

experiment B was performed at a later date than the pilot study, during which time the sequencing instrumentation within the Genomics Core Laboratory had been upgraded, different materials, methods, instrumentation and data processing steps were used for microbiome sequencing of samples. The DNeasy PowerSoil kit (Qiagen) was used for DNA isolation per the supplier's protocol. DNA concentrations and sample purity were determined using a UV spectrophotometer (NanoDrop 2000). All DNA samples were then diluted to 20 ng/mL in tris-EDTA buffer (TE, pH 8.0). Isolated fecal DNA was amplified using the Platinum HS PCR kit (Thermo Fisher). Forward and reverse primers, 16S-515F and 16S-806R, targeting the V4 region of the 16S rRNA [38] were obtained from Integrated DNA Technologies (Coralville, IA). PCR amplification was performed using the following protocol: 3 min at 94 °C; 35 cycles of 94 °C for 45 s, 50 °C for 60 s, 72 °C for 90 s; final annealing at 72 °C for 10 min; and hold at 4 °C. Next, each sample was assigned a set of barcoding primers, and a second round of PCR amplification was performed using the following protocol: 15 s at 94 °C; 10 cycles at 94 °C for 15 s, 72 °C for 60 s, 72 °C for 90 s; final annealing at 72 °C for 3 min; and hold at 4 °C. Electrophoresis was performed with the amplicons to confirm a product size of 254 bp.

Lastly, the final PCR products were purified using Agencourt AMPure beads (Beckman Coulter, Indianapolis, IN, USA) according to the manufacturer's instructions. Briefly, PCR products were diluted in the AMPure bead solution, incubated at room temperature for 5 min and then captured using a 96-well magnet for 2 min. The supernatant was removed, and then, the PCR products were rinsed twice with 70% (v/v) ethanol. DNA was eluted from the beads using TE buffer, and DNA concentrations were reconfirmed by fluorescence spectroscopy (Fluorometer 9300-002, Turner BioSystems, Sunnyvale, CA, USA) using the Quant-IT Picogreen dsDNA Assay (Thermo Fisher). Samples were diluted to 1 ng/ μ L, pooled and stored at -20 °C until sequencing at the Genomics Core Laboratory. Sequencing was performed using the MiSeq reagent kit v2 for a paired end 500 cycle (2 \times 250 bp) (Illumina, San Diego, CA, USA).

Microbiota sequences were processed using QIIME 2 [39] and DADA2 [40]. The DADA2 R package implements the full amplicon workflow (filtering, dereplication, chimera identification, merging paired end reads) and generates an amplicon sequence variant (ASV) table and representative sequences. To assign taxonomy, the Qiime feature-classifier classify-sklearn command was used with a classifier pre-trained for the V4 region, silva-138-99-515-806-nb-classifier.qza, and the most recent release of the Silva database (138 SSU) [41]. File 2.S2 provides the resulting count data at the species level.

2.2.5. Microbiome Sequencing Data Analysis

For all microbiome analyses, the cage was considered the biological unit, which avoided the potential confounding effects of coprophagia of mice that shared housing. For experiment A, the taxonomy and alpha and beta diversity analyses were performed using `core_diversity_analyses.py` script, as previously described [36]. For experiment B, sequence data were analyzed using Microbiome Analyst Marker Data Profiling module [42], with minimum count of four, a low count filter of 20% prevalence and low variance filter of 10% based on the inter-quantile range. The sequencing libraries were rarefied to the minimum library size with total sum scaling. For experiment A, sequencing data were analyzed for an effect of experimental diet within each time point. For experiment B, data were similarly analyzed for effect of treatment within a time point as well as longitudinally across time points within a treatment. Measures of α -diversity included the number of OTUs or ASVs (total number sequenced), Chao1 richness (number of species represented) and Shannon index (weighted abundance of species present). Beta diversity was determined using unweighted (qualitative measure, which is sensitive to low abundance features) and weighted (accounts for abundance of species) unifrac distance and was represented as principal coordinate plots (PCoA) of the first two coordinates. A permanova p value <0.01 for β -diversity was considered statistically significant. Taxonomic relative abundance data were analyzed using metagenomeSeq with a zero-inflated Gaussian fit, and false discovery

rate-adjusted p -value < 0.05 was considered statistically significant. ClustVis was used to perform unsupervised hierarchical cluster analyses using relative abundance data family taxonomic level [43]. Heat trees were constructed to show the relationships among differentially abundant taxa for selected pairwise comparisons. Heat tree analysis leverages the hierarchical structure of taxonomic classifications to quantitatively (using the median abundance) and statistically (using the non-parametric Wilcoxon rank sum test) depict taxonomic differences between microbial communities.

For experiment B only, heat trees were generated for pairwise comparisons by experimental diet or time point. The heat tree analysis leverages the hierarchical structure of taxonomic classifications to quantitatively (using median abundance) and statistically (non-parametric Wilcoxon rank sum test) depict taxonomic differences between microbial communities. Additionally, Tax4Fun was employed for functional potential prediction based on minimum 16S rRNA sequence similarity [44]. The resulting gene abundance tables were processed using the Microbiome Analyst Shotgun Data Profiling module with a minimum count of four, a low count filter of 20% and a low variance filter at 10% based on inter-quartile range. Data were total sum scaled and then analyzed by metagenomeSeq (zero-inflated Gaussian distribution with FDR $p < 0.05$) to identify differentially abundant KEGG orthology terms. The list of significant terms was then subject to pathway association analysis using the *globaltest* algorithm to identify significantly enriched functional pathways ($p < 0.05$). Additionally, to compare the shift in microbiome composition longitudinally in response to BRB intervention, both the taxonomy and functional gene sets were analyzed by non-metric multi-dimensional scaling (NDMS) using the Bray–Curtis dissimilarity method and visualized as principal coordinate plots with the first two coordinates.

2.2.6. Fecal Short-Chain Fatty Acid Analysis

Six acid standards (acetic, propionic, butyric, isobutyric, isovaleric and valeric acids) were prepared, and fecal materials from experiment B were processed for short-chain fatty acid analysis by gas chromatography using a Shimadzu GC2010 equipped with a ZB-FFAP column (30 m × 0.52 mm ID × 1.0 μm film thickness; Phenomenex, Torrance, CA, USA) and a flame ionization detector, as previously described [45].

2.2.7. Other Data Analyses

Statistical analyses for tumor incidence were performed using Fisher's exact test, followed by a Bonferroni adjustment to correct for multiple testing (Prism v. 8, GraphPad Software, San Diego, CA). Other data were analyzed using a generalized linear mixed model (GLMM) with cage as a nested, random factor using the restricted maximum likelihood (REML) estimation and the Tukey HSD post hoc test for multiple comparisons (JMP v.16.2.0, SAS Institute, Cary, NC, USA). For experiment A, the main effect of treatment was determined within each time point. For experiment B, the main effects of basal diet, BRB supplementation and diet*BRB interaction were determined within each time point. Suspected outliers were verified using the robust outlier test (ROUT) with a conservative Q value of 1% (Prism), meaning that there is a ≤1% chance of excluding a data point as an outlier in error. Data that did not meet the equal variance assumption were log₁₀ or square root transformed. For data that were not normally distributed or for which a transformation did not equalize variance, a non-parametric Steel–Dwass test was employed (JMP) to assess the main effects of diet and BRB intervention (no interaction test possible). However, if the results of the non-parametric Steel–Dwass tests were not different from the original GLMM analyses with respect to significant outcomes, the original GLMM test results are reported (with interactions for Experiment B) because the mixed model accounts for potential cage effects. A significant effect of the test variable was inferred when the adjusted *p* value was <0.05. Food and energy intakes were assessed on a per cage basis.

2.3. Results

2.3.1. Pilot Study with BRB Supplementation (Experiment A)

2.3.1.1. Food and Energy Intakes, Body Weight, Lean and Fat Mass, Glucose Tolerance (Experiment A)

In the pilot study, mice fed the TWD basal diet consumed fewer grams of food compared to those mice provided the AIN diet, although their energy intakes were not different (Figure 2.S2a,b), as has been observed previously [12]. The energy intake was significantly greater for mice provided TWD supplemented with either 5% or 10% BRB, corresponding to a significant concentration-dependent increase in final body weight (Figure 2.S2c) attributed to a significant increase in fat mass (Figure 2.S2e). However, the increase in body weight and altered body composition were not associated with impaired glucose metabolism, as glucose tolerance was not affected by BRB supplementation (Figure 2.S2f).

2.3.1.2. Symptoms of Colitis and Colon Tumor Outcomes (Experiment A)

Symptoms of colitis were assessed on experiment days 33 and 45 at the colitis and recovery time points, respectively (Figure 2.S1a). As expected, consumption of the TWD increased the DAI score during active colitis as compared to mice fed the AIN diet, and this response persisted to the recovery time point twelve days later (Figure 2.1a,b). Addition of BRB to the diet reduced TWD-enhanced colitis symptoms in a concentration-dependent manner, most notably by the recovery time point, at which time the symptoms of colitis in mice fed TWD with either 5% or 10% BRB were not different from mice fed the AIN diet.

At the end of the study, colon tumor incidence was not significantly different among the experimental groups (Figure 2.1c). However, as anticipated, mice fed TWD had more colon tumors, larger tumors and a significantly higher tumor burden than their AIN-fed counterparts (Figure 2.1d–f). Remarkably, supplementation of the TWD with 5% or 10% BRB suppressed

colon tumorigenesis, leading to fewer and smaller tumors and an overall reduced tumor burden, similar to mice provided the basal AIN diet (Figure 2.1d–f).

2.3.1.3. Microbiome Assessment (Experiment A)

A total of 9.9×10^6 amplicons were sequenced. After filtering for length, quality, and abundance and inspection for chimeras, 7.2×10^6 sequences were assigned to OTUs using the `pick_open_ref_otus` command (GreenGenes database `gg_13_8_otus`) for an average of 62,073 sequences per sample assigned to 1415 OTUs. The sequencing depth for diversity analyses was set to ~5500 sequences (Figure 2.S3).

Dietary supplementation with 5% or 10% black raspberry shifted the composition of the gut microbiome, primarily during the active colitis phase in this disease model (Figures 2.S4 and 2.S5, File 2.S3). At the phylum taxonomic level, the relative abundance of Actinobacteria was lower in mice fed the TWD basal diet at 13.6% compared to those fed the AIN basal diet at 20% during active colitis, although this difference was not statistically different. BRB supplementation significantly elevated the abundance of Actinobacteria in the fecal microbiome from 13.6% in TWD-fed mice to 21 to 23% in TWD-fed mice supplemented with 5% or 10% BRB. This change in Actinobacteria during colitis was largely attributed to shifts in the population of *Bifidobacterium pseudolongum* ($p = 0.0041$ and 0.0028 for 5 and 10% BRB diets, respectively) in the Bifidobacteriaceae family (Figure 2.S5b). However, also within the Actinobacteria phylum, the abundance of the family Coriobacteriaceae was suppressed with BRB supplementation during both active colitis ($p = 0.0587$ and 0.0048 for 5 and 10% BRB, respectively) and at the terminal time point (BRB treatments combined, $p = 0.0419$). Within the Bacteroidetes phylum (recently renamed Bacteroidota), a substantial decrease in Bacteroidaceae was observed, from 2.4% of the fecal microbiome in mice provided TWD only to just 0.23 to 0.32% in mice fed TWD + 5% or 10% BRB, respectively ($p = 1.68 \times 10^{-7}$ and 6.14×10^{-3} , respectively; Figure 2.S5b). Within the Firmicutes phylum (recently renamed Bacillota), the relative abundance of Erysipelotrichaceae

was elevated during colitis in mice provided TWD+5%BRB compared to those fed TWD only ($p = 3.25 \times 10^{-9}$), whereas the Ruminococcaceae family was less abundant in mice fed either TWD + 5% or 10% BRB compared to TWD only ($p = 0.0052$ or $=0.0023$, respectively). Through recovery and to the terminal time point, most of the BRB-induced changes in the microbiome population had resolved with few persistent shifts (e.g., Ruminococcaceae) with a few additional taxa responsive to the TWD + 5% BRB treatment compared to TWD only (e.g., Dehalobacteriaceae, Lachnospiraceae, Peptostreptococcaceae and Rikenellaceae) (File 2.S3). The ratio of Firmicutes:Bacteroidetes was variable across treatment groups and time points, with the only apparent significant difference noted during colitis when comparing the TWD versus the TWD + 5% BRB diet group ($p = 0.0079$) (Figure 2.S5c).

Alpha diversity was determined as the number of observed OTUs, the Chao1 index (count of species) and the Shannon index (accounts for proportional abundance) (Figure 2.S6). No significant differences in alpha diversity for observed OTUs or Chao1 index were noted among treatment groups at any of the study time points. However, at the pre-DSS time point, the Shannon alpha diversity was elevated in mice fed TWD+5% BRB compared to the AIN control (Figure 2.S6c). During active colitis, Shannon alpha diversity was significantly reduced in mice provided TWD + 5% or 10% BRB compared to TWD only. Yet, by the terminal time point, alpha diversity was elevated in mice fed TWD+5% BRB compared to TWD only but not the higher 10% concentration (Figure 2.S6c). When considering the differences in taxa represented in the fecal microbiome populations, more substantial distinctions were observed particularly for unweighted unifracs beta diversity, a measurement that favors the contribution of rare taxa (Figure 2.2). Following three weeks of exposure to the experimental diets, a clear separation of treatment groups by BRB supplementation was evident for unweighted unifracs distances (permanova $p = 0.009$). These measurably distinct microbiomes for those mice exposed or not exposed to BRB were evident during active colitis (permanova $p = 0.015$), recovery from gut injury ($p = 0.005$)

and colon tumorigenesis at the terminal time point (permanova $p = 0.002$) (Figure 2.2a).

Alternatively weighted unfrac distances, which account for the relative abundance of taxa, were not remarkably different ($p > 0.01$) (Figure 2.2b).

2.3.2. BRB Supplementation with Standard and Western Basal Diets (Experiment B)

2.3.2.1. Food and Energy Intake, Body Weight and Composition, Organ and Cecum Weight (Experiment B)

In control groups, the total food intake for mice fed AIN or TWD basal diets was consistent, leading to a higher overall total energy intake in mice fed the TWD due to that diet's higher energy density (Figures 2.3a,b and 2.S7). A significant interaction with the BRB diet was evident ($p = 0.0002$), with food intake at a significantly higher rate for mice fed TWD/BRB compared to their TWD/CON counterparts ($p < 0.0001$), leading to an increased energy intake of 33% compared to AIN/BRB-fed mice ($p < 0.0001$) and AIN/CON ($p < 0.0001$). Although a trend of increased body weight of mice fed the TWD/BRB diet compared to all other groups was evident throughout most of the study period, particularly following the AOM+DSS exposure period days 21–31 (Figure 2.3c), the final body weights were not significantly different among the experimental groups by day 115 at the study end (Figure 2.3d). Body composition determined by EchoMRI indicated that lean mass was lower and fat mass was higher, on average, in mice fed TWD/BRB compared to both the AIN/CON and AIN/BRB groups but not compared to mice fed the TWD/CON diet (Figure 2.3e,f).

Liver weight relative to body weight at the terminal time point was not significantly affected by basal diet or treatment (Figure 2.S8a), whereas kidney weights were slightly increased in mice fed TWD compared to those provided the AIN diet (main effect $p = 0.0163$) (Figure 2.S8b). Relative spleen weights were higher in mice fed the TWD compared to those provided AIN (diet main effect $p = 0.0005$) (Figure 2.S8c), reflecting the higher cancer burden for those animals, as has been noted previously [12]. Interestingly, a strong effect of BRB supplementation

was observed for cecum content weight, with the average relative cecum content mass for BRB-exposed mice about 52% greater than the control groups (main effect of treatment $p = 0.0010$) (Figure 2.S8d).

2.3.2.2. Symptoms of Colitis and Histopathology Scoring (Experiment B)

Compared to mice fed the AIN basal diet, consumption of the TWD markedly enhanced the symptoms of colitis as measured by the DAI score during active colitis on day 33 (diet main effect $p < 0.0001$) and continuing through recovery from gut injury at day 45 (diet main effect $p < 0.0001$) (Figure 2.4a). However, in Experiment B, there was no apparent effect of BRB supplementation on colitis symptoms at either time point (BRB main effect $p = 0.334$ and 0.6178 for colitis and recovery time points, respectively) (Figure 2.4a). This observation differs from that of the pilot study (Experiment A), in which supplementation of the TWD diet with 10% BRB significantly reduced the DAI at colitis and recovery time points compared to TWD alone (Figure 2.1a,b).

In a pattern such as that for the DAI score, significant main effects of diet on the colon histopathology inflammation score and mucosa injury scores were noted with higher scores observed in mice fed TWD compared to those provided the AIN diet, but no significant effects of BRB were noted in mice fed either basal diet (Figure 2.4b,c).

2.3.2.3. Colon Length and Tumorigenesis (Experiment B)

Colon tumor incidence in mice fed the AIN basal diet was lower in mice supplemented with BRB (52%) compared to their control counterparts (70%), although this difference was not statistically significant (Figure 2.5a). Similarly, tumor incidence for TWD/CON mice (88%) was no different from the TWD/BRB group (95%). However, incidence in mice provided TWD with BRB was significantly greater than AIN mice also provided BRB ($p = 0.0004$), pointing to an effect of basal diet (Figure 2.5a).

In mice necropsied on experiment day 115, colons excised from mice fed the TWD were shorter in length by 6.2% at 72.8 mm compared to those fed the AIN diet at 77.6 mm (diet main effect $p = 0.0003$); BRB supplementation significantly increased colon length by 3%, irrespective of basal diet (main effect $p = 0.0423$) (Figure 2.5b). As was observed repeatedly in this CAC mouse model, consumption of the TWD enhanced colon tumorigenesis, leading to a 4-fold increase in tumor multiplicity, a 15-fold increase in average tumor volume and a 13-fold increase in tumor burden (diet main effect $p < 0.0001$ for all three endpoints) (Figure 2.5c–e). A significant main effect of BRB treatment on colon tumor multiplicity was observed, with a 46% decline in mice fed BRB compared to controls, regardless of basal diet ($p = 0.0045$). Although tumor multiplicity in the AIN/BRB group was not significantly lower than in their AIN/CON counterparts, a trend of reduced multiplicity was apparent for mice in the TWD/BRB group compared to TWD/CON mice ($p = 0.0539$) (Figure 2.5c). However, BRB did not effectively reduce colon tumor size or tumor burden (Figure 2.5d,e).

2.3.2.4. Dynamics of the Fecal Microbiome in Response to BRB with Differing Basal Diets (Experiment B)

A total of 11.8×10^6 amplicons were sequenced. After filtering for length, quality, and abundance and inspection for chimeras, 7.5×10^6 sequences were assigned to ASVs (Silva database 138 SSU) using the `pick_open_ref_otus` command for an average of 67,443 sequences per sample assigned to 1415 ASVs. The sequencing depth for diversity analyses was set to 28,909 sequences (Figure 2.S9).

Given the multi-level experimental model incorporating multiple time points, two basal diets and two treatment conditions, our analyses of the fecal microbiome profiles proceeded in a stepwise fashion. First, we considered the overall dynamics of the microbiome in the context of this animal model of inflammation-associated colorectal cancer. Briefly, drastic changes in the composition of the gut microbiome were observed over the course of disease development, from

a healthy gut prior to AOM+DSS treatment, during active colitis and progressing through recovery to tumorigenesis, notwithstanding the basal diet or BRB supplement provided (Figures 2.6, 2.7, 2.8, 2.S10 and 2.S11). For example, a decrease in the relative abundance of Akkermansiaceae, specifically *A. muciniphila*, was observed in mice experiencing active colitis, with further loss through recovery to the terminal time point (Figure 2.S10a). The population of Enterobacteriaceae increased during active colitis; then, they were substantially reduced compared to both the colitis and pre-DSS time points with the lowest relative abundance evident at recovery and terminal time points. Bacteroidaceae and Clostridiaceae populations were similarly lower at recovery and terminal time points (Figure 2.S10a). Bifidobacteriaceae (*Bifidobacterium spp.*) were overall very slightly less abundant during colitis ($p = 0.0258$), yet 7% more abundant during the recovery phase before returning to baseline by the terminal time point. Alternatively, bacteria belonging to the Erysipelotrichaceae family were relatively more abundant from the colitis time point onward to the study end. Finally, populations of Lachnospiraceae, Muribaculaceae, Rikenellaceae and Ruminococcaceae were reduced in mice experiencing active colitis, yet appeared to recover shortly thereafter to pre-DSS abundance levels (Figure 2.S10a). Considered collectively, these changes in the microbiome population indicate an overall increase in the shift in the Firmicutes-to-Bacteroidetes ratio favoring firmicutes during active colitis and through recovery with a partial recovery back to the pre-DSS baseline in this mouse model of CAC (Figure 2.S10b).

The remainder of the analyses focused on effects of the basal diet and/or BRB supplement within each experimental time point. The pre-DSS time point revealed the impacts of basal diet on the gut microbiome prior to chemically triggered gut inflammation or carcinogen exposure. Relatively few significant effects of the AIN or TWD basal diets on the microbiome composition were noted (Figure 2.8a, File 2.S4). Of note, the population of Erysipelotrichaceae was 15% lower in TWD/CON-fed mice compared to AIN/CON ($p = 0.0237$), and that of

Clostridiaceae was 15% more abundant in TWD/CON compared to AIN/CON ($p = 0.0014$). During active colitis, the relative abundances of Akkermansiaceae and Lactobacillaceae were 470% greater or 73% lower, respectively, in mice fed the TWD/CON diet compared to AIN controls ($p = 0.0286$ or 0.0048 , respectively).

Consumption of BRB had profound effects on the fecal microbiome composition throughout the study, with apparent shifts in bacteria populations dependent on the basal diet at some time points (Figures 2.8 and 2.9, File 2.S4). Prior to induction of gut inflammation, BRB intake significantly reduced the population of Erysipelotrichaceae (primarily *Dubosiella newyorkensis*, *Erysipelatoclostridium spp.* and *Turicibacter spp.*) from 39% to just 15% of the fecal microbiome ($p = 0.0004$) in mice fed the AIN basal diet, whereas no change was apparent in mice provided the TWD diet (Figure 2.9b). This pattern was persistent through colitis and recovery time points, with significant reductions in Erysipelotrichaceae in mice fed the AIN diet, whereas the apparent lower abundance in TWD-fed mice was not statistically significant. BRB markedly reduced the relative abundance of Streptococcaceae (primarily *Lactococcus spp.*) in mice provided either the AIN or TWD diet at the pre-DSS time point ($p = 0.0045$ and 0.0006 , respectively) (Figure 2.9b). However, BRB was effective at lowering Streptococcaceae only in TWD-fed mice during active colitis, perhaps because the relative abundance of this taxa was notably lower in AIN-fed mice at this time point. No further effect of BRB on this population was evident during recovery or at the terminal time point.

BRB supplementation appeared to increase the population of Bifidobacteriaceae (*Bifidobacterium spp.*), as a significant main effect of BRB supplementation, irrespective of diet, was observed prior to DSS treatment and through active colitis and in mice fed the TWD diet at the terminal time point (Figure 2.9c). Similarly, the population of Rikenellaceae (*Alistipes uncultured bacterium*) increased from just 0.43% of the microbiome in CON mice to 1.9% in BRB-supplemented mice consuming the AIN diet and from 0.38% in CON to 3.0% in BRB-

supplemented mice provided the TWD diet at the pre-DSS time point ($p \leq 0.001$) (Figure 2.9d). Although less pronounced, this increase in Rikenellaceae was evident for AIN-fed mice during active colitis and through recovery, although not statistically significant by the terminal time point. In mice fed TWD, the effect of BRB was less pronounced during colitis and recovery but as significant at the terminal time point, with an increase from 0.26% in CON compared to 1.2% in BRB-supplemented mice ($p = 0.0008$). Prior to onset of colitis, Lachnospiraceae relative abundance was significantly greater in mice provided BRB on the AIN basal diet (10.3%) compared to controls (3.3%), although not in mice provided the TWD basal diet (Figure 2.9e). This pattern was consistent during active colitis, although by recovery from gut injury, BRB supplementation effectively increased the relative abundance of Lachnospiraceae for mice fed either the AIN or TWD basal diets. By the end of the study, an apparent greater abundance of this taxa persisted, although it was variable among the cages within the BRB supplemented groups and was not statistically significant for either basal diet.

BRB supplementation was also effective at shifting the relative abundance of Ruminococcaceae (including *Ruminoclostridium spp.*, *Oscillibacter* and *Instestimonas*) throughout the complete study, with an increase from 2.1% to 5.6% of the microbiome in CON compared to BRB-fed mice prior to DSS treatment ($p = 0.0006$), a dampened response during colitis (from 0.2% for CON to 1.4% for BRB; $p < 0.0001$), followed by robust increases through recovery (0.8% for CON and 3.6% for BRB; $p < 0.0001$) and the terminal time points (1.3% in CON increased to 4.3% for BRB; $p = 0.0482$) (Figure 2.9f). Although a similar trend of elevated population of Ruminococcaceae in TWD-fed mice was also apparent, this response did not reach statistical significance until the terminal time point ($p = 0.0089$). Lastly, of the selected taxa for discussion, Akkermansiaceae relative abundance was higher in mice fed the AIN diet with BRB supplementation during active colitis (increase from 1.2% of bacteria population to 5.1% with BRB; $p < 0.0001$) and through recovery (2.0% in CON increased to 5.6% in BRB-fed mice; $p =$

0.0023) (Figure 2.9g). BRB supplementation did not appear to affect Akkermansiaceae abundance in mice fed TWD at any study time point.

At the phylum level, these shifts in the microbiome over the course of disease development led to substantial alterations in the ratio of Firmicutes to Bacteroidetes (F:B), with significant main effect of BRB supplementation ($p = 0.0001$) but with a trend of effect of basal diet ($p = 0.084$) (Figure 2.10). The F:B ratio was overall lower prior to DSS treatment, with a significant decrease from 3.5 in CON mice to 1.7 for BRB-supplemented mice fed the AIN diet ($p = 0.0021$). Similarly, for mice provided TWD, the ratio decreased from 6.4 to 4.2 with addition of BRB ($p = 0.0013$). During colitis, the comparisons between BRB-supplemented and CON diets were not statistically significant for either AIN or TWD basal diets, although an overall main effect of BRB was evident ($p = 0.0025$). During recovery from DSS-induced gut injury, BRB was effective at reducing the F:B ratio from 20.7 to 6.1 in mice provided the AIN basal diet ($p = 0.0007$) but not in those provided TWD ($p = 0.3382$). By the end of the study, however, this pattern was reversed, with BRB effectively decreasing the F:B ratio from 21.6 to 8.5 in mice fed the TWD ($p = 0.0115$) but not the AIN diet ($p = 0.8144$).

2.3.2.5. Alpha and Beta Diversity of Fecal Microbiome (Experiment B)

Alpha diversity was determined using three measures: observed ASVs, Chao1 index and Shannon index. First considering the microbiome composition over the course of disease development, irrespective of basal diet or BRB supplementation, α -diversity was substantially reduced in mice experiencing colitis compared to pre-DSS baseline with prolonged loss of taxa through recovery ($p < 0.0001$ for all α -diversity measures; Figure 2.11, Table 2.S2). By the end of the study, α -diversity measures were more similar to the pre-DSS baseline ($p > 0.05$ for observed ASVs and Chao1 index), although when considered as a weighted measure by the Shannon index, the overall α -diversity was still significantly reduced ($p = 0.0008$; Table 2.S2).

The main model analyses revealed profound effects of BRB treatment on α -diversity throughout the study, with mostly consistent effects in mice provided either the AIN or TWD basal diets for observed ASVs and the Chao1 index (Figure 2.11a,b; Table 2.S3). One notable exception was noted during active colitis, when BRB supplementation appeared less effective in improving α -diversity in mice fed TWD. Furthermore, this pattern of reduced BRB efficacy in mice fed the TWD basal diet was further apparent for the Shannon index at the pre-DSS baseline, during colitis and through recovery (Figure 2.11c).

Beta diversity was determined using both weighted and unweighted unifracs distances to explore the microbiome community profiles based on relative abundance and rare taxa, respectively. As anticipated, for unweighted unifracs distance β -diversity (Figure 2.S12a), clear separations of microbiome samples were evident at each experimental time point with the most distinct profiles apparent in mice experiencing active colitis through the recovery period 14 days later (permanova $p < 0.001$ for each diet/supplement group). Interestingly, when considering the composition of the microbiome weighted for abundance, the pre-DSS baseline microbiome appeared most distinct (Figure 2.S12b) and still notably different from microbiomes at the terminal time point, suggesting that recovery from gut injury led to long-term changes in fecal microbiome profiles (permanova $p < 0.001$ for each diet/supplement group).

Dietary supplementation with BRB caused marked shifts in the composition of the fecal microbiome, as assessed using either weighted or unweighted unifracs distance measures (Figure 2.12), whereas basal diet appeared to have only modest or no apparent effects on bacteria profiles at any of the disease stages in this experiment. Following two weeks of experimental treatments at the pre-DSS baseline, BRB appeared to shift the microbiome composition, such that the profiles were clearly distinct compared to their CON counterparts. This pattern was mostly consistent at the colitis time point (permanova $p < 0.001$), although more overlap among experimental groups was apparent for weighted unifracs β -diversity. By the recovery time point,

the fecal microbiomes of TWD/BRB mice appeared less distinct from those provided the CON diet for either weighted or unweighted β -diversity, although AIN/BRB microbiomes were still distant. At the study end, unweighted β -diversity revealed persistent distinct microbiomes for mice supplemented with BRB fed either diet, whereas the weighted measure suggested only a strong segregation of microbiomes from AIN/BRB mice (Figure 2.12), suggesting that the long-term effects of BRB supplementation may be more profound for rarer taxa, which more heavily influenced the unweighted unifracs analysis.

2.3.2.6. Functional Metagenomics and Longitudinal Analyses (Experiment B)

Functional potential prediction revealed significant differences in the representation of KEGG orthology terms when comparing mice supplemented with BRB and the controls fed either the AIN or TWD basal diets (Figures 2.13a and 2.S13). At the pre-DSS baseline, the KEGG metabolism level 1 terms of glycan biosynthesis and metabolism, biosynthesis of other secondary metabolites and metabolism of other amino acids were significantly enriched in BRB-supplemented mice compared to CON counterparts for both basal diets. This pattern was consistent during active colitis, with one additional category, carbohydrate metabolism, slightly but significantly enriched in AIN/BRB mice only. During recovery, this effect of BRB was apparent only for AIN-fed mice, with the exception at this time point of carbohydrate metabolism being very slightly enriched for TWD-fed mice. By the study end, no significant enrichments in level 1 KEGG terms were noted.

The lists of significant terms identified via metagenomeSeq analyses were subject to pathway association analysis to identify enriched level 2 pathways for BRB supplementation, irrespective of basal diet, at each time point (Figure 2.13b). Addition of BRB to the mouse diet appeared to strongly shift the functional capacity of the gut microbiome in favor of carbon metabolism, pyruvate metabolism, butanoate metabolism and propanoate metabolism, along with several other pathways. Of note, only during active colitis, a very strong enrichment in taxa

associated with lipopolysaccharide biosynthesis was noted, as well as shifts favoring carbon fixation pathways in prokaryotes, pyruvate metabolism and fatty acid biosynthesis. Like the colitis time point, relatively few enriched functional pathways were identified for BRB-supplemented gut microbiomes during recovery from gut injury, with amino sugar and nucleotide sugar metabolism uniquely enriched along with pyruvate metabolism and carbon metabolism, as in prior stages. By the end of the experiment, functional analyses revealed a unique pathway set for BRB-supplemented mice, including purine metabolism, selenocompound metabolism, nicotinate and nicotinamide metabolism.

To explore longitudinal trends in microbiome taxonomic and functional diversity, Bray–Curtis β -diversity was analyzed using non-metric multi-dimensional scaling (NMDS) with the complete experimental data set across all time points. In this visualization, BRB supplementation appears to be the primary experimental factor driving taxonomic diversity, with time point as a probable secondary factor (Figure 2.14a). Alternatively, these distinctions are less clear when considering the microbiome functional capacity (Figure 2.14b). The longitudinal variation of samples along the first NMDS dimension shows how microbiome populations diverge with respect to taxonomy proximal to onset of colitis (circa day 33) with continued divergence persisting through recovery (circa day 45) and then largely resolving by the end of the experiment (Figures 2.S14 and 2.14c,d). Of note, a clear divergence in both taxonomic and functional variation is evident during active colitis for mice fed TWD as compared to the AIN diet without BRB supplementation (Figure 2.S14); yet, this divergence largely resolves through recovery and on to the tumorigenesis phase in this disease model. Furthermore, a strong taxonomic divergence was associated with response to BRB supplementation, although this appears more pronounced for mice fed the AIN diet compared to those provided TWD (Figure 2.14c). Longitudinal analysis of the gut microbiome functional capacity revealed similar divergence in microbiomes proximal

to colitis when fed either CON or BRB-supplemented diets, although resolution appears to be more rapid around the recovery time point (Figure 2.14d).

2.3.2.7. Fecal Short-Chain Fatty Acid Content (Experiment B)

Mice provided BRB in the context of the TWD basal diet produced significantly higher amounts of acetic (75% ↑, $p < 0.0001$), propionic (93% ↑, $p < 0.0001$), isobutyric (42% ↑, $p = 0.0389$), butyric (240% ↑, $p < 0.0001$) and valeric (52% ↑, $p = 0.0382$) acids compared to their AIN-fed counterparts during the initial phase of the study prior to DSS treatment (Figure 2.15, Tables 2.S5–2.S7). Notably, this observation correlates closely with the higher total food and energy intakes in mice provided the TWD/BRB diet in the first three weeks of the experiment (Figure 2.S7). During active colitis, the overall production of acetic, butyric, propionic and valeric acids was significantly elevated (Table 2.S5), although BRB supplementation did not significantly alter these specific SCFAs for mice fed either basal diet (Figure 2.15). Rather, isobutyric and isovaleric acids were significantly reduced by 67% ($p = 0.0005$) and 57% ($p = 0.0060$), respectively, in mice provided the TWD/BRB experimental diet compared to TWD/CON, while isovaleric acid was significantly elevated by 76% ($p = 0.0457$) in mice provided the AIN/BRB diet compared to AIN/CON. As the animals recovered from gut injury, BRB supplementation significantly reduced acetic acid (46% ↓, $p = 0.0047$) and isobutyric acid (47% ↓, $p = 0.0032$) in fecal samples from AIN-fed mice, whereas BRB elevated propionic (50% ↑, $p = 0.0467$), isobutyric (82% ↑, $p = 0.0043$) and isovaleric (79% ↑, $p = 0.0040$) acids in mice provided the TWD basal diet. By the study end, overall SCFA in fecal samples returned to the pre-DSS baseline (Table 2.S5). In the long term, compared to control mice, BRB supplementation increased butyric acid fecal concentration by about 2-fold ($p = 0.0021$) and valeric acid by 55% ($p = 0.0209$) in mice provided the TWD but not in their AIN-fed counterparts.

2.4. Discussion

Consumption of a rodent diet that emulates the typical American pattern with respect to macro- and micronutrient profiles has been repeatedly shown to enhance symptoms of colitis, inflammatory cell infiltration, mucosal injury and tumor development in murine models of colitis-associated colorectal cancer [12,35]. Herein, we report the findings from the first investigation to explore the purported benefit of dietary supplementation with BRB for gut health and modulation of the gut microbiome in a mouse model of Western-diet enhanced colitis and colitis-associated colorectal cancer. The results of a pilot study suggested that BRB supplementation ameliorated colitis symptoms and reduced colon tumorigenesis in mice provided the TWD. Moreover, assessment of the fecal microbiome suggested that BRB consumption led to shifts in the gut microbiome in favor of health-promoting species. However, in a more extensive follow-up study, the suppressive effects of BRB supplementation on colitis and CAC were mixed, with no apparent effects on colitis symptoms, colon inflammation or mucosa injury, yet an apparent improvement in colon length and reduced tumor multiplicity by the end of the experiment, irrespective of the basal diet provided. As observed in the pilot study, in the second experiment, BRB supplementation had profound effects on the composition of the fecal microbiome evident even before the onset of colitis, as evidenced by increased alpha diversity and distinct microbiome profiles throughout the study period, during colitis, recovery, and finally, tumorigenesis. Of interest, when considering changes in abundance of individual taxa, we observed more frequent significant changes in their relative abundance values in mice provided the AIN basal diet as compared to those fed TWD.

An unexpected finding in both experiments was the apparent increased energy intake for mice provided the TWD supplemented with BRB. In prior investigations employing the TWD, we observed that mice fed TWD typically consume less food, such that their overall energy intake is consistent with that of mice provided the AIN diet [12,13,35,46]. However, TWD/CON food

intake for experiment B of this study was statistically greater compared to their AIN/CON counterparts, leading to elevated energy intake. In both experiments of this investigation, addition of BRB to the TWD basal diet led to further increased intake of food, higher energy intake and, consequently, increased body weight and fat mass. However, these effects were not apparent for mice provided the AIN basal diet, pointing to an interaction between the TWD nutritional profile—with its higher energy density and unbalanced micronutrient composition—and dietary supplementation with BRB. Importantly, CON and BRB-supplemented diets were matched for total sugar and fat content. Thus, it is reasonable to surmise that the addition of BRB increased the palatability of the rodent diet, presumably due to the differing sugar profile of black raspberries (fructose and glucose) compared to the semi-purified diets containing only sucrose. Future studies should explore the potential adverse effects of the TWD on the gut–brain axis and neuroendocrine control of hunger and satiety—effects, which may explain why hyperphagia was notably pronounced in mice provided with the more palatable BRB diet.

As previously observed in multiple studies, mice consuming TWD experienced more severe colitis symptoms, increased inflammation and mucosal damage in the colon epithelium and elevated tumor development compared to mice consuming the standard AIN [12,35], a pattern that persisted in the current studies. Given the link between consumption of this Western diet by rodents and evident promotion of colitis and CAC, it is important to identify the functional foods abundant in bioactive chemicals with potent anti-inflammatory, antioxidant and/or anti-cancer properties. Herein, we report that BRB supplementation consistently reduced tumor multiplicity in a mouse model of Western-diet enhanced CAC. However, the findings for symptoms of colitis and colon inflammation were equivocal. Several previous studies have explored the effects of black-raspberry-supplemented diets in both murine cancer and inflammatory disease models, although not in the context of a Western dietary pattern. *Apc*^{Min/+} mice fed AIN76A supplemented with 5% whole freeze-dried BRB powder had a decrease in

polyp burden and size in the small intestine and colon compared to control diet [47]. Dong et al. compared different doses of protocatechuic acid (PCA) and 5% BRB supplemented in a AIN76A diet administered to *Apc^{Min/+}* mice, resulting in a greater effect of 5% BRB on polyp number and size, tumor incidence and shift of pro-inflammatory bacterial species to anti-inflammatory promoting taxa [48]. Using a similar experimental model of CAC in C57BL6/J mice, Chen et al. observed decreased colon tumor incidence and multiplicity for mice provided chow supplemented with 5 or 10% BRB [25]. When added to the AIN76 diet, black raspberries, their anthocyanin bioactives and a microbial metabolite of anthocyanins have also been shown to be effective at suppressing chemical carcinogenesis in a rat model of esophageal cancer [15,22].

In addition to its apparent anti-cancer properties, evidence also points to the anti-inflammatory effects of dietary supplementation with BRB in animal studies. Using a DSS-induced model of UC, Montrose et al. reported that addition of BRB to the AIN76 basal diet suppressed key pro-inflammatory cytokines, including tumor necrosis factor-alpha ($TNF\alpha$) and interleukin 1-beta ($IL1\beta$), thus inhibiting cyclooxygenase 2 (COX2) [23]. Wister rats fed a high-fat diet supplemented with 2.5% or 5% BRB freeze-dried powder for 8 weeks had decreased levels of $IL1\beta$, $IL6$ and COX2 [49]. Multiple studies using the *IL10* knockout mouse model for UC showed that supplementing the AIN76A diet with 5% BRB led to decreased inflammatory cell infiltration in colon tissues, which the authors concluded was due to the BRB supplement correcting dysregulated TLR4 in colonocytes, decreasing prostaglandin E2 and inhibiting aberrant epigenetic pathways by decreasing β -catenin translocation levels [50,51]. Additionally, BRB decreased NF- κ B p65 expression, which reduced aberrant DNA methylation of tumor suppression genes in the Wnt pathway in a C57BL/6J mouse model of UC using the AIN76A diet supplemented with 5% BRB powder [52]. Collectively, this evidence suggests that supplementation with BRB in mice consuming a standard diet decreased inflammatory cytokines, ameliorated TLR4 dysregulation and reduced methylation of tumor suppression genes.

A key finding of this investigation was that consumption of BRB markedly altered the composition of the fecal microbiome in a dynamic way over the course of disease development and, ultimately, tumorigenesis. Anthocyanin-rich BRB promoted growth of more diverse microbial communities in the colon, which were notably distinct from time-matched controls, as evidenced by elevated α -diversities and highly divergent β -diversities (experiment B). Comparable to these findings, Gu et al. reported that dietary supplementation of AIN93G with 10% freeze-dried BRB powder diet in healthy male mice increased richness of the mucosal and luminal microbiomes of the colon while also promoting growth of distinct microbiota populations [17]. In a UC model of C57BL/6J mice provided 1% DSS in water for two weeks, the AIN76A diet supplemented with 10% BRB powder had an attenuating effect on microbial richness compared to control diet and higher diversity than mice fed only the control diet [53]. Collectively, BRB supplementation promotes anti-inflammatory and anti-cancer properties while also enriching the gut microbiome.

Shifts in relative abundance in major phylum favoring Firmicutes compared to Bacteroidetes (F:B) has been previously linked to chronic inflammatory disease, including obesity and inflammatory bowel disease (IBD) [54,55]. As noted for the more extensive experiment B, the F:B ratio was consistently reduced in BRB-supplemented diets prior to onset of colitis, during active colitis, through recovery and colon tumorigenesis. Driving this decrease in the F:B ratio was a lower relative abundance of Erysipelotrichaceae and Streptococcaceae in BRB-fed mice compared to CON diet. Of note, members of these bacteria families have been previously found in high abundance in patients diagnosed with UC or Crohn's disease [56,57]. Schaubek et al. observed a significant increase in Erysipelotrichaceae in mice that developed tumor necrosis factor (TNF)-driven CD-like transmural inflammation [58]. In this investigation using a mouse model of colitis and CAC, the abundance of Erysipelotrichaceae was higher in mice (experiment B) during active colitis and remained elevated through recovery and colon

tumor development. Alternatively, an increased abundance in this bacteria family was associated with a 12% lower risk of IBD and 14% reduced risk of UC in humans [59]. Insulin-resistant mice fed a high-fat, high-sugar diet supplemented with cyanidin-3-glucoside (C3G) extract, commonly found in blueberries, reduced Erysipelotrichaceae and Streptococcaceae relative abundance [60], a finding similar to this study in which BRB supplementation reduced both Erysipelotrichaceae and Streptococcaceae prior to DSS-induced gut injury and during active colitis, with different outcomes depending on the basal diet provided.

Bacteria belonging to the Bifidobacteriaceae family (*Bifidobacterium pseudolongum* in experiment A and unidentified species in experiment B) were enriched with BRB supplementation in this investigation, most notably during active colitis in both experiments. Bifidobacteriaceae dominate the gut microbiome of infants but decrease in abundance by the time a child reaches three years of age [61]. Species belonging to the Bifidobacteriaceae family suppress the immune response, increase acetate production and improve intestinal barrier function in infants and provide protective effects in CD patients [62]. In a recent study that explored colon mucosa and tumor-associated microbiomes by comparing age-matched wild-type F344 rats and Apc-mutated Pirc rats, Vitali et al. reported that the colon tumor tissue-associated microbiome was enriched for Bifidobacteriaceae, suggesting a relationship between bacteria in this family and the tumor environment [63]. Previous studies exploring the effects of dietary supplementation with BRB in animal models of IBD or CAC did not report changes in abundance of Bifidobacteriaceae taxa, contrary to our findings [17,53].

In the current study, BRB supplementation increased the relative abundance of Lachnospiraceae, Ruminococcaceae and Rikenellaceae prior to, during and after carcinogen exposure. Members of the Lachnospiraceae family are butyrate-producing and degrades cellulose and hemicellulose derivatives of plant fibers, leading to increased bioavailability for host absorption and contributing to intestinal homeostasis [64]. In a study of 42 CRC patients and 89

matched controls, Sinha and colleagues determined a significant association of CRC diagnosis with reduced abundance of Lachnospiraceae in feces [65]. In addition, the relative abundance of Lachnospiraceae decreased with increasing severity of bowel inflammation in a study of Chinese patients with UC [66]. Multiple studies have shown that dietary supplementation with anthocyanin-rich foods alters Lachnospiraceae abundance in the gut with purported health benefits. For example, addition of an anthocyanin-rich extract from bilberries to the diet promoted the growth of Lachnospiraceae in aged rats [67]. Additionally, Chen et al. reported that treatment with the anthocyanin cyanidin-3-O-glucoside ameliorated chemically induced gut dysbiosis, including increased abundance of Lachnospiraceae_NK4A136_group, and protected against intestinal mucosa damage [68].

In this investigation, we observed different responses to BRB intervention for taxa in the Ruminococcaceae family, with apparent reduced abundance during active colitis in the pilot experiment and clearly elevated abundance in the more extensive study, most notably in mice fed the AIN diet prior to gut injury, during active colitis, through recovery and, for both basal diets, on to tumor development. Ruminococcaceae are butyrate-producing bacteria necessary for intestinal barrier functions, and a decrease in the relative abundance of Ruminococcaceae has been shown to promote secondary bile deficiencies and intestinal inflammation [69-71]. Interestingly, others have also reported mixed outcomes for Ruminococcaceae abundance following intervention with anthocyanin-rich foods. For example, Pan et al. reported that healthy F344 rats fed the AIN76G diet with 5% BRB had increased Ruminococcaceae in feces [24]. Alternatively, dietary supplementation with 5% BRB or protocatechuic acid, a microbial-derived metabolite of black raspberries, apparently decreased the relative abundance of fecal *Ruminococcus gnavus* in the APC^{Min/+} mouse model of small intestinal cancer [48]. Furthermore, in C57BL/6J mice fed a high-fat basal diet, blueberry and cranberry anthocyanin extracts were shown to reduce the relative abundance of Ruminococcaceae in the fecal microbiome as

compared to high-fat control mice [72]. Finally, Kennedy and colleagues reported that the relative abundance of Rikenellaceae is reduced in CD patients compared to healthy controls [73].

Anthocyanin extract from blueberries and cranberries added to a high-fat diet reduced the abundance of Rikenellaceae in C57BL/6J mice [72], while blue honeysuckle berries, containing mainly cyanidin 3-glucoside, added to a high-fat diet led to increased abundance of Rikenellaceae in the fecal microbiome of male mice [74].

Within the Verrucomicrobiaceae family, *A. muciniphila* is one of the most widely studied bacterium due to its apparent critical role in sustaining gut homeostasis via promotion of mucin secretion and maintenance of the mucosal layer. Thus, application of *A. muciniphila* as a probiotic or identification of diets that promote its abundance are of high interest to leverage its potential for sustaining gut health and supporting the intestinal immune response [75]. However, the relationship between *A. muciniphila* and intestinal inflammatory diseases is unclear (reviewed in Ref [reviewed in 76]), as multiple studies have reported equivocal findings in humans [77-81] and in animal models [82-84]. In this investigation, we observed a marked decrease in the abundance of Verrucomicrobiaceae (*Akkermansia* unclassified species) following DSS-induced injury to the gut epithelium, although less so during colitis for TWD-fed mice, suggesting that the highly inflamed and damaged tissue environment was not supportive for this bacterium. Furthermore, we reported that Akkermansiaceae was elevated in mice fed the AIN diet supplemented with BRB during active colitis and through recovery compared to controls, although not in TWD-fed mice (experiment B). Polyphenols derived from Concord grapes have been shown to increase Akkermansiaceae abundance, resulting in enhanced intestinal barrier function and suppression of inflammatory cells in mice fed a high-fat diet [85]. Additionally, multiple studies have shown that addition of either blueberry or cranberry powder or extract to a high-fat, high-sugar diet increased the abundance of *A. muciniphila* after 6 to 11 weeks [72,86]. In this study, we identified the key microbial taxa associated with gut inflammation as possible

biomarkers of disease. While this study included a dynamic assessment of the microbiome, it remains unclear whether changes in the abundance of bacteria, such as *A. muciniphila*, are indeed causative of altered colitis status or are a consequence of changes in gut inflammation status.

In a prior longitudinal study of the gut microbiome in a well-established mouse model of IBD, Sharpton et al. suggested that the taxonomic structure and functional capabilities of the gut microbiome shifted through disease development, and these changes correlated with immune activation [87]. In the current study, we observed transient, diet-dependent divergence of microbial taxonomic and functional diversity, most evident in the healthy mice before DSS-induced gut injury and during active colitis, which then resolved—especially with respect to functional diversity—during recovery from gut injury. This divergence was apparent for mice consuming both basal diets, although clearly more pronounced in mice fed the AIN. Prior to gut insult, our metagenomic analysis of BRB-fed mice compared to controls revealed differences in KEGG level 1 terms, including increased glycan biosynthesis and metabolism, biosynthesis of other secondary metabolites and metabolism of other amino acids. Moreover, enriched KEGG level 2 terms in mice provided BRB included pyruvate, butanoate and propanoate metabolism pathways, notably prior to gut injury. During active colitis and recovery of gut injury, lipopolysaccharide biosynthesis, carbon fixation and fatty acid metabolism pathways were enriched, likely a consequence of DSS-induced inflammation and disease progression.

Black raspberry polyphenols, such as phenolic acids, flavanols and anthocyanins [17], are broken down to secondary metabolites, such as SCFAs. For example, the black raspberry freeze-dried powder in this study had a 3.72% w/w of anthocyanin with cyanidin-3-*O*-glucoside being the dominant structure. The sugar moiety is removed from the cyanidin via β -glucosidase, which enhances glycan metabolism into butyrate [88]. Glucose is actively converted to pyruvate promoting the citric acid cycle, consequently stimulating metabolism of other amino acids. Further, cyanidin is hydrolyzed and cleaved into two important secondary metabolites,

protocatechuic acid and phloroglucinaldehyde [89]. Given the apparent shift in functional diversity of the gut microbiome in mice fed BRB-supplemented diets, we also determined the concentrations of SCFAs in fecal samples. Interestingly, the apparent change in the functional diversity of the gut microbiome associated with BRB supplementation, as indicated by enriched KEGG level 2 terms for pyruvate, butanoate and propanoate metabolism, was associated with shifts in fecal SCFA levels, specifically acetic, propionic and butyric acids prior to gut injury, especially in mice fed the TWD. However, it should also be noted that mice fed the TWD+BRB diet had higher overall energy intake compared to the other experimental groups, which could explain the higher concentration of SCFAs in the feces of these mice. Tu et al. reported that C57BL/6J mice fed the AIN76A diet with 10% BRB had similar increases in butyrate as compared to controls [90]. Butyrate is the least abundant SCFA and is the main energy source for colonocytes. Further, butyrate modulates the immune responses, intestinal barrier function, inhibits histone acetylation and has been shown to have anti-cancer properties (reviewed in Ref [reviewed in 91]).

This study has some limitations that should be considered. First among these are the apparent contradictory findings between the pilot study (experiment A) and the more extensive second study (experiment B), most notably for colitis disease activity index, the histopathology assessment of inflammation and mucosal injury, and tumor burden, although BRB supplementation similarly reduced tumor multiplicity in both studies. Additionally, different results were apparent for the relative abundance of specific microbiome taxa. With respect to microbiome analyses, the two key considerations are (1) the different sequencing technologies, with the methods for experiment B being more robust and achieving much improved sequencing depth to capture more rare taxa; and (2) fewer cages employed in the pilot study limited the statistical power. Given the different sequencing platforms and databases used for mapping sequences to bacteria, comparisons across the two experiments for specific bacteria taxa should

be made with caution. Additionally, fecal microbiome profiling determined the relative abundance of various taxa present rather than their absolute abundance; it is possible that apparent changes in the relative abundance of one species may not be due to changes in its actual population size but rather due to the growth or loss of other species in the community. The experimental model of CAC was the same for both studies, yielding the anticipated phenotype outcomes for colitis, histopathology and tumorigenesis for mice fed either the AIN or TWD, as has been observed in several prior studies by our group. Additionally, the diet formulations were consistent across the two experiments, as we used the same source of BRB freeze-dried powder with a consistent anthocyanin profile; thus, the experimental diets were not likely the driving factor in apparent differences in inflammatory response. At this point, we cannot posit a clear explanation for the apparent differences in inflammatory response evident in these experiments. However, we note that repeated pre-clinical experiments with dietary interventions for cancer prevention are rarely provided in the literature, and these mixed results give further weight to the need to consider the reproducibility of pre-clinical studies before advancing such work to clinical settings. Furthermore, the concentration of BRB in the mouse diets employed in this study would deliver a dose of anthocyanins (estimated 448 mg/kg per day with estimated human equivalent dose of 7.6 mg/kg based on surface area allometric scaling) approximately 5-fold greater than could reasonably be achieved in humans consuming black raspberries as part of a regular diet (approximately 460 mg anthocyanins in 100 g serving of fresh black raspberries, for a dose of 7.6 mg/kg). Moreover, these berries are a seasonal specialty crop and not widely available in local groceries. However, concentrated anthocyanin-rich extracts and freeze-dried fruit powders (as used in this study) are commercially available all year round.

2.5. Conclusions

In conclusion, dietary supplementation with freeze-dried black raspberry powder appeared to suppress colon tumorigenesis, as evidenced by reduced colon tumor multiplicity in

multiple experiments, although the effects on colitis symptoms, colonic inflammation and mucosal damage were inconsistent. Moreover, addition of BRB to the mouse diet shifted the fecal microbiome composition in favor of health-promoting taxa, increased alpha diversity and promoted growth of distinct microbiome populations compared to mice fed the control diets. Importantly, a significant interaction between basal diet and BRB supplement was evident for many experimental parameters, such as body weight and fat mass gain, alpha diversity and relative abundance of several bacteria families, pointing to the importance of the underlying nutritional status of the target population for intervention with functional foods. The key issues still left to be addressed in future investigations include the potential benefit of other anthocyanin-rich foods with differing anthocyanin profiles in this animal model of Western-diet enhanced CAC, the impact of varying anthocyanin-rich food intake patterns to emulate typical human diet (e.g., varied food items, varied intake schedule) and the duration of microbiome response to intervention with anthocyanin-rich foods. These investigations would better inform nutritionists working with IBD patients in real-world diet intervention scenarios to promote gut homeostasis, suppress inflammation and potentially reduce the risk of CAC.

References

1. Loddo, I.; Romano, C. Inflammatory bowel disease: genetics, epigenetics, and pathogenesis. *Front Immunol* **2015**, *6*, 551, doi:10.3389/fimmu.2015.00551.
2. Kelsen, J.R.; Russo, P.; Sullivan, K.E. Early-onset inflammatory bowel disease. *Immunol Allergy Clin North Am* **2019**, *39*, 63-79, doi:10.1016/j.iac.2018.08.008.
3. Xu, F.; Dahlhamer, J.M.; Zammitti, E.P.; Wheaton, A.G.; Croft, J.B. Health-risk behaviors and chronic conditions among adults with inflammatory bowel disease — United States, 2015 and 2016. *MMWR Morb Mortal Wkly Rep* **2018**, *67*, 190-195, doi:10.15585/mmwr.mm6706a4.
4. Piovani, D.; Danese, S.; Peyrin-Biroulet, L.; Bonovas, S. Inflammatory bowel disease: estimates from the global burden of disease 2017 study. *Aliment Pharmacol Ther* **2020**, *51*, 261-270, doi:10.1111/apt.15542.

5. Mattar, M.C.; Lough, D.; Pishvaian, M.J.; Charabaty, A. Current management of inflammatory bowel disease and colorectal cancer. *Gastrointest Cancer Res* **2011**, *4*, 53-61.
6. Keller, D.S.; Windsor, A.; Cohen, R.; Chand, M. Colorectal cancer in inflammatory bowel disease: review of the evidence. *Tech Coloproctol* **2019**, *23*, 3-13, doi:10.1007/s10151-019-1926-2.
7. Islami, F.; Ward, E.M.; Sung, H.; Cronin, K.A.; Tangka, F.K.L.; Sherman, R.L.; Zhao, J.; Anderson, R.N.; Henley, S.J.; Yabroff, K.R., et al. Annual report to the nation on the status of cancer, part 1: national cancer statistics. *J Natl Cancer Inst* **2021**, *113*, 1648-1669, doi:10.1093/jnci/djab131.
8. Windsor, J.W.; Kaplan, G.G. Evolving epidemiology of IBD. *Curr Gastroenterol Rep* **2019**, *21*, 40, doi:10.1007/s11894-019-0705-6.
9. Thanikachalam, K.; Khan, G. Colorectal cancer and nutrition. *Nutrients* **2019**, *11*, doi:10.3390/nu11010164.
10. Grant, W.B. Review of recent advances in understanding the role of vitamin D in reducing cancer risk: breast, colorectal, prostate, and overall cancer. *Anticancer Res* **2020**, *40*, 491-499, doi:10.21873/anticancer.13977.
11. Hintze, K.J.; Benninghoff, A.D.; Ward, R.E. Formulation of the total Western diet (TWD) as a basal diet for rodent cancer studies. *J Agric Food Chem* **2012**, *60*, 6736-6742, doi:10.1021/jf204509a.
12. Benninghoff, A.D.; Hintze, K.J.; Monsanto, S.P.; Rodriguez, D.M.; Hunter, A.H.; Phatak, S.; Pestka, J.J.; Wettere, A.J.V.; Ward, R.E. Consumption of the total Western diet promotes colitis and inflammation-associated colorectal cancer in mice. *Nutrients* **2020**, *12*, doi:10.3390/nu12020544.
13. Monsanto, S.P.; Hintze, K.J.; Ward, R.E.; Larson, D.P.; Lefevre, M.; Benninghoff, A.D. The new total Western diet for rodents does not induce an overweight phenotype or alter parameters of metabolic syndrome in mice. *Nutr Res* **2016**, *36*, 1031-1044, doi:10.1016/j.nutres.2016.06.002.
14. Panche, A.N.; Diwan, A.D.; Chandra, S.R. Flavonoids: an overview. *J Nutr Sci* **2016**, *5*, e47, doi:10.1017/jns.2016.41.
15. Peiffer, D.S.; Zimmerman, N.P.; Wang, L.S.; Ransom, B.W.; Carmella, S.G.; Kuo, C.T.; Siddiqui, J.; Chen, J.H.; Oshima, K.; Huang, Y.W., et al. Chemoprevention of esophageal cancer with black raspberries, their component anthocyanins, and a major anthocyanin metabolite, protocatechuic acid. *Cancer Prev Res (Phila)* **2014**, *7*, 574-584, doi:10.1158/1940-6207.CAPR-14-0003.
16. Cvorovic, J.; Tramer, F.; Granzotto, M.; Candussio, L.; Decorti, G.; Passamonti, S. Oxidative stress-based cytotoxicity of delphinidin and cyanidin in colon cancer cells. *Arch Biochem Biophys* **2010**, *501*, 151-157, doi:10.1016/j.abb.2010.05.019.

17. Gu, J.; Thomas-Ahner, J.M.; Riedl, K.M.; Bailey, M.T.; Vodovotz, Y.; Schwartz, S.J.; Clinton, S.K. Dietary black raspberries impact the colonic microbiome and phytochemical metabolites in mice. *Mol Nutr Food Res* **2019**, *63*, e1800636, doi:10.1002/mnfr.201800636.
18. Wu, X.; Beecher, G.R.; Holden, J.M.; Haytowitz, D.B.; Gebhardt, S.E.; Prior, R.L. Concentrations of anthocyanins in common foods in the United States and estimation of normal consumption. *J Agric Food Chem* **2006**, *54*, 4069-4075, doi:10.1021/jf0603001.
19. Wang, D.; Wei, X.; Yan, X.; Jin, T.; Ling, W. Protocatechuic acid, a metabolite of anthocyanins, inhibits monocyte adhesion and reduces atherosclerosis in apolipoprotein E-deficient mice. *J Agric Food Chem* **2010**, *58*, 12722-12728, doi:10.1021/jf103427j.
20. Acquaviva, R.; Tomasello, B.; Di Giacomo, C.; Santangelo, R.; La Mantia, A.; Naletova, I.; Sarpietro, M.G.; Castelli, F.; Malfa, G.A. Protocatechuic acid, a simple plant secondary metabolite, induced apoptosis by promoting oxidative stress through HO-1 downregulation and p21 upregulation in colon cancer cells. *Biomolecules* **2021**, *11*, doi:10.3390/biom11101485.
21. Khoo, H.E.; Azlan, A.; Tang, S.T.; Lim, S.M. Anthocyanidins and anthocyanins: colored pigments as food, pharmaceutical ingredients, and the potential health benefits. *Food Nutr Res* **2017**, *61*, 1361779, doi:10.1080/16546628.2017.1361779.
22. Wang, L.S.; Hecht, S.S.; Carmella, S.G.; Yu, N.; Larue, B.; Henry, C.; McIntyre, C.; Rocha, C.; Lechner, J.F.; Stoner, G.D. Anthocyanins in black raspberries prevent esophageal tumors in rats. *Cancer Prev Res (Phila)* **2009**, *2*, 84-93, doi:10.1158/1940-6207.CAPR-08-0155.
23. Montrose, D.C.; Horelik, N.A.; Madigan, J.P.; Stoner, G.D.; Wang, L.S.; Bruno, R.S.; Park, H.J.; Giardina, C.; Rosenberg, D.W. Anti-inflammatory effects of freeze-dried black raspberry powder in ulcerative colitis. *Carcinogenesis* **2011**, *32*, 343-350, doi:10.1093/carcin/bgq248.
24. Pan, P.; Lam, V.; Salzman, N.; Huang, Y.W.; Yu, J.; Zhang, J.; Wang, L.S. Black raspberries and their anthocyanin and fiber fractions alter the composition and diversity of gut microbiota in F-344 rats. *Nutr Cancer* **2017**, *69*, 943-951, doi:10.1080/01635581.2017.1340491.
25. Chen, L.; Jiang, B.; Zhong, C.; Guo, J.; Zhang, L.; Mu, T.; Zhang, Q.; Bi, X. Chemoprevention of colorectal cancer by black raspberry anthocyanins involved the modulation of gut microbiota and SFRP2 demethylation. *Carcinogenesis* **2018**, *39*, 471-481, doi:10.1093/carcin/bgy009.
26. Tu, P.; Bian, X.; Chi, L.; Gao, B.; Ru, H.; Knobloch, T.J.; Weghorst, C.M.; Lu, K. Characterization of the functional changes in mouse gut microbiome associated with increased *Akkermansia muciniphila* population modulated by dietary black raspberries. *ACS Omega* **2018**, *3*, 10927-10937, doi:10.1021/acsomega.8b00064.
27. Shi, N.; Li, N.; Duan, X.; Niu, H. Interaction between the gut microbiome and mucosal immune system. *Mil Med Res* **2017**, *4*, 14, doi:10.1186/s40779-017-0122-9.

28. Kamada, N.; Seo, S.U.; Chen, G.Y.; Nunez, G. Role of the gut microbiota in immunity and inflammatory disease. *Nature reviews. Immunology* **2013**, *13*, 321-335, doi:10.1038/nri3430.
29. Grivennikov, S.I. Inflammation and colorectal cancer: colitis-associated neoplasia. *Sem. Immunopath.* **2013**, *35*, 229-244, doi:10.1007/s00281-012-0352-6.
30. Frank, D.N.; St Amand, A.L.; Feldman, R.A.; Boedeker, E.C.; Harpaz, N.; Pace, N.R. Molecular-phylogenetic characterization of microbial community imbalances in human inflammatory bowel diseases. *Proc. Natl. Acad. Sci. USA* **2007**, *104*, 13780-13785, doi:10.1073/pnas.0706625104.
31. Ott, S.J.; Musfeldt, M.; Wenderoth, D.F.; Hampe, J.; Brant, O.; Folsch, U.R.; Timmis, K.N.; Schreiber, S. Reduction in diversity of the colonic mucosa associated bacterial microflora in patients with active inflammatory bowel disease. *Gut* **2004**, *53*, 685-693, doi:10.1136/gut.2003.025403.
32. Ott, S.J.; Plamondon, S.; Hart, A.; Begun, A.; Rehman, A.; Kamm, M.A.; Schreiber, S. Dynamics of the mucosa-associated flora in ulcerative colitis patients during remission and clinical relapse. *J Clin Microbiol* **2008**, *46*, 3510-3513, doi:10.1128/JCM.01512-08.
33. Wang, W.; Chen, L.; Zhou, R.; Wang, X.; Song, L.; Huang, S.; Wang, G.; Xia, B. Increased proportions of *Bifidobacterium* and the *Lactobacillus* group and loss of butyrate-producing bacteria in inflammatory bowel disease. *J Clin Microbiol* **2014**, *52*, 398-406, doi:10.1128/JCM.01500-13.
34. Schwab, C.; Berry, D.; Rauch, I.; Rennisch, I.; Ramesmayer, J.; Hainzl, E.; Heider, S.; Decker, T.; Kenner, L.; Muller, M., et al. Longitudinal study of murine microbiota activity and interactions with the host during acute inflammation and recovery. *ISME J* **2014**, *8*, 1101-1114, doi:10.1038/ismej.2013.223.
35. Aardema, N.D.; Rodriguez, D.M.; Van Wettene, A.J.; Benninghoff, A.D.; Hintze, K.J. The Western dietary pattern combined with vancomycin-mediated changes to the gut microbiome exacerbates colitis severity and colon tumorigenesis. *Nutrients* **2021**, *13*, doi:10.3390/nu13030881.
36. Rodriguez, D.M.; Benninghoff, A.D.; Aardema, N.D.J.; Phatak, S.; Hintze, K.J. Basal Diet Determined Long-Term Composition of the Gut Microbiome and Mouse Phenotype to a Greater Extent than Fecal Microbiome Transfer from Lean or Obese Human Donors. *Nutrients* **2019**, *11*, doi:10.3390/nu11071630.
37. Caporaso, J.G.; Kuczynski, J.; Stombaugh, J.; Bittinger, K.; Bushman, F.D.; Costello, E.K.; Fierer, N.; Pena, A.G.; Goodrich, J.K.; Gordon, J.I., et al. QIIME allows analysis of high-throughput community sequencing data. *Nat Methods* **2010**, *7*, 335-336, doi:10.1038/nmeth.f.303.
38. Nelson, M.C.; Morrison, H.G.; Benjamino, J.; Grim, S.L.; Graf, J. Analysis, optimization and verification of Illumina-generated 16S rRNA gene amplicon surveys. *PLoS One* **2014**, *9*, e94249, doi:10.1371/journal.pone.0094249.

39. Estaki, M.; Jiang, L.; Bokulich, N.A.; McDonald, D.; Gonzalez, A.; Kosciulek, T.; Martino, C.; Zhu, Q.; Birmingham, A.; Vazquez-Baeza, Y., et al. QIIME 2 enables comprehensive end-to-end analysis of diverse microbiome data and comparative studies with publicly available data. *Curr Protoc Bioinformatics* **2020**, *70*, e100, doi:10.1002/cpbi.100.
40. Callahan, B.J.; McMurdie, P.J.; Rosen, M.J.; Han, A.W.; Johnson, A.J.; Holmes, S.P. DADA2: High-resolution sample inference from Illumina amplicon data. *Nat Methods* **2016**, *13*, 581-583, doi:10.1038/nmeth.3869.
41. Quast, C.; Pruesse, E.; Yilmaz, P.; Gerken, J.; Schweer, T.; Yarza, P.; Peplies, J.; Glockner, F.O. The SILVA ribosomal RNA gene database project: improved data processing and web-based tools. *Nucleic Acids Res* **2013**, *41*, D590-596, doi:10.1093/nar/gks1219.
42. Chong, J.; Liu, P.; Zhou, G.; Xia, J. Using MicrobiomeAnalyst for comprehensive statistical, functional, and meta-analysis of microbiome data. *Nat Protoc* **2020**, *15*, 799-821, doi:10.1038/s41596-019-0264-1.
43. Metsalu, T.; Vilo, J. ClustVis: a web tool for visualizing clustering of multivariate data using Principal Component Analysis and heatmap. *Nucleic Acids Res* **2015**, *43*, W566-570, doi:10.1093/nar/gkv468.
44. Asshauer, K.P.; Wemheuer, B.; Daniel, R.; Meinicke, P. Tax4Fun: predicting functional profiles from metagenomic 16S rRNA data. *Bioinformatics* **2015**, *31*, 2882-2884, doi:10.1093/bioinformatics/btv287.
45. Smith, A.D.; Chen, C.; Cheung, L.; Ward, R.; Hintze, K.J.; Dawson, H.D. Resistant potato starch alters the cecal microbiome and gene expression in mice fed a western diet based on NHANES data. *Front Nutr* **2022**, *9*, 782667, doi:10.3389/fnut.2022.782667.
46. Ward, R.; Hintze, K.; Lefevre, M.; Benninghoff, A.; Li, M.H.; Rompato, G. Effects of green tea on the cecal metagenome of mice fed either the AIN-93 or Total Western Diet. In Proceedings of Faseb Journal, Apr.
47. Pan, P.; Skaer, C.W.; Wang, H.T.; Stirdivant, S.M.; Young, M.R.; Oshima, K.; Stoner, G.D.; Lechner, J.F.; Huang, Y.W.; Wang, L.S. Black raspberries suppress colonic adenoma development in ApcMin/+ mice: relation to metabolite profiles. *Carcinogenesis* **2015**, *36*, 1245-1253, doi:10.1093/carcin/bgv117.
48. Dong, A.; Lin, C.W.; Echeveste, C.E.; Huang, Y.W.; Oshima, K.; Yearsley, M.; Chen, X.; Yu, J.; Wang, L.S. Protocatechuic acid, a gut bacterial metabolite of black raspberries, inhibits adenoma development and alters gut microbiome profiles in Apc (Min/+) mice. *J Cancer Prev* **2022**, *27*, 50-57, doi:10.15430/JCP.2022.27.1.50.
49. Park, S.Y.; Jung, H.; Lin, Z.; Hwang, K.T.; Kwak, H.K. Black raspberry (*Rubus occidentalis*) attenuates inflammatory markers and vascular endothelial dysfunction in Wistar rats fed a high-fat diet with fructose solution. *J Food Biochem* **2021**, *45*, e13917, doi:10.1111/jfbc.13917.

50. Huang, Y.W.; Echeveste, C.E.; Oshima, K.; Zhang, J.; Yearsley, M.; Yu, J.; Wang, L.S. Anti-colonic inflammation by black raspberries through regulating Toll-like receptor-4 signaling in Interlukin-10 knockout mice. *J Cancer Prev* **2020**, *25*, 119-125, doi:10.15430/JCP.2020.25.2.119.
51. Wang, L.S.; Kuo, C.T.; Huang, T.H.; Yearsley, M.; Oshima, K.; Stoner, G.D.; Yu, J.; Lechner, J.F.; Huang, Y.W. Black raspberries protectively regulate methylation of Wnt pathway genes in precancerous colon tissue. *Cancer Prev Res (Phila)* **2013**, *6*, 1317-1327, doi:10.1158/1940-6207.CAPR-13-0077.
52. Wang, L.S.; Kuo, C.T.; Stoner, K.; Yearsley, M.; Oshima, K.; Yu, J.; Huang, T.H.; Rosenberg, D.; Peiffer, D.; Stoner, G., et al. Dietary black raspberries modulate DNA methylation in dextran sodium sulfate (DSS)-induced ulcerative colitis. *Carcinogenesis* **2013**, *34*, 2842-2850, doi:10.1093/carcin/bgt310.
53. Tu, P.; Chi, L.; Bian, X.; Gao, B.; Ru, H.; Lu, K. A black raspberry-rich diet protects from dextran sulfate sodium-induced intestinal inflammation and host metabolic perturbation in association with increased aryl hydrocarbon receptor ligands in the gut microbiota of mice. *Front Nutr* **2022**, *9*, 842298, doi:10.3389/fnut.2022.842298.
54. Shen, Z.H.; Zhu, C.X.; Quan, Y.S.; Yang, Z.Y.; Wu, S.; Luo, W.W.; Tan, B.; Wang, X.Y. Relationship between intestinal microbiota and ulcerative colitis: mechanisms and clinical application of probiotics and fecal microbiota transplantation. *World J Gastroenterol* **2018**, *24*, 5-14, doi:10.3748/wjg.v24.i1.5.
55. Turnbaugh, P.J.; Ley, R.E.; Mahowald, M.A.; Magrini, V.; Mardis, E.R.; Gordon, J.I. An obesity-associated gut microbiome with increased capacity for energy harvest. *Nature* **2006**, *444*, 1027-1031, doi:10.1038/nature05414.
56. Turpin, W.; Bedrani, L.; Espin-Garcia, O.; Xu, W.; Silverberg, M.S.; Smith, M.I.; Garay, J.A.R.; Lee, S.H.; Guttman, D.S.; Griffiths, A., et al. Associations of NOD2 polymorphisms with Erysipelotrichaceae in stool of in healthy first degree relatives of Crohn's disease subjects. *BMC Med Genet* **2020**, *21*, 204, doi:10.1186/s12881-020-01115-w.
57. Teofani, A.; Marafini, I.; Laudisi, F.; Pietrucci, D.; Salvatori, S.; Unida, V.; Biocca, S.; Monteleone, G.; Desideri, A. Intestinal taxa abundance and diversity in inflammatory bowel disease patients: an analysis including covariates and confounders. *Nutrients* **2022**, *14*, doi:10.3390/nu14020260.
58. Schaubeck, M.; Clavel, T.; Calasan, J.; Lagkouvardos, I.; Haange, S.B.; Jehmlich, N.; Basic, M.; Dupont, A.; Hornef, M.; von Bergen, M., et al. Dysbiotic gut microbiota causes transmissible Crohn's disease-like ileitis independent of failure in antimicrobial defence. *Gut* **2016**, *65*, 225-237, doi:10.1136/gutjnl-2015-309333.
59. Zhuang, Z.; Li, N.; Wang, J.; Yang, R.; Wang, W.; Liu, Z.; Huang, T. GWAS-associated bacteria and their metabolites appear to be causally related to the development of inflammatory bowel disease. *Eur J Clin Nutr* **2022**, 10.1038/s41430-022-01074-w, doi:10.1038/s41430-022-01074-w.

60. Huang, F.; Zhao, R.; Xia, M.; Shen, G.X. Impact of Cyanidin-3-Glucoside on gut microbiota and relationship with metabolism and inflammation in high fat-high sucrose diet-induced insulin resistant mice. *Microorganisms* **2020**, *8*, doi:10.3390/microorganisms8081238.
61. Tojo, R.; Suarez, A.; Clemente, M.G.; de los Reyes-Gavilan, C.G.; Margolles, A.; Gueimonde, M.; Ruas-Madiedo, P. Intestinal microbiota in health and disease: role of *Bifidobacteria* in gut homeostasis. *World J Gastroenterol* **2014**, *20*, 15163-15176, doi:10.3748/wjg.v20.i41.15163.
62. Yao, S.; Zhao, Z.; Wang, W.; Liu, X. *Bifidobacterium longum*: protection against inflammatory bowel disease. *J Immunol Res* **2021**, *2021*, 8030297, doi:10.1155/2021/8030297.
63. Vitali, F.; Tortora, K.; Di Paola, M.; Bartolucci, G.; Menicatti, M.; De Filippo, C.; Caderni, G. Intestinal microbiota profiles in a genetic model of colon tumorigenesis correlates with colon cancer biomarkers. *Sci Rep* **2022**, *12*, 1432, doi:10.1038/s41598-022-05249-0.
64. Vacca, M.; Celano, G.; Calabrese, F.M.; Portincasa, P.; Gobbetti, M.; De Angelis, M. The controversial role of human gut Lachnospiraceae. *Microorganisms* **2020**, *8*, doi:10.3390/microorganisms8040573.
65. Sinha, R.; Ahn, J.; Sampson, J.N.; Shi, J.; Yu, G.; Xiong, X.; Hayes, R.B.; Goedert, J.J. Fecal microbiota, fecal metabolome, and colorectal cancer interrelations. *PLoS One* **2016**, *11*, e0152126, doi:10.1371/journal.pone.0152126.
66. He, X.X.; Li, Y.H.; Yan, P.G.; Meng, X.C.; Chen, C.Y.; Li, K.M.; Li, J.N. Relationship between clinical features and intestinal microbiota in Chinese patients with ulcerative colitis. *World J Gastroenterol* **2021**, *27*, 4722-4737, doi:10.3748/wjg.v27.i28.4722.
67. Li, J.; Wu, T.; Li, N.; Wang, X.; Chen, G.; Lyu, X. Bilberry anthocyanin extract promotes intestinal barrier function and inhibits digestive enzyme activity by regulating the gut microbiota in aging rats. *Food Funct* **2019**, *10*, 333-343, doi:10.1039/c8fo01962b.
68. Chen, G.; Wang, G.; Zhu, C.; Jiang, X.; Sun, J.; Tian, L.; Bai, W. Effects of cyanidin-3-O-glucoside on 3-chloro-1,2-propanediol induced intestinal microbiota dysbiosis in rats. *Food Chem Toxicol* **2019**, *133*, 110767, doi:10.1016/j.fct.2019.110767.
69. Peng, L.; Li, Z.R.; Green, R.S.; Holzman, I.R.; Lin, J. Butyrate enhances the intestinal barrier by facilitating tight junction assembly via activation of AMP-activated protein kinase in Caco-2 cell monolayers. *J Nutr* **2009**, *139*, 1619-1625, doi:10.3945/jn.109.104638.
70. Vital, M.; Karch, A.; Pieper, D.H. Colonic butyrate-producing communities in humans: an overview using omics data. *mSystems* **2017**, *2*, doi:10.1128/mSystems.00130-17.
71. Sinha, S.R.; Haileselassie, Y.; Nguyen, L.P.; Tropini, C.; Wang, M.; Becker, L.S.; Sim, D.; Jarr, K.; Spear, E.T.; Singh, G., et al. Dysbiosis-induced secondary bile acid deficiency promotes intestinal inflammation. *Cell Host Microbe* **2020**, *27*, 659-670 e655, doi:10.1016/j.chom.2020.01.021.

72. Liu, J.; Hao, W.; He, Z.; Kwek, E.; Zhu, H.; Ma, N.; Ma, K.Y.; Chen, Z.Y. Blueberry and cranberry anthocyanin extracts reduce bodyweight and modulate gut microbiota in C57BL/6 J mice fed with a high-fat diet. *Eur J Nutr* **2021**, *60*, 2735-2746, doi:10.1007/s00394-020-02446-3.
73. Kennedy, N.A.; Lamb, C.A.; Berry, S.H.; Walker, A.W.; Mansfield, J.; Parkes, M.; Simpkins, R.; Tremelling, M.; Nutland, S.; Consortium, U.I.G., et al. The impact of NOD2 variants on fecal microbiota in Crohn's disease and controls without gastrointestinal disease. *Inflamm Bowel Dis* **2018**, *24*, 583-592, doi:10.1093/ibd/izx061.
74. Wu, S.; Hu, R.; Nakano, H.; Chen, K.; Liu, M.; He, X.; Zhang, H.; He, J.; Hou, D.X. Modulation of gut microbiota by *Lonicera caerulea* L. berry polyphenols in a mouse model of fatty liver induced by high fat diet. *Molecules* **2018**, *23*, doi:10.3390/molecules23123213.
75. Ansaldo, E.; Slayden, L.C.; Ching, K.L.; Koch, M.A.; Wolf, N.K.; Plichta, D.R.; Brown, E.M.; Graham, D.B.; Xavier, R.J.; Moon, J.J., et al. *Akkermansia muciniphila* induces intestinal adaptive immune responses during homeostasis. *Science* **2019**, *364*, 1179-1184, doi:10.1126/science.aaw7479.
76. Zhang, T.; Ji, X.; Lu, G.; Zhang, F. The potential of *Akkermansia muciniphila* in inflammatory bowel disease. *Appl Microbiol Biotechnol* **2021**, *105*, 5785-5794, doi:10.1007/s00253-021-11453-1.
77. Bajer, L.; Kverka, M.; Kostovcik, M.; Macinga, P.; Dvorak, J.; Stehlikova, Z.; Brezina, J.; Wohl, P.; Spicak, J.; Drastich, P. Distinct gut microbiota profiles in patients with primary sclerosing cholangitis and ulcerative colitis. *World J Gastroenterol* **2017**, *23*, 4548-4558, doi:10.3748/wjg.v23.i25.4548.
78. Danilova, N.A.; Abdulkhakov, S.R.; Grigoryeva, T.V.; Markelova, M.I.; Vasilyev, I.Y.; Boulygina, E.A.; Ardatskaya, M.D.; Pavlenko, A.V.; Tyakht, A.V.; Odintsova, A.K., et al. Markers of dysbiosis in patients with ulcerative colitis and Crohn's disease. *Ter Arkh* **2019**, *91*, 17-24, doi:10.26442/00403660.2019.04.000211.
79. Png, C.W.; Linden, S.K.; Gilshenan, K.S.; Zoetendal, E.G.; McSweeney, C.S.; Sly, L.I.; McGuckin, M.A.; Florin, T.H. Mucolytic bacteria with increased prevalence in IBD mucosa augment in vitro utilization of mucin by other bacteria. *Am J Gastroenterol* **2010**, *105*, 2420-2428, doi:10.1038/ajg.2010.281.
80. Pisani, A.; Rausch, P.; Bang, C.; Ellul, S.; Tabone, T.; Marantidis Cordina, C.; Zahra, G.; Franke, A.; Ellul, P. Dysbiosis in the gut microbiota in patients with inflammatory bowel disease during remission. *Microbiol Spectr* **2022**, *10*, e0061622, doi:10.1128/spectrum.00616-22.
81. Zhang, T.; Li, P.; Wu, X.; Lu, G.; Marcella, C.; Ji, X.; Ji, G.; Zhang, F. Alterations of *Akkermansia muciniphila* in the inflammatory bowel disease patients with washed microbiota transplantation. *Appl Microbiol Biotechnol* **2020**, *104*, 10203-10215, doi:10.1007/s00253-020-10948-7.
82. Bian, X.; Wu, W.; Yang, L.; Lv, L.; Wang, Q.; Li, Y.; Ye, J.; Fang, D.; Wu, J.; Jiang, X., et al. Administration of *Akkermansia muciniphila* ameliorates dextran sulfate sodium-

- induced ulcerative colitis in mice. *Front Microbiol* **2019**, *10*, 2259, doi:10.3389/fmicb.2019.02259.
83. Fan, L.; Xu, C.; Ge, Q.; Lin, Y.; Wong, C.C.; Qi, Y.; Ye, B.; Lian, Q.; Zhuo, W.; Si, J., et al. *A. Muciniphila* suppresses colorectal tumorigenesis by inducing TLR2/NLRP3-mediated M1-like TAMs. *Cancer Immunol Res* **2021**, *9*, 1111-1124, doi:10.1158/2326-6066.CIR-20-1019.
84. Seregin, S.S.; Golovchenko, N.; Schaf, B.; Chen, J.; Pudlo, N.A.; Mitchell, J.; Baxter, N.T.; Zhao, L.; Schloss, P.D.; Martens, E.C., et al. NLRP6 protects Il10(-/-) mice from colitis by limiting colonization of *Akkermansia muciniphila*. *Cell Rep* **2017**, *19*, 733-745, doi:10.1016/j.celrep.2017.03.080.
85. Roopchand, D.E.; Carmody, R.N.; Kuhn, P.; Moskal, K.; Rojas-Silva, P.; Turnbaugh, P.J.; Raskin, I. Dietary polyphenols promote growth of the gut bacterium *Akkermansia muciniphila* and attenuate high-fat diet-induced metabolic syndrome. *Diabetes* **2015**, *64*, 2847-2858, doi:10.2337/db14-1916.
86. Rodriguez-Daza, M.C.; Roquim, M.; Dudonne, S.; Pilon, G.; Levy, E.; Marette, A.; Roy, D.; Desjardins, Y. Berry polyphenols and fibers modulate distinct microbial metabolic functions and gut microbiota enterotype-like clustering in obese mice. *Front Microbiol* **2020**, *11*, 2032, doi:10.3389/fmicb.2020.02032.
87. Sharpton, T.; Lyalina, S.; Luong, J.; Pham, J.; Deal, E.M.; Armour, C.; Gaulke, C.; Sanjabi, S.; Pollard, K.S. Development of inflammatory bowel disease is linked to a longitudinal restructuring of the gut metagenome in mice. *mSystems* **2017**, *2*, doi:10.1128/mSystems.00036-17.
88. Parada Venegas, D.; De la Fuente, M.K.; Landskron, G.; Gonzalez, M.J.; Quera, R.; Dijkstra, G.; Harmsen, H.J.M.; Faber, K.N.; Hermoso, M.A. Short chain fatty Acids (SCFAs)-mediated gut epithelial and immune regulation and its relevance for inflammatory bowel diseases. *Front Immunol* **2019**, *10*, 277, doi:10.3389/fimmu.2019.00277.
89. Tan, J.; Li, Y.; Hou, D.X.; Wu, S. The effects and mechanisms of cyanidin-3-glucoside and its phenolic metabolites in maintaining intestinal integrity. *Antioxidants (Basel)* **2019**, *8*, doi:10.3390/antiox8100479.
90. Tu, P.; Bian, X.; Chi, L.; Xue, J.; Gao, B.; Lai, Y.; Ru, H.; Lu, K. Metabolite profiling of the gut microbiome in mice with dietary administration of black raspberries. *ACS Omega* **2020**, *5*, 1318-1325, doi:10.1021/acsomega.9b00237.
91. Liu, H.; Wang, J.; He, T.; Becker, S.; Zhang, G.; Li, D.; Ma, X. Butyrate: a double-edged sword for health? *Adv Nutr* **2018**, *9*, 21-29, doi:10.1093/advances/nmx009.

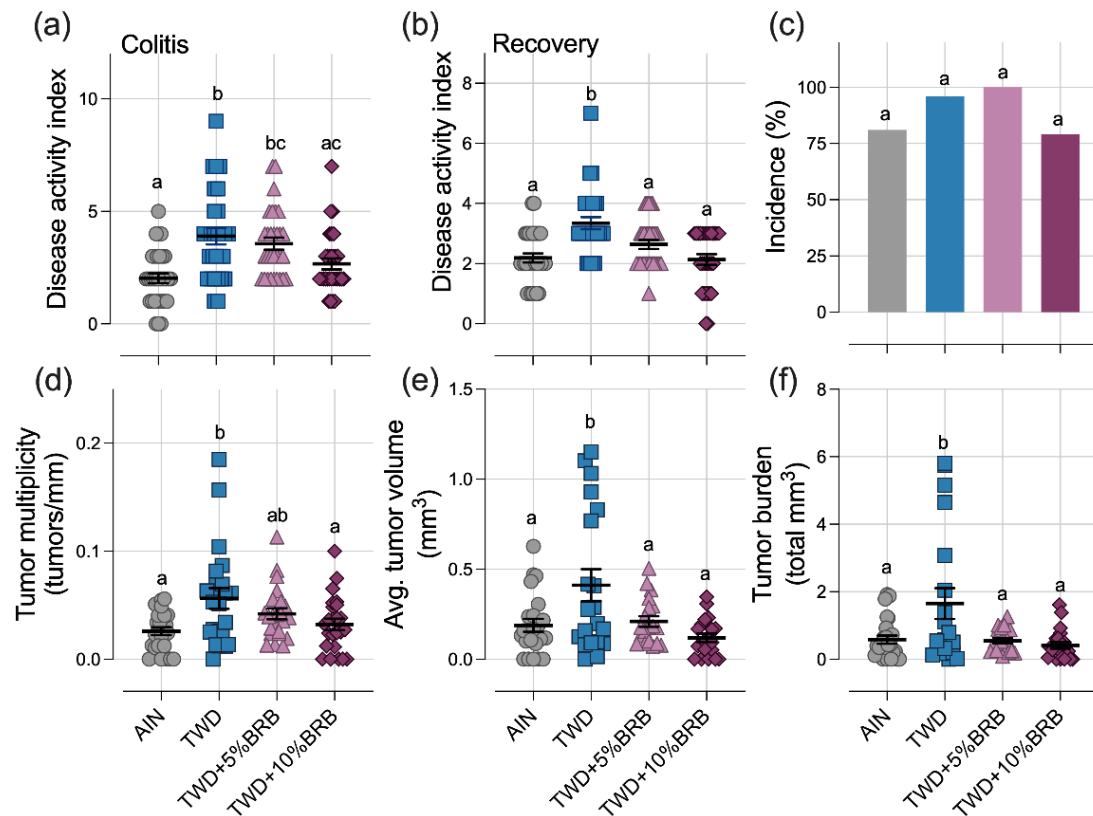


Figure 2.1. Dietary supplementation with 5 to 10% BRB suppressed symptoms of colitis and colon tumorigenesis in mice fed TWD (experiment A). **(a,b)** Disease activity index (DAI) score during active colitis on day 33 **(a)** and recovery from gut injury on day 45 **(b)**. **(c)** Incidence of colon tumors shown as the percent of mice with tumors. **(d)** Colon tumor multiplicity (number of tumors per mm colon length). **(e)** Average tumor volume. **(f)** Tumor burden (total volume). For **(a,b)** and **(d-f)**, data are shown as individual values with mean \pm SE. Different letters indicate that treatment groups are significantly different ($p < 0.05$), as determined by statistical methods outlined in the Materials and Methods section.

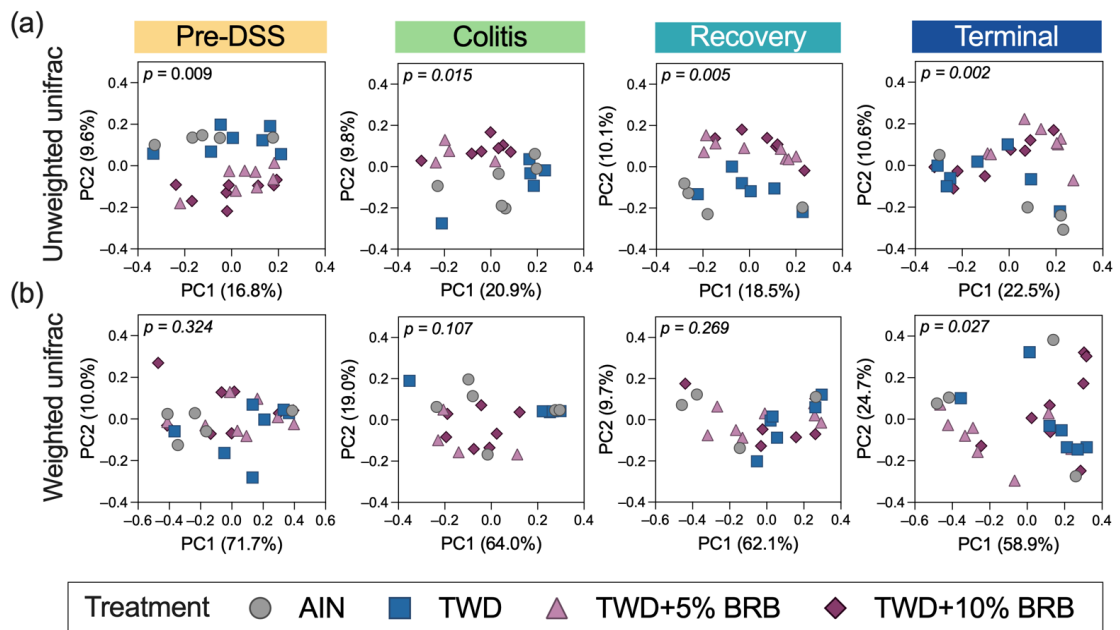


Figure 2.2. Beta diversity of mouse microbiomes at each experimental time point (experiment A). Principal coordinate plots depicting fecal microbiome beta diversity using (a) unweighted or (b) weighted unifracs distances are shown with the two components. The variation attributed to PC1 and PC2 along with the permanova p -values are provided for each plot.

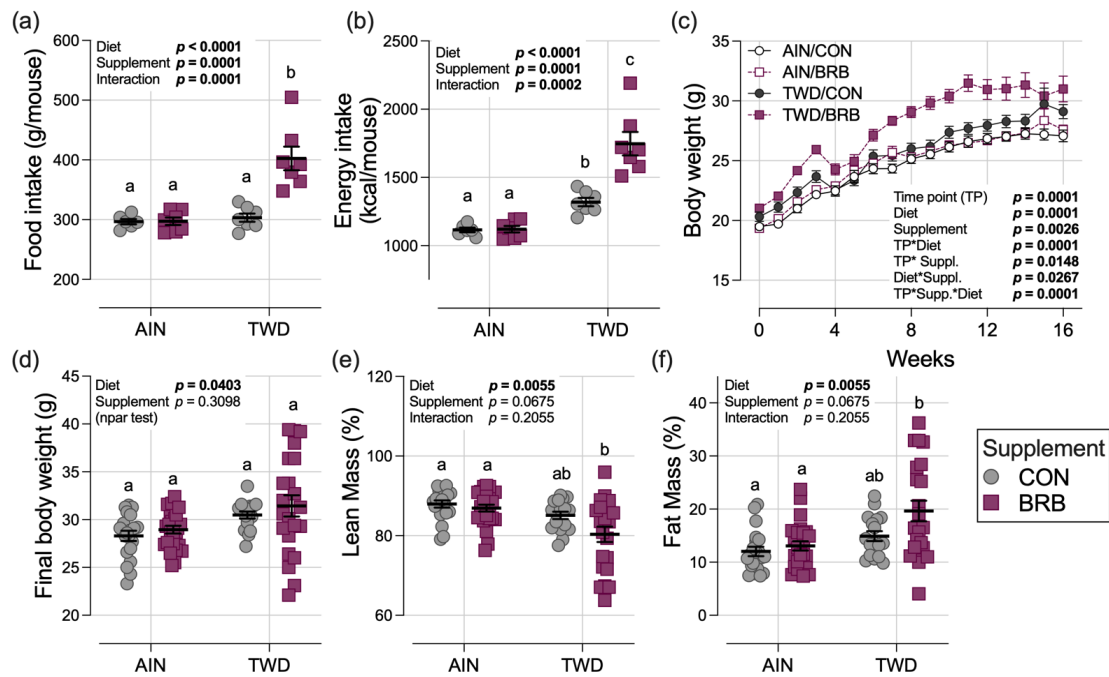


Figure 2.3. Food and energy intakes, body weight and body composition (experiment B). **(a,b)** Estimated total daily food and energy intake per mouse. See Figure 2.S7 for longitudinal food and energy intake data. **(c)** Body weight gain over the study period. **(d)** Final body weight at study end on day 115. **(e,f)** Lean and fat mass as percentage of body weight. Data are shown as the individual measurements (except **(c)**) with the mean \pm SE **(a,b,d-f)**. Inset tables show the statistical model main effects for diet, treatment and their interaction or “npar test” if a non-parametric test was required, and different letters indicate that experimental groups are significantly different ($p < 0.05$), as determined by statistical methods outlined in Materials and Methods.

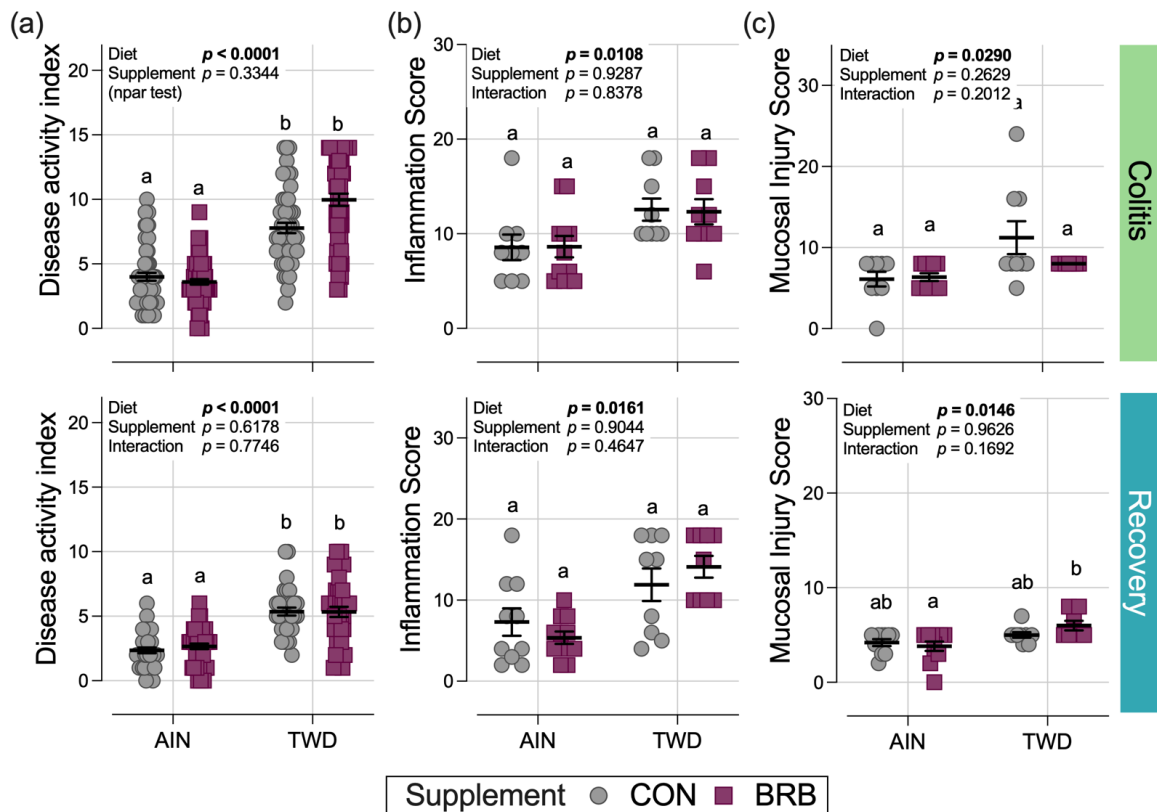


Figure 2.4. Disease activity index and colon histopathology (experiment B). Scores for the disease activity index (DAI) (a), histopathology inflammation score (b) and histopathology mucosal injury score (c) are shown for active colitis on day 33 and recovery from gut injury on day 45. Data are shown as individual values with mean \pm SE. Inset tables provide the statistical model main effects for diet, treatment and their interaction or “npar test” if a non-parametric test was required, and different letters indicate that experimental groups are significantly different ($p < 0.05$), as determined by statistical methods outlined in the Materials and Methods section.

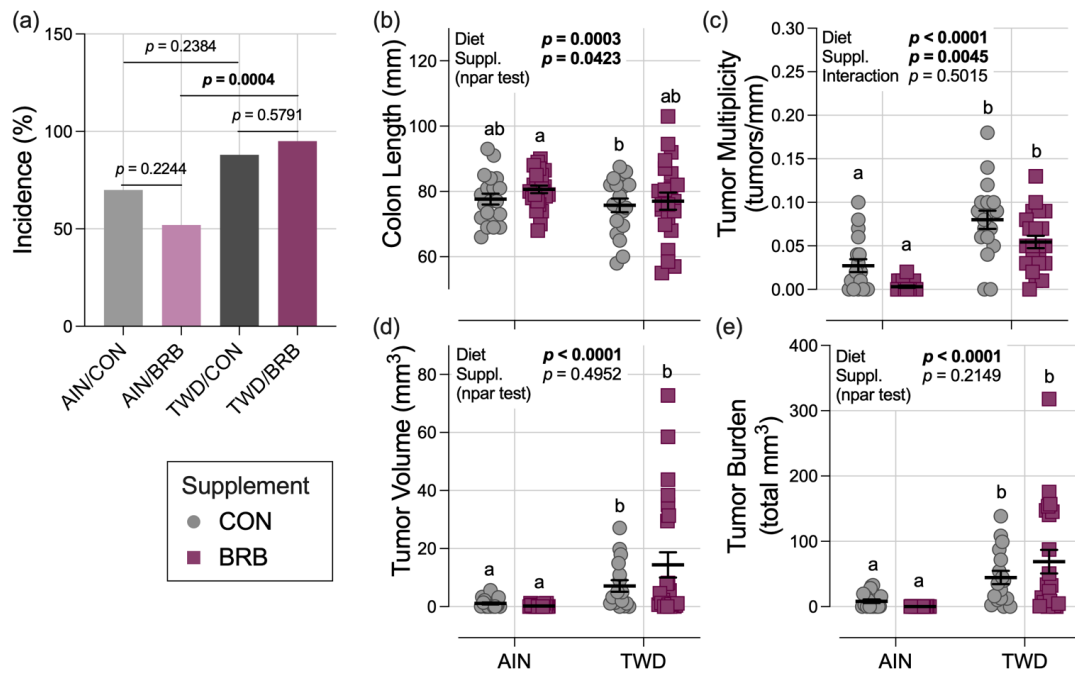


Figure 2.5. Effect of BRB supplementation on colon length and colon tumorigenesis in mice fed AIN or TWD basal diets (experiment B). (a) Incidence of colon tumors shown as the percent of mice with tumors at the terminal time point. P-values from pairwise Fisher exact tests (selected *a priori*) are shown. (b) Colon length. (c) Colon tumor multiplicity (number of tumors per mm colon length). (d) Average tumor volume. (e) Tumor burden (total volume). For (b–e), data are shown as individual values with mean \pm SE. Inset tables show the statistical model main effects for diet, treatment and their interaction or “npar test” if a non-parametric test was required, and different letters indicate that experimental groups are significantly different ($p < 0.05$), as determined by statistical methods outlined in the Materials and Methods section.

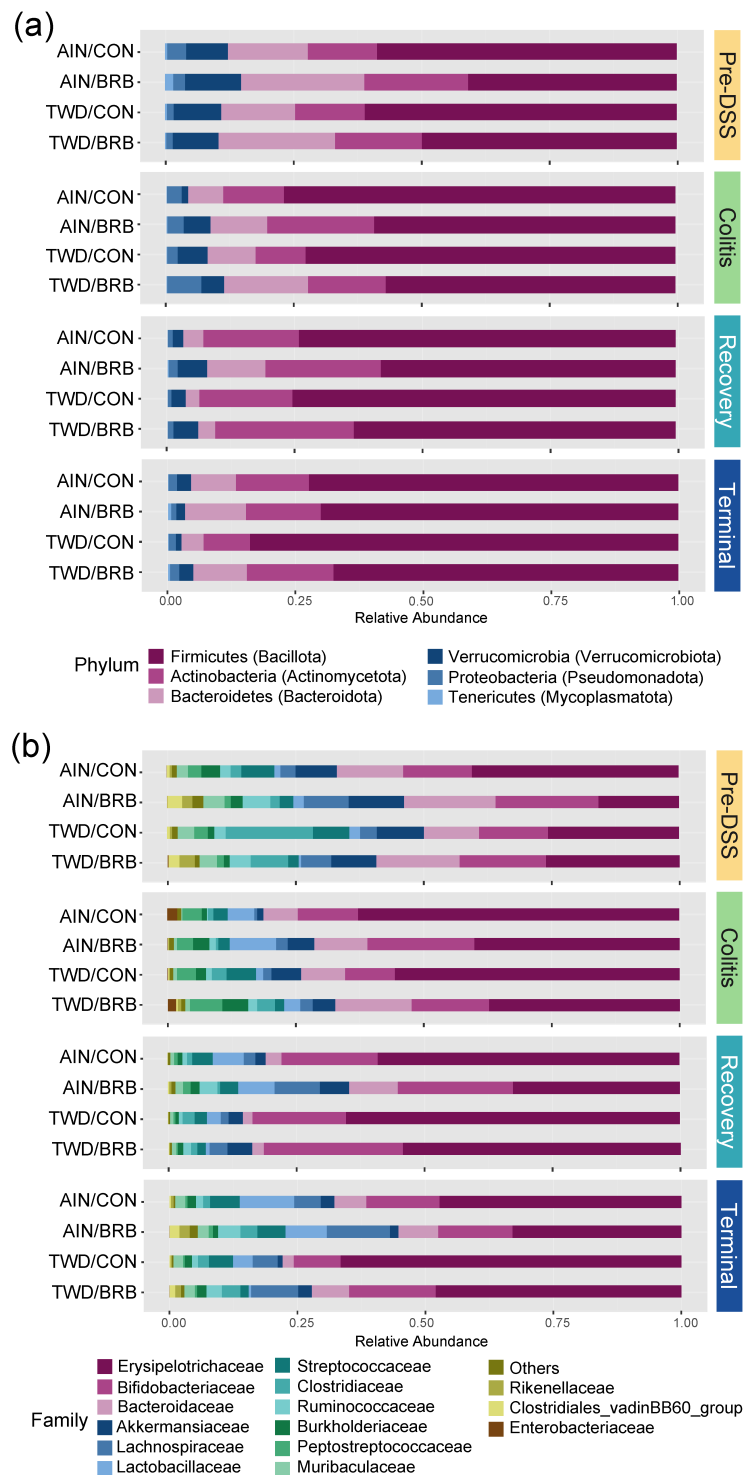


Figure 2.6. Taxonomic classification of mouse fecal bacteria (experiment B). Data shown are the relative normalized abundance of bacteria annotated to phylum (a) or family (b) taxonomic levels for the top 15 most abundant taxa for each experimental group for each experimental time point. New phylum level taxonomic designations are indicated in parentheses (a).

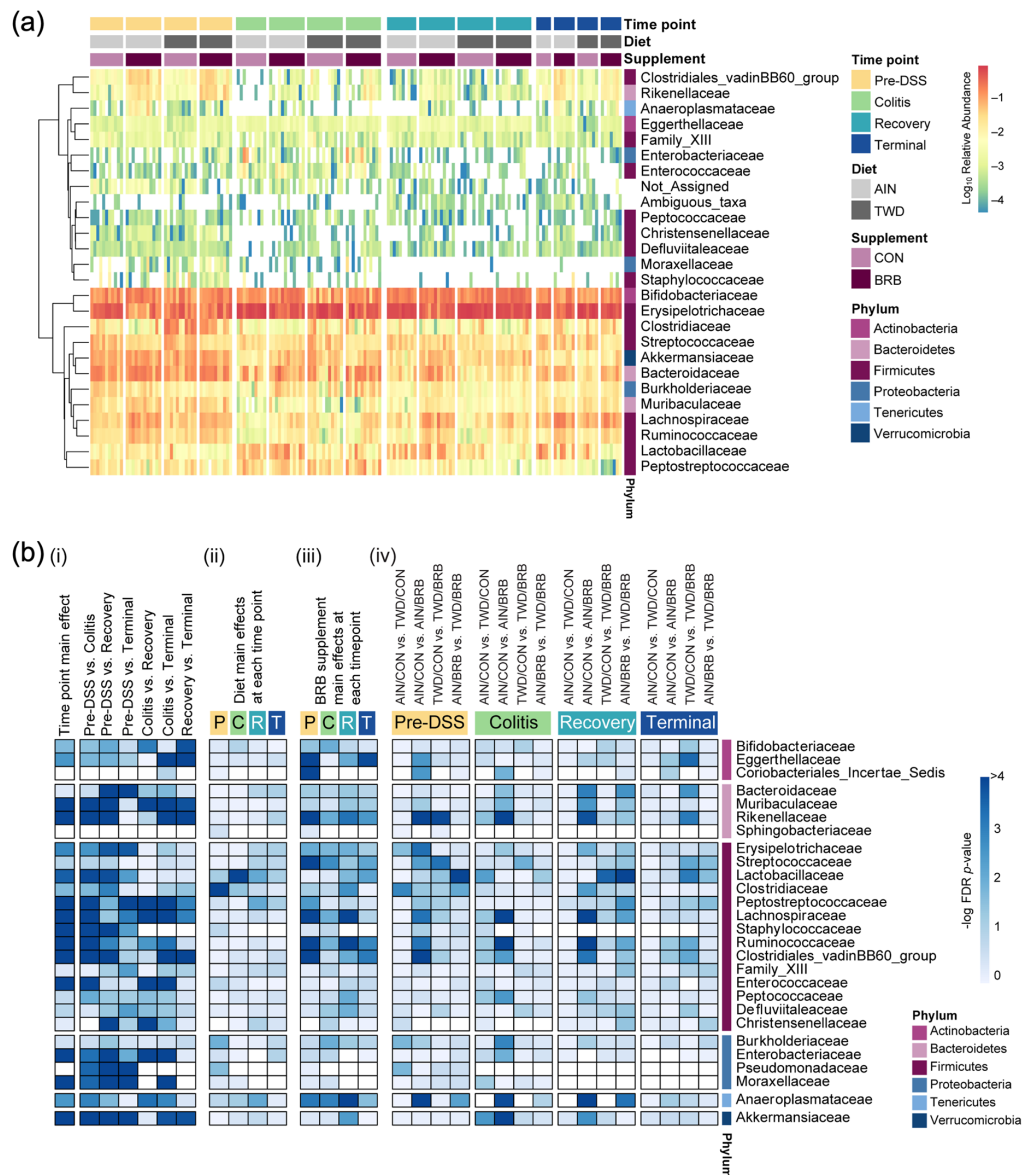


Figure 2.7. Relative abundance of fecal microbiome at the family taxonomic level with summary of results of metagenomeSeq statistical analyses (experiment B). **(a)** Unsupervised hierarchical cluster analysis shows the \log_{10} relative abundance with clustering by taxa using the Euclidean distance with average linkage. **(b)** Summary plot shows the \log_{10} FDR-adjusted p -values obtained from metagenomeSeq analyses of fecal microbiome profiles. All tests were determined *a priori*, and complete results are provided in File 2.S4. (i) Analyses for main effects of time point and pairwise comparisons across time points, irrespective of basal diet or BRB supplementation. (ii) Analyses for diet main effects, irrespective of BRB supplementation, at each time point. (iii) Analyses for BRB supplementation main effects, irrespective of basal diet, at each time point. (iv) Selected pairwise tests for basal diet and BRB supplement combinations within each study time point. A significant effect was inferred for FDR-adjusted p -values < 0.05 (increasing blue on the color scale).

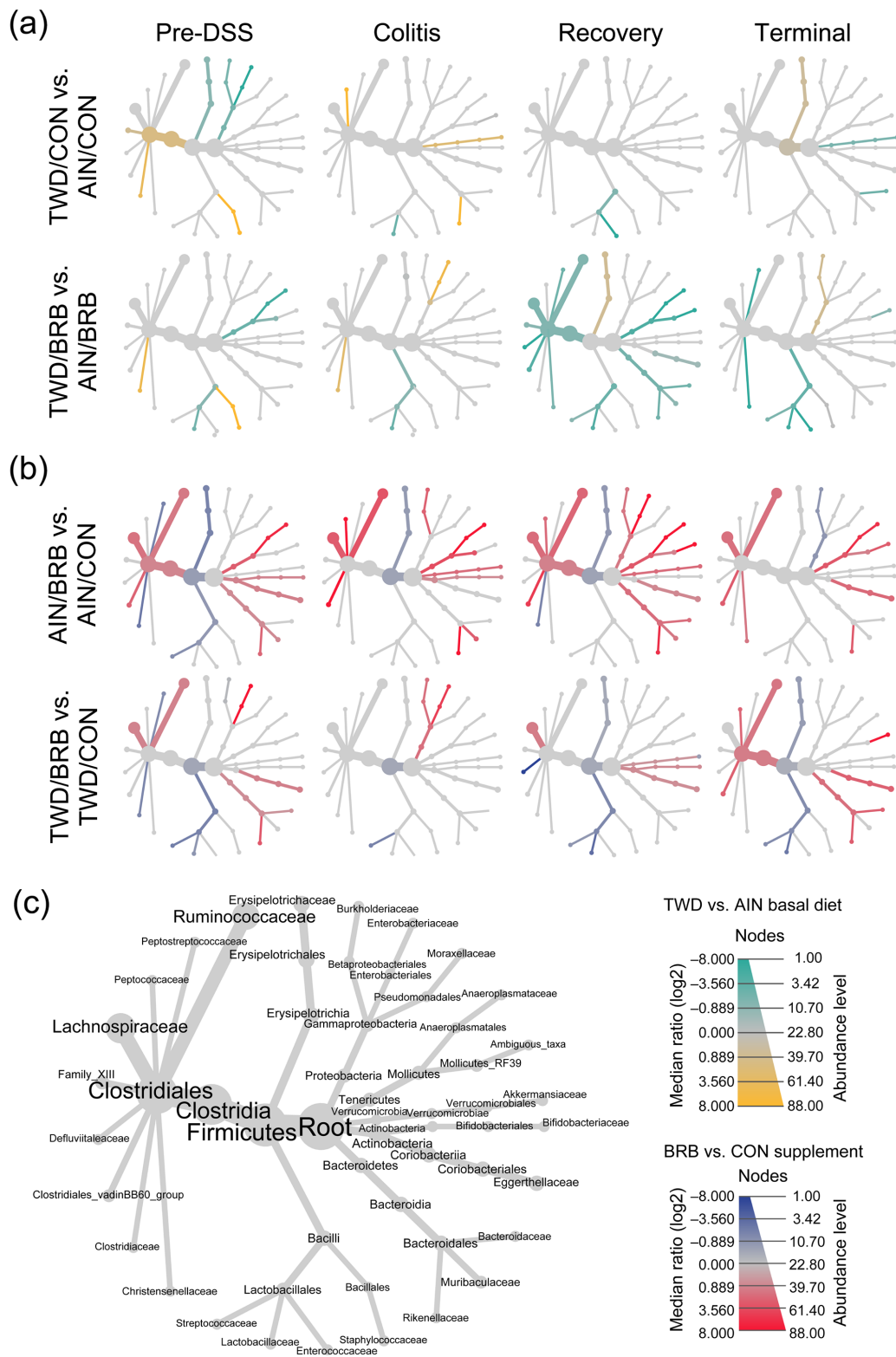


Figure 2.8. Fecal microbiome community structures depicted as heat trees showing the relative abundance ratios for selected comparisons of basal diet and BRB supplement at each experimental time point (experiment B). **(a)** Comparisons of TWD versus AIN basal diet with or without BRB supplementation (green-to-yellow color bar, with yellow indicating greater abundance in TWD-fed mice; top legend). **(b)** Comparisons of BRB versus CON supplement for AIN or TWD basal diets (blue-to-red color bar, with red indicating greater abundance in BRB-supplemented mice; bottom legend). **(c)** Phylogenetic structure of fecal microbiome bacteria community.

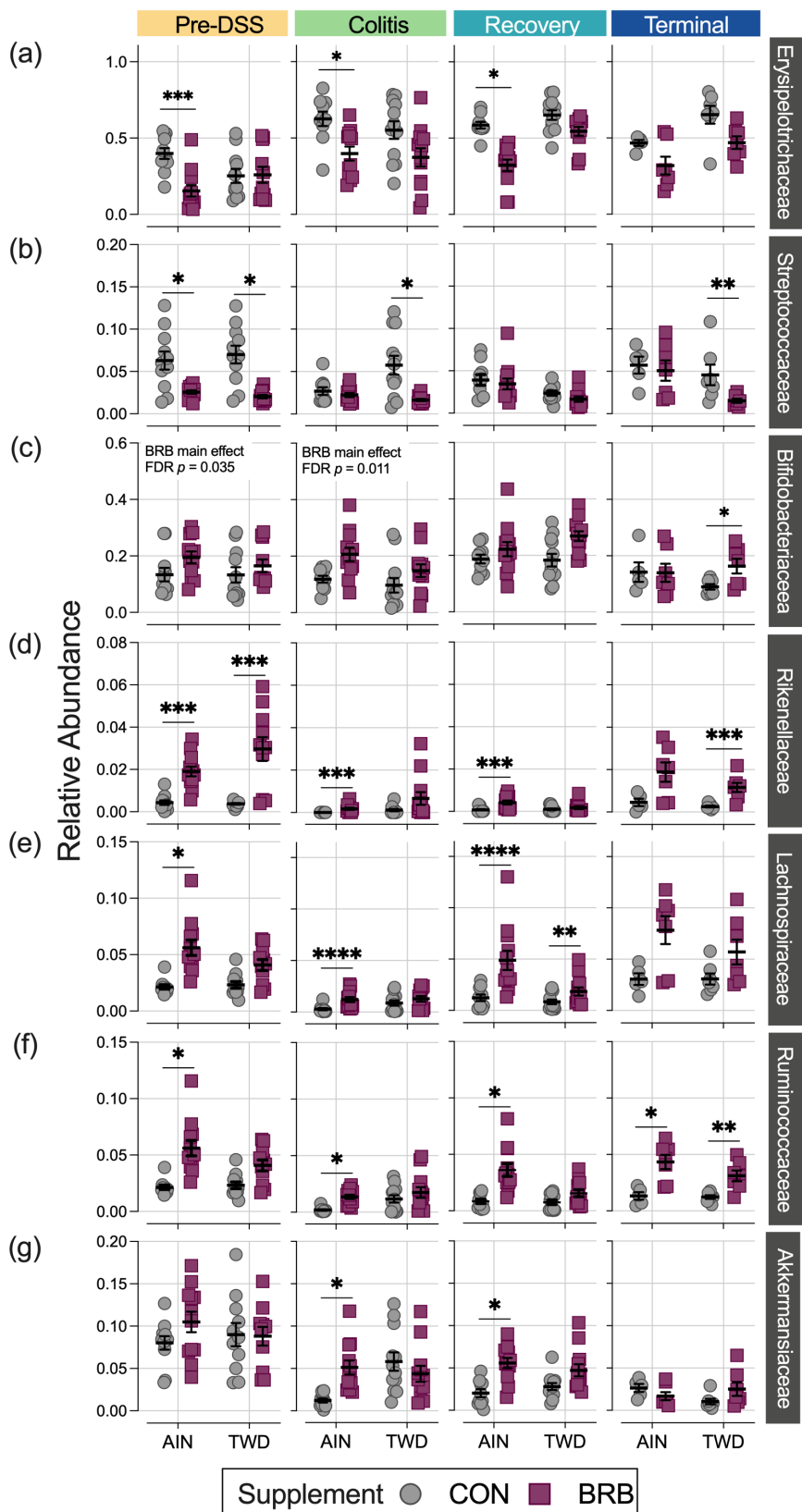


Figure 2.9. Relative abundance of select bacteria families of interest for each experimental time point (experiment B). **(a)** Erysipelotrichaceae, **(b)** Streptococcaceae, **(c)** Bifidobacteriaceae, **(d)** Lachnospiraceae, **(e)** Rikenellaceae, **(f)** Ruminococcaceae and **(g)** Akkermansiaceae. Data are shown as individual values that represent each cage (as the biological unit) with mean \pm SE. For simplified visualization, this plot shows only the statistical results as FDR-corrected p -values for comparisons between CON and BRB-supplemented diets as indicated: *, $p < 0.05$; **, $p < 0.01$; and ***, $p < 0.001$, as outlined in Materials and Methods. Complete results of all metagenome-Seq statistical analyses, including pairwise comparisons by basal diet and across time points, are provided in File 2.S4.

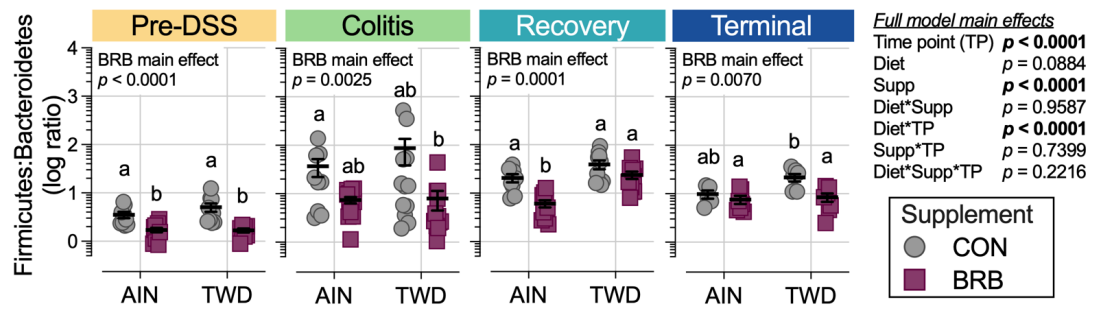


Figure 2.10. Ratio of Firmicutes to Bacteroidetes for each experimental time point (experiment B). Ratios were determined using normalized count data for each phylum. Data are shown as individual values representing each cage (as the biological unit) with mean \pm SE. The table shows the statistical model main effects, including all experimental factors, and different letters indicate that experimental groups are significantly different ($p < 0.05$), as determined by statistical methods outlined in the Materials and Methods section.

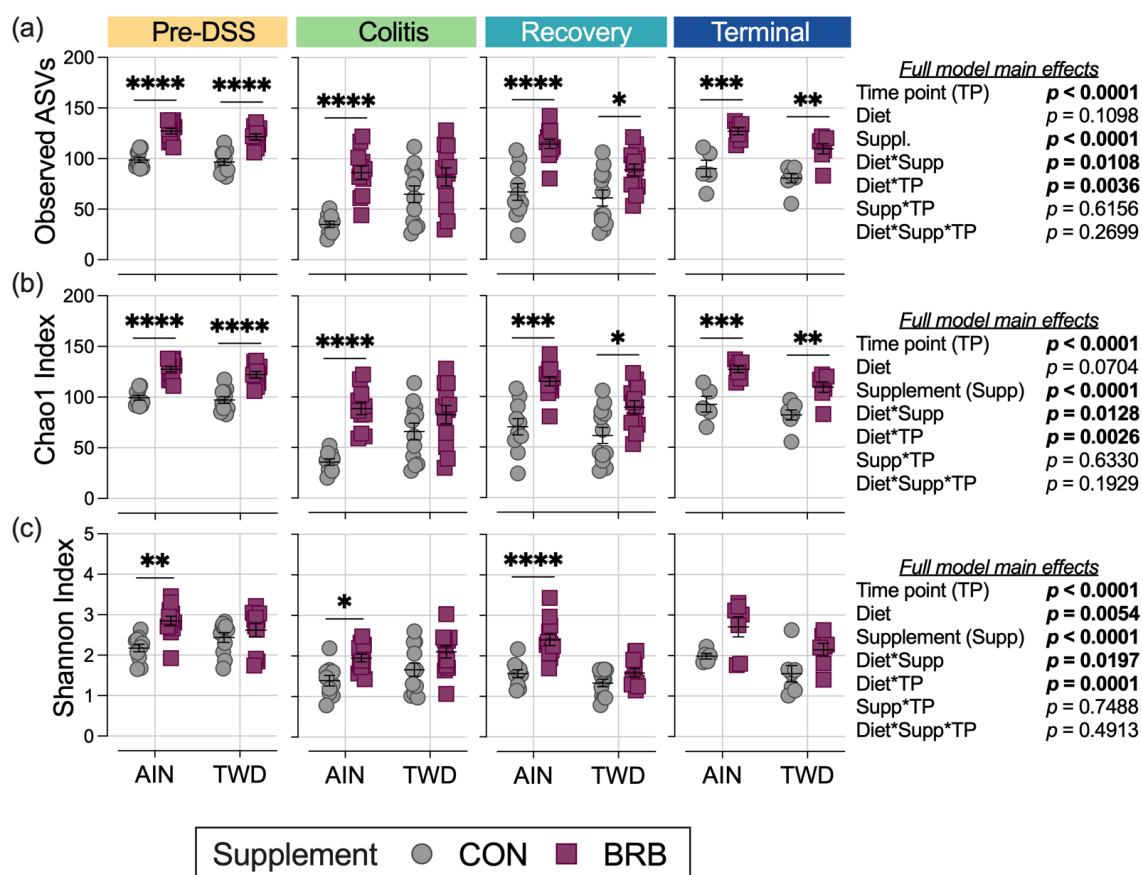


Figure 2.11. Alpha diversity of mouse fecal microbiomes for each experimental time point (experiment B). Alpha diversity measures include (a) observed ASVs, (b) the Chao1 index and (c) the Shannon index. Data are shown as individual values representing each cage (as the biological unit) with mean \pm SE. Inset tables show the statistical model main effects, including all experimental factors, for each α -diversity measure. For simplified visualization, this plot shows only the statistical results for comparisons between CON and BRB-supplemented diets, as indicated: *, $p < 0.05$; **, $p < 0.01$; ***, $p < 0.001$; and ****, $p < 0.0001$, as outlined in Materials and Methods. Complete results of these statistical analyses, including comparisons within and across time points, are provided in Tables 3.S2–3.S4.

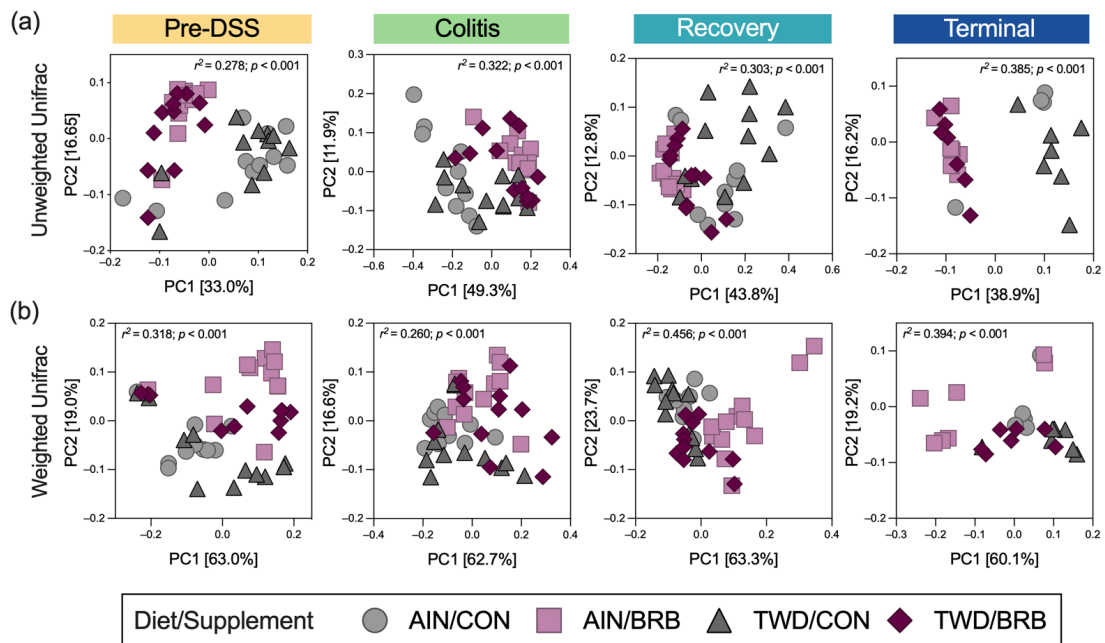


Figure 2.12. Beta diversity of mouse fecal microbiomes for each experimental time point (experiment B). Principal coordinate plots depicting fecal microbiome beta diversity using (a) unweighted or (b) weighted unifracs distances are shown using the first two components. The variations attributed to PC1 and PC2 are shown along with the r^2 and permanova p -values for each plot.

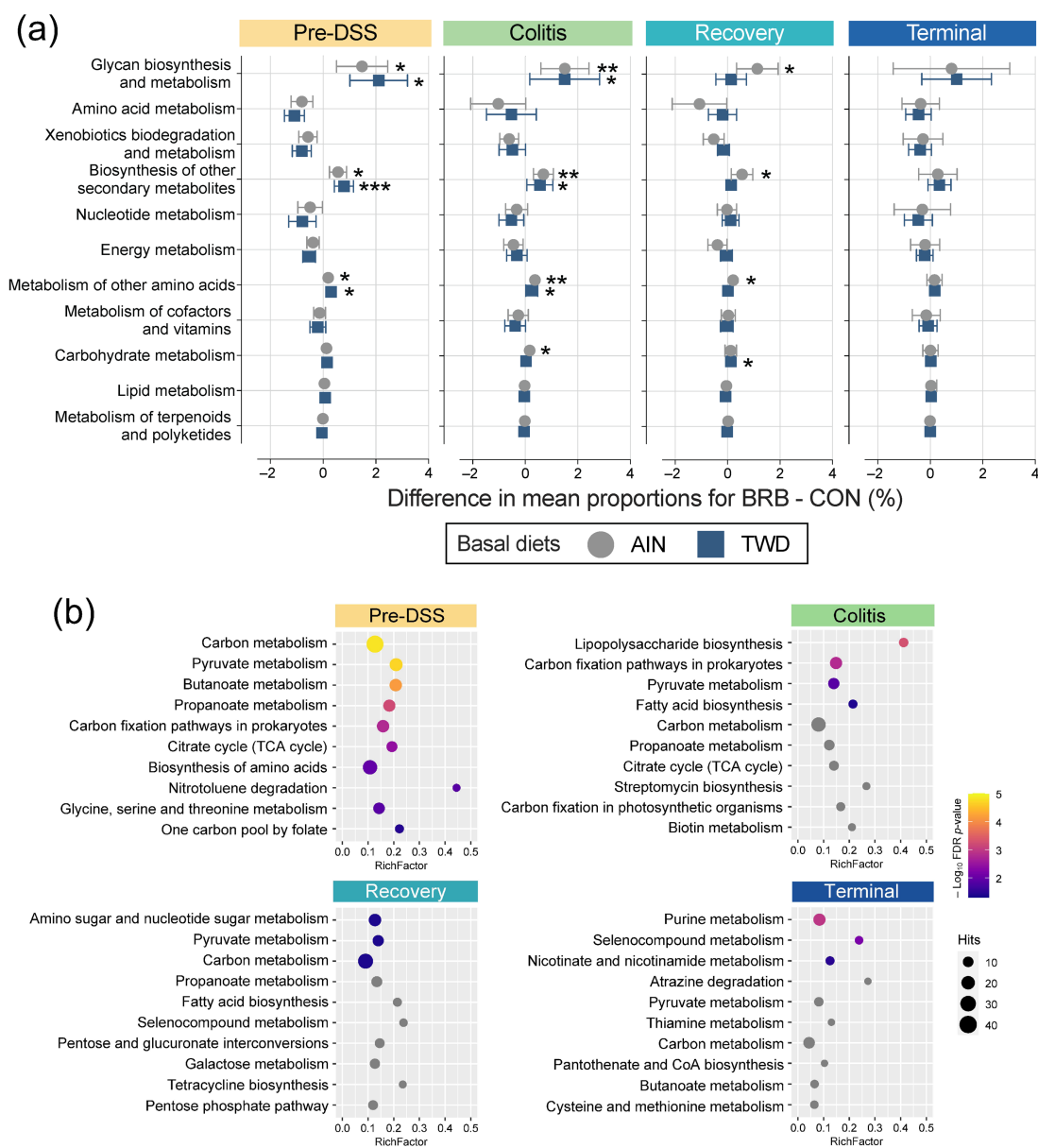


Figure 2.13. Metagenome predicted functions classified using KEGG metabolism orthology with tax4fun (experiment B). (a) Differences in mean proportions for BRB-supplemented and CON treatments for mice fed either AIN or TWD basal diets. Values are the differences between proportions with 95% confidence intervals. *, $p < 0.05$; **, $p < 0.01$; and ***, $p < 0.001$, as determined by Fisher's exact test followed by Benjamini–Hochberg method to adjust for multiple comparisons for the full data set. Proportions for each diet and supplement combination at each time point are provided in Figure 2.S13b. (b) Pathway enrichment of significant KEGG level 2 terms associated with the fecal microbiome of BRB-fed mice (AIN- and TWD-fed combined). Values shown are the term count (number of terms associated with the metabolism pathway), the enrichment factor (number of significant terms/total terms in pathway) and the FDR-corrected p -value.

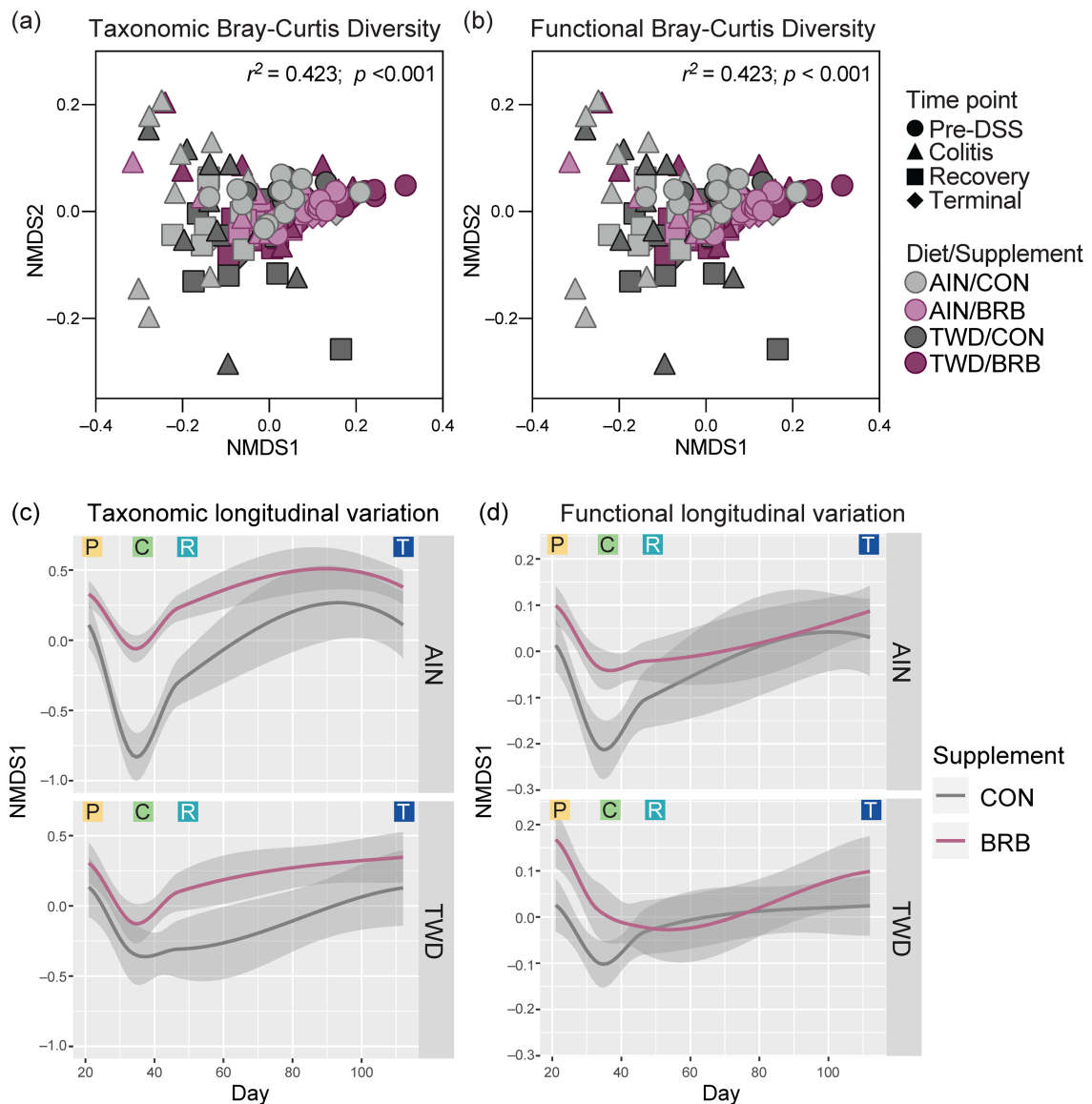


Figure 2.14. Longitudinal analysis of fecal microbiome taxonomy and functional capacity (experiment B). (a,b) NMDS ordination plots of the taxonomic (a) and functional (b) β -diversity for fecal microbiomes of mice fed either CON or BRB-supplemented diet with either AIN or TWD basal diets for all experimental time points. Functional beta diversity was measured as the Bray–Curtis dissimilarity based on KEGG term abundances, while taxonomic beta-diversity values represent the Bray–Curtis dissimilarity based on ASV abundances. (c,d) Longitudinal variation shown as the first dimension plotted over experimental day for taxonomic (c) and functional (d) diversity. Loess-smoothed trajectories of microbiomes from each experimental group are plotted; gray shading represents the 95% confidence interval. P, pre-DSS; C, colitis; R, recovery; and T, terminal time points.

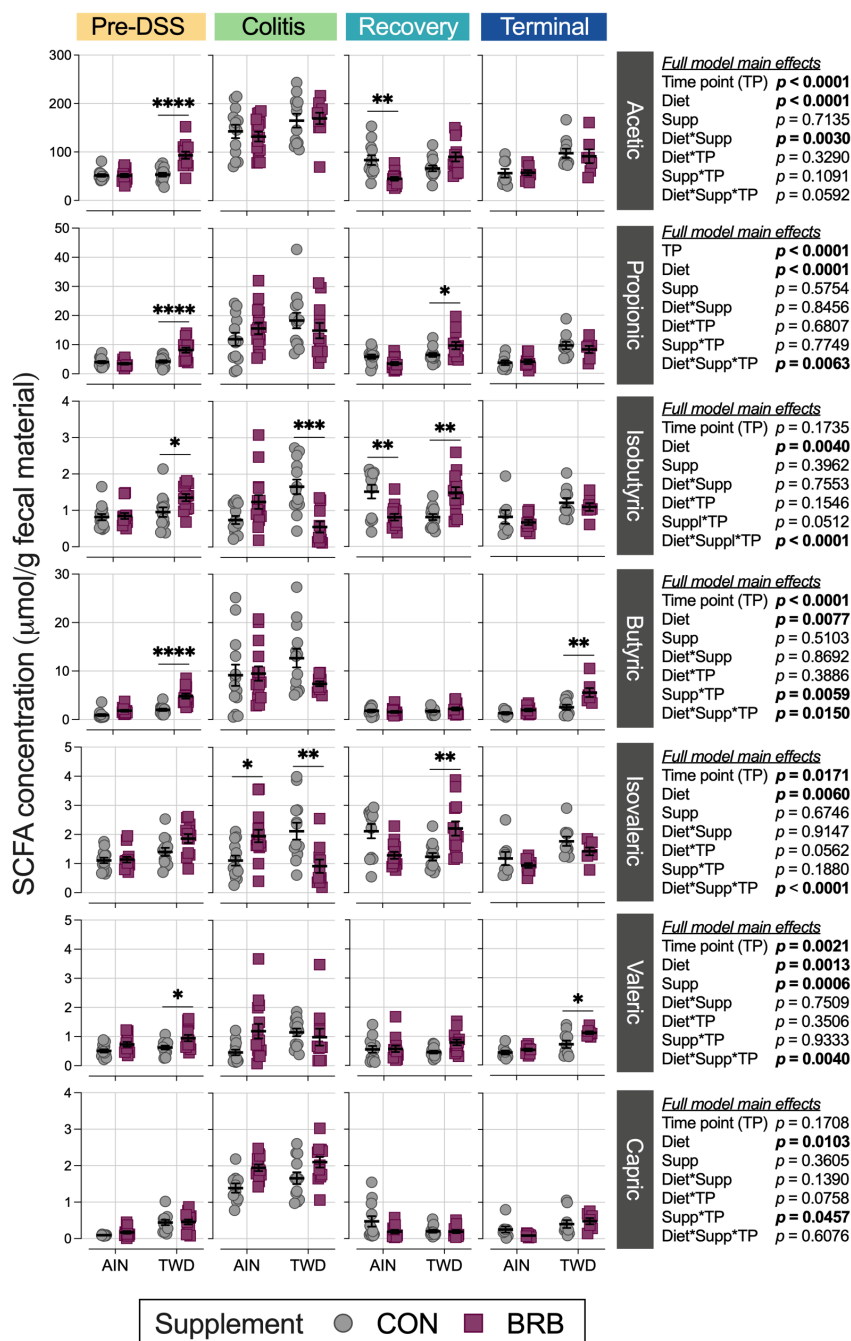


Figure 2.15. Short-chain fatty acid concentrations in fecal samples from mice fed CON or BRB-supplemented diets at each experimental time point (experiment B). Data are shown as individual values that represent each cage (as the biological unit) with mean \pm SE. For simplified visualization, this plot shows only the statistical results as FDR-corrected p -values for comparisons between CON and BRB-supplemented diets, as indicated: *, $p < 0.05$; **, $p < 0.01$; ***, $p < 0.001$; and ****, $p < 0.0001$, as outlined in Materials and Methods. Complete results of all statistical analyses, including pairwise comparisons by basal diet and across time points, are provided in Tables 3.S5–3.S7.

CHAPTER 3

BASAL DIET FED TO RECIPIENT MICE WAS THE DRIVING FACTOR FOR COLITIS AND COLON TUMORIGENESIS, DESPITE FECAL MICROBIOTA TRANSFER FROM MICE WITH SEVERE OR MILD DISEASE²

Abstract

Consumption of the total Western diet (TWD) in mice has been shown to increase gut inflammation, promote colon tumorigenesis, and alter fecal microbiome composition when compared to mice fed a healthy diet, i.e., AIN93G (AIN). However, it is unclear whether the gut microbiome contributes directly to colitis-associated CRC in this model. The objective of this study was to determine whether dynamic fecal microbiota transfer (FMT) from donor mice fed either the AIN basal diet or the TWD would alter colitis symptoms or colitis-associated CRC in recipient mice, which were fed either the AIN diet or the TWD, using a 2×2 factorial experiment design. Time-matched FMT from the donor mice fed the TWD did not significantly enhance symptoms of colitis, colon epithelial inflammation, mucosal injury, or colon tumor burden in the recipient mice fed the AIN diet. Conversely, FMT from the AIN-fed donors did not impart a protective effect on the recipient mice fed the TWD. Likewise, the composition of fecal microbiomes of the recipient mice was also affected to a much greater extent by the diet they consumed than by the source of FMT. In summary, FMT from the donor mice fed either basal diet with differing colitis or tumor outcomes did not shift colitis symptoms or colon

² This chapter has been previously published in: Rodriguez, D.M.; Hintze, K.J.; Rompato, G.; Stewart, E.C.; Barton, A.H.; Mortensen-Curtis, E.; Green, P.A.; Van Wettene, A.J.; Thomas, A.J.; Benninghoff, A.D. Basal diet fed to recipient mice was the driving factor for colitis and colon tumorigenesis, despite fecal microbiota transfer from mice with severe or mild disease. *Nutrients* **2023**, *15*, doi:10.3390/nu15061338. Author Contributions: Conceptualization, D.M.R., K.J.H. and A.D.B.; methodology, D.M.R., K.J.H., G.R., E.C.S., A.H.B., E.M.-C., P.A.G., A.J.V.W., A.J.T. and A.D.B.; data curation, D.M.R. and A.D.B.; writing—original draft preparation, D.M.R. and A.D.B.; writing—reviewing and editing, D.M.R., K.J.H. and A.D.B.; visualization, D.M.R. and A.D.B.; project administration, A.D.B.; funding acquisition, A.D.B.

tumorigenesis in the recipient mice, regardless of the basal diet they consumed. These observations suggest that the gut microbiome may not contribute directly to the development of disease in this animal model.

3.1. Introduction

The microbiome is a vast collection of microorganisms that live in association with the human body, including bacteria, viruses, fungi, and protists that reside on various surfaces, such as the skin, mouth, nose, lung, gastrointestinal tract, and genital tract [1]. The colon microbiome, which is composed of microbes that cohabit with each other and with local host cells, has an essential role in the host digestive system [2]. Gut homeostasis represents a state of equilibrium between the microbiome and host cells, resulting in a symbiotic or commensal association [3]. Microorganisms profit from a favorable environment and steady nutrient availability, and, in turn, these microorganisms support the host via microbial degradation of indigestible dietary components, stimulation of immune functions, production of certain vitamins, and other essential functions [4]. Understanding the dynamic relationship between the intestinal microbiome and gut health has prompted the development of murine and other animal models to further characterize microbiota profiles and their functionality.

Human and rodent gut microbiomes are largely similar and comprised of four dominant phyla: Firmicutes, Bacteroidetes, Actinobacteria, and Proteobacteria. The National Center for Biotechnology Information in the U.S. recently renamed these phyla as Bacillota, Bacteroidota, Actinomycetota, and Pseudomonadota, respectively, to improve systemic taxonomic nomenclature [5], although both designations are used synonymously nowadays. Modifiable lifestyle factors, such as the consumption of antibiotics, alcohol, or tobacco; the prevalence of chronic inflammatory disease; and diet can potentially change the gut microbiome [6]. The Western diet is characterized by high consumption of red meat, animal fat, and sugar, along with low fiber intake, and is considered a risk factor for many chronic diseases, such as inflammatory

bowel disease (IBD) and colorectal cancer (CRC) [7]. The Western dietary pattern results in chronic deficiency of essential micronutrients, leading to a disruption of metabolic and biological pathways [8]. To investigate the interaction between the Western dietary pattern and the development of inflammation-associated colorectal cancer, we previously developed the total Western diet (TWD) for rodents based on the typical nutrient intake of Americans on an energy density basis [7]. In repeated studies, we had shown that chronic consumption of the TWD enhanced symptoms of colitis; increased inflammation and injury to colon mucosa; altered inflammation and immune signaling in mucosal tissues; and promoted colon tumorigenesis in a murine model of colitis-associated colorectal cancer (CAC) [9].

The involvement of the gut microbiome—considered either as a whole community of bacteria or in part with a focus on specific pathobionts—in the development of chronic intestinal inflammation and/or the development of colorectal cancer has been a subject of intense investigation in recent years. Importantly, individuals suffering from chronic colitis are at a two- to three-fold greater risk of developing CAC compared to healthy population [10]. IBD patients typically have a lower microbial load, reduced diversity in their gut microbiome, an elevated abundance of pro-inflammatory taxa, and greater quantities of bacteria belonging to the Erysipelotrichaceae and Streptococcaceae families (both within the Firmicutes phylum) [11]. Certain bacterial species have been shown to have pro-inflammatory properties by invading epithelial cells and inducing cytokine production, creating an ideal microenvironment for tumor development. Yu et al. reported that *Fusobacterium nucleatum* was abundant in the colorectal cancer tissues of CRC patients and suggested that it modulates innate immune signaling and promotes resistance to chemotherapy [12]. Furthermore, *F. nucleatum* selectively binds to E-cadherin, thereby increasing membrane permeability and activating the β -catenin signaling pathway, which upregulates the expression of oncogenic and pro-inflammatory genes in humans and mice [13]. Similarly, enterotoxigenic *Bacteroides fragilis*, a Gram-negative bacterium,

triggers pathways leading to cleavage of E-cadherin, activation of the Wnt/ β -catenin pathway and subsequent induction of the production of interleukin-17A and tumor necrosis factor; all of these collectively contribute to a pro-inflammatory tumor microenvironment [14]. Bonnet et al. reported that *Escherichia coli*, a Gram-negative bacterium belonging to the Enterobacteriaceae family, was more abundant in the tumor tissues obtained from CRC patients when compared to normal adjacent tissues, as well as when compared to the normal mucosa of control patients; of note, *E. coli* colonization was more pronounced in patients with advanced disease [15]. Mucosa-associated adhesive-invasive *E. coli* strains invade the mucosa, triggering the production of cancer-driving reactive oxygen species [15]. *Enterococcus faecalis*, a Gram-positive bacterium belonging to the Enterococcaceae family, promotes colon inflammation by generating extracellular superoxide and hydrogen peroxide, which leads to elevated DNA damage, increased expression of tumor growth factor-beta (TGF β), activation of the SMAD signaling pathways, and upregulation of cyclooxygenase-2 [16]. Finally, *Peptostreptococcus anaerobius* (Clostridiaceae family), a Gram-positive oral bacterium generally found in mucosal tissue, was detected in high abundance in the stool samples and colon mucosa obtained from CRC patients; *P. anaerobius* was also shown to promote colon tumorigenesis in mice, enhance proliferation of human colon normal and cancer cell lines in vitro, and alter oncogenic pathways including cholesterol biosynthesis and TLR signaling, among others [17].

The mounting evidence pointing to an association, and perhaps a causal role, of gut bacteria in the pathogenesis of chronic inflammation and/or colon tumorigenesis has led to the development of multiple pre-clinical murine models in which the composition of the gut microbiome is manipulated to determine subsequent effects on gut health parameters. First among these is the gnotobiotic mouse, for which the composition of the microbiome is known. Generally, gnotobiotic (GB) mice are developed from a germ-free animal, either conceived via in vitro fertilization of a germ-free dam or birthed via cesarian section and then maintained in a

pathogen-free environment. Then, the desired microbe(s) can be introduced via various means (e.g., co-housing, shared bedding, and inoculation) to colonize the germ-free mouse and establish a gnotobiotic model [18]. While the use of GB murine models is critical to understanding key microbial interactions within the gut, these models do have limitations in that they may lack important commensal resident bacteria that are essential for establishing gut homeostasis. Furthermore, laboratory mice bred in germ-free conditions develop anatomical, physiological, and immunological abnormalities [19]. In addition, GB colonies are expensive and difficult to maintain, and few facilities are available to sustain a germ-free environment. These limitations have led to the development of alternative models, including the use of antibiotics and antifungal drugs to deplete the resident microbiome of recipient mice prior to the transfer of fecal material from a donor animal in a process called fecal microbiota transfer (FMT) [20]. Hintze et al. depleted the gut microbiome of commonly used C57BL/6J mice with broad-scope antibiotics using this approach, followed by four weekly transfers of fecal material from two human donors; the authors found that the recipient mice's microbiomes reflected approximately 68 to 75% of the human microbiome sequence mass [20]. We employed a similar antibiotic approach in a human-to-mouse FMT experiment in which fecal material from either obese or lean human donors was transferred to mice fed either a healthy diet, a high-fat diet, or a complete Western diet [21]. Interestingly, we found that the diet fed to the recipient mice was the driving force in shaping the gut microbiome of the recipient mice as opposed to the source of the donated microbiota. The recipient mice that received FMT from obese human donors and were fed a standard diet did not acquire an overweight phenotype, nor did FMT from lean donors protect the mice that were fed a high-fat diet from gaining excess weight [21]. These findings point to the critical need to consider the diet fed to recipient mice when performing FMT experiments to determine if gut bacteria from donors may confer host traits to recipients.

While multiple studies have pointed to gut dysbiosis as a common feature of colitis and/or colon tumorigenesis in humans and animal models, it is not clear whether changes in the gut microbiome composition associated with different nutritional patterns are the drivers of this disease process, leading to the progression from initial inflammation to neoplasia and then advanced tumorigenesis. Therefore, to better understand the involvement of the microbiome in the development and/or exacerbation of colitis and colon tumorigenesis, we designed an FMT experiment using fecal material collected from a prior study, in which donor mice were fed either the AIN93G diet or the TWD and subjected to our standard protocol for mouse CAC [22]. This experimental design incorporated the standard AIN93G diet or the total Western diet for the donor animals as well as for the recipient mice in a 2×2 factorial design. We hypothesized that FMT from the donor mice that were fed the TWD and experienced severe colitis and high tumor burden would exacerbate symptoms of colitis and increase tumorigenesis in the recipient mice that were fed the AIN93G diet. Conversely, we hypothesized that FMT from the donor mice that were fed the AIN93G diet and had mild colitis and low tumor burden would alleviate colitis symptoms and reduce tumorigenesis in the recipient mice that were fed the TWD.

3.2. Materials and Methods

3.2.1. Chemicals and Reagents

Azoxymethane (AOM) was purchased from Sigma-Aldrich (St. Louis, MO, USA; CAS No. 25843-45-2). Dextran sodium sulfate (DSS; reagent grade at mol. wt. ~40 kDa) was obtained from Thermo Fisher Scientific (Waltham, MA, USA). All other chemicals were obtained from general laboratory suppliers at reagent grade. Other reagents and kits are described below.

3.2.2. Experimental Animals

The Utah State University Institutional Animal Care and Use Committee approved all procedures for the handling and treatment of mice used for this study (protocol no. 11562). The

husbandry procedures and facilities for housing the mice were exactly the same as described in a previous study [22].

3.2.3. Collection of Fecal Material from Donor Mice

The principal research question of this study is whether the fecal microbiome associated with a Western diet enhances colitis symptoms, colon tumorigenesis, and microbiome modulation, when it is transferred into recipient mice fed either a healthy diet (AIN93G) or the total Western diet (TWD). Fecal material was collected weekly in a previous study [22] from mice that were fed either the AIN basal diet or the TWD in a longitudinal study employing the AOM + DSS model of chemical carcinogenesis (Figure 3.S1a) and was used for FMT to recipients, as outlined below. The fecal samples were collected and stored in a -80°C freezer. To prepare the material for FMT, these fecal samples were pooled by basal diet and experimental week (Figure 3.S1a) and diluted to 1 g/mL in sterile saline one week prior to their use for FMT, and stored at -20°C . On the day of transfer, the samples were thawed on ice and then used for oral gavage, as described below.

3.2.4. Experimental Diets for Recipient Mice

The experimental diets were formulated by Envigo (Hackensack, NJ, USA; formerly Harlan Teklad) as outlined in Table 3.S1; they were obtained from the vendor as one lot and maintained at 4°C for the duration of the study. The two basal diets were the AIN93G diet (AIN, cat. No. TD.94045), formulated to promote rodent health with an energy density of 3.8 kcal/g, and the total Western diet (TWD, cat. No. TD.180497), the formulation of which was previously published [7], with an energy density of 4.4 kcal/g, and which was designed to emulate typical macro- and micronutrient intakes on an energy density basis. The diets were administered, and food intake was monitored as previously described [22].

3.2.5. Microbiota Depletion and Fecal Microbiota Transfer from Mouse Donors

The depletion of the recipient mice's resident microbiome was achieved using a previously described protocol [20]. Twelve hours after the last antibiotic treatment, each mouse was dosed by oral gavage with the fecal matter diluted in sterile saline (1 g/mL) from its assigned FMT source group, which included either AIN-fed or TWD-fed donor mice. FMT continued weekly in a time-matched fashion (Figure 3.S1b) until the end of the study.

3.2.6. Experimental Design

A 2×2 factorial design was employed with the basal diet fed to the FMT recipients (referred to henceforth as “basal diet”) and the basal diet fed to the FMT donors (henceforth, “FMT source”) as the two main experimental factors, resulting in the following experimental groups (basal diet/FMT source): (1) fed AIN/fmt AIN, (2) fed AIN/fmt TWD, (3) fed TWD/fmt AIN, and (4) fed TWD/fmt TWD (Figure 3.S1b). The mice were assigned to one of these experimental groups at 5 weeks of age using a random block design to standardize body weights among the experimental groups. The recipient mice were provided one of the two basal diets, AIN93G (group 1–2) or TWD (group 3–4), for 3 days before starting the antibiotic regimen.

The protocol for inducing colitis and colon tumorigenesis had been described in a previous study [22] and was followed in this experiment with only slight modifications. On day 14, the mice were dosed *i.p.* with 10 mg/kg of AOM prepared in sterile PBS and provided 1% (*w/v*) DSS via drinking water for 10 days, followed by plain drinking water for the remainder of the experiment. On days 26 and 38, the mice were temporarily placed in new cages blinded to treatment, and the DAI score was determined as described in a previous study [9]. Additionally, on days 26 and 38, a randomly selected subset of mice from each group ($n = 7$ to 11 per group) was euthanized by CO₂ asphyxiation and necropsied, as outlined in a previous study [9]. The histopathological assessment of epithelial inflammation and mucosal injury was performed by a board-certified veterinary pathologist at the Utah Veterinary Diagnostic Laboratory using a

scoring system as previously described [9]. On day 105, body composition was determined for all mice using an MRI scan (EchoMRI-700). On day 115, the remaining mice ($n = 22$ to 27 per group) were euthanized by CO₂ asphyxiation and necropsied, as described in a previous study [9]. A randomly selected subset of colon tissues ($n = 13$ to 17 per group) was preserved for histopathological verification of cancer stage.

3.2.7. Microbiota Profiling by 16S rRNA Sequencing

Sequencing of fecal microbiome was performed using the MiSeq reagent kit v2 for a paired-end 500 cycle (2×250 bp) (Illumina, San Diego, CA, USA), as previously described [22]. Fresh fecal samples were collected by cage on day 14 (pre-DSS), day 26 (colitis), day 38 (recovery), and day 115 (terminal), and stored at -80 °C until analysis. The methods for DNA isolation, amplification, purification, quantitation, and sequencing were as previously outlined [22]. The microbiota sequences were processed using QIIME 2 [23] and DADA2 [24]. Briefly, the DADA2 R package with a full amplicon workflow, including filtering, dereplication, chimera identification, and merging paired-end reads, generated an amplicon sequence variant (ASV) table and representative sequences. To assign taxonomy, the Qiime feature-classifier classify-sklearn command was used with a pre-trained classifier for the v4 region, silva-138-99-515-806-nb-classifier.qza, and the most recent release of the SILVA database [25]. Supplementary File 3.S1 provides the resulting count data collapsed to the family level.

3.2.8. Microbiome Sequencing Data Analysis

The sequence data were analyzed using the Microbiome Analyst Marker Data Profiling module [26] as previously described [22]. The data were analyzed for the main effects of *basal diet* and *FMT source*, as well as for selected a priori pair-wise comparisons as follows: (1) fed TWD/fmt AIN vs. fed AIN/fmt AIN (effect of basal diets in mice given fmt from AIN-fed donors); (2) fed TWD/fmt TWD vs. fed AIN/fmt TWD (effect of basal diets in mice given fmt

from TWD-fed donors); (3) fed AIN/fmt TWD vs. fed AIN/fmt AIN (effect of fmt from different donors on mice fed the AIN basal diet); and (4) fed TWD/fmt TWD vs. fed TWD/fmt AIN (effect of fmt from different donors on mice fed the TWD). Alpha diversity (number ASVs, Chao1 richness, and Shannon index) and beta diversity (unweighted and weighted unifrac distances) were assessed as described in a previous study [22]. A permanova p -value < 0.01 for β -diversity was considered statistically significant. The taxonomic relative abundance data were analyzed using the metagenomeSeq with a zero-inflated Gaussian fit, and a false discovery rate-adjusted p -value < 0.05 was considered statistically significant. Clustvis was used to perform unsupervised, bidirectional hierarchical cluster analyses using the relative abundance data at the family taxonomical level [27]. Heat trees representing the hierarchical structure of the taxonomic classifications were generated for the pairwise comparisons listed above (for the non-parametric Wilcoxon rank-sum test, a p -value < 0.05 was considered significant).

3.2.9. Statistical Analysis

Statistical analyses for tumor incidence were performed using the Fisher's exact test, followed by a Bonferroni adjustment to correct for multiple testing (Prism v. 8, GraphPad Software, San Diego, CA, USA). Other data were analyzed using a generalized linear mixed model (GLMM) with cage as a nested, random factor and using the restricted maximum likelihood (REML) estimation and Tukey's HSD post hoc test for multiple comparisons (JMP v.16.2.0, SAS Institute, Cary, NC, USA). The main effects of basal diet and FMT source, and their interaction, were determined for each time point. Suspected outliers were verified using the robust outlier test (ROUT) with a conservative Q value of 1% (Prism), meaning that there is a $\leq 1\%$ chance of excluding a data point as an outlier in error. Data that did not meet the equal variance assumption were \log_{10} or square root transformed. For data that were not normally distributed or for which a transformation did not equalize variance, a nonparametric Steel–Dwass test was employed (JMP) to assess the main effects of diet and FMT source (no interaction test

possible). However, if the results of the nonparametric Steel–Dwass tests were not different from the original GLMM analyses with respect to significant outcomes, the original GLMM test results were reported because the mixed model accounts for potential cage effects. A significant effect of the test variable was inferred when the adjusted p -value was <0.05 .

3.3. Results

3.3.1. Food and Energy Intakes, Body Weight and Composition, and Organ Weights

Total food intake for the study period was not significantly different among the diet or FMT source groups, whereas energy intake was significantly higher (9.6% overall) in the recipient mice fed the TWD compared to those fed the AIN diet (diet main effect, $p = 0.0002$), reflecting the higher energy density of the TWD (Figure 3.1a,b). This increased energy intake led to a small but significant increase in final body weight of 3.3% in the recipient mice fed the TWD (diet main effect, $p = 0.0394$) (Figure 3.1c,d). However, the basal diet fed to the recipient mice did not significantly alter either lean or fat mass composition (Figure 3.1e,f), although liver, spleen, and kidney weights were all higher in the TWD-fed recipients (Figure 3.S2). Of note, FMT from the TWD-fed donor mice, when compared to the AIN-fed donors, did not significantly affect food intake, energy intake, body weight gain, lean or fat mass composition, relative liver weight, relative kidney weight, or cecum content (Figure 3.1 and Figure 3.S2). However, relative spleen weight in the TWD-fed recipients that received FMT from the TWD-fed donors was significantly reduced compared to their counterparts that received FMT from the AIN-fed donors (Figure 3.S2b). The relative mass of cecum contents was not affected by diet or FMT donor source (Figure 3.S2d).

3.3.2. Symptoms of Colitis and Histopathological Scoring

Compared to the recipient mice fed the AIN diet, consumption of the TWD increased symptoms of colitis, as measured by the DAI score, by 1.8-fold during active colitis on day 26,

although this elevation during active disease did not persist through the recovery phase in this study (Figure 3.2a). However, FMT from the AIN- or TWD-fed donor mice did not alter colitis symptoms at either time point. The histopathological assessment of colon inflammation and mucosal injury indicated a strong promoting effect of the TWD on the recipient mice during active colitis (diet main effect, $p < 0.0001$ and $=0.0109$, respectively), with the prolonged elevation of colon inflammation in the TWD-fed mice persisting through recovery (diet main effect, $p < 0.0001$) and to the terminal time point at day 112 (diet main effect, $p < 0.0001$) (Figure 3.2b,c). However, the mucosal injury had largely resolved by the recovery time point, with no further apparent effect of the TWD. For colitis symptoms and mucosal injury, FMT from the donor mice fed either the AIN diet or the TWD did not have any apparent significant effects (Figure 3.2). However, a significant main effect of FMT from the donor mice fed the TWD was noted for inflammation scores at the recovery time point ($p = 0.0392$), suggesting that the microbiota transferred from previously TWD-fed mice exacerbated colon inflammation well into recovery due to DSS-induced gut injury (Figure 3.2b).

3.3.3. Colon Length and Tumorigenesis

The basal diet fed to the recipient mice significantly altered the incidence of colon tumors. Specifically, for mice that received FMT from the AIN-fed donors, tumor incidence in the TWD-fed recipients was 100% compared to only 56% for their AIN-fed counterparts ($p = 0.0004$); similarly, for mice that received FMT from the TWD-fed donors, tumor incidence was 100% versus 65% for the AIN-fed recipients ($p = 0.0152$) (Figure 3.3a). Alternatively, within each basal diet group, FMT from either the AIN- or TWD-fed donors did not alter tumor incidence.

In the mice that were necropsied at the study end point, the average colon length of the recipient mice was affected by both experimental factors, namely the basal diet fed to the recipient and the FMT donor source (Figure 3.3b). First, when considering only the effect of basal

diet, colon length was 7.0% shorter in the TWD-fed recipients compared to their AIN-fed counterparts (diet main effect, $p = 0.0005$). Next, considering the effect of the FMT source, the colons of the mice that received FMT from the TWD-fed donors were 6.4% longer on average (FMT source main effect, $p = 0.0020$). However, no interaction between basal diet and FMT source was noted, indicating that the effect of FMT was consistent regardless of the basal diet fed to the recipient mice.

As expected, the recipient mice fed the TWD experienced a 5-fold increase in tumor multiplicity, a 5-fold increase in tumor volume, and an 11-fold increase in tumor burden (diet main effect, $p < 0.0001$), irrespective of FMT donor (Figure 3.3c–e). FMT from the AIN- or TWD-fed donors did not significantly alter tumor multiplicity or tumor burden, and FMT from the TWD-fed donors appeared to reduce average tumor volume (FMT source main effect, $p = 0.0133$); however, this effect was not dependent on the basal diet as there was no interaction between FMT source and basal diet ($p = 0.6581$) (Figure 3.3d).

3.3.4. Fecal Microbiome Response to FMT Source and Basal Diet

After fecal bacterial DNA isolation, a total of 12.3×10^6 amplicons were sequenced and filtered for length, quality, and chimeras, leaving 8.3×10^6 total sequences for an average of 38,713 sequence reads per sample assigned to 3101 ASVs. The sequencing depth was set to ~4444 sequences for diversity analyses (Figure 3.S3).

This experimental design included multiple factors to explore the dynamics of the mouse gut microbiome after antibiotic depletion of resident microbiota, followed by FMT from the donor mice and then the standard AOM + DSS regimen to induce colitis and colon tumorigenesis in the mice fed either the standard AIN diet or the TWD. Thus, the statistical analyses were performed in a stepwise manner, considering first the overall effect of the study time point, and then the effects of basal diet and FMT source within each time point. First, the taxonomic composition of the fecal microbiome was greatly affected by the chemical induction of colitis, as

indicated by an overall increase in the relative abundances of Erysipelotrichaceae (primarily *Dubosiella newyorkensis* and *Turicibacter* spp.) from 41% to 57% ($p = 0.0001$) and Bifidobacteriaceae (*Bifidobacterium* spp.) from 3.4% to 16.9% ($p < 0.0001$) in the fecal microbiome, regardless of the basal diet or FMT source, whereas the relative abundances of other taxa decreased, such as Akkermansiaceae (*Akkermansia muciniphila*) from 13.4% to 5.6% ($p = 0.0067$), Streptococcaceae (*Lactococcus* spp.) from 11.8% to 6.6% ($p = 0.0216$), Lachnospiraceae (primarily *Lachnoclostridium*, *A2*, *Marvinbryantia*, and other unclassified genera) from 4.4% to 1.4% ($p \leq 0.0001$), and Bacteroidaceae (*Bacteroides* spp.) from 9.6 to 1.2% ($p < 0.0001$) (Figure 3.4 and Figure 3.5, Supplementary Figures 3.S4 and 3.S5 and File 3.S2). These shifts in relative abundance persisted for the most part through the recovery phase, although the abundance of Lachnospiraceae increased from 1.2% at the colitis time point to 4.5% at recovery ($p < 0.0001$), showing a level similar to the pre-DSS abundance of 3.8% (Figure 3.S5). However, the fecal microbiome at the terminal time point was distinct with a notable marked increase in Eubacteriaceae, comprising 26% of the microbiome on average ($p < 0.0001$ for all time points), irrespective of the basal diet or FMT source. This increase in Eubacteriaceae corresponded to a proportional decrease of 20% for Erysipelotrichaceae ($p < 0.0001$) and of 10.5% for Bifidobacteriaceae ($p < 0.0001$) at the terminal time point compared to recovery, so that their relative abundance was more similar to that prior to DSS-induced gut injury. Additionally, of note, the relative abundance of Sutterellaceae (*Parasutterella uncultured_organism*) was different over the course of disease development, with the relative abundance of this taxon being significantly different at the pre-DSS (0.82% of the population), colitis (0.37%), and recovery (0.42%) time points when compared to the terminal time point (1.15%) ($p < 0.0001$ for all comparisons to the terminal time point) (Figure 3.S5).

The taxonomic composition of the fecal microbiome of the recipient mice reflected their basal diet to a much greater extent than the FMT donor source at each experimental stage,

although most profoundly at the terminal time point (Figure 3.4, Figure 3.5 and Figure 3.S4). It should be noted that the microbiome profiles shown for the donor mice are from the most proximal weekly collection before the indicated study time point for the recipients (i.e., collection 2 for the pre-DSS time point, collection 3 for the colitis time point, collection 5 for the recovery time point, and collection 5 for the terminal time point) (Figure 3.S1). The statistical analyses of microbiome taxonomic abundance via either metagenomeSeq (Figure 3.5b and Supplementary File 3.S2) or nonparametric heat tree analyses (Figure 3.6) showed that many more significant differences were detected when comparing the experimental groups according to the basal diet as opposed to comparing them according to the FMT source. For example, at the pre-DSS time point, the relative abundance of Erysipelotrichaceae (*D. newyorkensis*) in the mice fed the TWD diet was significantly greater compared to the AIN-fed mice that received FMT from AIN-fed donors ($p = 0.0002$) or TWD-fed donors ($p = 0.0153$) (Figure 3.6a and Figure 3.7a). An overall greater abundance of this bacterial family was also noted during active colitis (diet main effect, $p = 0.0430$), although not at later time point. However, there was no apparent effect of the FMT source on the abundance of Erysipelotrichaceae (Figure 3.6a and Figure 3.7a). While changes in the relative abundance of Bifidobacteriaceae were apparent when considering microbiome composition over time, as noted above, our analyses for the other two experimental factors – basal diet and FMT source – did not reveal any significant effects on this bacterial family (Figure 3.7b).

Significant effects of the basal diet were also apparent for Streptococcaceae (primarily the genus *Lactococcus*) throughout the study, with the relative abundance of this family being significantly higher in the mice fed the AIN diet compared to the mice fed the TWD before the induction of colitis, regardless of the FMT source ($p < 0.01$) (Figure 3.6a and Figure 3.7c). By the colitis time point, this trend was altered for those mice that received FMT from TWD-fed donors, with the relative abundance of Streptococcaceae higher in the AIN-fed mice compared to their

TWD-fed counterparts ($p = 0.0272$). By the recovery and terminal time points, however, the relative abundance of this family was again similar to the original pre-DSS values, with higher percentages for mice fed the AIN basal diet than for those fed the TWD (diet main effects, $p = 0.0014$ and <0.0001 for recovery and terminal time points, respectively). Again, no significant effects of the FMT source were noted for Streptococcaceae at any point during the study. A similar result was evident for *A. muciniphila* of the Akkermansiaceae family, as no effect of FMT source was apparent. However, the relative abundance of this species increased during active colitis and at the terminal time point for the mice fed the TWD compared to those fed the AIN diet, regardless of the FMT source (Figure 3.6a and Figure 3.7d).

The relative abundance of bacteria belonging to the Lachnospiraceae family was higher in the recipient mice fed the AIN diet compared to those provided the TWD, regardless of the FMT donor source, before the induction of colitis at the pre-DSS time point (Figure 3.6a and Figure 3.8a). This trend appeared disrupted during active colitis and recovery, with no effect of basal diet observed, but it appeared to be restored at the terminal time point, especially for mice that received FMT from the AIN-fed donor group ($p = 0.0008$). The relative abundance of Lachnospiraceae was not significantly impacted by the FMT source. The relative abundance of Lactobacillaceae also appeared to be reduced in the TWD-fed recipients compared to their AIN-fed counterparts, irrespective of the FMT source, with significant main effects of diet noted prior to the DSS treatment, during active colitis, and at the study end point (Figure 3.8b). However, as with most other taxa, the FMT source did not alter the relative abundance of this bacterial family either.

FMT from AIN- or TWD-fed donor mice did not alter the relative abundance of most of the taxa identified in this microbiome sequencing study, with a couple of exceptions. Before the onset of colitis, Clostridia_UCG-014 abundance was significantly reduced in the mice that received FMT from the TWD-fed donors (FMT main effect, $p < 4.25 \times 10^{-8}$), most notably for

mice that were fed the AIN basal diet ($p = 0.0002$) (Figure 3.8c). However, this pattern did not persist throughout the study; instead, significant main effects of basal diet were apparent, regardless of FMT source, with *Clostridia_UCG-014* being more abundant in the mice fed the TWD during recovery (diet main effect, $p = 0.0002$) and then less abundant by the terminal time point ($p = 0.0089$). Similarly, the relative abundance of another relatively rare bacterial family, Eubacteriaceae, was higher in mice receiving FMT from the AIN-fed donors, showing a higher abundance at 0.085% of the fecal microbiome compared to their counterparts that received FMT from the TWD-fed donors at 0.056% (FMT main effect, $p = 0.0292$), as observed prior to the DSS treatment (Figure 3.8d). Conversely, FMT from the TWD-fed donors significantly increased the relative abundance of Sutterellaceae compared to the AIN-fed donors (FMT main effect, $p = 0.0292$), an effect that was most evident in mice provided the TWD ($p = 0.0153$) (Figure 3.8e). However, these apparent effects of FMT source on the abundance of Eubacteriaceae and Sutterellaceae in the fecal microbiome were transient and did not persist through the colitis, recovery, or terminal time points.

Prior to gut insult, the mice fed the TWD as a basal diet had a significantly higher Firmicute-to-Bacteroidetes ratio (F:B) compared to the mice fed the AIN diet, but only for those recipients that received FMT from the AIN-fed donors (Figure 3.9). The F:B ratio was higher for all groups during the active colitis and recovery time points compared to pre-DSS, although there were no differences in this ratio among the experimental groups. By the end of the study, significant main effects of both diet ($p = 0.0067$) and FMT source ($p = 0.0440$) were observed, with one significant pairwise comparison among the experimental groups for the recipient mice fed the AIN diet with FMT from the AIN-fed donors compared to the recipient mice fed the TWD with FMT from the TWD-fed donors (Figure 3.9).

3.3.5. Alpha and Beta Diversity of Fecal Microbiome

The richness and evenness of microbial communities were determined using three indices of alpha diversity measures: observed ASVs (count of sequence variants), Chao1 index (species richness), and Shannon index (community evenness). In a pattern similar to past studies, prior to carcinogen exposure, the alpha diversity was higher in the AIN-fed mice compared to the TWD-fed mice, notwithstanding the FMT source (diet main effect, $p < 0.05$ for all alpha diversity measures) (Figure 3.10). Compared to the initial alpha diversity measurements, observed ASVs, Chao1, and Shannon indices were markedly lower during the active colitis and recovery phases of this disease model (time point main effect, $p < 0.0001$ for all comparisons) (Table 3.S2). During active colitis, the recipient mice fed the TWD had a higher Shannon index compared to their counterparts fed the AIN basal diet overall (diet main effect, $p = 0.0067$), but this effect was most pronounced when compared to the recipients that were fed the AIN diet and received FMT from the TWD-fed donors (Figure 3.10c). This pattern was reversed during recovery, as the recipient mice fed the AIN diet had a greater Shannon index compared to the recipient mice fed the TWD (diet main effect, $p = 0.0395$), although none of the pairwise comparisons among the separate experimental groups were significant. Likewise, during the colitis and recovery phases, no differences in the species richness measurements were noted (Figure 3.10a,b). By the terminal time point, the main effects of diet were apparent for all alpha diversity measurements, with overall higher scores in the recipient mice fed the AIN diet compared to their TWD-fed counterparts. No main effects of FMT source were noted, although observed ASVs and Shannon index was significantly greater in the recipient mice fed the AIN diet and received FMT from the AIN-fed donors when compared to the recipient mice fed the TWD and received FMT from the TWD-fed donors ($p = 0.0248$ and $=0.0023$ for ASVs and Shannon index, respectively) (Table 3.S3).

Beta diversity was determined using weighted and unweighted unfrac distance measurements to account for the relative abundance of taxa and the presence of rare taxa, respectively, in the fecal microbiome populations. Before the induction of colitis, clear distinctions in the beta diversity of the fecal microbiome were apparent, with individual samples (corresponding to cages) being grouped more closely according to the diet fed to the recipient mice (permanova $p < 0.001$ for unweighted and $p = 0.004$ for weighted unfrac analyses) (Figure 3.11). During active colitis, the unweighted unfrac analysis suggested less distinction for these microbiomes, indicating a reduced contribution of rare species during this time point (permanova $p = 0.038$ with low $r^2 = 0.08$). Alternatively, the weighted analysis suggested some distinction between the recipient mice fed the AIN diet compared to those fed the TWD (permanova $p = 0.003$). During recovery, however, neither beta diversity analysis suggested that the microbiomes were substantially distinct. By the study end point, the microbiomes of the recipient mice fed the AIN diet were distinct from those fed the TWD (permanova $p < 0.001$ for both weighted and unweighted unfrac analyses). Additionally, considering the weighted unfrac analysis at the terminal time point, a moderate separation between the mice that received FMT from the AIN-fed donors and the mice that received FMT from the TWD-fed donors was evident along the second principal coordinate. Otherwise, distinctions among the microbiomes according to the FMT source were not evident at any other time point during the study.

3.4. Discussion

The gut microbiome modulates physiological functions related to cancer development, including inflammation, cell proliferation, apoptosis, and angiogenesis. Thus, it is likely that the gut microbiome directly affects colon tumorigenesis. Patients with IBD or colon tumors have often been observed to have distinct microbiomes, a phenomenon that has also been observed in animal models of these diseases, although a consensus cancer-related gut microbiome has not been identified to date. In this study, we sought to better understand how diet-driven changes in

the gut microbiome of donor mice could influence inflammation-associated colorectal carcinogenesis in recipient mice by employing FMT. Importantly, the study design considered the impact of basal diet during disease development for recipient mice that were colonized by fecal microbiomes transferred from mice experiencing either mild or severe colitis and colon tumorigenesis. If our hypothesis that the composition of the gut microbiome is a driving factor in disease development was correct, we would have expected to observe worse colitis symptoms, greater colon tissue inflammation and damage, and a higher tumor incidence in the recipient mice that received FMT from the TWD-fed donors, especially for the recipients that were fed the AIN basal diet, which is known from several previous studies to induce only mild colitis and low tumorigenesis [9]. However, we observed that FMT from either donor had little to no effect on colitis symptoms, colon tissue inflammation, or mucosal injury. Interestingly, the effects of FMT from the TWD-fed donors suggested a potential protective effect against colon tumorigenesis, as reflected by significantly increased colon length and smaller tumor volume as well as trends for reduced tumor multiplicity and volume, although this pattern of response did not align with the observations on gut inflammation as would be expected from our prior work in this CAC model. Importantly, our findings suggest that the basal diet fed to the recipient mice was the major driver of disease progression in this experiment. Likewise, the composition of the fecal microbiomes of the recipient mice was also affected to a much greater extent by the diet they consumed as opposed to the source of FMT.

FMT is a useful approach for shifting the gut microbiome population in favor of health-promoting bacteria and, potentially, reversing gut dysbiosis [28]. Previously, FMT was shown to be successful in the treatment of *Clostridium difficile* infection [29]. However, in 2019, the U.S. Food and Drug Administration warned of a high transmission risk of pathogenic, drug-resistant bacteria following FMT intended to treat *C. difficile* infection [30]. As reviewed recently by Waller et al. [31], the evidence for the use of FMT to induce remission in patients with mild-to-

moderate IBD is substantial, as multiple randomized, controlled trials have yielded positive results after 8 to 12 weeks and noted benefit compared to placebo. While FMT from a healthy microbiome appears to assist in disease management, FMT from an unhealthy source may potentially lead to unfavorable outcomes.

As observed repeatedly in this murine model of CAC [9,22,32], mice fed the TWD (irrespective of FMT source) had shorter colon length, more severe colitis symptoms, higher inflammation and mucosa injury scores, higher tumor multiplicity, larger average tumor volume, and higher tumor burden compared to their AIN-fed counterparts. Interestingly, in this experiment, we also observed a marked increase in colon tumor incidence in the TWD-fed recipient mice. Furthermore, the mice fed the TWD consumed the same amount of food as the mice fed the AIN diet, resulting in increased energy consumption in the mice fed the TWD due to its higher energy density. However, final body weight and body composition were not significantly affected. In summary, in this study, the diet fed to the recipient mice was the main driver for inflammation response during active colitis, recovery from gut injury, and tumorigenesis. Interestingly, we arrived at a similar conclusion in a prior study using donor fecal material from obese and lean human donors transferred to recipient mice fed different basal diets, including the AIN93G diet and TWD [21]; in that human-to-mouse FMT experiment, the basal diet fed to the recipient mice was the primary driver for the development of metabolic syndrome and obesity.

However, a few outcomes of this study were significantly affected by the FMT source, namely AIN-fed versus TWD-fed donor mice. Of note, while the inflammation score at the recovery time point and the ratio of Firmicutes: Bacteroidetes at the terminal time point increased with FMT from the TWD-fed donors, an improvement in colon length and average tumor volume was observed in the recipient mice that received FMT from the TWD-fed donors compared to those that received FMT from the AIN-fed donors, irrespective of the basal diet they consumed.

However, an explanation for the contradictory pattern in these outcomes is not entirely straightforward. First, greater colon length is generally associated with reduced inflammation and a lower Firmicutes: Bacteroidetes ratio [9,33,34]. Furthermore, the higher inflammation score observed during recovery for the mice that received FMT from the TWD-fed donors compared to the mice that received FMT from the AIN-fed donors (significant main effect of FMT source) suggests that the microbiome associated with the TWD might delay recovery from gut injury. However, these higher inflammation scores during recovery do not correlate with the observed lower average tumor multiplicity, average tumor volume, and tumor burden measures at the terminal time point for those mice that received FMT from the TWD-fed donors. Rather, based on our prior observations [9], we would have expected more severe tumorigenesis in mice that experienced prolonged inflammation through the recovery period. Additionally, the evidence for an association of a higher abundance of Firmicutes in the fecal microbiome with IBD and CRC is equivocal [35,36,37,38,39]. For example, in a metagenomic analysis of fecal samples obtained from 290 healthy subjects, 512 IBD patients, and 285 CRC patients, Ma et al. reported that IBD patients had low microbial diversity, whereas diversity was elevated in CRC patients. Furthermore, they found that the ratio of Firmicutes: Bacteroidetes was lower in these patients compared to their healthy counterparts [40]. This pattern differs from our findings, which showed that the overall Firmicutes: Bacteroidetes ratio was elevated during colitis; furthermore, the ratio was also elevated in the mice that experienced more severe tumorigenesis at the study end point (i.e., those recipient mice that were fed the TWD).

The application of FMT to ameliorate adverse side effects, such as mucosal inflammation, associated with some common chemotherapies used to treat CRC in humans has gained interest recently. For example, Chang et al. showed that FMT from healthy mice reduced mucosal inflammation and improved gut barrier integrity in Balb/c mice implanted with syngeneic CT26 colon adenocarcinoma cells on a FOLFOX regimen [41]. Additionally,

vancomycin-pretreated Balb/c mice administered 5-fluorouracil to induce mucositis were treated with FMT from a pool of healthy mice donors, resulting in the prevention of weight loss and colon shortening [42]. Finally, in a CAC model employing AOM with three cycles of DSS, female Balb/c mice were administered oral FMT from healthy, age- and sex-matched donors following DSS treatments, leading to less severe disease response as indicated by longer colon length, reduced gut inflammation, and reduced tumor burden, compared to mice that did not receive FMT [43]. Of note, none of these studies considered the role of basal diet given to recipient mice in mitigating or accentuating the effects of FMT on colitis or colon carcinogenesis. Furthermore, FMT was typically administered in combination with or following intense gut injury caused by chemical exposure, including treatments that likely depleted the resident gut microbiome, allowing for more efficient colonization by bacteria through FMT.

In this study, FMT from the donor mice fed either the AIN diet or the TWD diet did not significantly affect the richness or evenness of the fecal microbiome of the recipient mice. Likewise, neither weighted nor unweighted unifracs β -diversity analyses suggested that the populations of bacteria in the stool samples of the recipient mice were different according to the FMT source. However, we did observe that FMT from the donor mice fed the TWD, before DSS-induced colitis, reduced the relative abundance of two bacterial families, Clostridia_UCG-014 and Eubacteriaceae, both in the order Clostridia. In a study involving patients diagnosed with Crohn's disease and a cohort of healthy first-degree relatives, Leibovitch et al. determined that the abundance of Clostridia_UCG-014 was associated with impaired intestinal permeability, although this association appeared to be independent of gut inflammation [44]. A recent fecal microbiota analysis of UC patients indicated a reduced abundance of *Clostridium cluster IV* and *Eubacterium rectale* compared to healthy controls [45]. Of note, in the current study, the overall abundance of Clostridia_UCG-014 was not significantly different in the mice experiencing colitis compared to the pre-DSS baseline measurement, although reduced

abundance was evident in the mice recovering from colitis and at the study end point.

Alternatively, the relative abundance of Eubacteriaceae was not altered during active colitis or recovery, but it was notably elevated by the terminal time point. Species belonging to the Eubacteriaceae family have demonstrated anti-inflammatory properties and have been reported in reduced amounts in animal models of CAC and IBD patients [46,47]. Eubacteria species are butyrate producers, which are the main source of colonocyte energy, potentially explaining the increase in this species in mice with significant tumor development [48].

Another bacterial species notably affected by FMT from the TWD-fed donor mice before the induction of colitis was *Parasutterella uncultured_organism* (family Sutterellaceae); furthermore, this species was substantially more abundant at the terminal time point compared to all prior time points, regardless of the experimental group. In a cross-sectional study of an Italian cohort of IBD patients, the researchers determined that *Sutterella spp.* was elevated in the stool of IBD patients compared to healthy controls [49]. However, as noted by Kaakoush [50], while a high abundance of *Sutterella* has been associated with UC, evidence suggests that this species does not induce gut inflammation, but rather it degrades gut-associated immunoglobulin A, which is essential for protection against bacterial invasion [50]. Given the strong association of *Sutterella* with colitis, the observation that the mice that received FMT from the TWD-fed donors harbored a greater abundance of *Parasutterella* before colitis induction, and the functional similarity of both *Sutterella* and *Parasutterella* [51], it would be reasonable to expect that FMT from the TWD-fed mice might lead to more severe colitis in the recipient mice, especially those recipients fed the AIN diet, for which a mild inflammatory response would otherwise be expected without any intervention. However, this was not the case in our study, and no further effect of FMT on *Parasutterella* abundance was noted throughout the experiment.

In this study, the basal diet fed to the recipient mice had much more profound effects on the fecal microbiomes of the recipient mice than did FMT from the donor mice fed either the AIN

diet or the TWD. Prior to the induction of colitis, α -diversity was significantly higher in the mice fed the standard AIN diet when compared to their TWD-fed counterparts. While species richness was generally low for all experimental groups during active colitis and recovery from gut injury, this trend returned by the end of the study, with the AIN-fed mice having more taxa present in their fecal microbiomes than the mice provided the TWD. A similar pattern for beta diversity was also evident, particularly when considering the most abundant species in the fecal microbiomes of the recipient mice; the microbiomes of the mice provided the AIN diet, irrespective of FMT source, were notably distinct from their TWD-fed counterparts before the onset of colitis and at the study end point. The negative impact of the Western dietary pattern on gut microbiome diversity compared to healthier diets, such as those high in fiber and polyunsaturated fatty acids similar to the Mediterranean or Japanese diets, has been well established [52,53,54,55].

A. muciniphila is a highly studied anaerobic bacterium that resides within the mucosal layer of the intestinal mucosa; this mucin-degrading bacterium is thought to contribute to intestinal homeostasis and gut health [56,57,58]. However, the role of *A. muciniphila* in the development of gastrointestinal disease is not yet well understood. Some studies have reported an elevated abundance of this bacterium in CRC patients [59,60], whereas others have reported reduced abundance in patients diagnosed with IBD [45,61,62,63]. Håkansson and colleagues measured a higher abundance of *A. muciniphila* in the colon mucosal tissue of mice with DSS-induced colitis compared to non-treated controls [64], a finding that does not agree with the overall lower abundance of this bacterium during DSS-induced colitis in this study and our prior work [9], although the experimental protocols were notably different (10 mg/kg AOM + 1% DSS for 10 days in this study vs. 4% DSS for 7 days in Håkansson et al.). Of interest, Qu et al. reported that oral administration of *A. muciniphila* ameliorated symptoms of DSS-induced colitis in mice [65]. Collectively, these data point to a complicated role of *A. muciniphila* in gut homeostasis and disease development.

Several of the taxa that demonstrated dynamic relative abundance throughout disease development in response to the basal diet have also been implicated in IBD and/or CRC. We determined that members of the Lachnospiraceae family (genera *Lachnospiraceae* - *NK4A136_group*, *Lachnospiraceae_A2*, *Blautia*, *Marvinbryantia*, and *Lachnoclostridium*) were less abundant in the TWD-fed recipient mice compared to their AIN-fed counterparts prior to gut injury, and at the study end point in mice with high tumor burden. Several studies have reported reduced levels of *Blautia spp.* in the fecal microbiome of CRC patients compared to healthy controls [66,67,68]. Wang et al. reported a decrease in the abundance of *Lachnoclostridium sp.* in both wild-type and TGF β -deficient mice after the induction of colorectal carcinogenesis by AOM + DSS [69], a finding that appears to differ from our observations for the Lachnospiraceae family, including *Lachnoclostridium spp.*; however, we do note that the abundance of this taxa is reduced at the study end point in mice fed the TWD, which have much more severe tumor outcomes.

Similar to the findings reported in our prior study [22], we observed in this experiment that the relative abundances of bacteria in the Erysipelotrichaceae (e.g., *Turicibacter spp.* and *D. newyorkensis*) and Bifidobacteriaceae (*Bifidobacterium spp.*) families were elevated in the fecal microbiomes of mice experiencing active colitis compared to their pre-DSS counterparts. A greater abundance of Erysipelotrichaceae in the fecal microbiome has been found in the lumen of CRC patients compared to a healthy control group and to other gut diseases [70,71]. Additionally, in a murine colitis model, consumption of a choline-deficient diet led to a decrease in relative abundance of Erysipelotrichaceae [72]. Moreover, *Bifidobacterium* appears to increase in abundance during active IBD and has been reported as a predominant genus in the microbiome of Taiwanese IBD patients [73,74,75,76]. On the other hand, administration of *Bifidobacterium longum* suppressed development of preneoplastic lesions in mice and appeared to induce expression of tumor-suppressing microRNAs [77], whereas *Bifidobacterium infantis* conferred protection against DSS-induced colitis and abnormal immune signaling [77,78]. Additionally,

various strains of *Bifidobacterium* have anti-cancer properties and have been used as probiotics [79,80].

This study had several limitations to consider. Although a universal protocol for FMT has not yet been established, researchers have determined that FMT into recipients with a depleted gut microbiome—either via the use of antibiotic or polyethylene glycol administration or via the use of germ-free organisms—is more successful than FMT into recipients with intact gut microbiomes [81]. In this experiment, broad-scope antibiotics were used to deplete the resident microbiome of the recipient mice prior to FMT and implementation of the AOM/DSS to induce colitis and colon tumorigenesis. However, with this method, it is possible that some microbiota persisted, and antibiotic use could select for resistant bacteria or allow the overgrowth of other microbes. These drawbacks could be avoided by using germ-free mice [82]. However, germ-free mice present other disadvantages, and chief among them is an improperly developed gut immune system. Furthermore, FMT does not provide a perfect transplantation of donor microbiome to the gut of the recipient. Some species are unable to successfully colonize the recipient's gut, although this issue is less of a concern in the present study, which employed mouse-to-mouse FMT, compared to human-to-mouse FMT studies. Furthermore, the collection and storage methods used in this study might not have preserved all bacterial species, such as obligate anaerobes [81]. Additionally, the 16s rRNA sequencing analyses of fecal microbiomes generated the data for the relative abundance of bacteria, not their numerical abundance in the experimental samples. Thus, apparent changes in relative abundance of a particular taxon should not be interpreted as a change in its actual population size; rather, it is possible that the relative abundance could reflect a growth or a loss of other bacteria in the fecal microbiome community. Another limitation of this work was the narrow focus of the experimental design, which centered on the question of whether the gut microbiome from mice experiencing Western diet-enhanced colitis and colon tumorigenesis could exacerbate disease in recipient mice that would otherwise experience mild

symptoms (e.g., the AIN-fed recipients). This study's design did not address the question of whether the gut microbiome of mice with diet-driven severe disease would induce disease in otherwise healthy mice, which was beyond the scope of this work. Finally, this murine model of CAC allows the generation of colon adenocarcinomas within about six months of tumor initiation by AOM + DSS; however, this model is not generally used to assess the effects of diet or the influence of the gut microbiome on progression to advanced metastatic disease as the rapid growth of colon polyps often requires humane euthanasia of experimental animals due to bowel obstruction.

3.5. Conclusions

In conclusion, the findings of the present study did not support our hypothesis that FMT from mice fed a Western diet, which enhanced colitis and colon tumorigenesis in donor mice, would exacerbate disease symptoms in recipients fed the standard AIN diet. FMT from the donor mice that were fed the TWD and had a severe disease phenotype led to only minor changes in the recipient fecal microbiome and did not worsen disease symptoms in the mice fed the AIN diet. Conversely, FMT from the healthy mice with only mild colitis symptoms did not confer protection against gut inflammation or dysbiosis in the recipient mice fed the TWD. Instead, we determined that the basal diet fed to the recipient mice had a much more substantial effect on colitis, colon tumorigenesis, and fecal microbiome profile of recipient mice, a finding that is consistent with prior work by our group that employed FMT from obese or lean human donors to mice fed differing basal diets [21]. Collectively, these findings point to the need to appropriately consider the influence of basal diet on a recipient's microbiome in future pre-clinical FMT experiments. Additionally, these observations suggest that the nutritional status of a patient and their routine dietary intakes must be considered when employing FMT as a therapeutic approach for ameliorating gut inflammation. Lastly, future pre-clinical studies may consider whether gut microbiome associated with chronic intake of a Western type of diet may contribute to gut

inflammation and/or development of colorectal cancer in otherwise healthy mice by employing a long-term, repeated FMT protocol without the AOM + DSS protocol to initiate CAC.

References

1. Sekirov, I.; Russell, S.L.; Antunes, L.C.; Finlay, B.B. Gut microbiota in health and disease. *Physiol Rev* **2010**, *90*, 859-904, doi:10.1152/physrev.00045.2009.
2. Barko, P.C.; McMichael, M.A.; Swanson, K.S.; Williams, D.A. The gastrointestinal microbiome: a review. *J Vet Intern Med* **2018**, *32*, 9-25, doi:10.1111/jvim.14875.
3. Choo, J.; Glisovic, N.; Matic Vignjevic, D. Gut homeostasis at a glance. *J Cell Sci* **2022**, *135*, doi:10.1242/jcs.260248.
4. Durack, J.; Lynch, S.V. The gut microbiome: relationships with disease and opportunities for therapy. *J Exp Med* **2019**, *216*, 20-40, doi:10.1084/jem.20180448.
5. Oren, A.; Garrity, G.M. Valid publication of the names of forty-two phyla of prokaryotes. *Int J Syst Evol Microbiol* **2021**, *71*, doi:10.1099/ijsem.0.005056.
6. Song, M.; Chan, A.T.; Sun, J. Influence of the gut microbiome, diet, and environment on risk of colorectal cancer. *Gastroenterology* **2020**, *158*, 322-340, doi:10.1053/j.gastro.2019.06.048.
7. Hintze, K.J.; Benninghoff, A.D.; Ward, R.E. Formulation of the total Western diet (TWD) as a basal diet for rodent cancer studies. *J Agric Food Chem* **2012**, *60*, 6736-6742, doi:10.1021/jf204509a.
8. Turnbaugh, P.J.; Ridaura, V.K.; Faith, J.J.; Rey, F.E.; Knight, R.; Gordon, J.I. The effect of diet on the human gut microbiome: a metagenomic analysis in humanized gnotobiotic mice. *Sci Transl Med* **2009**, *1*, 6ra14, doi:10.1126/scitranslmed.3000322.
9. Benninghoff, A.D.; Hintze, K.J.; Monsanto, S.P.; Rodriguez, D.M.; Hunter, A.H.; Phatak, S.; Pestka, J.J.; Wettere, A.J.V.; Ward, R.E. Consumption of the total Western diet promotes colitis and inflammation-associated colorectal cancer in mice. *Nutrients* **2020**, *12*, doi:10.3390/nu12020544.
10. Shah, S.C.; Itzkowitz, S.H. Colorectal cancer in inflammatory bowel disease: mechanisms and management. *Gastroenterology* **2022**, *162*, 715-730 e713, doi:10.1053/j.gastro.2021.10.035.
11. Hansen, J.J. Immune responses to intestinal microbes in inflammatory bowel diseases. *Curr Allergy Asthma Rep* **2015**, *15*, 61, doi:10.1007/s11882-015-0562-9.
12. Yu, T.; Guo, F.; Yu, Y.; Sun, T.; Ma, D.; Han, J.; Qian, Y.; Kryczek, I.; Sun, D.; Nagarsheth, N., et al. *Fusobacterium nucleatum* promotes chemoresistance to colorectal cancer by modulating autophagy. *Cell* **2017**, *170*, 548-563 e516, doi:10.1016/j.cell.2017.07.008.

13. Ye, X.; Wang, R.; Bhattacharya, R.; Boulbes, D.R.; Fan, F.; Xia, L.; Adoni, H.; Ajami, N.J.; Wong, M.C.; Smith, D.P., et al. *Fusobacterium nucleatum* subspecies *animalis* influences proinflammatory cytokine expression and monocyte activation in human colorectal tumors. *Cancer Prev Res (Phila)* **2017**, *10*, 398-409, doi:10.1158/1940-6207.CAPR-16-0178.
14. Sears, C.L.; Geis, A.L.; Housseau, F. *Bacteroides fragilis* subverts mucosal biology: from symbiont to colon carcinogenesis. *J Clin Invest* **2014**, *124*, 4166-4172, doi:10.1172/JCI72334.
15. Bonnet, M.; Buc, E.; Sauvanet, P.; Darcha, C.; Dubois, D.; Pereira, B.; Dechelotte, P.; Bonnet, R.; Pezet, D.; Darfeuille-Michaud, A. Colonization of the human gut by *E. coli* and colorectal cancer risk. *Clin Cancer Res* **2014**, *20*, 859-867, doi:10.1158/1078-0432.CCR-13-1343.
16. Steck, N.; Hoffmann, M.; Sava, I.G.; Kim, S.C.; Hahne, H.; Tonkonogy, S.L.; Mair, K.; Krueger, D.; Pruteanu, M.; Shanahan, F., et al. *Enterococcus faecalis* metalloprotease compromises epithelial barrier and contributes to intestinal inflammation. *Gastroenterology* **2011**, *141*, 959-971, doi:10.1053/j.gastro.2011.05.035.
17. Tsoi, H.; Chu, E.S.H.; Zhang, X.; Sheng, J.; Nakatsu, G.; Ng, S.C.; Chan, A.W.H.; Chan, F.K.L.; Sung, J.J.Y.; Yu, J. *Peptostreptococcus anaerobius* induces intracellular cholesterol biosynthesis in colon cells to induce proliferation and causes dysplasia in mice. *Gastroenterology* **2017**, *152*, 1419-1433 e1415, doi:10.1053/j.gastro.2017.01.009.
18. Gheorghe, C.E.; Ritz, N.L.; Martin, J.A.; Wardill, H.R.; Cryan, J.F.; Clarke, G. Investigating causality with fecal microbiota transplantation in rodents: applications, recommendations and pitfalls. *Gut Microbes* **2021**, *13*, 1941711, doi:10.1080/19490976.2021.1941711.
19. Fiebigler, U.; Bereswill, S.; Heimesaat, M.M. Dissecting the interplay between intestinal microbiota and host immunity in health and disease: lessons learned from germfree and gnotobiotic animal models. *Eur J Microbiol Immunol (Bp)* **2016**, *6*, 253-271, doi:10.1556/1886.2016.00036.
20. Hintze, K.J.; Cox, J.E.; Rompato, G.; Benninghoff, A.D.; Ward, R.E.; Broadbent, J.; Lefevre, M. Broad scope method for creating humanized animal models for animal health and disease research through antibiotic treatment and human fecal transfer. *Gut Microbes* **2014**, *5*, 183-191, doi:10.4161/gmic.28403.
21. Rodriguez, D.M.; Benninghoff, A.D.; Aardema, N.D.J.; Phatak, S.; Hintze, K.J. Basal diet determined long-term composition of the gut microbiome and mouse phenotype to a greater extent than fecal microbiome transfer from lean or obese human donors. *Nutrients* **2019**, *11*, doi:10.3390/nu11071630.
22. Rodriguez, D.M.; Hintze, K.J.; Rompato, G.; Wettter, A.J.V.; Ward, R.E.; Phatak, S.; Neal, C.; Armbrust, T.; Stewart, E.C.; Thomas, A.J., et al. Dietary supplementation with black raspberries altered the gut microbiome composition in a mouse model of colitis-associated colorectal cancer, although with differing effects for a healthy versus a Western basal diet. *Nutrients* **2022**, *14*, doi:10.3390/nu14245270.

23. Estaki, M.; Jiang, L.; Bokulich, N.A.; McDonald, D.; Gonzalez, A.; Kosciulek, T.; Martino, C.; Zhu, Q.; Birmingham, A.; Vazquez-Baeza, Y., et al. QIIME 2 enables comprehensive end-to-end analysis of diverse microbiome data and comparative studies with publicly available data. *Curr Protoc Bioinformatics* **2020**, *70*, e100, doi:10.1002/cpbi.100.
24. Callahan, B.J.; McMurdie, P.J.; Rosen, M.J.; Han, A.W.; Johnson, A.J.; Holmes, S.P. DADA2: High-resolution sample inference from Illumina amplicon data. *Nat Methods* **2016**, *13*, 581-583, doi:10.1038/nmeth.3869.
25. Quast, C.; Pruesse, E.; Yilmaz, P.; Gerken, J.; Schweer, T.; Yarza, P.; Peplies, J.; Glockner, F.O. The SILVA ribosomal RNA gene database project: improved data processing and web-based tools. *Nucleic Acids Res* **2013**, *41*, D590-596, doi:10.1093/nar/gks1219.
26. Chong, J.; Liu, P.; Zhou, G.; Xia, J. Using MicrobiomeAnalyst for comprehensive statistical, functional, and meta-analysis of microbiome data. *Nat Protoc* **2020**, *15*, 799-821, doi:10.1038/s41596-019-0264-1.
27. Metsalu, T.; Vilo, J. ClustVis: a web tool for visualizing clustering of multivariate data using Principal Component Analysis and heatmap. *Nucleic Acids Res* **2015**, *43*, W566-570, doi:10.1093/nar/gkv468.
28. Vindigni, S.M.; Surawicz, C.M. Fecal microbiota transplantation. *Gastroenterol Clin North Am* **2017**, *46*, 171-185, doi:10.1016/j.gtc.2016.09.012.
29. Bakken, J.S.; Borody, T.; Brandt, L.J.; Brill, J.V.; Demarco, D.C.; Franzos, M.A.; Kelly, C.; Khoruts, A.; Louie, T.; Martinelli, L.P., et al. Treating *Clostridium difficile* infection with fecal microbiota transplantation. *Clin Gastroenterol Hepatol* **2011**, *9*, 1044-1049, doi:10.1016/j.cgh.2011.08.014.
30. U.S. Food and Drug Administration. Important safety alert regarding use of fecal microbiota for transplantation and risk of serious adverse reactions due to transmission of multi-drug resistant organisms. Available online: <https://www.fda.gov/vaccines-blood-biologics/safety-availability-biologics/important-safety-alert-regarding-use-fecal-microbiota-transplantation-and-risk-serious-adverse> (accessed on January 10, 2023).
31. Waller, K.M.J.; Leong, R.W.; Paramsothy, S. An update on fecal microbiota transplantation for the treatment of gastrointestinal diseases. *J Gastroenterol Hepatol* **2022**, *37*, 246-255, doi:10.1111/jgh.15731.
32. Aardema, N.D.; Rodriguez, D.M.; Van Wettere, A.J.; Benninghoff, A.D.; Hintze, K.J. The Western dietary pattern combined with vancomycin-mediated changes to the gut microbiome exacerbates colitis severity and colon tumorigenesis. *Nutrients* **2021**, *13*, doi:10.3390/nu13030881.
33. Lippert, E.; Ruellemele, P.; Obermeier, F.; Goelder, S.; Kunst, C.; Rogler, G.; Dunger, N.; Messmann, H.; Hartmann, A.; Endlicher, E. Anthocyanins Prevent Colorectal Cancer Development in a Mouse Model. *Digestion* **2017**, *95*, 275-280, doi:10.1159/000475524.

34. Wang, F.; Cai, K.; Xiao, Q.; He, L.; Xie, L.; Liu, Z. *Akkermansia muciniphila* administration exacerbated the development of colitis-associated colorectal cancer in mice. *J Cancer* **2022**, *13*, 124-133, doi:10.7150/jca.63578.
35. Zhang, Y.K.; Zhang, Q.; Wang, Y.L.; Zhang, W.Y.; Hu, H.Q.; Wu, H.Y.; Sheng, X.Z.; Luo, K.J.; Zhang, H.; Wang, M., et al. A comparison study of age and colorectal cancer-related gut bacteria. *Front Cell Infect Microbiol* **2021**, *11*, 606490, doi:10.3389/fcimb.2021.606490.
36. Russo, E.; Bacci, G.; Chiellini, C.; Fagorzi, C.; Niccolai, E.; Taddei, A.; Ricci, F.; Ringressi, M.N.; Borrelli, R.; Melli, F., et al. Preliminary comparison of oral and intestinal human microbiota in patients with colorectal cancer: a pilot study. *Front Microbiol* **2017**, *8*, 2699, doi:10.3389/fmicb.2017.02699.
37. Zhang, W.; Zou, G.; Li, B.; Du, X.; Sun, Z.; Sun, Y.; Jiang, X. Fecal microbiota transplantation (FMT) alleviates experimental colitis in mice by gut microbiota regulation. *J Microbiol Biotechnol* **2020**, *30*, 1132-1141, doi:10.4014/jmb.2002.02044.
38. Lin, H.; Ma, X.; Yang, X.; Chen, Q.; Wen, Z.; Yang, M.; Fu, J.; Yin, T.; Lu, G.; Qi, J., et al. Natural shikonin and acetyl-shikonin improve intestinal microbial and protein composition to alleviate colitis-associated colorectal cancer. *Int Immunopharmacol* **2022**, *111*, 109097, doi:10.1016/j.intimp.2022.109097.
39. Liu, W.; Zhang, R.; Shu, R.; Yu, J.; Li, H.; Long, H.; Jin, S.; Li, S.; Hu, Q.; Yao, F., et al. Study of the relationship between microbiome and colorectal cancer susceptibility using 16SrRNA sequencing. *Biomed Res Int* **2020**, *2020*, 7828392, doi:10.1155/2020/7828392.
40. Ma, Y.; Zhang, Y.; Xiang, J.; Xiang, S.; Zhao, Y.; Xiao, M.; Du, F.; Ji, H.; Kaboli, P.J.; Wu, X., et al. Metagenome analysis of intestinal bacteria in healthy people, patients with inflammatory bowel disease and colorectal cancer. *Front Cell Infect Microbiol* **2021**, *11*, 599734, doi:10.3389/fcimb.2021.599734.
41. Chang, C.W.; Lee, H.C.; Li, L.H.; Chiang Chiau, J.S.; Wang, T.E.; Chuang, W.H.; Chen, M.J.; Wang, H.Y.; Shih, S.C.; Liu, C.Y., et al. Fecal microbiota transplantation prevents intestinal injury, upregulation of toll-like receptors, and 5-fluorouracil/oxaliplatin-induced toxicity in colorectal cancer. *Int J Mol Sci* **2020**, *21*, doi:10.3390/ijms21020386.
42. Li, H.L.; Lu, L.; Wang, X.S.; Qin, L.Y.; Wang, P.; Qiu, S.P.; Wu, H.; Huang, F.; Zhang, B.B.; Shi, H.L., et al. Alteration of gut microbiota and inflammatory cytokine/chemokine profiles in 5-fluorouracil Induced intestinal mucositis. *Front Cell Infect Microbiol* **2017**, *7*, 455, doi:10.3389/fcimb.2017.00455.
43. Wang, Z.; Hua, W.; Li, C.; Chang, H.; Liu, R.; Ni, Y.; Sun, H.; Li, Y.; Wang, X.; Hou, M., et al. Protective role of fecal microbiota transplantation on colitis and colitis-associated colon cancer in mice is associated with Treg cells. *Front Microbiol* **2019**, *10*, 2498, doi:10.3389/fmicb.2019.02498.
44. Leibovitz, H.; Lee, S.H.; Xue, M.; Raygoza Garay, J.A.; Hernandez-Rocha, C.; Madsen, K.L.; Meddings, J.B.; Guttman, D.S.; Espin-Garcia, O.; Smith, M.I., et al. Altered gut microbiome composition and function are associated with gut barrier dysfunction in

- healthy relatives of patients with Crohn's disease. *Gastroenterology* **2022**, *163*, 1364-1376 e1310, doi:10.1053/j.gastro.2022.07.004.
45. Rajilic-Stojanovic, M.; Shanahan, F.; Guarner, F.; de Vos, W.M. Phylogenetic analysis of dysbiosis in ulcerative colitis during remission. *Inflamm Bowel Dis* **2013**, *19*, 481-488, doi:10.1097/MIB.0b013e31827fec6d.
 46. Zhu, Q.; Jin, Z.; Wu, W.; Gao, R.; Guo, B.; Gao, Z.; Yang, Y.; Qin, H. Analysis of the intestinal lumen microbiota in an animal model of colorectal cancer. *PLoS One* **2014**, *9*, e90849, doi:10.1371/journal.pone.0090849.
 47. Kolho, K.L.; Korpela, K.; Jaakkola, T.; Pichai, M.V.; Zoetendal, E.G.; Salonen, A.; de Vos, W.M. Fecal microbiota in pediatric inflammatory bowel disease and its relation to inflammation. *Am J Gastroenterol* **2015**, *110*, 921-930, doi:10.1038/ajg.2015.149.
 48. Mukherjee, A.; Lordan, C.; Ross, R.P.; Cotter, P.D. Gut microbes from the phylogenetically diverse genus *Eubacterium* and their various contributions to gut health. *Gut Microbes* **2020**, *12*, 1802866, doi:10.1080/19490976.2020.1802866.
 49. Santoru, M.L.; Piras, C.; Murgia, A.; Palmas, V.; Camboni, T.; Liggi, S.; Ibba, I.; Lai, M.A.; Orru, S.; Blois, S., et al. Cross sectional evaluation of the gut-microbiome metabolome axis in an Italian cohort of IBD patients. *Sci Rep* **2017**, *7*, 9523, doi:10.1038/s41598-017-10034-5.
 50. Kaakoush, N.O. *Sutterella* species, IgA-degrading bacteria in ulcerative colitis. *Trends Microbiol* **2020**, *28*, 519-522, doi:10.1016/j.tim.2020.02.018.
 51. Morotomi, M.; Nagai, F.; Watanabe, Y. *Parasutterella secunda* sp. nov., isolated from human faeces and proposal of Sutterellaceae fam. nov. in the order Burkholderiales. *Int J Syst Evol Microbiol* **2011**, *61*, 637-643, doi:10.1099/ijs.0.023556-0.
 52. Zeng, H.; Safratowich, B.D.; Liu, Z.; Bukowski, M.R.; Ishaq, S.L. Adequacy of calcium and vitamin D reduces inflammation, beta-catenin signaling, and dysbiotic *Parasutterella* bacteria in the colon of C57BL/6 mice fed a western-style diet. *J Nutr Biochem* **2021**, *92*, 108613, doi:10.1016/j.jnutbio.2021.108613.
 53. Wang, C.Z.; Huang, W.H.; Zhang, C.F.; Wan, J.Y.; Wang, Y.; Yu, C.; Williams, S.; He, T.C.; Du, W.; Musch, M.W., et al. Role of intestinal microbiome in American ginseng-mediated colon cancer prevention in high fat diet-fed AOM/DSS mice [corrected]. *Clin Transl Oncol* **2018**, *20*, 302-312, doi:10.1007/s12094-017-1717-z.
 54. Huda, M.N.; Salvador, A.C.; Barrington, W.T.; Gacasan, C.A.; D'Souza, E.M.; Deus Ramirez, L.; Threadgill, D.W.; Bennett, B.J. Gut microbiota and host genetics modulate the effect of diverse diet patterns on metabolic health. *Front Nutr* **2022**, *9*, 896348, doi:10.3389/fnut.2022.896348.
 55. Miller, C.B.; Benny, P.; Riel, J.; Boushey, C.; Perez, R.; Khadka, V.; Qin, Y.; Maunakea, A.K.; Lee, M.J. Adherence to Mediterranean diet impacts gastrointestinal microbial diversity throughout pregnancy. *BMC Pregnancy Childbirth* **2021**, *21*, 558, doi:10.1186/s12884-021-04033-8.

56. Ottman, N.; Davids, M.; Suarez-Diez, M.; Boeren, S.; Schaap, P.J.; Martins Dos Santos, V.A.P.; Smidt, H.; Belzer, C.; de Vos, W.M. Genome-scale model and omics analysis of metabolic capacities of *Akkermansia muciniphila* reveal a preferential mucin-degrading lifestyle. *Appl Environ Microbiol* **2017**, *83*, doi:10.1128/AEM.01014-17.
57. Dingemans, C.; Belzer, C.; van Hijum, S.A.; Gunthel, M.; Salvatori, D.; den Dunnen, J.T.; Kuijper, E.J.; Devilee, P.; de Vos, W.M.; van Ommen, G.B., et al. *Akkermansia muciniphila* and *Helicobacter typhlonius* modulate intestinal tumor development in mice. *Carcinogenesis* **2015**, *36*, 1388-1396, doi:10.1093/carcin/bgv120.
58. Zhang, T.; Li, Q.; Cheng, L.; Buch, H.; Zhang, F. *Akkermansia muciniphila* is a promising probiotic. *Microb Biotechnol* **2019**, *12*, 1109-1125, doi:10.1111/1751-7915.13410.
59. Weir, T.L.; Manter, D.K.; Sheflin, A.M.; Barnett, B.A.; Heuberger, A.L.; Ryan, E.P. Stool microbiome and metabolome differences between colorectal cancer patients and healthy adults. *PLoS One* **2013**, *8*, e70803, doi:10.1371/journal.pone.0070803.
60. Sanapareddy, N.; Legge, R.M.; Jovov, B.; McCoy, A.; Burcal, L.; Araujo-Perez, F.; Randall, T.A.; Galanko, J.; Benson, A.; Sandler, R.S., et al. Increased rectal microbial richness is associated with the presence of colorectal adenomas in humans. *ISME J* **2012**, *6*, 1858-1868, doi:10.1038/ismej.2012.43.
61. Png, C.W.; Linden, S.K.; Gilshenan, K.S.; Zoetendal, E.G.; McSweeney, C.S.; Sly, L.I.; McGuckin, M.A.; Florin, T.H. Mucolytic bacteria with increased prevalence in IBD mucosa augment in vitro utilization of mucin by other bacteria. *Am J Gastroenterol* **2010**, *105*, 2420-2428, doi:10.1038/ajg.2010.281.
62. Rodrigues, V.F.; Elias-Oliveira, J.; Pereira, I.S.; Pereira, J.A.; Barbosa, S.C.; Machado, M.S.G.; Carlos, D. *Akkermansia muciniphila* and gut immune system: a good friendship that attenuates inflammatory bowel disease, obesity, and diabetes. *Front Immunol* **2022**, *13*, 934695, doi:10.3389/fimmu.2022.934695.
63. Pittayanon, R.; Lau, J.T.; Leontiadis, G.I.; Tse, F.; Yuan, Y.; Surette, M.; Moayyedi, P. Differences in gut microbiota in patients with vs without inflammatory bowel diseases: a systematic review. *Gastroenterology* **2020**, *158*, 930-946 e931, doi:10.1053/j.gastro.2019.11.294.
64. Hakansson, A.; Tormo-Badia, N.; Baridi, A.; Xu, J.; Molin, G.; Hagslatt, M.L.; Karlsson, C.; Jeppsson, B.; Cilio, C.M.; Ahrne, S. Immunological alteration and changes of gut microbiota after dextran sulfate sodium (DSS) administration in mice. *Clin Exp Med* **2015**, *15*, 107-120, doi:10.1007/s10238-013-0270-5.
65. Qu, S.; Fan, L.; Qi, Y.; Xu, C.; Hu, Y.; Chen, S.; Liu, W.; Liu, W.; Si, J. *Akkermansia muciniphila* alleviates dextran sulfate sodium (DSS)-induced acute colitis by NLRP3 activation. *Microbiol Spectr* **2021**, *9*, e0073021, doi:10.1128/Spectrum.00730-21.
66. Du, X.; Li, Q.; Tang, Z.; Yan, L.; Zhang, L.; Zheng, Q.; Zeng, X.; Chen, G.; Yue, H.; Li, J., et al. Alterations of the gut microbiome and fecal metabolome in colorectal cancer: implication of intestinal metabolism for tumorigenesis. *Front Physiol* **2022**, *13*, 854545, doi:10.3389/fphys.2022.854545.

67. Wang, J.; Wang, Y.; Li, Z.; Gao, X.; Huang, D. Global analysis of microbiota signatures in four major types of gastrointestinal cancer. *Front Oncol* **2021**, *11*, 685641, doi:10.3389/fonc.2021.685641.
68. Han, S.; Zhuang, J.; Pan, Y.; Wu, W.; Ding, K. Different characteristics in gut microbiome between advanced adenoma patients and colorectal cancer patients by metagenomic analysis. *Microbiol Spectr* **2022**, *10*, e0159322, doi:10.1128/spectrum.01593-22.
69. Wang, Z.; Hopson, L.M.; Singleton, S.S.; Yang, X.; Jogunoori, W.; Mazumder, R.; Obias, V.; Lin, P.; Nguyen, B.N.; Yao, M., et al. Mice with dysfunctional TGF-beta signaling develop altered intestinal microbiome and colorectal cancer resistant to 5FU. *Biochim Biophys Acta Mol Basis Dis* **2021**, *1867*, 166179, doi:10.1016/j.bbadis.2021.166179.
70. Chen, W.; Liu, F.; Ling, Z.; Tong, X.; Xiang, C. Human intestinal lumen and mucosa-associated microbiota in patients with colorectal cancer. *PLoS One* **2012**, *7*, e39743, doi:10.1371/journal.pone.0039743.
71. Mancabelli, L.; Milani, C.; Lugli, G.A.; Turroni, F.; Cocconi, D.; van Sinderen, D.; Ventura, M. Identification of universal gut microbial biomarkers of common human intestinal diseases by meta-analysis. *FEMS Microbiol Ecol* **2017**, *93*, doi:10.1093/femsec/fix153.
72. Ju, T.; Kennelly, J.P.; Jacobs, R.L.; Willing, B.P. Insufficient dietary choline aggravates disease severity in a mouse model of *Citrobacter rodentium*-induced colitis. *Br J Nutr* **2021**, *125*, 50-61, doi:10.1017/S0007114520002639.
73. Gueimonde, M.; Ouwehand, A.; Huhtinen, H.; Salminen, E.; Salminen, S. Qualitative and quantitative analyses of the bifidobacterial microbiota in the colonic mucosa of patients with colorectal cancer, diverticulitis and inflammatory bowel disease. *World J Gastroenterol* **2007**, *13*, 3985-3989, doi:10.3748/wjg.v13.i29.3985.
74. Cardoneanu, A.; Mihai, C.; Rezus, E.; Burlui, A.; Popa, I.; Cijevschi Prelicean, C. Gut microbiota changes in inflammatory bowel diseases and ankylosing spondylitis. *J Gastrointest Liver Dis* **2021**, *30*, 46-54, doi:10.15403/jgld-2823.
75. Teofani, A.; Marafini, I.; Laudisi, F.; Pietrucci, D.; Salvatori, S.; Unida, V.; Biocca, S.; Monteleone, G.; Desideri, A. Intestinal taxa abundance and diversity in inflammatory bowel disease patients: an analysis including covariates and confounders. *Nutrients* **2022**, *14*, doi:10.3390/nu14020260.
76. Wang, W.; Chen, L.; Zhou, R.; Wang, X.; Song, L.; Huang, S.; Wang, G.; Xia, B. Increased proportions of *Bifidobacterium* and the *Lactobacillus* group and loss of butyrate-producing bacteria in inflammatory bowel disease. *J Clin Microbiol* **2014**, *52*, 398-406, doi:10.1128/JCM.01500-13.
77. Fahmy, C.A.; Gamal-Eldeen, A.M.; El-Hussieny, E.A.; Raafat, B.M.; Mehanna, N.S.; Talaat, R.M.; Shaaban, M.T. *Bifidobacterium longum* suppresses murine colorectal cancer through the modulation of oncomiRs and tumor suppressor miRNAs. *Nutr Cancer* **2019**, *71*, 688-700, doi:10.1080/01635581.2019.1577984.

78. Zhou, L.; Liu, D.; Xie, Y.; Yao, X.; Li, Y. *Bifidobacterium infantis* induces protective colonic PD-L1 and Foxp3 regulatory T cells in an acute murine experimental model of inflammatory bowel disease. *Gut Liver* **2019**, *13*, 430-439, doi:10.5009/gnl18316.
79. Tojo, R.; Suarez, A.; Clemente, M.G.; de los Reyes-Gavilan, C.G.; Margolles, A.; Gueimonde, M.; Ruas-Madiedo, P. Intestinal microbiota in health and disease: role of *Bifidobacteria* in gut homeostasis. *World J Gastroenterol* **2014**, *20*, 15163-15176, doi:10.3748/wjg.v20.i41.15163.
80. Asadollahi, P.; Ghanavati, R.; Rohani, M.; Razavi, S.; Esghaei, M.; Talebi, M. Anti-cancer effects of *Bifidobacterium* species in colon cancer cells and a mouse model of carcinogenesis. *PLoS One* **2020**, *15*, e0232930, doi:10.1371/journal.pone.0232930.
81. Bokoliya, S.C.; Dorsett, Y.; Panier, H.; Zhou, Y. Procedures for fecal microbiota transplantation in murine microbiome studies. *Front Cell Infect Microbiol* **2021**, *11*, 711055, doi:10.3389/fcimb.2021.711055.
82. Kennedy, E.A.; King, K.Y.; Baldrige, M.T. Mouse microbiota models: comparing germ-free mice and antibiotics treatment as tools for modifying gut bacteria. *Front Physiol* **2018**, *9*, 1534, doi:10.3389/fphys.2018.01534.

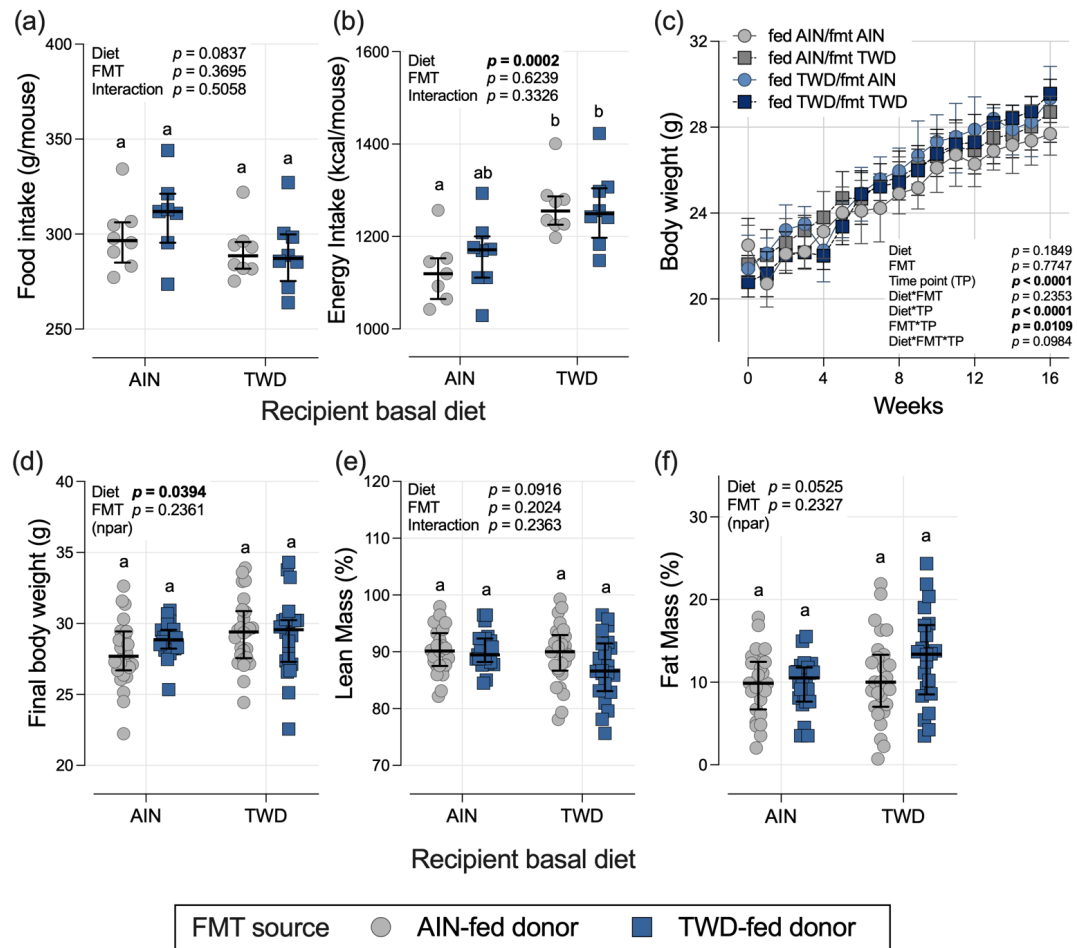


Figure 3.1. Food and energy intakes, body weight, and body composition. **(a,b)** Estimated total daily food and energy intakes per mouse per cage ($n = 7$ to 8 cages per group). **(c)** Body weight gain over the study period ($n = 22$ to 27 mice per group). **(d)** Final body weight at the study end point on day 112 ($n = 22$ to 27 mice per group). **(e,f)** Lean and fat mass as percentage of body weight. ($n = 22$ to 27 mice per group). The data are shown as individual measurements (except (c)) with the median \pm interquartile range (a,b,d-f). The inserted values show the statistical model's main effects for recipient basal diet and FMT source, and their interaction, or "npar" if a non-parametric test was required, and different letters indicate that the experimental groups are significantly different ($p < 0.05$), as determined by the statistical methods outlined in the Materials and Methods section.

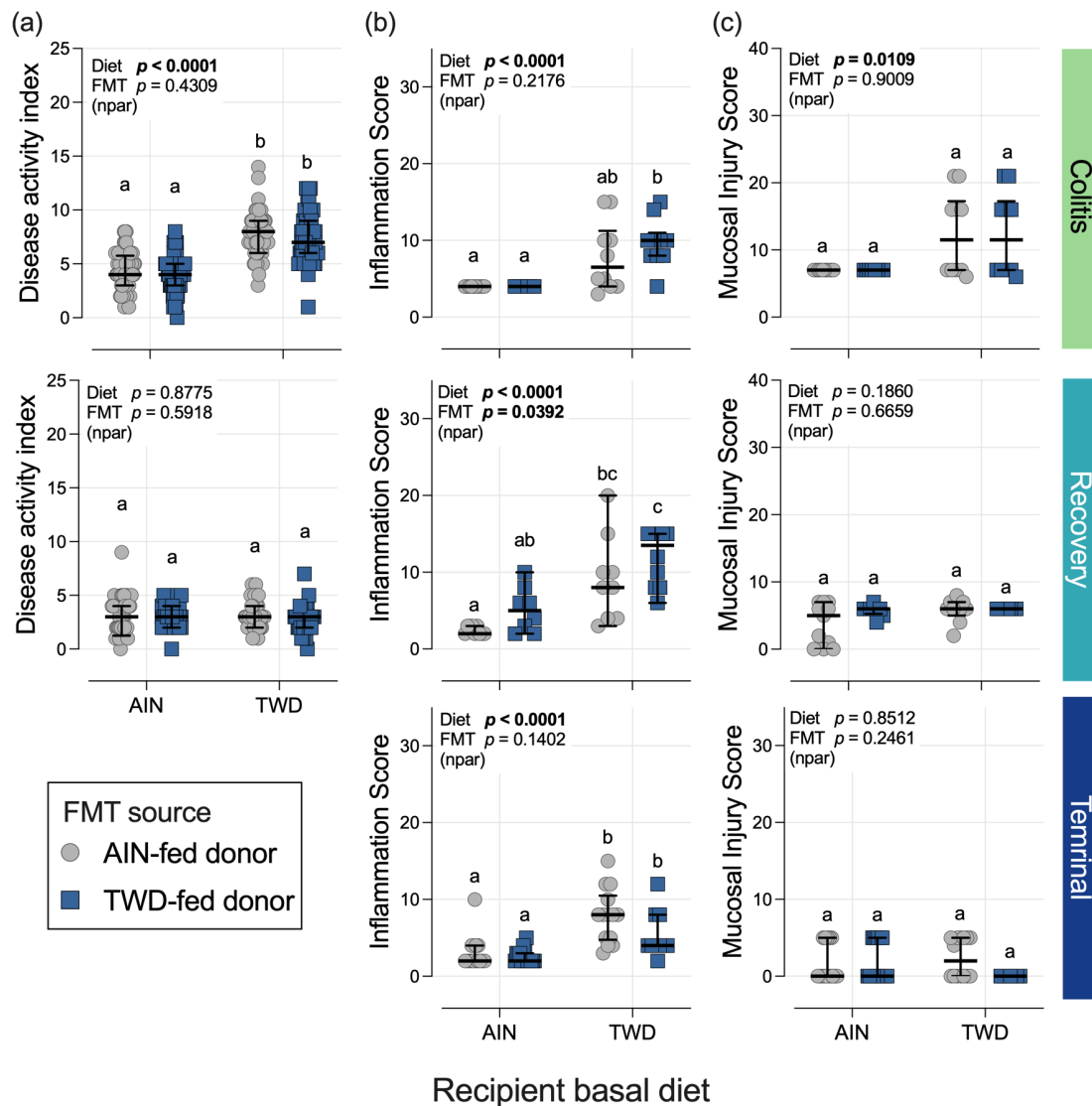


Figure 3.2. Disease activity index and colon histopathology. Scores for the disease activity index (DAI) (a), mucosal inflammation (b), and mucosal injury (c) are shown for active colitis on day 26, for recovery from gut injury on day 38, and for the terminal time point on day 112. The data are shown as individual values with median \pm interquartile range. For the DAI score, $n = 53$ to 64 mice per group at the active colitis time point and $n = 37$ to 44 mice per group at the recovery time point. For inflammation and mucosal injury scores, $n = 10$ to 11 mice per group at the active colitis time point, $n = 7$ to 11 mice per group at the recovery time point, and $n = 10$ to 16 mice per group at the terminal time point. The inserted values provide the statistical model's main effects for recipient basal diet and FMT source, and their interaction, or "npar" if a non-parametric test was required, and different letters indicate that the experimental groups are significantly different ($p < 0.05$), as determined by the statistical methods outlined in the Materials and Methods section.

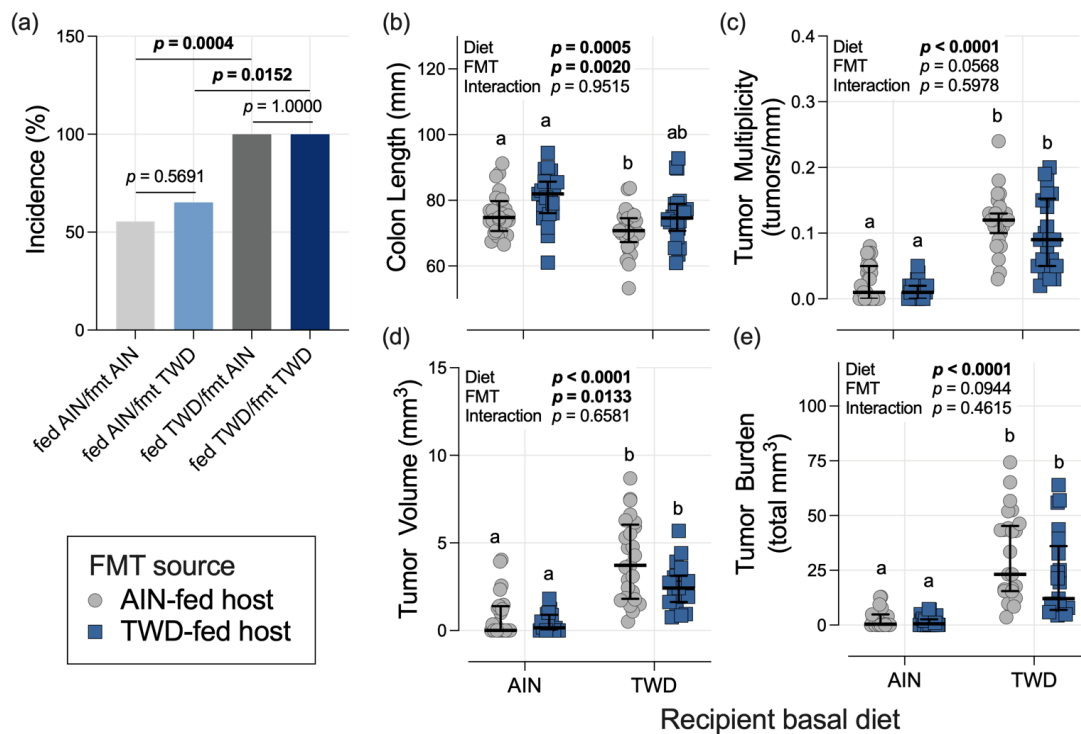


Figure 3.3. Effect of recipient basal diet and FMT source on colon length and colon tumorigenesis. **(a)** Incidence of colon tumors shown as the percentage of mice with tumors at the terminal time point ($n = 22$ to 27 mice per group). p -values from pairwise Fisher's exact tests (selected a priori) are shown. **(b)** Colon length ($n = 22$ to 27 mice per group). **(c)** Colon tumor multiplicity (number of tumors per mm colon length) ($n = 19$ to 27 mice per group). **(d)** Average tumor volume ($n = 18$ to 25 mice per group). **(e)** Tumor burden (total volume) ($n = 20$ to 25 mice per group). For **(b–e)**, the data are shown as individual values with median \pm interquartile range. The inserted values provide the statistical model's main effects for recipient basal diet and FMT source, and their interaction, and different letters indicate that the experimental groups are significantly different ($p < 0.05$), as determined by the statistical methods outlined in the Materials and Methods section.

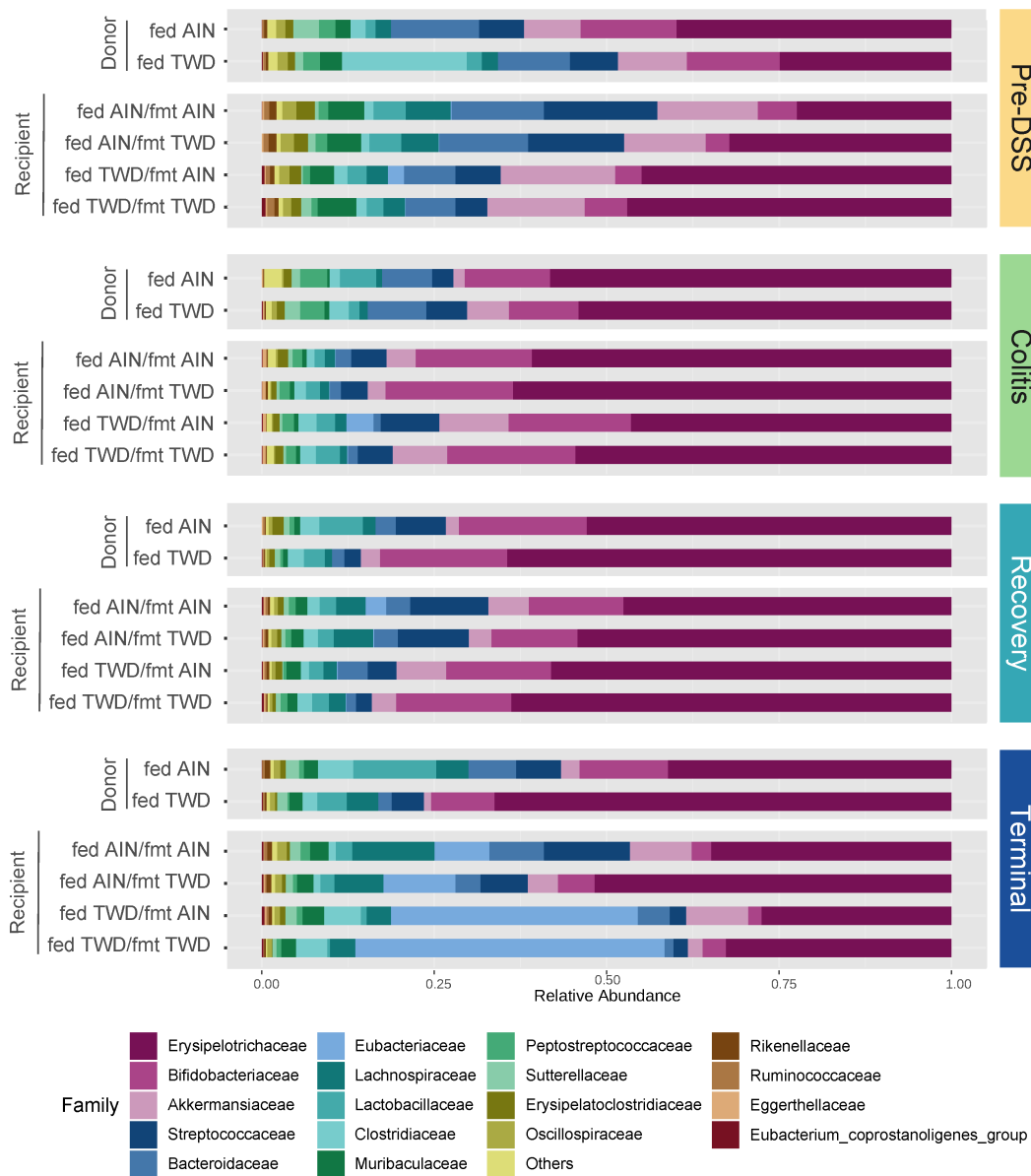


Figure 3.4. Taxonomic classification of mouse fecal bacteria. The data shown are the average relative normalized abundance of bacteria annotated to the family taxonomic level for the top 18 most abundant taxa for each experimental group at each time point ($n = 19$ to 20 cages per group at the pre-DSS time point, $n = 17$ to 18 cages per group at the active colitis time point, $n = 12$ to 13 cages per group at the recovery time point, and $n = 7$ to 8 cages per group at the terminal time point). The donor fecal microbiome sequence data are obtained from Rodriguez et al [22]. However, the donor sequence data were reprocessed in conjunction with the recipient fecal microbiome sequence data in this study so that the normalization for both donor and recipient data sets was consistent. The data for the phylum taxonomic level are available in Figure 3.S4.

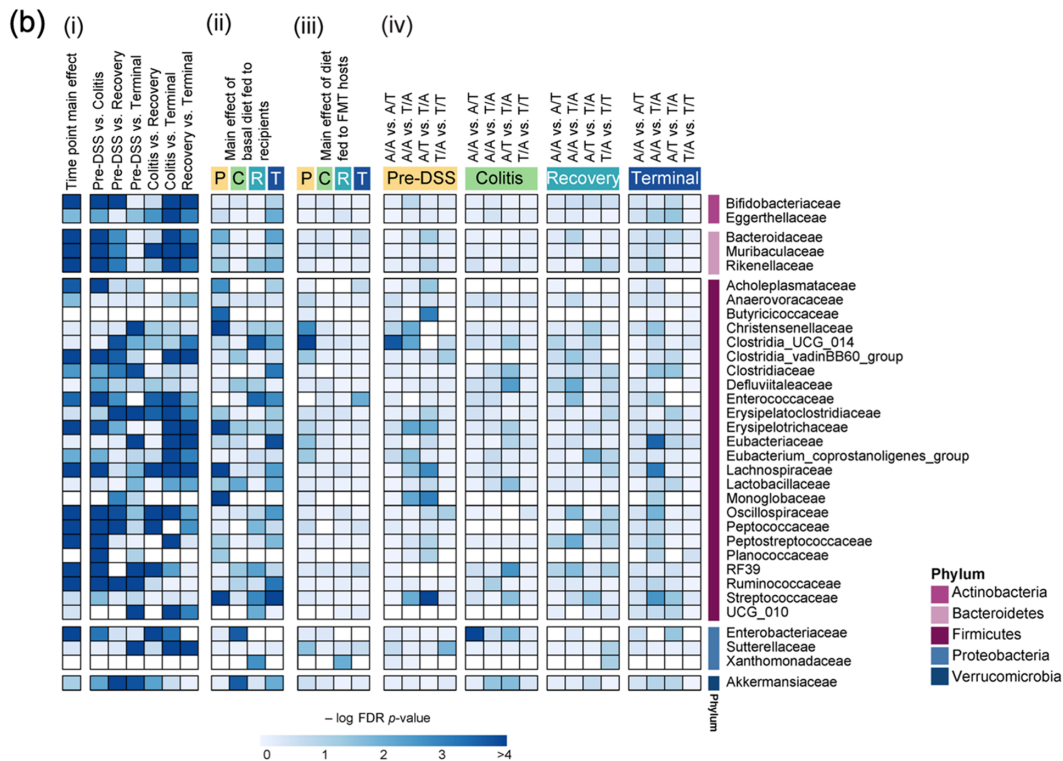
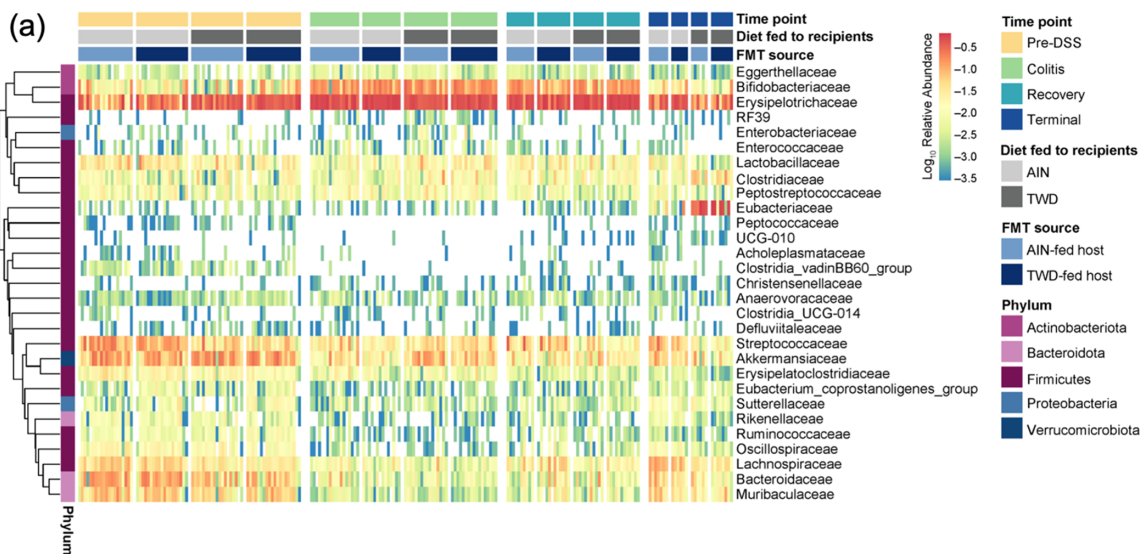


Figure 3.5. Relative abundance of fecal microbiome at the family taxonomic level with a summary of the results from the metagenomeSeq statistical analyses. **(a)** Unsupervised hierarchical cluster analysis shows the \log_{10} relative abundance with clustering by taxa using the Euclidean distance with average linkage ($n = 19$ to 20 cages per group at the pre-DSS time point, $n = 17$ to 18 cages per group at the active colitis time point, $n = 12$ to 13 cages per group at the recovery time point, and $n = 7$ to 8 cages per group at the terminal time point). **(b)** Summary plot shows the \log_{10} FDR-adjusted p -values obtained from the metagenomeSeq analyses of fecal microbiome profiles. All tests were determined a priori, and the complete results are provided in Supplementary File 3.S2. (i) Analyses for the main effects of time point and pairwise comparisons across time points, irrespective of basal diet or FMT source. (ii) Analyses for diet main effects, irrespective of FMT source, at each time point. (iii) Analyses for FMT source main effects, irrespective of basal diet, at each time point. (iv) Selected pairwise tests for basal diet and FMT source combinations within each study time point. The abbreviations for the recipient basal diet/FMT source are as follows: A/A, fed AIN/fmt AIN; A/T, fed AIN/fmt TWD; T/A, fed TWD/fmt AIN; and T/T, fed TWD/fmt TWD. A significant effect is inferred for FDR-adjusted p -values < 0.05 (increasing blue on the color scale).

Figure 3.6. Fecal microbiome community structures depicted as heat trees, showing the relative abundance ratios for selected comparisons of recipient basal diet and FMT source at each experimental time point. **(a)** Comparisons of effects of recipient basal diet on mice receiving FMT from either an AIN-fed or a TWD-fed donor (green-to-yellow color bar, with yellow indicating greater abundance in the TWD-fed mice; top legend). **(b)** Comparisons for effects of FMT source on recipient mice fed either the AIN basal diet or the TWD (blue-to-red color bar, with red indicating greater abundance in FMT from the TWD-fed donors; bottom legend). **(c)** Phylogenetic structure of fecal microbiome bacterial community.

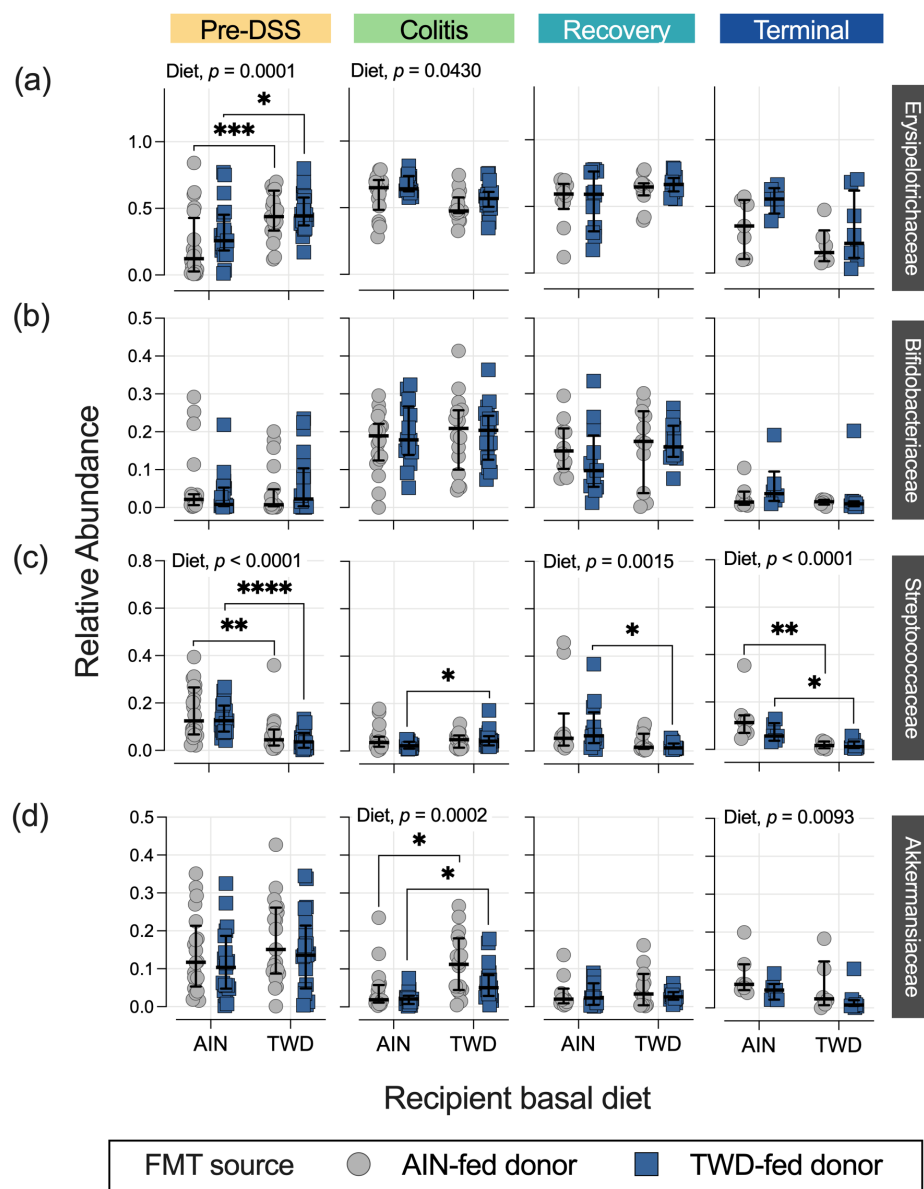


Figure 3.7. Relative abundance for selected bacterial families of interest at each experimental time point: **(a)** Erysipelotrichaceae, **(b)** Bifidobacteriaceae, **(c)** Streptococcaceae, and **(d)** Akkermansiaceae. The data are shown as individual values that represent each cage (as the biological unit) with median \pm interquartile range ($n = 19$ to 20 cages per group at the pre-DSS time point, $n = 17$ to 18 cages per group at the active colitis time point, $n = 12$ to 13 cages per group at the recovery time point, and $n = 7$ to 8 cages per group at the terminal time point). For simplified visualization, this plot shows only the statistical results as FDR-corrected p -values for significant main effects or the post hoc comparisons of FMT from the AIN-fed or TWD-fed donors: *, $p < 0.05$; **, $p < 0.01$; ***, $p < 0.001$; and ****, $p < 0.0001$, as outlined in the Materials and Methods section. The complete results of all metagenomeSeq statistical analyses, including pairwise comparisons by recipient basal diet and across time points, are provided in Supplementary File 3.S2.

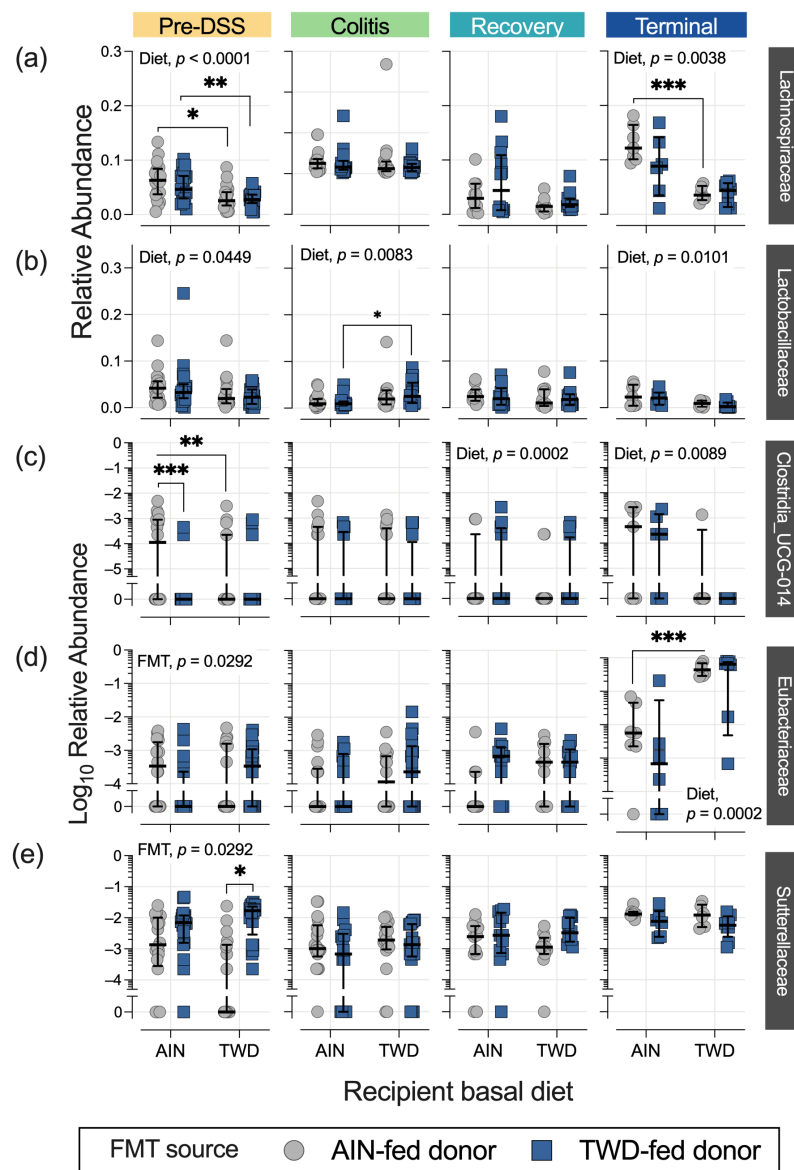


Figure 3.8. Relative abundance of additional bacterial families of interest at each experimental time point: **(a)** Lachnospiraceae, **(b)** Lactobacillaceae, **(c)** Clostridia_UCG_014, **(d)** Eubacteriaceae, and **(e)** Sutterellaceae. The data are shown as individual values that represent each cage (as the biological unit) with median \pm interquartile range ($n = 19$ to 20 cages per group at the pre-DSS time point, $n = 17$ to 18 cages per group at the active colitis time point, $n = 12$ to 13 cages per group at the recovery time point, and $n = 7$ to 8 cages per group at the terminal time point). For simplified visualization, this plot shows only the statistical results as FDR-corrected p -values for significant main effects or the post hoc comparisons of FMT from the AIN-fed or TWD-fed donors: *, $p < 0.05$; **, $p < 0.01$; and ***, $p < 0.001$, as outlined in the Materials and Methods section. The complete results of all metagenomeSeq statistical analyses, including pairwise comparisons by recipient basal diet and across time points, are provided in Supplementary File 3.S2.

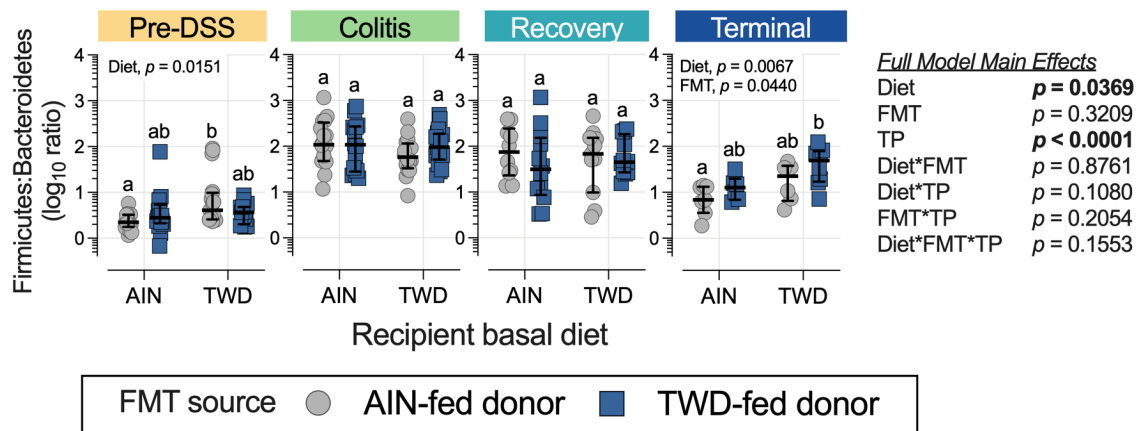


Figure 3.9. Ratio of Firmicutes to Bacteroidetes at each experimental time point. The ratios were determined using normalized count data for each phylum. The data are shown as individual values representing each cage (as the biological unit) with median \pm interquartile range. ($n = 19$ to 20 cages per group at the pre-DSS time point, $n = 17$ to 18 cages per group at the active colitis time point, $n = 12$ to 13 cages per group at the recovery time point, and $n = 7$ to 8 cages per group at the terminal time point). The table shows the statistical model's main effects, including all experimental factors, and different letters indicate that the experimental groups are significantly different ($p < 0.05$), as determined by the statistical methods outlined in the Materials and Methods section.

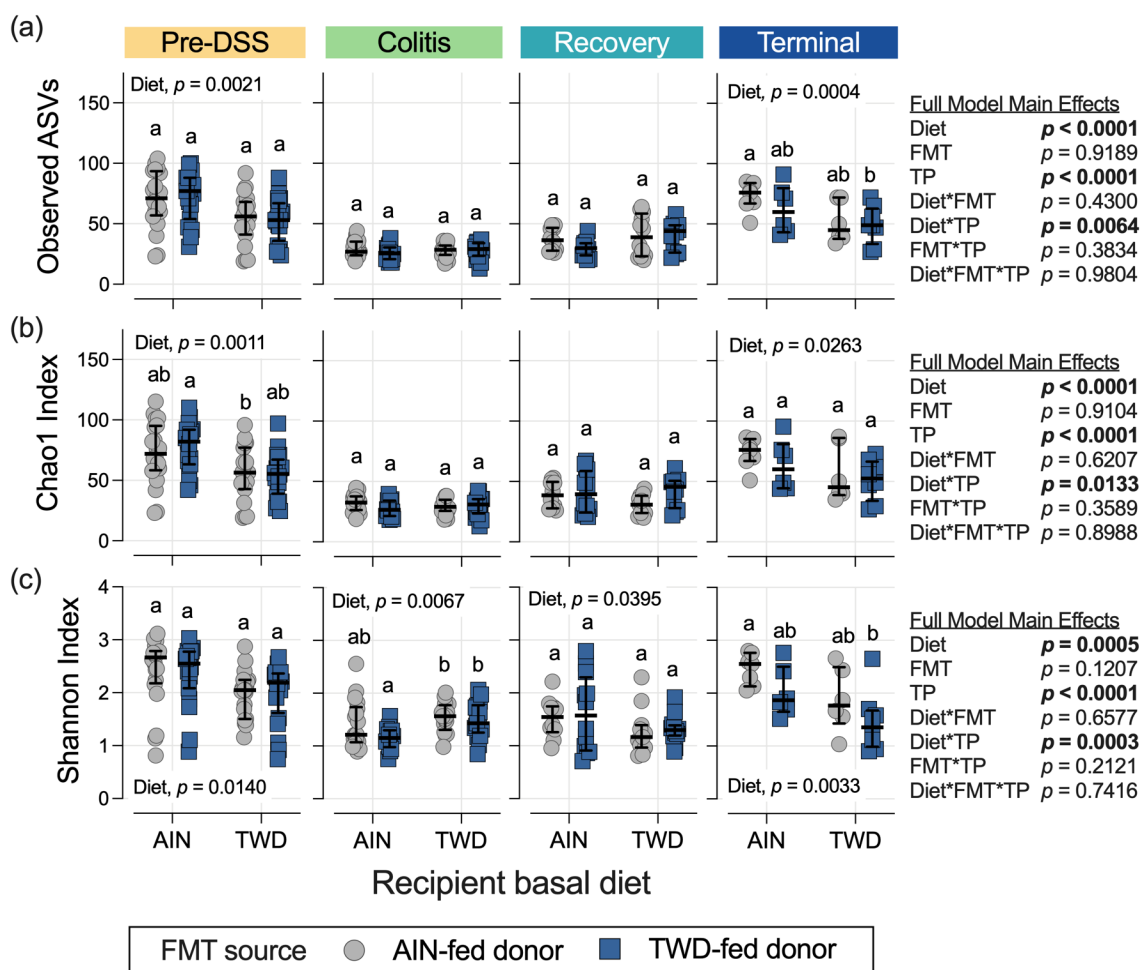


Figure 3.10. Alpha diversity of mouse fecal microbiomes at each experimental time point. Alpha diversity measures include (a) observed ASVs, (b) the Chao1 index, and (c) the Shannon index. The data are shown as individual values representing each cage (as the biological unit) with median \pm interquartile range ($n = 19$ to 20 cages per group at the pre-DSS time point, $n = 17$ to 18 cages per group at the active colitis time point, $n = 12$ to 13 cages per group at the recovery time point, and $n = 7$ to 8 cages per group at the terminal time point). The inserted tables show the statistical model's main effects, including all experimental factors, for each α -diversity measure. Different letters indicate that the experimental groups are significantly different ($p < 0.05$), as outlined in the Materials and Methods section. Significant main effects of either recipient basal diet or FMT source are also shown. The complete results of these statistical analyses, including all comparisons within and across time points, are found in Tables 3.S2–3.S4.

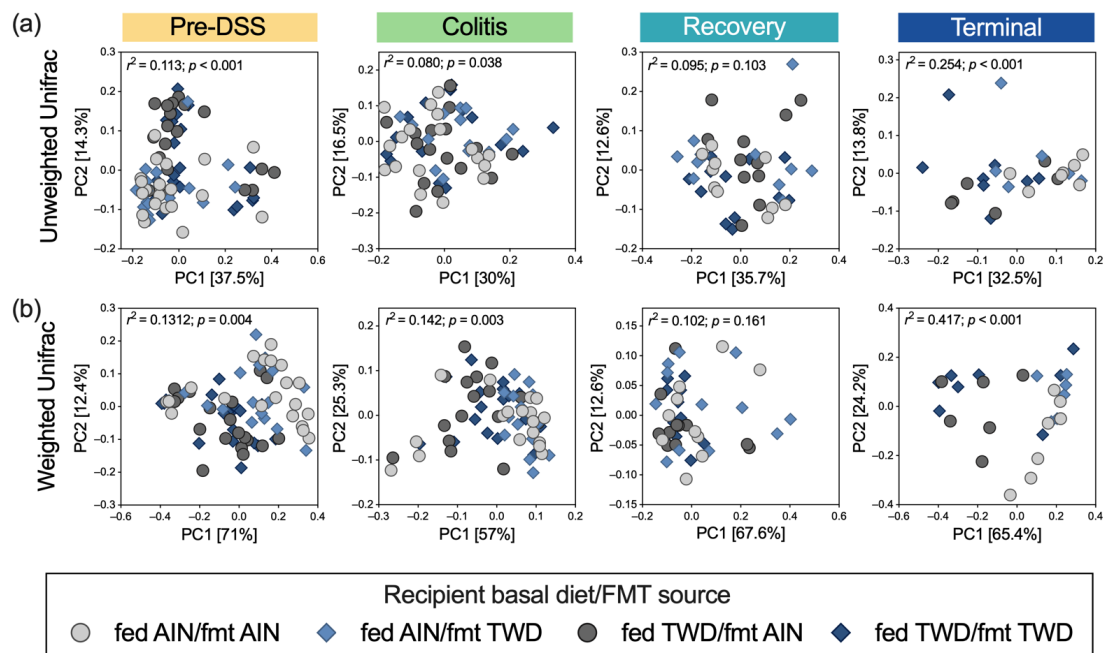


Figure 3.11. Beta diversity of mouse fecal microbiomes at each experimental time point. The principal coordinate plots depicting fecal microbiome beta diversity using (a) unweighted or (b) weighted unifrac distances are shown using the first two components ($n = 19$ to 20 cages per group at the pre-DSS time point, $n = 17$ to 18 cages per group at the active colitis time point, $n = 12$ to 13 cages per group at the recovery time point, and $n = 7$ to 8 cages per group at the terminal time point). The variations attributed to PC1 and PC2 are shown, along with the r^2 and permanova p -values for each plot.

CHAPTER 4

CONCLUSIONS

The overarching goal of the studies described in this dissertation was to better understand the contribution of the gut microbiome on the development of colon inflammation and subsequent colon tumorigenesis. Gut dysbiosis is a common feature of colitis and/or colon tumorigenesis in human and animal models. However, a specific cancer or disease-related gut microbiome has not been identified. To study this complex relationship, we designed two studies that approached the research question by either modulating the diet consumed or directly changing the microbiome composition in mice fed a healthy or Western-style basal diet on a colitis-associated colorectal cancer (CAC) model. Altogether, results of the pre-clinical mouse studies described in this dissertation suggest that the basal diet fed to mice appears to be the main factor impacting colitis symptoms, colon epithelial inflammation and mucosal injury, colon tumorigenesis and gut microbiome composition despite constant intervention by functional foods or fecal microbiome transfer.

Supplementation of anthocyanin-rich foods, such as black raspberries (BRB), was previously shown to exert a protective effect against colon inflammation and, in some cases, tumor development. In Chapter 2, we hypothesized that the BRB supplement would improve gut inflammation, and tumorigenesis and promote homeostasis in the gut microbiome; moreover, these beneficial effects would be more pronounced in mice fed a Western-style basal diet. However, we determined that supplementation of BRB in mice fed a Western-style basal diet resulted in inconsistent effects with respect to gut inflammation, although consistent suppression of colon tumorigenesis for mice fed a

healthy or Western diet. Additionally, mice fed BRB-supplemented diets had a distinct, more diverse microbiome favoring glycan and secondary metabolite metabolism, notably prior to gut injury.

For Chapter 3, we hypothesized that the microbiome of donor mice previously fed a Western-style diet would have detrimental effects on gut inflammation and tumorigenesis while promoting gut dysbiosis. However, the effect of the microbiome on disease development remains elusive as mice exposed to fecal microbiota transfer (FMT) from donor mice previously fed a Western-style diet and characterized by high inflammation and tumor burden resulted in delayed recovery from gut inflammation, improved colon lengths and tumor volumes compared to counterparts. Furthermore, the FMT source had minimal effect on the microbiome as basal diet seemed to be the driving factor of gut inflammation and tumorigenesis.

A Western-style diet is composed of high quantities of simple carbohydrates, processed foods, red meat and suboptimal levels of essential micronutrients and minerals. This dietary pattern is associated with colitis, colon tumorigenesis and gut microbial dysbiosis in multiple animal models [1,2], inflammatory bowel disease (IBD) patients [3-6] and colorectal cancer (CRC) patients [7-10]. Dietary patterns that consist of consuming whole fruits, vegetables, nuts and fish have been reported to be composed of compounds that contain anti-inflammatory, anti-cancer and antioxidant properties providing a potential preventative dietary strategy against IBD and CRC progression [11-14]. Moreover, diet composition influences the gut microenvironment by modulating microbes and microbial byproducts [15]. Diet-induced gut microbial dysbiosis is associated with gut inflammation and mucosal injury, potentially supporting abnormal

growth and further carcinogenesis. To understand the interaction between the host nutritional status and dietary or microbial interventions, we incorporated the total Western diet (TWD) for rodents in our study designs; the TWD has been shown to enhance colitis and colon tumorigenesis in models of colorectal cancer [2,16-19].

Consumption of BRB has been reported to have health benefits against colitis and colon tumorigenesis. However, BRB intake had not been studied in the context of supplementation to a Western diet. Based on previous reports stating the protective effects of BRB supplementation, the first study aimed to determine its effects on colitis symptoms, colon inflammation and mucosal injury, colon tumorigenesis and microbiome modulation of mice consuming a Western-style basal diet compared to a healthy mouse diet. Although we hypothesized that consumption of BRB would improve colitis symptoms, colon inflammation and consequent tumor development, our findings indicated a complicated effect when consuming a Western-style basal diet. Dietary supplementation of BRB had inconsistent effects on colitis and mucosal injury with reduced tumor multiplicity, regardless of the basal diet provided to mice. Furthermore, BRB-supplemented diets had extensive effects on the gut microbiome observed by increased alpha diversity, reduced Firmicute to Bacteroidetes ratio, and distinct microbiome compared to control diets. Further metagenome analysis revealed that before gut injury, mice fed a diet supplemented with BRB, harbored microbial species that prioritized glycan and secondary metabolite biosynthesis, and glycan, carbohydrate and amino acid absorption. Mice fed a Western-style diet supplemented with BRB had elevated fecal concentrations of short-chain fatty acids (SCFAs) such as acetic acid, propionic and butyric acid, although higher concentrations of fecal SCFAs may be

explained by increased food intake for those mice provided the BRB-supplemented Western-style diet. Finally, the interaction of basal diet and BRB supplement was significant in various metabolic and microbial factors, indicating a complex relationship between functional foods, basal diet and the gut microbiome. Interestingly, basal diet had the strongest impact on colitis and colon tumorigenesis, reaffirming not only the importance of incorporating animal diets representing target populations when exploring gut health, disease and therapeutics, but also the detrimental effects of a Western-style dietary pattern. Black raspberries contain many health benefits however, the basal diet has an extensive impact on gut health indicating that basal diet should be taken into high consideration when deliberating therapeutics for individuals to restore or maintain gut health.

For the second study described in Chapter 3, we reviewed multiple studies that pointed to gut dysbiosis as a common feature of colitis and/or colon tumorigenesis in humans and animal models, although it is not clear whether changes in the gut microbiome population associated with different nutritional patterns are drivers or a consequence of this disease process. Thus, to understand the potential effects of a diet-driven colitis-associated gut microbiome on colon tumor development, we designed a fecal microbiota transplant experiment using samples collected from mice in the first study (Chapter 2). We sought to understand whether diet-driven changes in the gut microbiome of donor mice influence the microbiome of recipient mice following FMT, where recipient mice consumed a healthy or Western-style diet. Findings herein indicate the basal diet consumed by the recipient mice was the main driver of gut microbial composition, colon inflammation and consequent tumorigenesis. FMT source – whether

from a donor mouse that consumed a Western-style diet – had minimal, although significant effects on colon inflammation during gut recovery, average tumor volume and relative abundance of taxa belonging to the Firmicute phylum, which resulted in a high Firmicute to Bacteroidetes ratio by study end. Unexpectedly, FMT from donors fed a Western-style diet improved colon length, average tumor volume in recipient mice and delayed recovery from gut injury. These findings are contradictory as greater colon length is generally associated with reduced inflammation and a lower Firmicutes to Bacteroidetes ratio [2,20,21]. Meanwhile, higher inflammation scores normally correlate with lower multiplicity, tumor volume and tumor burden [2], unlike the findings reported here. Although the current studies aimed to determine how dietary supplementation or microbial modulation affected colon inflammation in associated colorectal murine cancer models, findings suggest the basal diet is the main driver of gut health.

Naturally, this work had limitations that need to be taken into consideration. As the bioinformatics field expands, methods and techniques improve, and higher reliability of the identification of bacterial sequences and rare taxa is observed. In addition, microbiome samples were stored frozen for months and thawed prior to the administration of FMT, resulting in the possible loss of important anaerobic microorganisms. Although freezing fecal samples is the most commonly used method for bacteria cryoprotection, a recent review described the best way of freezing fecal samples for FMT is to aliquot samples into saline before freezing [22]. We looked at the functionality of the bacterial microbiome but did not consider other microorganisms that are present in the gut microbiome and their biological functions. Additionally, we observed relative abundance of the fecal microbiome, not absolute abundance, meaning

significant differences between populations can be due to changes or the absence of associated taxa. A consensus cancer-related gut microbiome is yet to be determined leaving the question of whether the microbiome shift is the cause or effect of disease progression or other external factors. While the mouse model of CAC employed in this work is useful for providing insight into the longitudinal progression of colon tumorigenesis, the strong tumor response to the TWD (i.e., development of very large adenomas and adenocarcinoma) required relatively early study termination at about 6 months of age due to morbidity. Thus, the model does not allow for examination of advanced disease or metastasis or exploration of the gut microbiome associated with late progression of the disease. Moreover, using animal models provides insight into changes in their microbiome but might not translate when considering the human microbiome as the human intestinal environment may harbor different gut microbes. Finally, the variation of dietary patterns among individuals, or even the variation of an individual's day-to-day eating pattern, creates a strong limitation in identifying a universal microbiome representing CRC.

Studies herein determined that the basal diet fed to recipient mice had an extensive effect on colitis, colon tumorigenesis and the fecal microbiome profile. While FMT is a very useful tool when trying to repopulate the gut microbiome after gut injury, dietary interventions such as anthocyanin-rich foods demonstrated a stronger effect on the gut microbiome and tumor multiplicity. A more robust assessment of the recipient mice microbiome needs to be researched observing changes before, during and following antibiotic treatment prior to FMT administration. With the wide selection of functional foods, understanding the biological function of food bio-actives is essential to prevent

diet-driven disease. Investigating anthocyanin-rich and similar functional foods can provide insight into how a balanced diet is necessary for biological function.

Incorporating the dynamic pattern of normal human consumption, for example, various foods and intake times, can provide real-world dietary intervention tools to promote gut homeostasis, and reduce inflammation and subsequent CAC risk. In addition, adding whole-food products that contain essential micronutrients regularly depleted in a Western-style diet, can be an opportunity to improve personalized nutrition plans.

An important aspect to consider is the reproducibility of the data, as seen in Chapter 2; despite using similar animal models, BRB and diet sources, the findings were not in complete agreement. These observations point to the need for robust approaches in similar pre-clinical studies, including replication of findings in repeated experiments. Furthermore, future work should consider alternate animal models of CAC and different genetic strains, which may respond differently to the total Western diet or dietary interventions with functional foods. This dissertation focused on an inflammation-associated model of CRC. Future studies should also consider the effect of a Western-style diet using a spontaneous model CRC, in the absence of chemically-induced inflammation; such studies would likely require an extended follow-up period of up to 12 months. Furthermore, given the apparent close relationship between the diet consumed and the composition of the fecal microbiome, future studies should focus on specific changes to the nutritional profile of the Western diet to improve disease outcomes, including specific micro- and micronutrients in addition to supplementation with functional foods. This work could lead to the identification of a nutritional profile that favors a health-promoting gut microbiome in healthy individuals and improve nutritional

strategies for patients suffering from dysbiosis-associated diseases, such as those with IBD or CRC.

In conclusion, the results of this dissertation point to the critical role of the basal diet in driving the composition of the microbiome and disease response in a mouse model of inflammation-associated colorectal cancer. Further, this work underscores the need to consider the Western nutritional pattern in pre-clinical animal models of human disease [23]. Consumption of a healthy or an unhealthy diet appears to be the main contributing factor influencing colon inflammation and tumorigenesis, pointing to the need for further research into how a basal diet influences the development of IBD, CRC and other metabolic diseases that are likely influenced by the gut microbiome. In closing, “Tell me what you eat, and I will tell you what you are”, as wisely noted in 1825 by the famous French gastronome Jean Anthelme Brillat-Savarin [24].

References

1. Ward, R.E.; Benninghoff, A.D.; Healy, B.J.; Li, M.; Vagu, B.; Hintze, K.J. Consumption of the total Western diet differentially affects the response to green tea in rodent models of chronic disease compared to the AIN93G diet. *Mol Nutr Food Res* **2017**, *61*, doi:10.1002/mnfr.201600720.
2. Benninghoff, A.D.; Hintze, K.J.; Monsanto, S.P.; Rodriguez, D.M.; Hunter, A.H.; Phatak, S.; Pestka, J.J.; Wettore, A.J.V.; Ward, R.E. Consumption of the total Western diet promotes colitis and inflammation-associated colorectal cancer in mice. *Nutrients* **2020**, *12*, doi:10.3390/nu12020544.
3. Narula, N.; Wong, E.C.L.; Dehghan, M.; Mente, A.; Rangarajan, S.; Lanas, F.; Lopez-Jaramillo, P.; Rohatgi, P.; Lakshmi, P.V.M.; Varma, R.P., et al. Association of ultra-processed food intake with risk of inflammatory bowel disease: prospective cohort study. *BMJ* **2021**, *374*, n1554, doi:10.1136/bmj.n1554.
4. Laudisi, F.; Stolfi, C.; Monteleone, G. Impact of food additives on gut homeostasis. *Nutrients* **2019**, *11*, doi:10.3390/nu11102334.
5. Li, T.; Qiu, Y.; Yang, H.S.; Li, M.Y.; Zhuang, X.J.; Zhang, S.H.; Feng, R.; Chen, B.L.; He, Y.; Zeng, Z.R., et al. Systematic review and meta-analysis: Association of a pre-

- illness Western dietary pattern with the risk of developing inflammatory bowel disease. *J Dig Dis* **2020**, *21*, 362-371, doi:10.1111/1751-2980.12910.
6. Khan, S.; Waliullah, S.; Godfrey, V.; Khan, M.A.W.; Ramachandran, R.A.; Cantarel, B.L.; Behrendt, C.; Peng, L.; Hooper, L.V.; Zaki, H. Dietary simple sugars alter microbial ecology in the gut and promote colitis in mice. *Sci Transl Med* **2020**, *12*, doi:10.1126/scitranslmed.aay6218.
 7. Tayyem, R.F.; Bawadi, H.A.; Shehadah, I.; Agraib, L.M.; AbuMweis, S.S.; Al-Jaberi, T.; Al-Nusairr, M.; Bani-Hani, K.E.; Heath, D.D. Dietary patterns and colorectal cancer. *Clin Nutr* **2017**, *36*, 848-852, doi:10.1016/j.clnu.2016.04.029.
 8. Barbirou, M.; Woldu, H.G.; Sghaier, I.; Bedoui, S.A.; Mokrani, A.; Aami, R.; Mezlini, A.; Yacoubi-Loueslati, B.; Tonellato, P.J.; Bouhaouala-Zahar, B. Western influenced lifestyle and Kv2.1 association as predicted biomarkers for Tunisian colorectal cancer. *BMC Cancer* **2020**, *20*, 1086, doi:10.1186/s12885-020-07605-7.
 9. Zheng, X.; Hur, J.; Nguyen, L.H.; Liu, J.; Song, M.; Wu, K.; Smith-Warner, S.A.; Ogino, S.; Willett, W.C.; Chan, A.T., et al. Comprehensive assessment of diet quality and risk of precursors of early-onset colorectal cancer. *J Natl Cancer Inst* **2021**, *113*, 543-552, doi:10.1093/jnci/djaa164.
 10. Mehta, R.S.; Song, M.; Nishihara, R.; Drew, D.A.; Wu, K.; Qian, Z.R.; Fung, T.T.; Hamada, T.; Masugi, Y.; da Silva, A., et al. Dietary patterns and risk of colorectal cancer: analysis by tumor location and molecular subtypes. *Gastroenterology* **2017**, *152*, 1944-1953 e1941, doi:10.1053/j.gastro.2017.02.015.
 11. Castello, A.; Amiano, P.; Fernandez de Larrea, N.; Martin, V.; Alonso, M.H.; Castano-Vinyals, G.; Perez-Gomez, B.; Olmedo-Requena, R.; Guevara, M.; Fernandez-Tardon, G., et al. Low adherence to the western and high adherence to the mediterranean dietary patterns could prevent colorectal cancer. *Eur J Nutr* **2019**, *58*, 1495-1505, doi:10.1007/s00394-018-1674-5.
 12. Fritsch, J.; Garces, L.; Quintero, M.A.; Pignac-Kobinger, J.; Santander, A.M.; Fernandez, I.; Ban, Y.J.; Kwon, D.; Phillips, M.C.; Knight, K., et al. Low-fat, high-fiber diet reduces markers of inflammation and dysbiosis and improves quality of life in patients with ulcerative colitis. *Clin Gastroenterol Hepatol* **2021**, *19*, 1189-1199 e1130, doi:10.1016/j.cgh.2020.05.026.
 13. Groschel, C.; Prinz-Wohlgenannt, M.; Mesteri, I.; Karuthedom George, S.; Trawnicek, L.; Heiden, D.; Aggarwal, A.; Tennakoon, S.; Baumgartner, M.; Gasche, C., et al. Switching to a healthy diet prevents the detrimental effects of Western diet in a colitis-associated colorectal cancer model. *Nutrients* **2019**, *12*, doi:10.3390/nu12010045.
 14. Whalen, K.A.; McCullough, M.; Flanders, W.D.; Hartman, T.J.; Judd, S.; Bostick, R.M. Paleolithic and Mediterranean diet pattern scores and risk of incident, sporadic colorectal adenomas. *Am J Epidemiol* **2014**, *180*, 1088-1097, doi:10.1093/aje/kwu235.
 15. Yang, J.; Wei, H.; Zhou, Y.; Szeto, C.H.; Li, C.; Lin, Y.; Coker, O.O.; Lau, H.C.H.; Chan, A.W.H.; Sung, J.J.Y., et al. High-fat diet promotes colorectal tumorigenesis

- through modulating gut microbiota and metabolites. *Gastroenterology* **2022**, *162*, 135-149 e132, doi:10.1053/j.gastro.2021.08.041.
16. Aardema, N.D.; Rodriguez, D.M.; Van Wettere, A.J.; Benninghoff, A.D.; Hintze, K.J. The Western dietary pattern combined with vancomycin-mediated changes to the gut microbiome exacerbates colitis severity and colon tumorigenesis. *Nutrients* **2021**, *13*, doi:10.3390/nu13030881.
 17. Rodriguez, D.M.; Hintze, K.J.; Rompato, G.; Wettere, A.J.V.; Ward, R.E.; Phatak, S.; Neal, C.; Armbrust, T.; Stewart, E.C.; Thomas, A.J., et al. Dietary supplementation with black raspberries altered the gut microbiome composition in a mouse model of colitis-associated colorectal cancer, although with differing effects for a healthy versus a Western basal diet. *Nutrients* **2022**, *14*, doi:10.3390/nu14245270.
 18. Hintze, K.J.; Benninghoff, A.D.; Ward, R.E. Formulation of the total Western diet (TWD) as a basal diet for rodent cancer studies. *J Agric Food Chem* **2012**, *60*, 6736-6742, doi:10.1021/jf204509a.
 19. Kim, S.; Abernathy, B.E.; Trudo, S.P.; Gallaher, D.D. Colon cancer risk of a Westernized diet Is reduced in mice by reeding cruciferous or apiaceous vegetables at a lower dose of carcinogen but not a higher dose. *J Cancer Prev* **2020**, *25*, 223-233, doi:10.15430/JCP.2020.25.4.223.
 20. Lippert, E.; Ruellemele, P.; Obermeier, F.; Goelder, S.; Kunst, C.; Rogler, G.; Dunger, N.; Messmann, H.; Hartmann, A.; Endlicher, E. Anthocyanins prevent colorectal cancer development in a mouse model. *Digestion* **2017**, *95*, 275-280, doi:10.1159/000475524.
 21. Wang, F.; Cai, K.; Xiao, Q.; He, L.; Xie, L.; Liu, Z. *Akkermansia muciniphila* administration exacerbated the development of colitis-associated colorectal cancer in mice. *J Cancer* **2022**, *13*, 124-133, doi:10.7150/jca.63578.
 22. Nicco, C.; Paule, A.; Konturek, P.; Edeas, M. From donor to patient: collection, preparation and cryopreservation of fecal samples for fecal microbiota transplantation. *Diseases* **2020**, *8*, doi:10.3390/diseases8020009.
 23. Hintze, K.J.; Benninghoff, A.D.; Ward, R.E. Improving Laboratory Mice Diets to Increase Relevance to Human Populations. *Functional Foods in Health and Disease* **2017**, *7*, 329-337.
 24. Brillat-Savarin, J.A. *The Physiology of Taste*; Lindsay & Blakiston: Philadelphia, 1854.

APPENDICES

Appendix A. Publication Licensing Information

MDPI Open Access Information and Policy

All articles published by MDPI are made immediately available worldwide under an open access license. This means:

- everyone has free and unlimited access to the full-text of *all* articles published in MDPI journals;
- everyone is free to re-use the published material if proper accreditation/citation of the original publication is given;
- open access publication is supported by the authors' institutes or research funding agencies by payment of a comparatively low **Article Processing Charge (APC)** for accepted articles.

Permissions

No special permission is required to reuse all or part of article published by MDPI, including figures and tables. For articles published under an open access Creative Common CC BY license, any part of the article may be reused without permission provided that the original article is clearly cited. Reuse of an article does not imply endorsement by the authors or MDPI.

Figure A.1. Screen capture from *Nutrients* journal website outlining the publisher's licensing policy. <https://www.mdpi.com/openaccess> (Accessed 24 January 2023).

Creative Commons Legal Code

Attribution 4.0 International

Official translations of this license are available [in other languages](#).

Creative Commons Corporation (“Creative Commons”) is not a law firm and does not provide legal services or legal advice. Distribution of Creative Commons public licenses does not create a lawyer-client or other relationship. Creative Commons makes its licenses and related information available on an “as-is” basis. Creative Commons gives no warranties regarding its licenses, any material licensed under their terms and conditions, or any related information. Creative Commons disclaims all liability for damages resulting from their use to the fullest extent possible.

Using Creative Commons Public Licenses

Creative Commons public licenses provide a standard set of terms and conditions that creators and other rights holders may use to share original works of authorship and other material subject to copyright and certain other rights specified in the public license below. The following considerations are for informational purposes only, are not exhaustive, and do not form part of our licenses.

Considerations for licensors: Our public licenses are intended for use by those authorized to give the public permission to use material in ways otherwise restricted by copyright and certain other rights. Our licenses are irrevocable. Licensors should read and understand the terms and conditions of the license they choose before applying it. Licensors should also secure all rights necessary before applying our licenses so that the public can reuse the material as expected. Licensors should clearly mark any material not subject to the license. This includes other CC-licensed material, or material used under an exception or limitation to copyright.

Considerations for the public: By using one of our public licenses, a licensor grants the public permission to use the licensed material under specified terms and conditions. If the licensor’s permission is not necessary for any reason—for example, because of any applicable exception or limitation to copyright—then that use is not regulated by the license. Our licenses grant only permissions under copyright and certain other rights that a licensor has authority to grant. Use of the licensed material may still be restricted for other reasons, including because others have copyright or

other rights in the material. A licensor may make special requests, such as asking that all changes be marked or described. Although not required by our licenses, you are encouraged to respect those requests where reasonable.

Creative Commons Attribution 4.0 International Public License

By exercising the Licensed Rights (defined below), You accept and agree to be bound by the terms and conditions of this Creative Commons Attribution 4.0 International Public License ("Public License"). To the extent this Public License may be interpreted as a contract, You are granted the Licensed Rights in consideration of Your acceptance of these terms and conditions, and the Licensor grants You such rights in consideration of benefits the Licensor receives from making the Licensed Material available under these terms and conditions.

Section 1 – Definitions.

- a. **Adapted Material** means material subject to Copyright and Similar Rights that is derived from or based upon the Licensed Material and in which the Licensed Material is translated, altered, arranged, transformed, or otherwise modified in a manner requiring permission under the Copyright and Similar Rights held by the Licensor. For purposes of this Public License, where the Licensed Material is a musical work, performance, or sound recording, Adapted Material is always produced where the Licensed Material is synched in timed relation with a moving image.
- b. **Adapter's License** means the license You apply to Your Copyright and Similar Rights in Your contributions to Adapted Material in accordance with the terms and conditions of this Public License.
- c. **Copyright and Similar Rights** means copyright and/or similar rights closely related to copyright including, without limitation, performance, broadcast, sound recording, and Sui Generis Database Rights, without regard to how the rights are labeled or categorized. For purposes of this Public License, the rights specified in Section 2(b)(1)-(2) are not Copyright and Similar Rights.
- d. **Effective Technological Measures** means those measures that, in the absence of proper authority, may not be circumvented under laws fulfilling obligations under Article 11 of the WIPO Copyright Treaty adopted on December 20, 1996, and/or similar international agreements.
- e. **Exceptions and Limitations** means fair use, fair dealing, and/or any other exception or limitation to Copyright and Similar Rights that applies to Your use of the Licensed Material.
- f. **Licensed Material** means the artistic or literary work, database, or other material to which the Licensor applied this Public License.
- g. **Licensed Rights** means the rights granted to You subject to the terms and conditions of this Public License, which are limited to all Copyright and Similar Rights that apply to Your use of the Licensed Material and that the Licensor has authority to license.

- h. **Licensor** means the individual(s) or entity(ies) granting rights under this Public License.
- i. **Share** means to provide material to the public by any means or process that requires permission under the Licensed Rights, such as reproduction, public display, public performance, distribution, dissemination, communication, or importation, and to make material available to the public including in ways that members of the public may access the material from a place and at a time individually chosen by them.
- j. **Sui Generis Database Rights** means rights other than copyright resulting from Directive 96/9/EC of the European Parliament and of the Council of 11 March 1996 on the legal protection of databases, as amended and/or succeeded, as well as other essentially equivalent rights anywhere in the world.
- k. **You** means the individual or entity exercising the Licensed Rights under this Public License. **Your** has a corresponding meaning.

Section 2 – Scope.

a. License grant.

1. Subject to the terms and conditions of this Public License, the Licensor hereby grants You a worldwide, royalty-free, non-sublicensable, non-exclusive, irrevocable license to exercise the Licensed Rights in the Licensed Material to:
 - A. reproduce and Share the Licensed Material, in whole or in part; and
 - B. produce, reproduce, and Share Adapted Material.
2. Exceptions and Limitations. For the avoidance of doubt, where Exceptions and Limitations apply to Your use, this Public License does not apply, and You do not need to comply with its terms and conditions.
3. Term. The term of this Public License is specified in Section 6(a).
4. Media and formats; technical modifications allowed. The Licensor authorizes You to exercise the Licensed Rights in all media and formats whether now known or hereafter created, and to make technical modifications necessary to do so. The Licensor waives and/or agrees not to assert any right or authority to forbid You from making technical modifications necessary to exercise the Licensed Rights, including technical modifications necessary to circumvent Effective Technological Measures. For purposes of this Public License, simply making modifications authorized by this Section 2(a)(4) never produces Adapted Material.
5. Downstream recipients.
 - A. Offer from the Licensor – Licensed Material. Every recipient of the Licensed Material automatically receives an offer from the Licensor to exercise the Licensed Rights under the terms and conditions of this Public License.
 - B. No downstream restrictions. You may not offer or impose any additional or different terms or conditions on, or apply any Effective Technological Measures to, the Licensed Material if

doing so restricts exercise of the Licensed Rights by any recipient of the Licensed Material.

6. No endorsement. Nothing in this Public License constitutes or may be construed as permission to assert or imply that You are, or that Your use of the Licensed Material is, connected with, or sponsored, endorsed, or granted official status by, the Licensor or others designated to receive attribution as provided in Section 3(a)(1)(A)(i).

b. Other rights.

1. Moral rights, such as the right of integrity, are not licensed under this Public License, nor are publicity, privacy, and/or other similar personality rights; however, to the extent possible, the Licensor waives and/or agrees not to assert any such rights held by the Licensor to the limited extent necessary to allow You to exercise the Licensed Rights, but not otherwise.
2. Patent and trademark rights are not licensed under this Public License.
3. To the extent possible, the Licensor waives any right to collect royalties from You for the exercise of the Licensed Rights, whether directly or through a collecting society under any voluntary or waivable statutory or compulsory licensing scheme. In all other cases the Licensor expressly reserves any right to collect such royalties.

Section 3 – License Conditions.

Your exercise of the Licensed Rights is expressly made subject to the following conditions.

a. Attribution.

1. If You Share the Licensed Material (including in modified form), You must:
 - A. retain the following if it is supplied by the Licensor with the Licensed Material:
 - i. identification of the creator(s) of the Licensed Material and any others designated to receive attribution, in any reasonable manner requested by the Licensor (including by pseudonym if designated);
 - ii. a copyright notice;
 - iii. a notice that refers to this Public License;
 - iv. a notice that refers to the disclaimer of warranties;
 - v. a URI or hyperlink to the Licensed Material to the extent reasonably practicable;
 - B. indicate if You modified the Licensed Material and retain an indication of any previous modifications; and
 - C. indicate the Licensed Material is licensed under this Public License, and include the text of,

- or the URI or hyperlink to, this Public License.
2. You may satisfy the conditions in Section 3(a)(1) in any reasonable manner based on the medium, means, and context in which You Share the Licensed Material. For example, it may be reasonable to satisfy the conditions by providing a URI or hyperlink to a resource that includes the required information.
 3. If requested by the Licensor, You must remove any of the information required by Section 3(a)(1)(A) to the extent reasonably practicable.
 4. If You Share Adapted Material You produce, the Adapter's License You apply must not prevent recipients of the Adapted Material from complying with this Public License.

Section 4 – Sui Generis Database Rights.

Where the Licensed Rights include Sui Generis Database Rights that apply to Your use of the Licensed Material:

- a. for the avoidance of doubt, Section 2(a)(1) grants You the right to extract, reuse, reproduce, and Share all or a substantial portion of the contents of the database;
- b. if You include all or a substantial portion of the database contents in a database in which You have Sui Generis Database Rights, then the database in which You have Sui Generis Database Rights (but not its individual contents) is Adapted Material; and
- c. You must comply with the conditions in Section 3(a) if You Share all or a substantial portion of the contents of the database.

For the avoidance of doubt, this Section 4 supplements and does not replace Your obligations under this Public License where the Licensed Rights include other Copyright and Similar Rights.

Section 5 – Disclaimer of Warranties and Limitation of Liability.

- a. **Unless otherwise separately undertaken by the Licensor, to the extent possible, the Licensor offers the Licensed Material as-is and as-available, and makes no representations or warranties of any kind concerning the Licensed Material, whether express, implied, statutory, or other. This includes, without limitation, warranties of title, merchantability, fitness for a particular purpose, non-infringement, absence of latent or other defects, accuracy, or the presence or absence of errors, whether or not known or discoverable. Where disclaimers of warranties are not allowed in full or in part, this disclaimer may not apply to You.**
- b. **To the extent possible, in no event will the Licensor be liable to You on any legal theory (including, without limitation, negligence) or otherwise for any direct, special, indirect,**

incidental, consequential, punitive, exemplary, or other losses, costs, expenses, or damages arising out of this Public License or use of the Licensed Material, even if the Licensor has been advised of the possibility of such losses, costs, expenses, or damages. Where a limitation of liability is not allowed in full or in part, this limitation may not apply to You.

- c. The disclaimer of warranties and limitation of liability provided above shall be interpreted in a manner that, to the extent possible, most closely approximates an absolute disclaimer and waiver of all liability.

Section 6 – Term and Termination.

- a. This Public License applies for the term of the Copyright and Similar Rights licensed here. However, if You fail to comply with this Public License, then Your rights under this Public License terminate automatically.
- b. Where Your right to use the Licensed Material has terminated under Section 6(a), it reinstates:
 - 1. automatically as of the date the violation is cured, provided it is cured within 30 days of Your discovery of the violation; or
 - 2. upon express reinstatement by the Licensor.For the avoidance of doubt, this Section 6(b) does not affect any right the Licensor may have to seek remedies for Your violations of this Public License.
- c. For the avoidance of doubt, the Licensor may also offer the Licensed Material under separate terms or conditions or stop distributing the Licensed Material at any time; however, doing so will not terminate this Public License.
- d. Sections 1, 5, 6, 7, and 8 survive termination of this Public License.

Section 7 – Other Terms and Conditions.

- a. The Licensor shall not be bound by any additional or different terms or conditions communicated by You unless expressly agreed.
- b. Any arrangements, understandings, or agreements regarding the Licensed Material not stated herein are separate from and independent of the terms and conditions of this Public License.

Section 8 – Interpretation.

- a. For the avoidance of doubt, this Public License does not, and shall not be interpreted to, reduce,

limit, restrict, or impose conditions on any use of the Licensed Material that could lawfully be made without permission under this Public License.

- b. To the extent possible, if any provision of this Public License is deemed unenforceable, it shall be automatically reformed to the minimum extent necessary to make it enforceable. If the provision cannot be reformed, it shall be severed from this Public License without affecting the enforceability of the remaining terms and conditions.
- c. No term or condition of this Public License will be waived and no failure to comply consented to unless expressly agreed to by the Licensor.
- d. Nothing in this Public License constitutes or may be interpreted as a limitation upon, or waiver of, any privileges and immunities that apply to the Licensor or You, including from the legal processes of any jurisdiction or authority.

Creative Commons is not a party to its public licenses. Notwithstanding, Creative Commons may elect to apply one of its public licenses to material it publishes and in those instances will be considered the “Licensor.” The text of the Creative Commons public licenses is dedicated to the public domain under the [CC0 Public Domain Dedication](#). Except for the limited purpose of indicating that material is shared under a Creative Commons public license or as otherwise permitted by the Creative Commons policies published at creativecommons.org/policies, Creative Commons does not authorize the use of the trademark “Creative Commons” or any other trademark or logo of Creative Commons without its prior written consent including, without limitation, in connection with any unauthorized modifications to any of its public licenses or any other arrangements, understandings, or agreements concerning use of licensed material. For the avoidance of doubt, this paragraph does not form part of the public licenses.

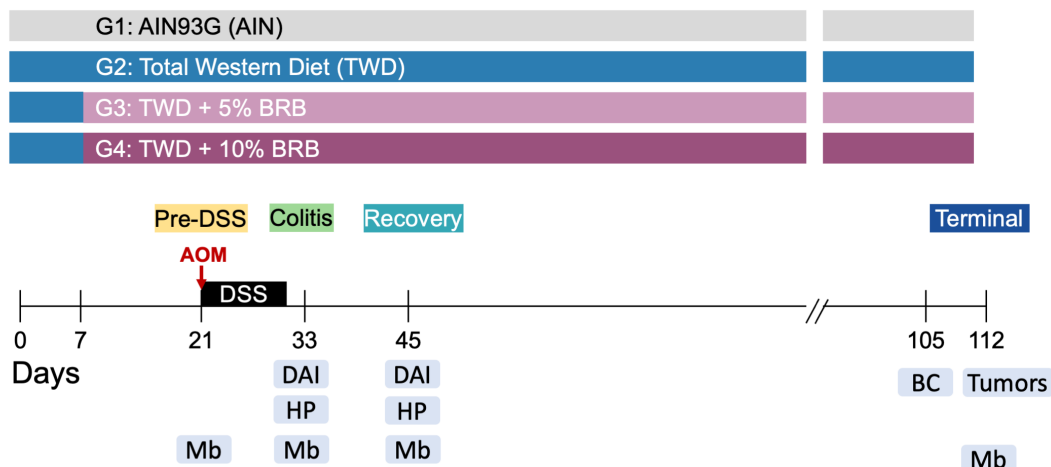
Creative Commons may be contacted at creativecommons.org.

Additional languages available: العربية, čeština, Deutsch, Ελληνικά, Español, euskara, suomeksi, français, hrvatski, Bahasa Indonesia, italiano, 日本語, 한국어, Lietuvių, latviski, te reo Māori, Nederlands, norsk, polski, português, română, русский, Slovenščina, svenska, Türkçe, українська, 中文, 華語. Please read the [FAQ](#) for more information about official translations.

Appendix B. Supplementary Material Associated with Chapter 2

Supplementary Figures

(a) Experiment A (pilot)



(b) Experiment B (basal diet comparison)

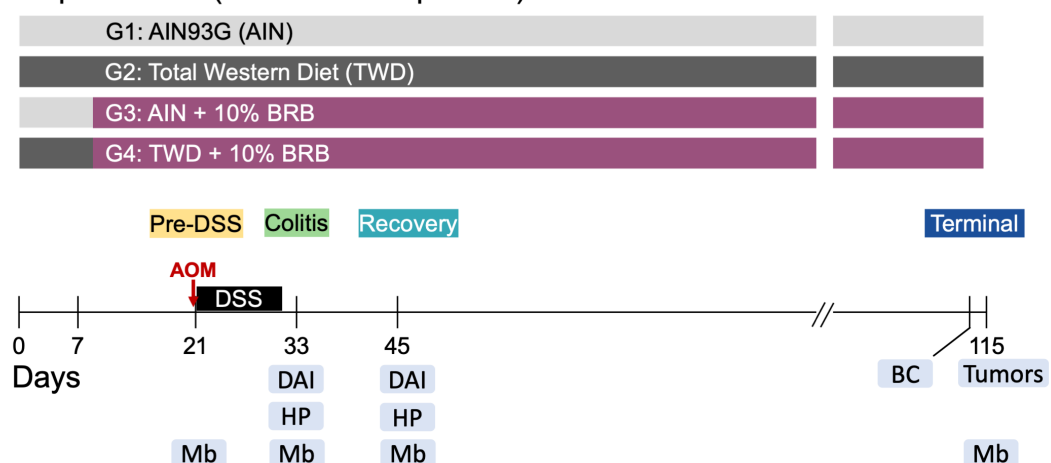


Figure 2.S1. Diagram depicting design of the pilot study (experiment A) and the black raspberry supplementation with standard and Western basal diets study (experiment B). **(a)** For experiment A, basal diets are represented as gray (AIN) or blue (TWD) bars with supplementation of low concentration black raspberry (5% BRB) and high concentration (10% BRB) depicted as light and dark pink, respectively. Experimental time points include pre-DSS (day 21), colitis (day 33), recovery (day 45) and terminal (day 112). Endpoints measured are indicated below the timeline, including the disease activity index (DAI), histopathology (HP), fecal microbiome profiling (Mb), body composition (BC) and colon tumors. **(b)** For experiment B, basal diets AIN and TWD are represented as light gray or dark gray bars, respectively, with 10% black raspberry supplementation shown as dark pink. Time points are as for experiment A, except for tumors assessed at day 115. Endpoints are indicated below the timeline. Other abbreviations are as follows: azoxymethane, AOM; dextran sodium sulfate, DSS.

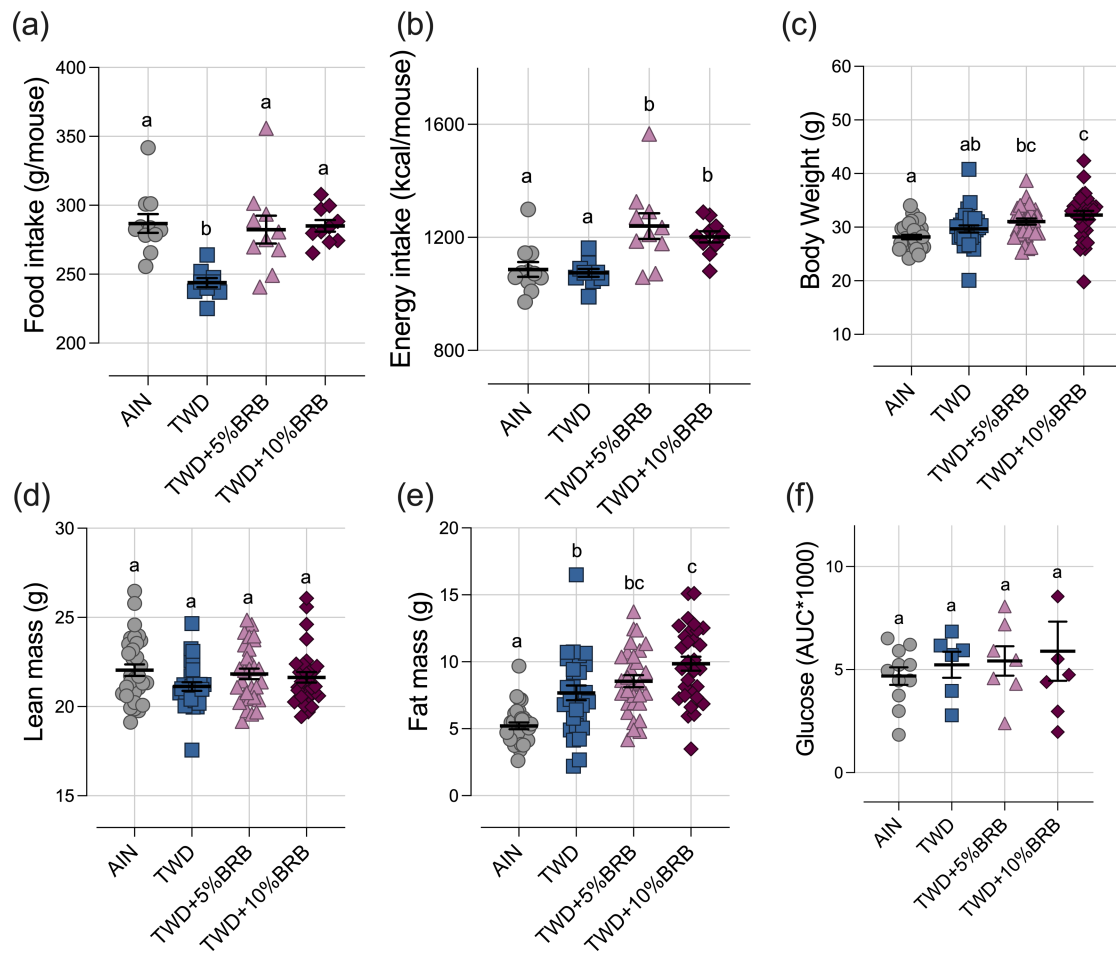


Figure 2.S2. Food and energy intake, final body weight, final lean and fat mass, and glucose tolerance (experiment A). Food (a) and energy (b) intakes per cage ($n=10-11$) for the study period are shown for each individual mouse with the mean \pm SD. Final body weight (c), lean mass (d), and fat mass (e) values are shown for each individual mouse ($n=29-32$) with the mean \pm SE. (f) Glucose tolerance expressed as the area under the curve (AUC) determined at the terminal time point shown for individual mice ($n=6$ to 11) with the mean \pm SE. Different letters indicate groups are significantly different ($p < 0.05$) as outlined in Materials and Methods.

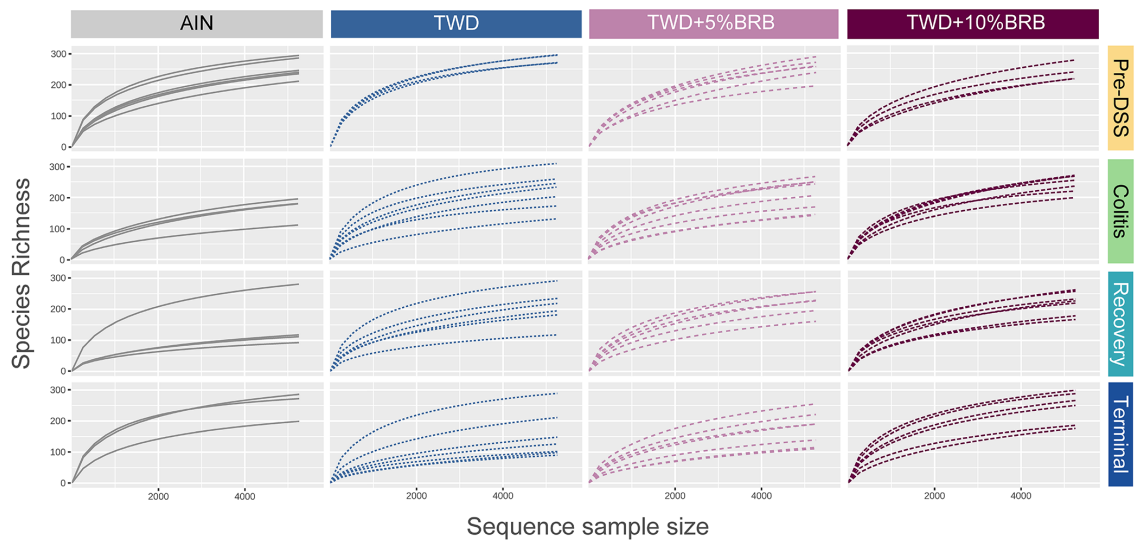


Figure 2.S3. Rarefaction curve analysis by experimental group and time point (experiment A). Curves plot species richness as a function of sequence sample size. For comparisons across experimental groups, data were rarefied to ~5,500 sequences, the lowest total among all the samples.

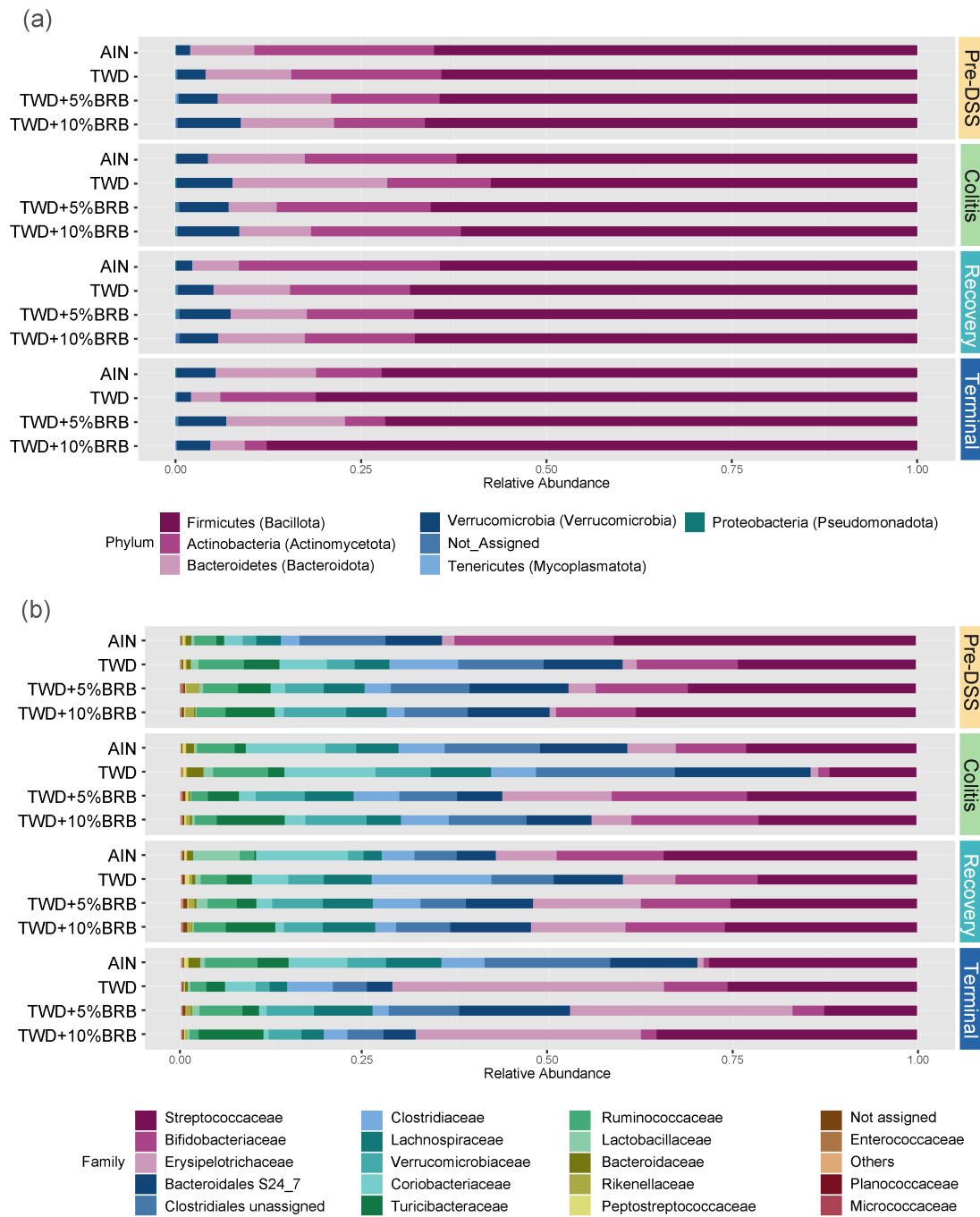


Figure 2.S4. Taxonomic classification of mouse fecal bacteria (experiment A). Data shown are the relative normalized abundance of bacteria annotated to phylum (a) or family (b) taxonomic levels for the most abundant taxa for each experimental group for each experimental time point. New phylum level taxonomic designations are indicated in parentheses (a).

Figure 2.S5. Relative abundance of fecal microbiome at the family taxonomic level (experiment A). **(a)** Unsupervised hierarchical cluster analysis of the bacteria families comprising a least 1% of fecal microbiome. The heatmap was constructed with clustering by taxa using the Euclidean distance with average clustering, and the color scale represents the \log_{10} relative abundance. **(b)** Relative abundance of select bacteria families of interest for each experimental time point, including Coriobacteriaceae, Bifidobacteriaceae, Bacteroidaceae, Ruminococcaceae, and Erysipelotrichaceae. **(c)** Ratio of Firmicutes:Bacteroidetes by experimental time point. Ratios were determined using normalized count data for each phylum. For (b) and (c), data are shown as individual values that represent each cage (as the biological unit) with mean \pm SE. *, $p < 0.05$; **, $p < 0.01$; and ****, $p < 0.0001$ as outlined in Materials and Methods. Complete results of all metagenomeSeq statistical analyses, including selected pairwise comparisons by experimental group, are provided in File 2.S3.

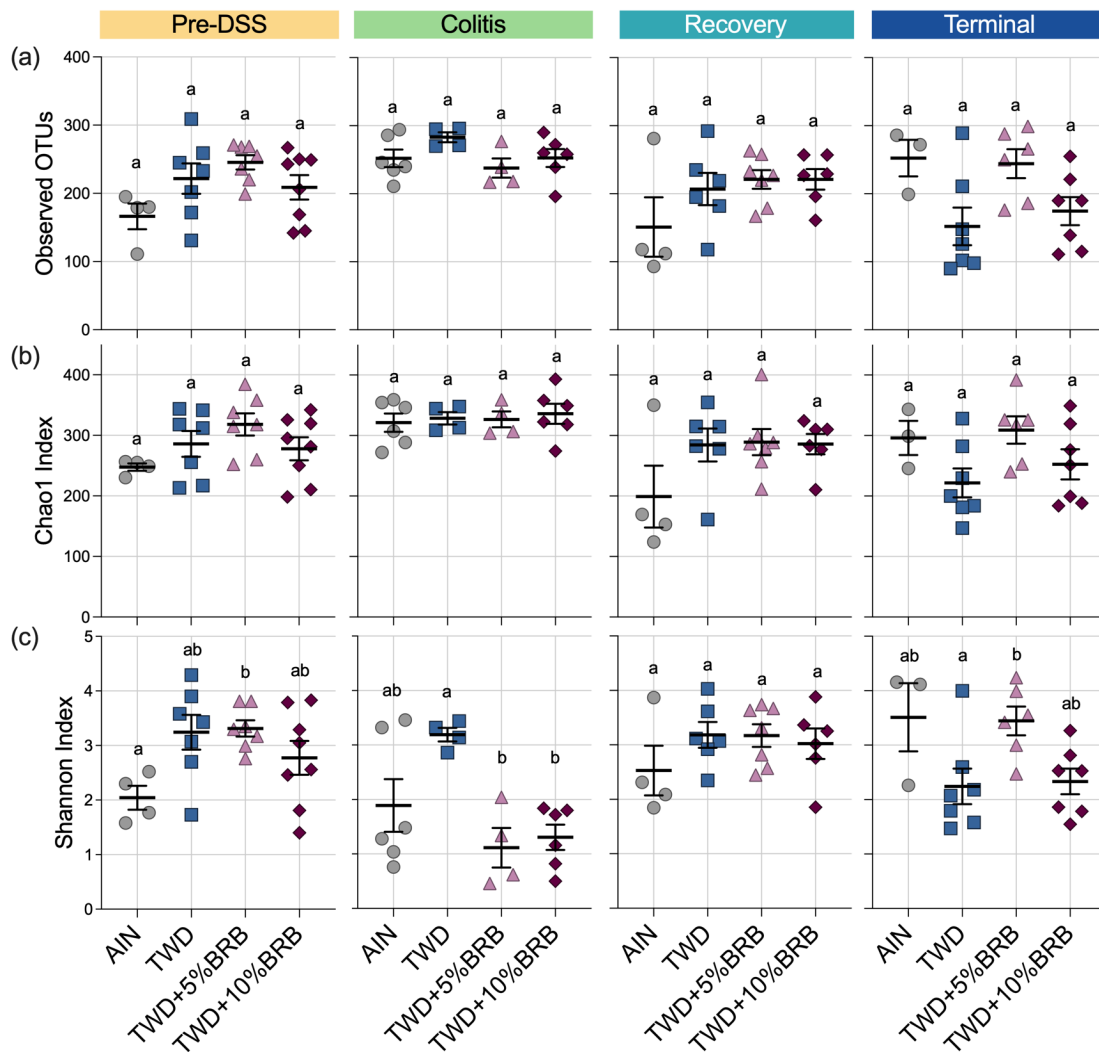


Figure 2.S6. Alpha diversity of mouse fecal microbiomes for each experimental time point (experiment A). Alpha diversity measures include (a) observed OTUs, (b) the Chao1 index, and (c) the Shannon index. Data are shown as individual values representing each cage (as the biological unit) with mean \pm SE. Inset tables show the statistical model main effects including all experimental factors for each α -diversity measure. Different letters indicate groups are significantly different ($p < 0.05$) as outlined in Materials and Methods.

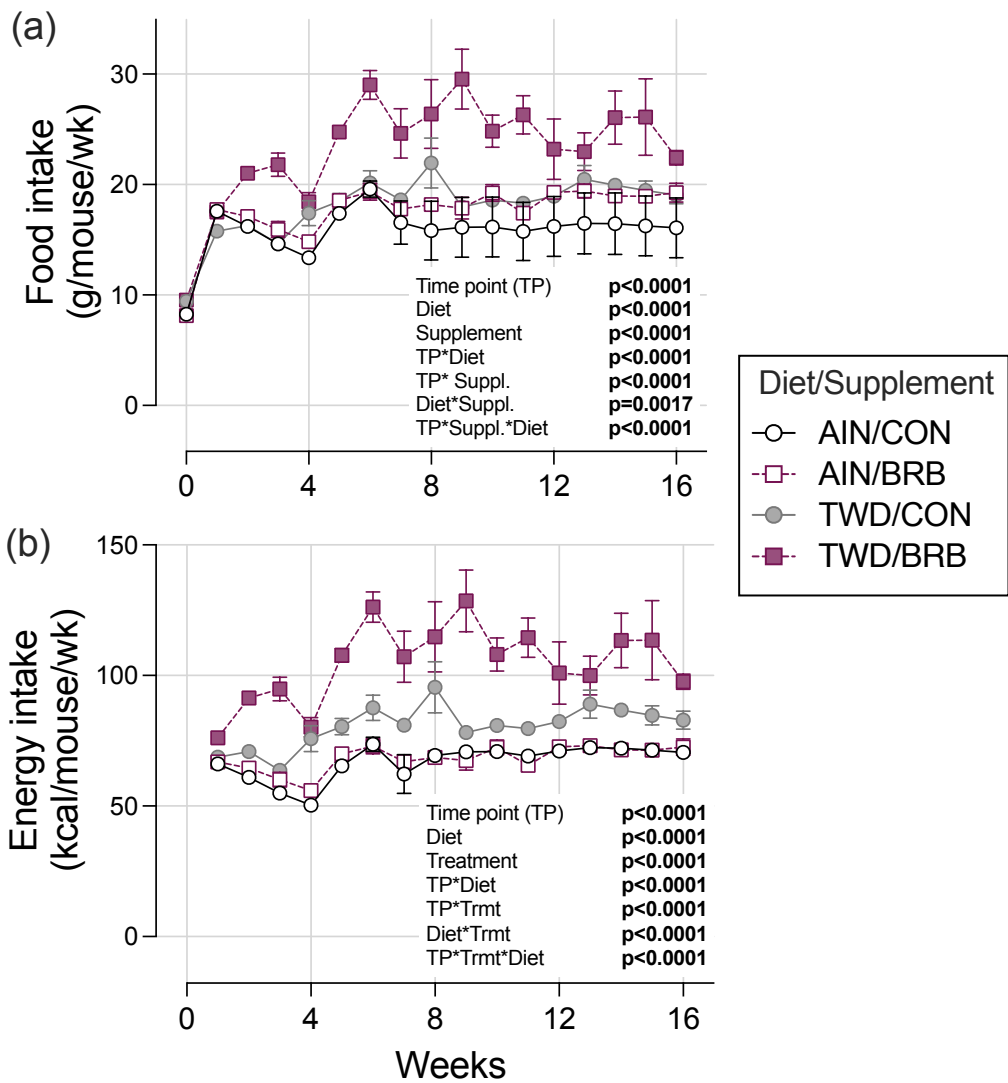


Figure 2.S7. Food and energy intake over the study period (experiment B). Values shown are the average estimated food intake **(a)** and energy intake **(b)** per mouse per week \pm SE. Inset tables show the statistical model main effects for time point (TP), basal diet (Diet), and BRB treatment (Trmt) and all possible interactions determined by statistical methods outlined in Materials and Methods.

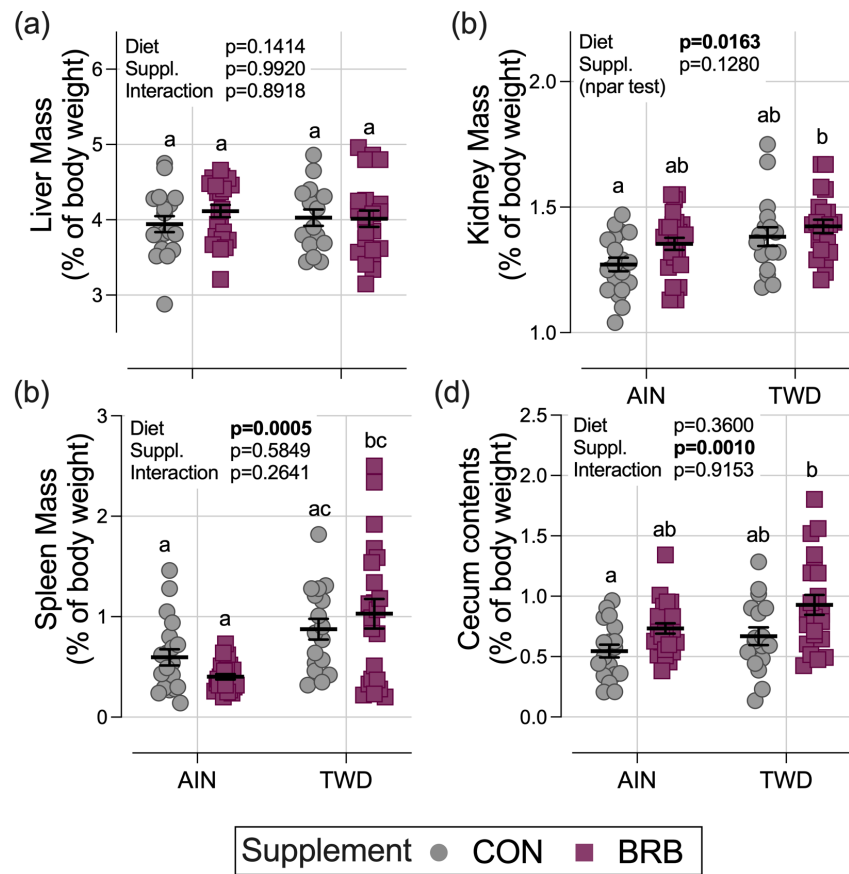


Figure 2.S8. Relative liver, kidney, spleen, and cecum content weights (experiment B). Data for liver (a), kidney (b), spleen (c), and cecum content (d) weights are shown as a proportion of the final body weight. Values for individual mice ($n=17-25$) are shown with mean \pm SE. Inset tables provide the model main effects for diet, treatment, and their interaction or “npar test” if a nonparametric test was required, and different letters indicate groups are significantly different ($p < 0.05$) as determined by statistical methods outlined in Materials and Methods.

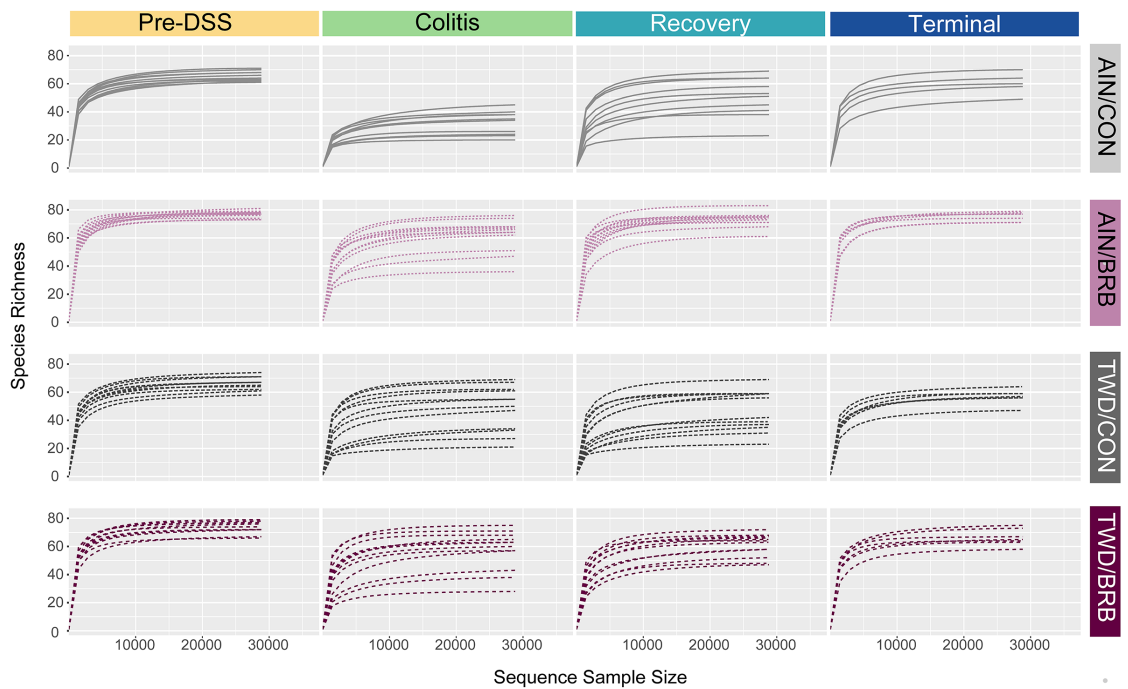


Figure 2.S9. Rarefaction curve analysis by experimental group and time point (experiment B). Curves plot species richness as a function of sequence sample size. For comparisons across experimental groups, data were rarefied to 28,909 sequences, the lowest total among all the samples. These curves indicate that saturation was reached satisfactorily for most samples and that additional sequence reads were unlikely to substantially increase the number of species detected.

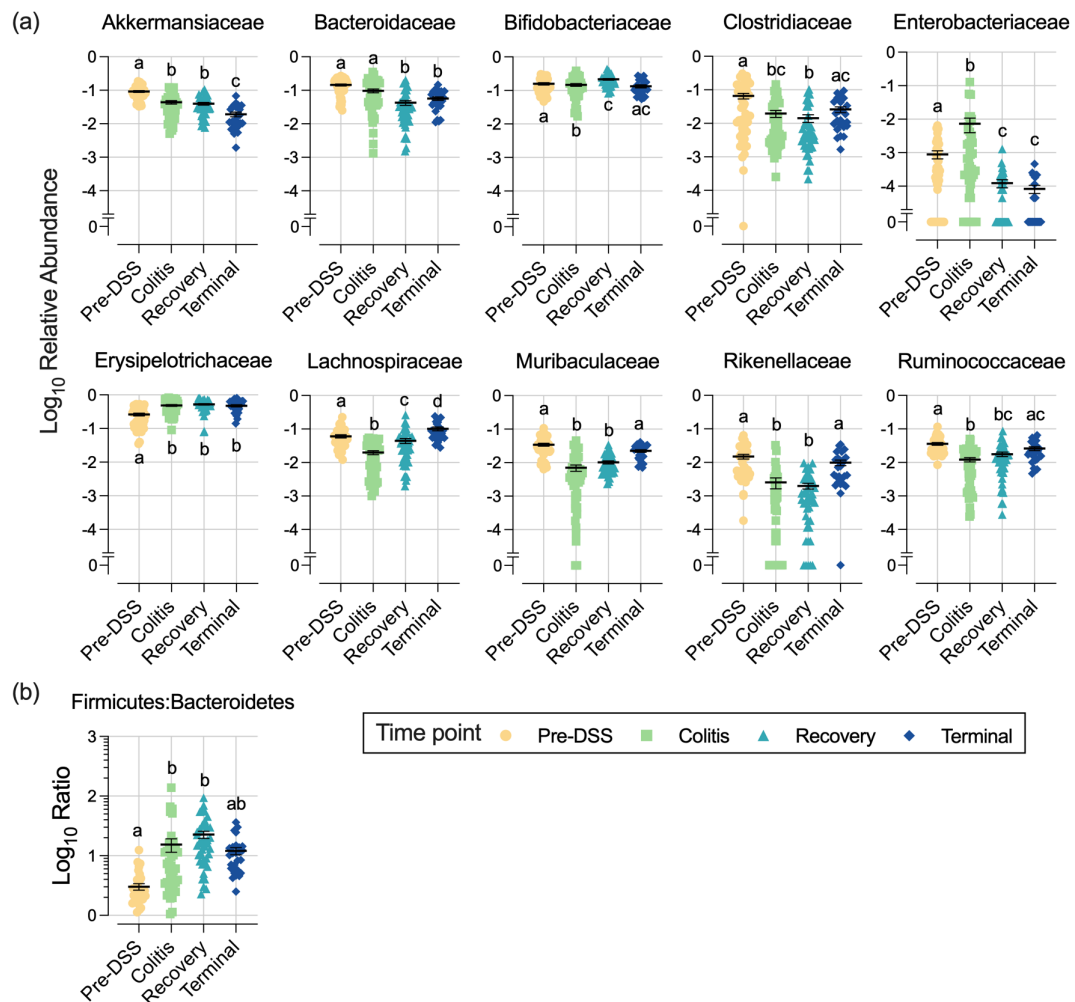


Figure 2.S10. Relative abundance of selected bacteria families of interest and the ratio of Firmicutes-to-Bacteroidetes over the study time points (experiment B). The \log_{10} relative abundance values for selected taxa (a) and the \log_{10} ratio values for Firmicutes-to-Bacteroidetes (b) are shown, irrespective of basal diet or BRB supplementation, for each experimental time point for individual mice with the mean \pm SE. Different letters indicate that relative abundances or ratios for time points are significantly different ($p < 0.05$) as determined by statistical methods outlined in Materials and Methods. Complete results of all metagenomeSeq statistical analyses are provided in File 2.S4.

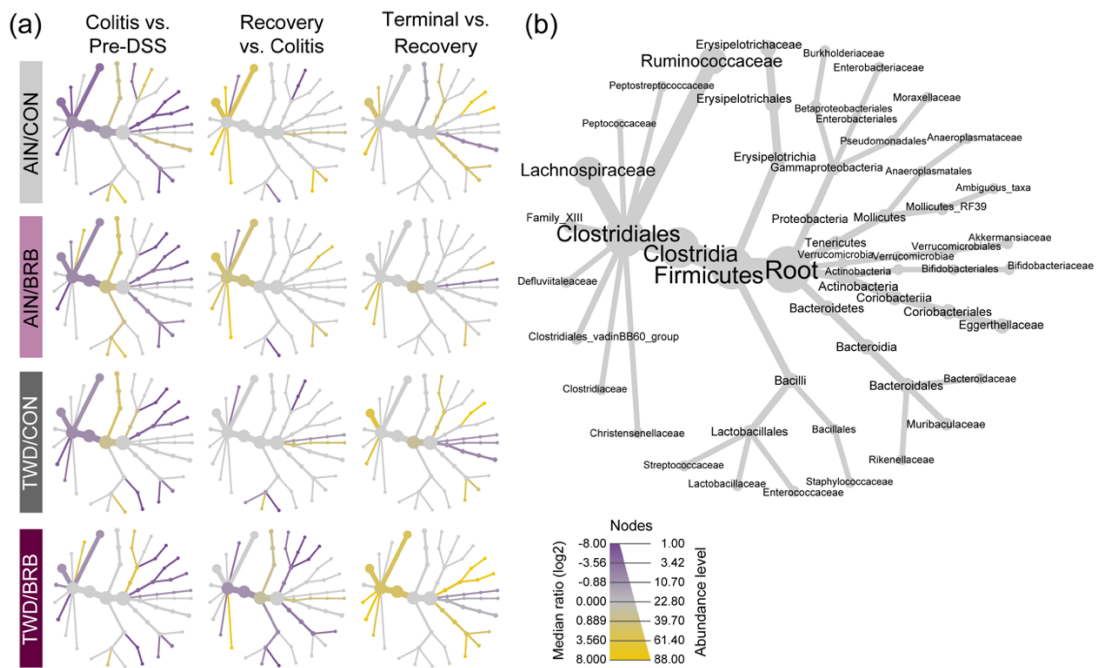


Figure 2.S11. Fecal microbiome community structures depicted as heat trees showing the relative abundance ratios for comparisons across study time points within each experimental diet group (experiment B). The heat tree analysis leverages the hierarchical structure of taxonomic classifications to quantitatively (using the median abundance) and statistically (using the non-parametric Wilcoxon Rank Sum test) depict taxonomic differences between microbial communities. **(a)** Comparisons of colitis vs. pre-DSS, recovery vs. colitis, and terminal vs. recovery time points with yellow indicating increase abundance with disease progression (advancing time point) and purple indicating reduced abundance as indicated by the scale. For example, relative abundance of Ruminococcaceae is increased (yellow) at recovery vs. colitis time point for the AIN/CON experimental diet group, whereas Enterobacteriaceae is less abundant (purple). **(b)** Phylogenetic structure of fecal microbiome bacteria community.

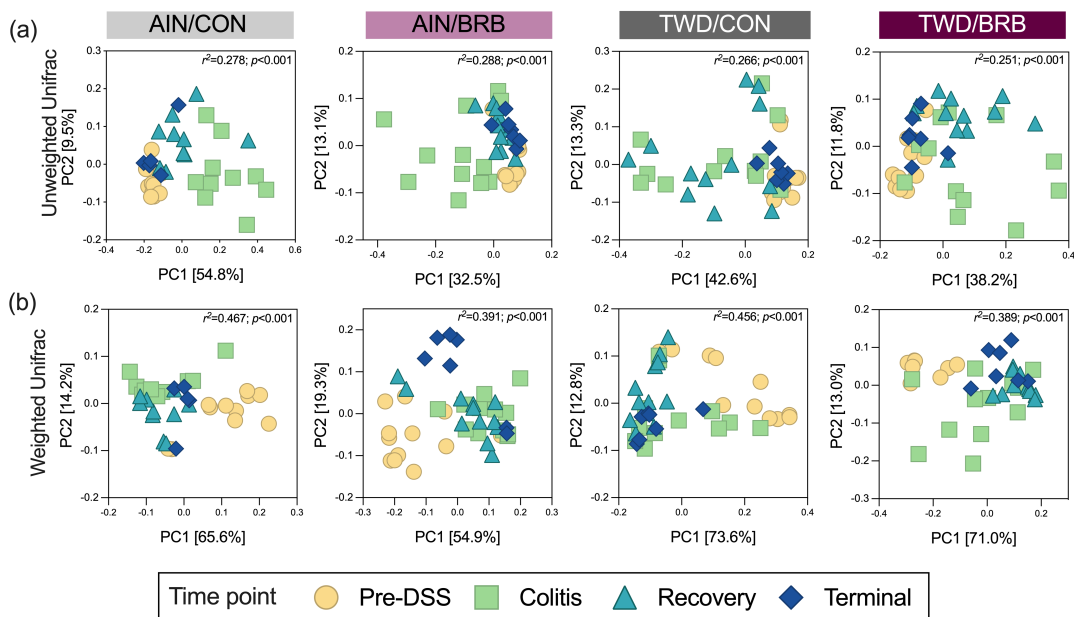


Figure 2.S12. Beta diversity of mouse fecal microbiomes over each time point within each experimental diet group (experiment B). Principal coordinate plots depicting fecal microbiome beta diversity using (a) unweighted or (b) weighted unifrac distances are shown using the first two components. The variation attributed to PC1 and PC2 are shown along with the r^2 and permanova p -values for each plot.

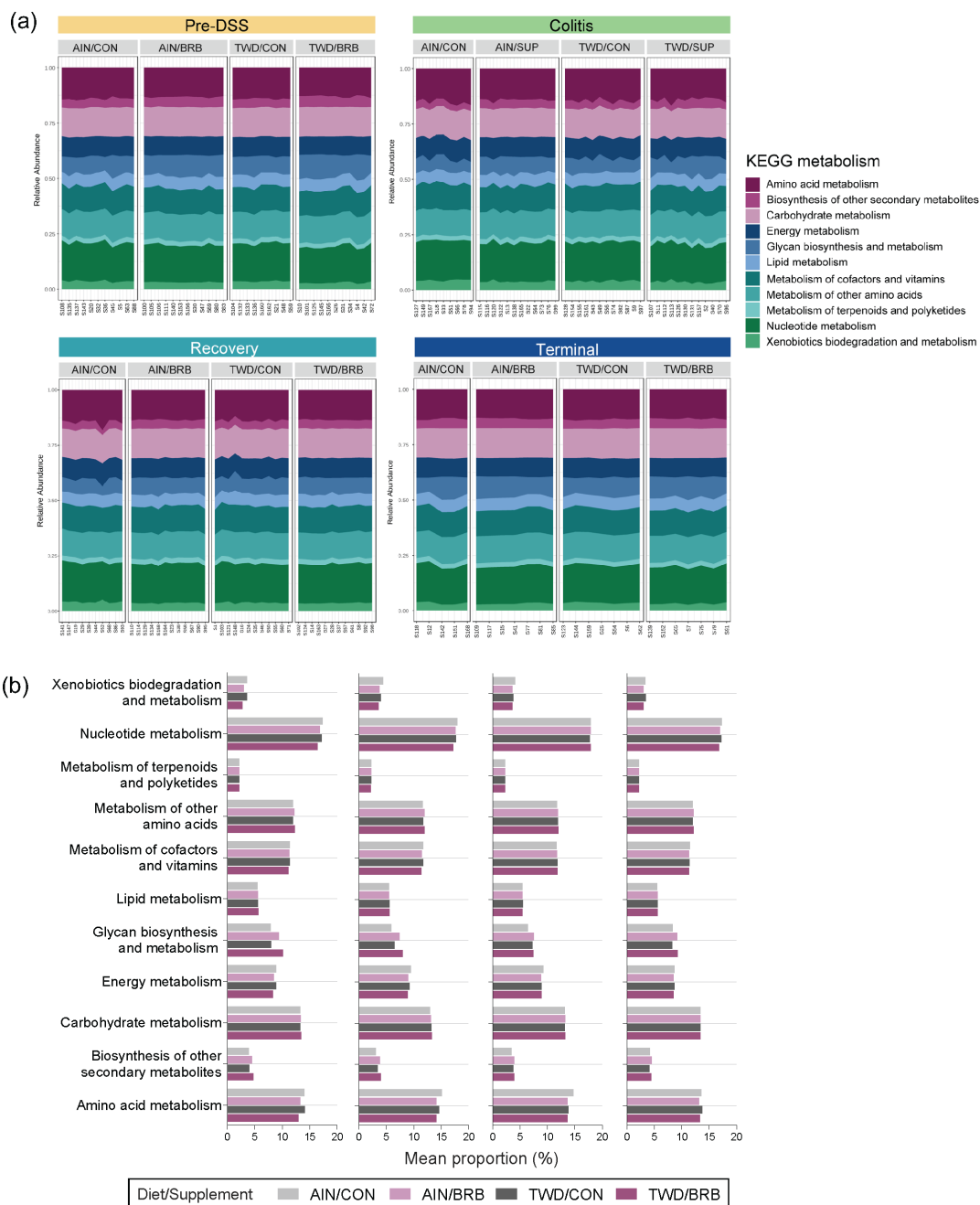


Figure 2.S13. Metagenome predicted functions classified using KEGG metabolism orthology with tax4fun (experiment B). (a) Stacked area plots show the total hits normalized by category size for KEGG level 1 metabolism terms. (b) Mean proportions (%) for KEGG metabolism categories for each experimental diet group.

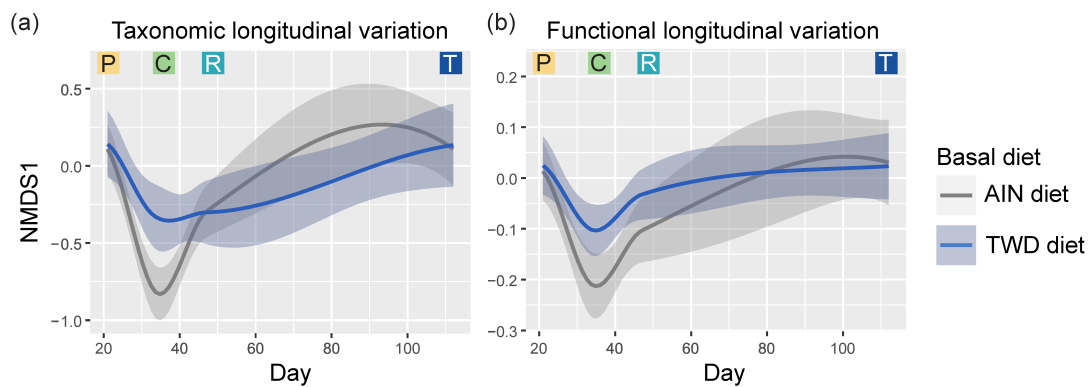


Figure 2.S14. Longitudinal analysis of fecal microbiome taxonomy and functional capacity (experiment B) for AIN and TWD basal diets without BRB supplementation (AIN/CON and BRB/CON groups). Longitudinal variation is shown as the first dimension of Bray-Curtis dissimilarity beta-diversity for taxonomy based on ASV abundances (**a**) or function based on KEGG term abundances (**b**). Loess-smoothed trajectories of sample microbiomes from each experimental group are plotted with gray areas representing the 95% confidence interval. P, pre-DSS; C, colitis; R, recovery; and T, terminal time points.

Supplementary Tables

Table 2.S1. Experimental diet formulations						
			AIN93G		TWD	
			AIN93G	+ 10% BRB	TWD	+ 10% BRB
Energy density (kcal/g)			3.76	3.77	4.35	4.34
Macro-nutrients	Carbohydrates (g/kg diet)	BRB powder		100		100
		Corn Starch	397.5	374.3	230	201
		Maltodextrin	132	132	70	70
		Sucrose	100	73.2	261.2	232.8
		Cellulose	50	12.5	30	
		<i>Kcal (% of total)</i>		<i>63.9%</i>	<i>63.9%</i>	<i>50.0%</i>
	Proteins (g/kg)	Casein	200	187.5	190	177.5
		L-cystine	3	3	2.85	2.85
		<i>Kcal (% of total)</i>		<i>18.8%</i>	<i>18.9%</i>	<i>15.5%</i>
	Fats (g/kg)	Soybean oil	70	70	31.4	31.4
Anhydrous milk fat				36.3	36.3	
Olive Oil				28.0	28.0	
Lard				28.0	28.0	
Beef tallow				24.8	24.8	
Corn oil				16.5	16.5	
Cholesterol				0.4	0.4	
<i>Kcal (% of total)</i>			<i>17.2%</i>	<i>17.1%</i>	<i>34.5%</i>	<i>34.6%</i>
Micro-nutrients	Minerals (mg/kg)	Calcium	5000	5000	2011	2011
		Phosphorus	3000	3000	2757	2757
		Sodium	1019	1019	7078	7078
		Potassium	3600	3600	5333	5333
		Magnesium	507	507	589	589
		Iron	35	35	31	31
		Zinc	30	30	25	25
		Copper	6	6	2.6	2.6
		Selenium	0.15	0.15	0.2	0.2
	Vitamins (unit/kg)	Thiamin (mg)	5	5	3.5	3.5
		Riboflavin (mg)	6	6	4.4	4.4
		Niacin (mg)	30	30	50.6	50.6
		Pyridoxine (mg)	6	6	3.9	3.9
		Folate (mg)	2	2	1.3	1.3
		Vitamin B ₁₂ (μg)	25	25	11	11
		Vitamin A (IU)	4000	4000	4300	4300
		Vitamin D (IU)	1000	1000	391	391
		Vitamin E (IU)	75	75	24.6	24.6
		Vitamin K (μg)	750	750	189	189
		Choline (mg)	1027	1027	648	648

Note: Abbreviations for diets are the following: total Western diet, TWD. Composition of the TWD was published previously.³ No data are available in NHANES for chloride, manganese, iodine, pantothenic acid, biotin, or ultra-trace minerals. Levels of these components mimics that of the basal diet to formulate BRB supplemented diets.

³ Hintze, K.J.; Benninghoff, A.D.; Ward, R.E. Formulation of the total western diet (TWD) as a basal diet for rodent cancer studies. *J. Agric. Food Chem.* **2012**, *60*, 6736-6742, doi:10.1021/jf204509a.

Table 2.S2.

Time point comparison	Alpha Diversity Measure		
	Observed ASVs	Chao1 index	Shannon Index
Pre-DSS vs. Colitis	0.0001	0.0001	0.0001
Pre-DSS vs. Recovery	0.0001	0.0001	0.0001
Pre-DSS vs. Terminal	0.2246	0.2742	0.0008
Colitis vs. Recovery	0.0012	0.0007	0.9090
Colitis vs. Terminal	0.0001	0.0001	0.0163
Recovery vs. Terminal	0.0006	0.0007	0.0027

Values shown are the Tukey HSD post-hoc comparison p -values for each pairwise comparison between experimental diet groups within each time point following a generalized linear model analysis. Main effects of all experimental factors are presented in Figure 2.11.

Table 2.S3. Alpha diversity pairwise comparisons by experimental group within time points (experiment B)

Time point	Comparison	Alpha Diversity Measure		
		Observed ASVs	Chao1 index	Shannon Index
Pre-DSS	AIN/CON vs. AIN/BRB	0.0001	0.0001	0.0020
Pre-DSS	AIN/CON vs. TWD/CON	0.9588	0.9448	0.4599
Pre-DSS	AIN/CON vs. TWD/BRB	0.0001	0.0001	0.0741
Pre-DSS	AIN/BRB vs. TWD/CON	0.0001	0.0001	0.0988
Pre-DSS	AIN/BRB vs. TWD/BRB	0.5004	0.5545	0.5540
Pre-DSS	TWD/CON vs. TWD/BRB	0.0001	0.0001	0.7349
Colitis	AIN/CON vs. AIN/BRB	0.0001	0.0001	0.0373
Colitis	AIN/CON vs. TWD/CON	0.0386	0.0299	0.5323
Colitis	AIN/CON vs. TWD/BRB	0.0004	0.0003	0.0048
Colitis	AIN/BRB vs. TWD/CON	0.1733	0.1204	0.4408
Colitis	AIN/BRB vs. TWD/BRB	0.9740	0.9295	0.8456
Colitis	TWD/CON vs. TWD/BRB	0.3547	0.3529	0.1079
Recovery	AIN/CON vs. AIN/BRB	0.0001	0.0002	0.0001
Recovery	AIN/CON vs. TWD/CON	0.9294	0.8141	0.4909
Recovery	AIN/CON vs. TWD/BRB	0.1359	0.2147	0.9996
Recovery	AIN/BRB vs. TWD/CON	0.0001	0.0001	0.0001
Recovery	AIN/BRB vs. TWD/BRB	0.0424	0.0444	0.0001
Recovery	TWD/CON vs. TWD/BRB	0.0251	0.0229	0.3867
Terminal	AIN/CON vs. AIN/BRB	0.0005	0.0010	0.0915
Terminal	AIN/CON vs. TWD/CON	0.6076	0.5214	0.4618
Terminal	AIN/CON vs. TWD/BRB	0.0811	0.1548	0.9460
Terminal	AIN/BRB vs. TWD/CON	0.0001	0.0871	0.0014
Terminal	AIN/BRB vs. TWD/BRB	0.0916	0.0001	0.1797
Terminal	TWD/CON vs. TWD/BRB	0.0022	0.0037	0.1464

Values shown are the Tukey HSD post-hoc comparison p -values for each pairwise comparison between experimental diet groups within each time point following a generalized linear model analysis.

Table 2.S4. Alpha diversity pairwise comparisons by time point within experimental group (experiment B)

Diet/Treatment	Comparison	Alpha Diversity Measure		
		Observed ASVs	Chao1 index	Shannon index
AIN/BRB	Pre-DSS vs. Colitis	0.0001	0.0001	0.0001
AIN/BRB	Pre-DSS vs. Recovery	0.0008	0.1908	0.0831
AIN/BRB	Pre-DSS vs. Terminal	0.7791	1.0000	0.9157
AIN/BRB	Colitis vs. Recovery	0.0011	0.0005	0.0871
AIN/BRB	Colitis vs. Terminal	0.0001	0.0001	0.0054
AIN/BRB	Recovery vs. Terminal	0.0758	0.3309	0.4702
AIN/CON	Pre-DSS vs. Colitis	0.0001	0.0001	0.0001
AIN/CON	Pre-DSS vs. Recovery	0.1916	0.0017	0.0007
AIN/CON	Pre-DSS vs. Terminal	1.0000	0.8782	0.7015
AIN/CON	Colitis vs. Recovery	0.0006	0.0003	0.6517
AIN/CON	Colitis vs. Terminal	0.0001	0.0001	0.0106
AIN/CON	Recovery vs. Terminal	0.3235	0.0799	0.0978
TWD/BRB	Pre-DSS vs. Colitis	0.0098	0.0005	0.0549
TWD/BRB	Pre-DSS vs. Recovery	0.0029	0.0046	0.0001
TWD/BRB	Pre-DSS vs. Terminal	0.4629	0.6254	0.1714
TWD/BRB	Colitis vs. Recovery	0.9695	0.8556	0.0404
TWD/BRB	Colitis vs. Terminal	0.4866	0.0569	0.9976
TWD/BRB	Recovery vs. Terminal	0.2803	0.2263	0.0650
TWD/CON	Pre-DSS vs. Colitis	0.0004	0.0110	0.0014
TWD/CON	Pre-DSS vs. Recovery	0.0034	0.0031	0.0001
TWD/CON	Pre-DSS vs. Terminal	0.6498	0.5255	0.0017
TWD/CON	Colitis vs. Recovery	0.8779	0.9658	0.3080
TWD/CON	Colitis vs. Terminal	0.0458	0.4471	0.9588
TWD/CON	Recovery vs. Terminal	0.1768	0.2445	0.7434

Values shown are the Tukey HSD post-hoc comparison p -values for each pairwise comparison across time points within each experimental diet group following a generalized linear model analysis.

Table 2.S5. Short-chain fatty acids pairwise comparisons for effects of time point only, irrespective of basal diet or BRB supplement (experiment B)

Time point comparison	Alpha Diversity Measure						
	Acetic	Butyric	Capric	Isobutyric	Isovaleric	Propionic	Valeric
Pre-DSS vs. Colitis	0.0001	0.0001	0.2944	0.9368	0.6528	0.0001	0.0472
Pre-DSS vs. Recovery	0.4378	0.8214	0.9956	0.3249	0.0422	0.4953	0.6444
Pre-DSS vs. Terminal	0.1946	0.9286	0.9993	0.9417	0.9671	0.6054	0.9998
Colitis vs. Recovery	0.0001	0.0001	0.1861	0.6898	0.4568	0.0001	0.0012
Colitis vs. Terminal	0.0001	0.0001	0.4586	0.7046	0.4512	0.0001	0.0816
Recovery vs. Terminal	0.9144	0.5192	0.9869	0.1689	0.0285	1.0000	0.7716

Values shown are the Tukey HSD post-hoc comparison p -values for each pairwise comparison between experimental diet groups within each time point following a generalized linear model analysis. Main effects of all experimental factors are presented in Figure 2.15.

Table 2.S6. Short chain fatty acids pairwise comparisons by experimental group within time points (experiment B)

Time point	Comparison	Short Chain Fatty Acid						
		Acetic	Butyric	Capric	Isobutyric	Isovaleric	Propionic	Valeric
Pre-DSS	AIN/BRB vs. AIN/CON	1.0000	0.1788	0.7720	0.9964	0.9987	0.9230	0.2039
Pre-DSS	AIN/CON vs. TWD/CON	0.9943	0.0768	0.0006	0.7623	0.3289	0.9928	0.7336
Pre-DSS	AIN/CON vs. TWD/BRB	0.0001	0.0001	0.0003	0.0023	0.0003	0.0001	0.0015
Pre-DSS	AIN/BRB vs. TWD/CON	0.9931	0.9779	0.0051	0.8768	0.4285	0.8190	0.8000
Pre-DSS	AIN/BRB vs. TWD/BRB	0.0001	0.0001	0.0024	0.0052	0.0007	0.0001	0.2409
Pre-DSS	TWD/BRB vs. TWD/CON	0.0001	0.0001	0.9977	0.0389	0.0524	0.0001	0.0382
Colitis	AIN/BRB vs. AIN/CON	0.9185	0.9988	0.9614	0.1625	0.0457	0.6694	0.0579
Colitis	AIN/CON vs. TWD/CON	0.5982	0.4734	0.9796	0.0024	0.0158	0.2397	0.0983
Colitis	AIN/CON vs. TWD/BRB	0.4656	0.9061	0.1242	0.8806	0.9439	0.8243	0.3198
Colitis	AIN/BRB vs. TWD/CON	0.2340	0.5319	0.9998	0.2901	0.9519	0.8376	0.9987
Colitis	AIN/BRB vs. TWD/BRB	0.1604	0.8391	0.2637	0.0429	0.0174	0.9962	0.8983
Colitis	TWD/BRB vs. TWD/CON	0.9951	0.1917	0.2551	0.0005	0.0060	0.7480	0.9508
Recovery	AIN/BRB vs. AIN/CON	0.0047	0.9157	0.0742	0.0032	0.0205	0.2150	0.9992
Recovery	AIN/CON vs. TWD/CON	0.3944	0.9963	0.0821	0.0034	0.0126	0.9597	0.9030
Recovery	AIN/CON vs. TWD/BRB	0.9282	0.6859	0.0768	0.9987	0.9868	0.0152	0.3071
Recovery	AIN/BRB vs. TWD/CON	0.1997	0.9715	0.9997	1.0000	0.9977	0.0708	0.8408
Recovery	AIN/BRB vs. TWD/BRB	0.0006	0.2893	1.0000	0.0040	0.0068	0.0001	0.3552
Recovery	TWD/BRB vs. TWD/CON	0.1261	0.5335	0.9998	0.0043	0.0040	0.0467	0.0747
Terminal	AIN/BRB vs. AIN/CON	0.9999	0.8229	0.4981	0.8417	0.7079	0.9962	0.8788
Terminal	AIN/CON vs. TWD/CON	0.0204	0.3536	0.5689	0.1634	0.0520	0.0019	0.1227
Terminal	AIN/CON vs. TWD/BRB	0.0951	0.0001	0.2772	0.5177	0.7375	0.0391	0.0001
Terminal	AIN/BRB vs. TWD/CON	0.0191	0.8465	0.0377	0.0215	0.0025	0.0026	0.4049
Terminal	AIN/BRB vs. TWD/BRB	0.0956	0.0004	0.0142	0.1410	0.1808	0.0531	0.0006
Terminal	TWD/BRB vs. TWD/CON	0.9694	0.0021	0.9060	0.9296	0.4350	0.8049	0.0209

Values shown are the Tukey HSD post-hoc comparison p -values for each pairwise comparison between experimental diet groups within each time point following a generalized linear model analysis.

Table 2.S7. Short-chain fatty acids pairwise comparisons by time point within experimental group (experiment B)

Time point	Comparison	Short Chain Fatty Acid						
		Acetic	Butyric	Capric	Isobutyric	Isovaleric	Propionic	Valeric
AIN/CON	Colitis vs. Pre-DSS	0.0001	0.0001	0.8603	0.9785	1.0000	0.0004	0.9763
AIN/CON	Pre-DSS vs. Recovery	0.0859	0.9540	0.0177	0.0035	0.0010	0.7319	0.9799
AIN/CON	Pre-DSS vs. Terminal	0.9858	0.9966	0.6435	1.0000	0.9974	0.9982	0.9447
AIN/CON	Colitis vs. Recovery	0.0004	0.0005	0.0759	0.0014	0.0013	0.0115	0.8647
AIN/CON	Colitis vs. Terminal	0.0001	0.0010	0.9565	0.9913	0.9972	0.0015	0.9973
AIN/CON	Recovery vs. Terminal	0.3048	0.9949	0.3424	0.0126	0.0092	0.7187	0.8187
AIN/BRB	Colitis vs. Pre-DSS	0.0001	0.0001	0.5511	0.1450	0.0017	0.0001	0.1855
AIN/BRB	Pre-DSS vs. Recovery	0.9153	0.9965	0.9993	0.9963	0.9023	1.0000	0.8997
AIN/BRB	Pre-DSS vs. Terminal	0.9359	0.9996	0.9580	0.7819	0.8089	0.9945	0.8508
AIN/BRB	Colitis vs. Recovery	0.0001	0.0001	0.6479	0.0910	0.0130	0.0001	0.0394
AIN/BRB	Colitis vs. Terminal	0.0001	0.0001	0.3309	0.0264	0.0003	0.0001	0.0493
AIN/BRB	Recovery vs. Terminal	0.6468	0.9911	0.9297	0.8775	0.4388	0.9941	0.9979
TWD/CON	Colitis vs. Pre-DSS	0.0001	0.0001	0.6908	0.0050	0.0501	0.0001	0.0024
TWD/CON	Pre-DSS vs. Recovery	0.7001	0.9970	0.0690	0.8876	0.9232	0.7206	0.6337
TWD/CON	Pre-DSS vs. Terminal	0.0077	0.9857	0.9813	0.6796	0.6126	0.1069	0.9305
TWD/CON	Colitis vs. Recovery	0.0001	0.0001	0.4705	0.0006	0.0101	0.0001	0.0001
TWD/CON	Colitis vs. Terminal	0.0001	0.0001	0.9104	0.1426	0.5935	0.0026	0.0222
TWD/CON	Recovery vs. Terminal	0.0957	0.9504	0.1951	0.2899	0.2814	0.5382	0.3105
TWD/BRB	Colitis vs. Pre-DSS	0.0001	0.0050	0.4426	0.0007	0.0111	0.0270	0.9987
TWD/BRB	Pre-DSS vs. Recovery	0.9967	0.0021	0.9136	0.8813	0.5796	0.8995	0.8928
TWD/BRB	Pre-DSS vs. Terminal	0.9997	0.7847	0.9999	0.5666	0.4994	1.0000	0.9289
TWD/BRB	Colitis vs. Recovery	0.0001	0.0001	0.1644	0.0001	0.0004	0.1258	0.8395
TWD/BRB	Colitis vs. Terminal	0.0001	0.1524	0.6239	0.0942	0.4701	0.0860	0.9670
TWD/BRB	Recovery vs. Terminal	0.9998	0.0009	0.9287	0.2365	0.0781	0.9470	0.6293

Values shown are the Tukey HSD post-hoc comparison *p*-values for each pairwise comparison between experimental diet groups within each time point following a generalized linear model analysis.

Supplementary Files and Supporting Data

File 2.S1. Experiment A (pilot study) microbiome count data.xlsx. Microsoft Office Excel document with curated microbiome count data for experiment A annotated with GreenGenes taxonomy. File accessible online <https://doi.org/10.3390/nu14245270>.

File 2.S2. Experiment B (diet comparison) microbiome count data.xlsx. Microsoft Office Excel document with curated microbiome count data for experiment B annotated with Silva taxonomy. File accessible online <https://doi.org/10.3390/nu14245270>.

File 2.S3: Experiment A metagenomeSeq statistics.xlsx. Microsoft Office Excel data with FDR p -values for all MetagenomeSeq data analyses of bacteria families for experiment A. File accessible online <https://doi.org/10.3390/nu14245270>.

File 2.S4: Experiment B metagenomeSeq statistics.xlsx. Microsoft Office Excel data with FDR p -values for all MetagenomeSeq data analyses of bacteria families for experiment B. File accessible online <https://doi.org/10.3390/nu14245270>.

All raw data supporting this work are freely available via the Utah State University Digital Commons Data Repository at <https://doi.org/10.26078/ats5-4m77>, including:

1. Benninghoff_Experiment_A_mapping_file.csv provides the sample identification details including the time point, basal diet, black raspberry (BRB) supplementation for each sample ID.
2. Benninghoff_Experiment_A_OTU_table.csv provides the 16S rRNA sequence count data for all samples for each operational taxonomic unit identified.
3. Benninghoff_Experiment_A_taxonomy.csv provides the mapping of operational taxonomic units to bacteria taxonomy.
4. Benninghoff_Experiment_B_mapping_file.csv provides the sample identification details including the time point, basal diet, black raspberry (BRB) supplementation for each sample ID.
5. Benninghoff_Experiment_A_ASV_table.csv provides the 16S rRNA sequence count data for all samples for each amplicon sequence variant identified.
6. Benninghoff_Experiment_A_taxonomy.csv provides the mapping of amplicon sequence variants to bacteria taxonomy.
7. Readme.txt

Appendix C. Supplementary Material Associated with Chapter 3

Supplementary Figures

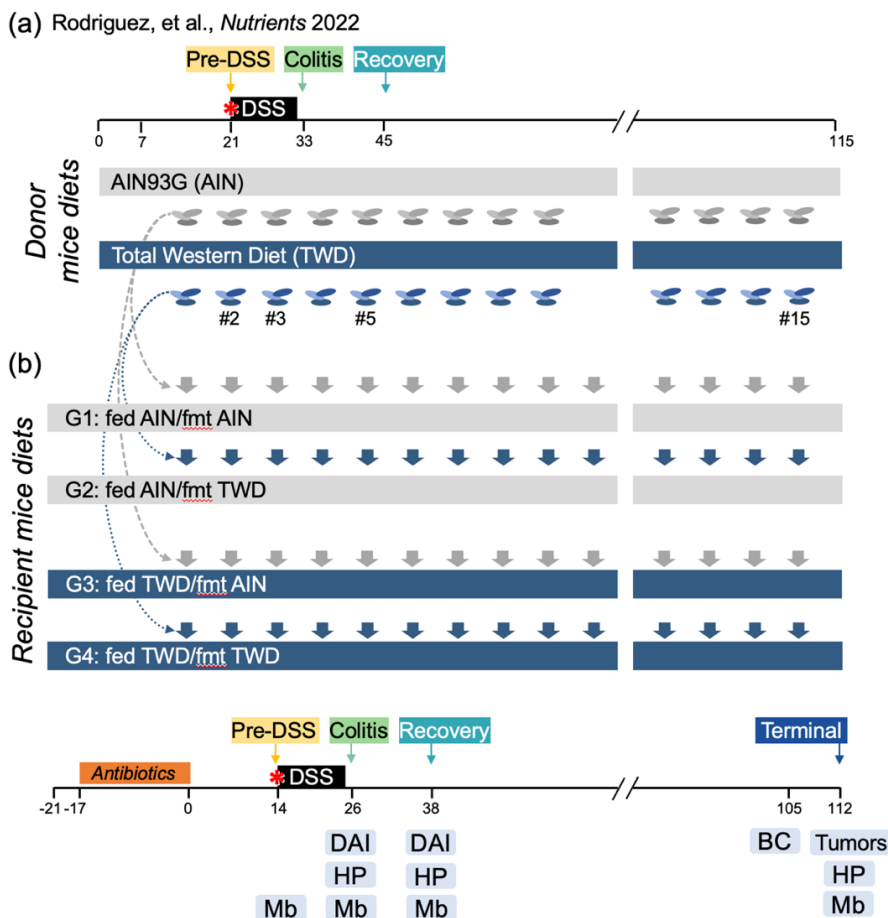


Figure 3.S1. Experimental design. **(a)** Diagram outlines the experimental design for the treatment of donor mice with azoxymethane (red asterisk) and dextran sodium sulfate (DSS) to induce colitis and colon tumorigenesis. Also shown are the time points for weekly collection of fecal samples for each basal diet group. Full experimental details are outlined in Rodriguez, et al.⁴ **(b)** Diagram outlines the experiment design for this study, described in detail in the Materials and Methods. Basal diets are represented as gray (AIN) or blue (TWD) bars with FMT from AIN-fed donors (grey arrows) and FMT from TWD-fed donor mice (blue arrows). Numbers below each FMT donor represents the week of collection that was then to time-matched for recipient mice. For example, collection 3 occurred while the donor mice were experience active colitis and was used to inoculate recipient mice just prior to DSS treatment. In this study, the endpoints assessed are shown, including the disease activity index (DAI), histopathology (HP), fecal microbiome profile (Mb), body composition (BC) and colon tumor incidence, multiplicity and burden (tumors).

⁴ Rodriguez, D.M.; Hintze, K.J.; Rompato, G.; Wettore, A.J.V.; Ward, R.E.; Phatak, S.; Neal, C.; Armbrust, T.; Stewart, E.C.; Thomas, A.J., et al. Dietary supplementation with black raspberries altered the gut microbiome composition in a mouse model of colitis-associated colorectal cancer, although with differing effects for a healthy versus a Western basal diet. *Nutrients* **2022**, *14*, doi:10.3390/nu14245270.

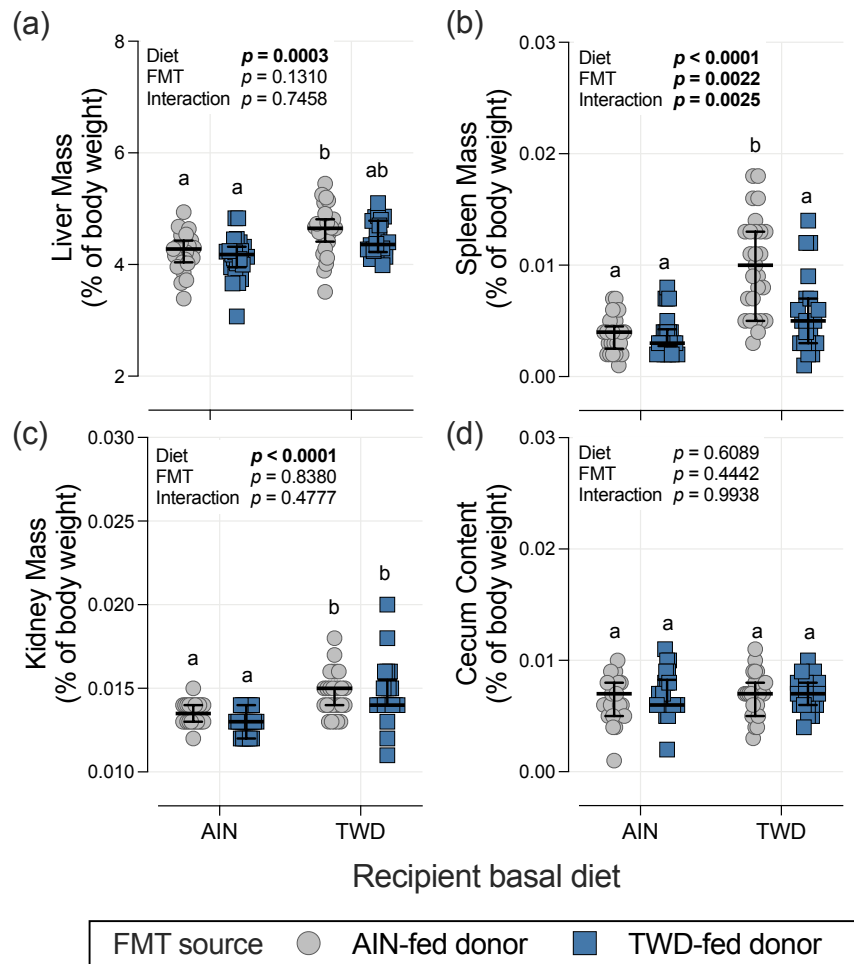


Figure 3.S2. Relative liver, kidney, spleen, and cecum content weights. Data for liver (a), kidney (b), spleen (c), and cecum content (d) weights are shown as a proportion of the final body weight. Values for individual mice are shown with median \pm interquartile range. Inset tables provide the model main effects for diet, treatment, and their interaction, and different letters indicate groups are significantly different ($p < 0.05$) as outlined in Materials and Methods.

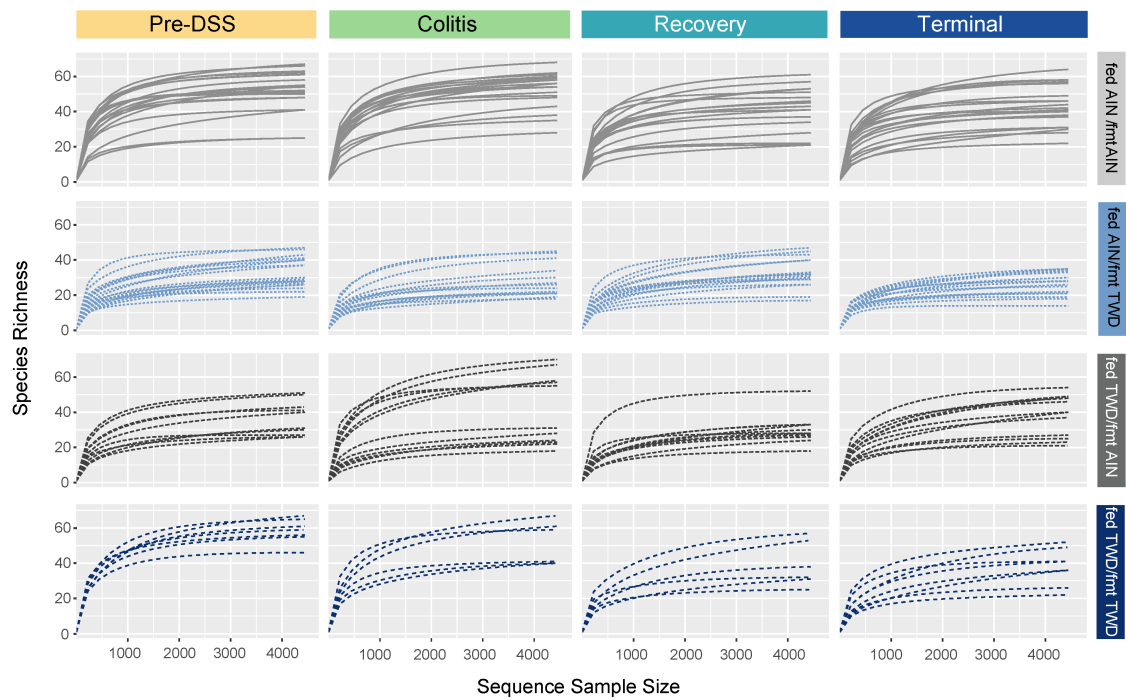


Figure 3.S3. Rarefaction curve analysis by experimental group and time point. Rarefaction curve analysis by experimental group and time point. Curves plot species richness as a function of sequence sample size. For comparisons across experimental groups, data were rarefied to ~4,400 sequences, the lowest total among all the samples. These curves indicate that saturation was reached satisfactorily for most samples and that additional sequence reads were unlikely to substantially increase the number of species detected.

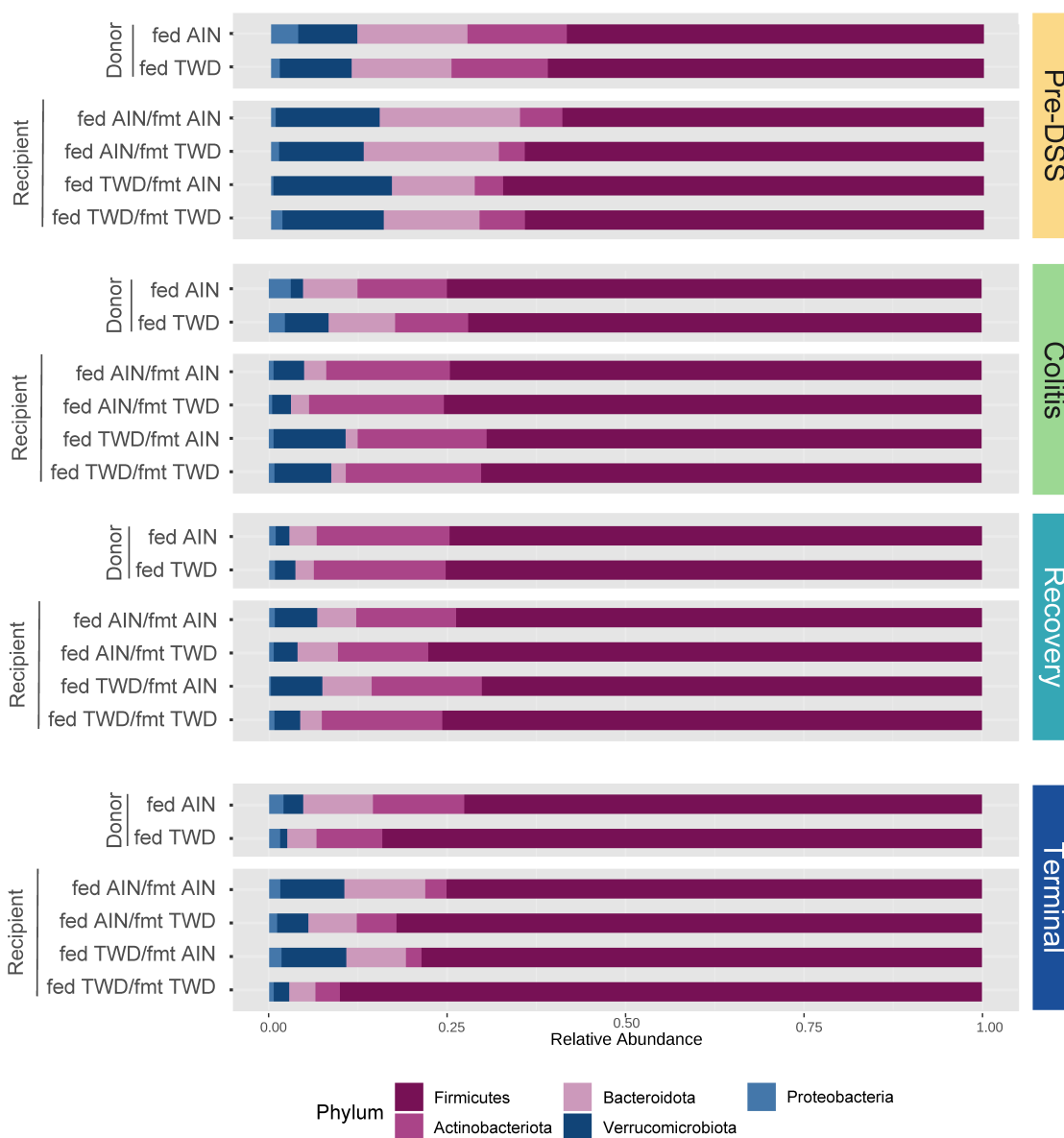


Figure 3.S4. Taxonomic classification of mouse fecal bacteria at the phylum level. Data shown are the relative normalized abundance of bacteria annotated to the phylum level.

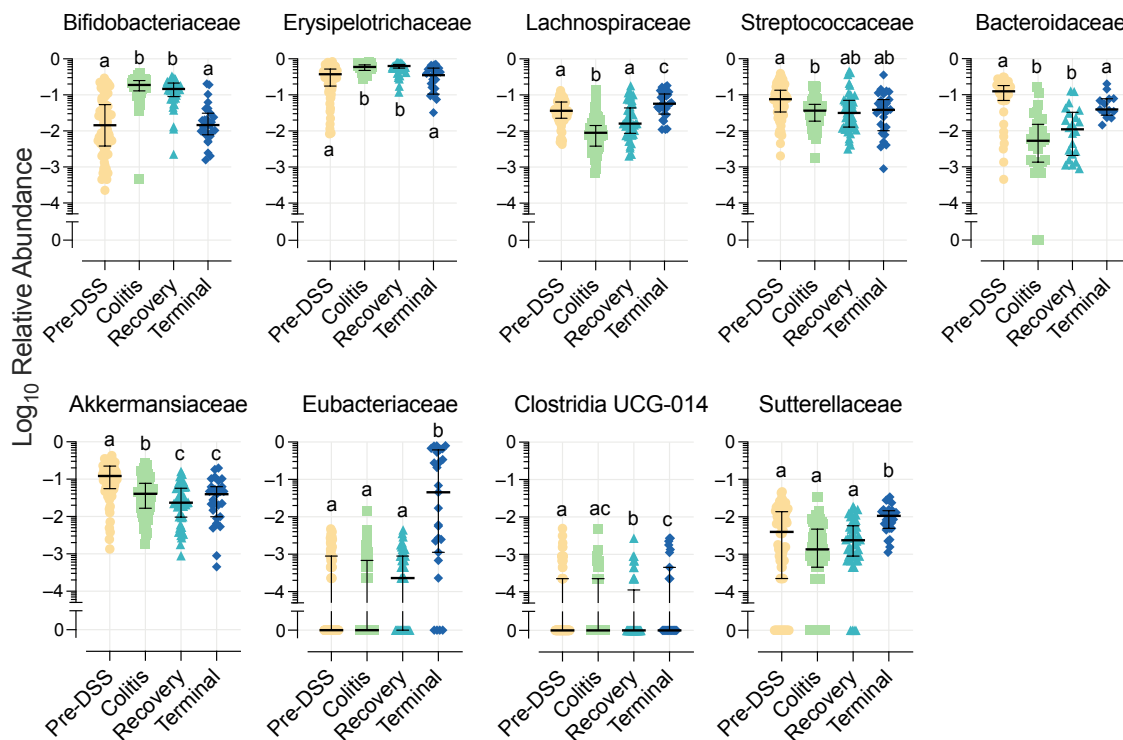


Figure 3.S5. Relative abundance of selected bacteria families of interest over the study time points. The log₁₀ relative abundance values for representing each cage (as the biological unit) with the median \pm interquartile range are shown for selected taxa, irrespective of basal diet or FMT donor source, for each experimental time point. Different letters indicate that relative abundances for time points are significantly different ($p < 0.05$) as determined by statistical methods outlined in Materials and Methods.

Table 3.S1. Experimental diet formulations

		AIN93G	TWD
Energy density (kcal/g)		3.76	4.35
Macronutrients	Carbohydrates (g/kg diet)		
	Corn Starch	397.5	230
	Maltodextrin	132	70
	Sucrose	100	261.2
	Cellulose	50	30
	Kcal (% of total)	63.9%	50.0%
	Proteins (g/kg)		
	Casein	200	190
	L-cystine	3	2.85
	Kcal (% of total)	18.8%	15.5%
	Fats (g/kg)		
	Soybean oil	70	31.4
	Anhydrous milk fat		36.3
	Olive Oil		28
	Lard		28
	Beef tallow		24.8
	Corn oil		16.5
	Cholesterol		0.4
	Kcal (% of total)	17.2%	34.5%
Micronutrients	Minerals (mg/kg)		
	Calcium	5000	2011
	Phosphorus	3000	2757
	Sodium	1019	7078
	Potassium	3600	5333
	Magnesium	507	589
	Iron	35	31
	Zinc	30	25
	Copper	6	2.6
	Selenium	0.15	0.2
	Vitamins (unit/kg)		
	Thiamin (mg)	5	3.5
	Riboflavin (mg)	6	4.4
	Niacin (mg)	30	50.6
	Pyridoxine (mg)	6	3.9
	Folate (mg)	2	1.3
	Vitamin B12 (µg)	25	11
	Vitamin A (IU)	4000	4300
	Vitamin D (IU)	1000	391
	Vitamin E (IU)	75	24.6
	Vitamin K (µg)	750	189
	Choline (mg)	1027	648

Note: TWD, total Western diet. Composition of the TWD was published previously.⁵ No data are available in NHANES for chloride, manganese, iodine, pantothenic acid, biotin, or ultra-trace minerals.

⁵ Hintze, K.J.; Benninghoff, A.D.; Ward, R.E. Formulation of the total western diet (TWD) as a basal diet for rodent cancer studies. *J. Agric. Food Chem.* 2012, 60, 6736-6742, doi:10.1021/jf204509a.

Table 3.S2. Alpha diversity pairwise comparisons for effects of time point only, irrespective of basal diet or FMT source

Time point comparison	Alpha Diversity Measure		
	Observed ASVs	Chao1 index	Shannon Index
Pre-DSS vs. Colitis	0.0001	0.0001	0.0001
Pre-DSS vs. Recovery	0.0001	0.0001	0.0001
Pre-DSS vs. Terminal	0.7358	0.7080	0.1370
Colitis vs. Recovery	0.0235	0.0444	0.9776
Colitis vs. Terminal	0.0001	0.0001	0.0001
Recovery vs. Terminal	0.0001	0.0001	0.0005

Values shown are the Tukey HSD post-hoc comparison *p*-values for each pairwise comparison between experimental diet groups within each timepoint following a generalized linear model analysis. Main effects of all experimental factors are presented in Figure 3.10.

Table 3.S3. Alpha diversity pairwise comparisons by experimental group within time points

Timepoint	Comparison	Alpha Diversity Measure		
		Observed ASVs	Chao1 index	Shannon Index
Pre-DSS	fed AIN/fmt AIN vs. fed AIN/fmt TWD	0.9999	0.9646	0.9298
Pre-DSS	fed AIN/fmt AIN vs. fed TWD/fmt AIN	0.0971	0.1128	0.0876
Pre-DSS	fed AIN/fmt AIN vs. fed TWD/fmt TWD	0.1385	0.1578	0.2483
Pre-DSS	fed AIN/fmt TWD vs. fed TWD/fmt AIN	0.1026	0.0470	0.3331
Pre-DSS	fed AIN/fmt TWD vs. fed TWD/fmt TWD	0.1450	0.0669	0.6455
Pre-DSS	fed TWD/fmt AIN vs. fed TWD/fmt TWD	0.9945	0.9950	0.9324
Colitis	fed AIN/fmt AIN vs. fed AIN/fmt TWD	0.2367	0.3275	0.1366
Colitis	fed AIN/fmt AIN vs. fed TWD/fmt AIN	0.7934	0.6447	0.6840
Colitis	fed AIN/fmt AIN vs. fed TWD/fmt TWD	0.7091	0.6474	0.8974
Colitis	fed AIN/fmt TWD vs. fed TWD/fmt AIN	0.7558	0.9430	0.0121
Colitis	fed AIN/fmt TWD vs. fed TWD/fmt TWD	0.8159	0.9344	0.0320
Colitis	fed TWD/fmt AIN vs. fed TWD/fmt TWD	0.9992	0.9999	0.9752
Recovery	fed AIN/fmt AIN vs. fed AIN/fmt TWD	0.8925	0.9361	0.9176
Recovery	fed AIN/fmt AIN vs. fed TWD/fmt AIN	0.4851	0.4855	0.6247
Recovery	fed AIN/fmt AIN vs. fed TWD/fmt TWD	0.9771	0.9831	0.6889
Recovery	fed AIN/fmt TWD vs. fed TWD/fmt AIN	0.1407	0.1802	0.2450
Recovery	fed AIN/fmt TWD vs. fed TWD/fmt TWD	0.9862	0.9945	0.2792
Recovery	fed TWD/fmt AIN vs. fed TWD/fmt TWD	0.2247	0.2418	0.9986
Terminal	fed AIN/fmt AIN vs. fed AIN/fmt TWD	0.8964	0.9356	0.6431
Terminal	fed AIN/fmt AIN vs. fed TWD/fmt AIN	0.0916	0.3458	0.1600
Terminal	fed AIN/fmt AIN vs. fed TWD/fmt TWD	0.0248	0.0841	0.0023
Terminal	fed AIN/fmt TWD vs. fed TWD/fmt AIN	0.4012	0.7522	0.8278
Terminal	fed AIN/fmt TWD vs. fed TWD/fmt TWD	0.1969	0.3678	0.0944
Terminal	fed TWD/fmt AIN vs. fed TWD/fmt TWD	0.9855	0.9284	0.3889

Values shown are the Tukey HSD post-hoc comparison *p*-values for each pairwise comparison between experimental diet groups within each timepoint following a generalized linear model analysis.

Table 3.S4. Alpha diversity pairwise comparisons by time point within experimental group

Diet/Treatment	Comparison	Alpha Diversity Measure		
		Observed ASVs	Chao1 index	Shannon index
fed AIN/fmt AIN	Pre-DSS vs. Colitis	0.0001	0.0001	0.0001
fed AIN/fmt AIN	Pre-DSS vs. Recovery	0.0001	0.0001	0.0003
fed AIN/fmt AIN	Pre-DSS vs. Terminal	0.9860	0.9989	0.9961
fed AIN/fmt AIN	Colitis vs. Recovery	0.6488	0.7368	0.9490
fed AIN/fmt AIN	Colitis vs. Terminal	0.0001	0.0001	0.0002
fed AIN/fmt AIN	Recovery vs. Terminal	0.0003	0.0012	0.0031
fed AIN/fmt TWD	Pre-DSS vs. Colitis	0.0001	0.0001	0.0001
fed AIN/fmt TWD	Pre-DSS vs. Recovery	0.0003	0.0001	0.0207
fed AIN/fmt TWD	Pre-DSS vs. Terminal	0.9547	0.7479	0.9239
fed AIN/fmt TWD	Colitis vs. Recovery	0.1196	0.1449	0.0986
fed AIN/fmt TWD	Colitis vs. Terminal	0.0002	0.0003	0.0063
fed AIN/fmt TWD	Recovery vs. Terminal	0.0415	0.0413	0.3971
fed TWD/fmt AIN	Pre-DSS vs. Colitis	0.0001	0.0001	0.0263
fed TWD/fmt AIN	Pre-DSS vs. Recovery	0.0003	0.0013	0.0004
fed TWD/fmt AIN	Pre-DSS vs. Terminal	0.9728	0.9999	0.9635
fed TWD/fmt AIN	Colitis vs. Recovery	0.9896	0.9914	0.3445
fed TWD/fmt AIN	Colitis vs. Terminal	0.0085	0.0067	0.3866
fed TWD/fmt AIN	Recovery vs. Terminal	0.0268	0.0211	0.0349
fed TWD/fmt TWD	Pre-DSS vs. Colitis	0.0001	0.0001	0.0019
fed TWD/fmt TWD	Pre-DSS vs. Recovery	0.0118	0.0146	0.0001
fed TWD/fmt TWD	Pre-DSS vs. Terminal	0.5775	0.6378	0.0081
fed TWD/fmt TWD	Colitis vs. Recovery	0.1399	0.1632	0.6640
fed TWD/fmt TWD	Colitis vs. Terminal	0.0060	0.0067	0.9968
fed TWD/fmt TWD	Recovery vs. Terminal	0.4997	0.4828	0.8651

Values shown are the Tukey HSD post-hoc comparison p -values for each pairwise comparison across time points within each experimental diet group following a generalized linear model analysis.

Supplementary Files and Supporting Data

File 3.S1. Microbiome count data.xlsx. Microsoft Office Excel document with curated microbiome count data annotated with Silva taxonomy. File accessible online <https://doi.org/10.26078/z54v-8j64>.

File 3.S2. MetagenomeSeq statistics.xlsx. Microsoft Office Excel data with FDR p -values for all MetagenomeSeq data analyses of bacteria families for experiment B. File accessible online <https://doi.org/10.26078/z54v-8j64>

All raw data supporting this work are freely available via the Utah State University Digital Commons Data Repository at <https://doi.org/10.26078/z54v-8j64>, including:

1. Benninghoff_Project N_Mapping.csv provides the sample identification details including the time point, basal diet and FMT source for each sample ID.
2. Benninghoff_Project N_Taxonomy.csv provides the mapping of amplicon sequence variants to bacteria taxonomy using the Silva database.
3. Benninghoff_Project N_ASV_counts.csv provides the 16S rRNA sequence count data for all samples for each amplicon sequence variant identified.
4. Readme.txt

VITA

Daphne Rodriguez was born in Santo Domingo, Dominican Republic where she resided until she was about seven years of age. In hopes of a better life, her family moved to Orange County, California where she resided until her teenage years, traveling back to Dominican Republic where she finished high school and attended Universidad Nacional Pedro Henriquez Urena aspiring to be a Doctor in Veterinary Medicine. Ms. Rodriguez received a governmental scholarship from the Dominican Republic to continue her educational career at Utah State University, where she completed her Bachelor's degree in the Department of Animal, Dairy and Veterinary Science. During her undergraduate studies, she began working as a research assistant under the mentorship of Dr. Abby Benninghoff, and then pursued a Master's degree in animal, dairy and veterinary sciences under co-mentorship of Dr. Benninghoff and Dr. Korry Hintze, from the Department of Nutrition, Dietetics and Food Sciences. After completion of her Master's research focusing on the gut microbiome and obesity, she then matriculated as a doctoral candidate under the continued guidance of Dr. Benninghoff, with funding support from the U.S Department of Agriculture. Her doctoral research focused on nutrition, the gut microbiome and colorectal cancer development. During her research career at Utah State, she co-authored five scientific publications detailing work on nutritional interventions to modulate the gut microbiome and colon carcinogenesis in mouse models and the use of fecal microbiota transfer to determine direct effects of disease-related microbiomes on disease development in recipients. Ms. Rodriguez will continue her scientific training as postdoctoral scholar in University of Texas Southwestern, continuing her research focusing on gut health and the microbiome.